
New Multinuclear Copper and Silver Clusters Protected by Phosphine Ligands

Zur Erlangung des akademischen Grades eines

DOKTORS DER NATURWISSENSCHAFTEN

(**Dr. rer. nat.**)

von der KIT-Fakultät für Chemie und Biowissenschaften

des Karlsruher Instituts für Technologie (KIT)

genehmigte

DISSERTATION

von

M.S.-Material. Minting Hao

aus

Xiangyang, Hubei, China

KIT-Dekan: Prof. Dr. Hans Achim Wagenknecht

Referent: Prof. Dr. Dieter Fenske

Korreferent: Prof. Dr. Peter W. Roesky

Tag der mündlichen Prüfung: 21.07.2022

This Ph.D. project was carried out from November 2018 to July 2022 at the institute of Inorganic Chemistry (AOC) and Institute of Nanotechnology (INT) of Karlsruhe Institute of Technology (KIT) under the direction of Prof. Dr. Dieter Fenske. This project was financially supported by China Scholarship Council.

I declare that this thesis was written independently and that any sources or resources other than those indicated has not been used and that the quotations has been identified. The dissertation has not yet been submitted to any other college or university.

宣传就是聚焦高光时刻，拿出亮丽好看的数据，其本质是一种误导。

Propaganda is to focus on high-light moments and come up with bright and beautiful data, which is essentially misleading.

From a non-famous journalist

TABLE OF CONTENT

1 Introduction

Synthesis, structures and properties of coinage metal chalcogenide clusters have been widely investigated[1] during the past decades with development of modern analysis technologies, for instance in the field of transmission electron microscope (TEM), nuclear magnetic resonance (NMR), electrospray ionization-mass spectrometry (ESI-MS). Due to their tiny sizes (≤ 10 nm), chalcogenide clusters can be seen as nano-particles with precise structural information. Herein, the advantage of metal chalcogenide clusters residues in two main aspects:

(1) Structurally, they own precise information of structure, composition and perfect size homogeneity,[2] which is beneficial of describing the relationship between structure and properties.[3] Therefore, they can be seen as a bridge between smaller molecules and bulk binary materials.[4] Some of them act as nodes to combine different ligands with various functions.[5]

(2) In terms of performance, they present special properties similar with common nanoparticles such as quantum confinement effect and quantum tunnelling effect.[6]

Gold clusters and nano-particles have been deeply studied and many of them display remarkable size-dependent properties.[7] However, compared with similar gold compounds,[7-8] silver and copper chalcogenides have been less reported. This situation might be caused by their instability and difficulty of crystallization. Herein, several approaches have been figured out to stabilize the final cluster at least kinetically, which will be introduced later. But no matter which kind of routine that has been described, one of the vital points is finding the effective strategy to get rid of their aggregation. After years of exploration, several synthetic strategies have been discovered to make stable copper or silver chalcogenide clusters available.

1.1 Synthetic methods

1.1.1 Anion-templated method

The anion-templated method is a widely used strategy in the synthesis of multinuclear silver clusters with core-shell geometry. The number of relevant reports in the field of copper clusters is relatively smaller. Hydrides[9] and halogenides[10] as inorganic anions have been testified as effective templates. As for the synthesis of silver clusters a stepwise process is possible: Firstly, reagents e.g. inorganic silver salts, sulphur sources and polyoxometalates are dissolved into solvents, forming cationic and anionic species such as single Ag^+, multiple Ag_n^{m+} kernels[11] and in situ anions. Secondly, formation of nucleation centres of these clusters. Thirdly, this core is covered by the other cations, commonly Ag^+. Finally, this metastable intermediate species is wrapped by remaining anions or ligands such as thiolates or neutral ligands.

A lot of anions have been used to synthesize clusters such as $Cl^–$[12], $CF_3COO^–$[13], $CO_3^{2–}$[14] and polyoxometalates (POMs)[15]. It seems that different anionic templates determine the size and geometry of the cluster. For example, the fundamental building unit of $\{[S@Ag_{12}@(n\mathrm{BuPO}_3)_9@Ag_{36}(t\mathrm{BuS})_{23}(CH_3O)_2(NO_3)_3]\cdot 2CH_3OH\}_n$[16] (*n*Bu = normal butyl; *t*Bu = *tert*-butyl) templated by central $S^{2–}$ can be regarded as consisting of a core of $[S@Ag_{12}@(n\mathrm{BuPO}_3)_9]^{8–}$ encapsulated by a shell of $[Ag_{36}(t\mathrm{BuS})_{23}]^{13+}$. However, when $S^{2–}$ was replaced by $MoO_4^{2–}$, namely in compound $[CH_3OH_2]_6\{MoO_4@Ag_{12}@(n\mathrm{BuPO}_3)_8S_6@Ag_{36}(t\mathrm{BuS})_{24}\}$, the building unit of this compound became core of six $S^{2–}$ capped by a distorted Ag_{12} cuboctahedron surrounded by a shell of $[Ag_{36}(t\mathrm{BuS})_{24}]^{12+}$. The framework of the structure displays a tetradecahedron with a two-fold rotation axis. Another example is that the size of $[SO_4@Ag_{20}(i\mathrm{BuS})_{10}(PhSO_3)_8(H_2O)_4\cdot 2H_2O]_n$ (*i*Bu = isobutyl) is smaller than that of $[(\alpha\text{-}Mo_5O_{18})@Ag_{36}(i\mathrm{PrS})_{18}(PhSO_3)_{12}(DMF)_6]$ (*i*Pr = isopropyl; DMF = N,N’-dimethylformamide) and $\{(n\mathrm{Bu}_4NH)[(\beta\text{-}Mo_5O_{18})@Ag_{36}(i\mathrm{BuS})_{18}(PhSO_3)_{13}(CH_3OH)]\}_n$.[17] Similarly, by this principle one can conclude that POMs as bigger anions approach to more complicated and larger structures. In 2018, $[SO_4@Ag_{78}S_{15}(CpS)_{27}(CF_3CO_2)_{12}](CF_3CO_2)_7$ (CpSH = cyclopentanethiol)[18] has been successfully synthesized using the $SO_4^{2–}$ anion as a template. Another example of the influence of a template anion to the final structure has been published in 2018 by Zheng et al.[19] They reported the first example of a mixed anion-templated structure, namely

$[(SO_4)_2(W_5O_{19})_2@Ag_{90}(tBuC_6H_4S)_{44}(PhCOO)_{24}(DMF)_2(H_2O)_2]\cdot 2PhCOO$, whose anions $W_5O_{19}^{8-}$ and SO_4^{2-} generated in-situ by decomposition of $[\alpha\text{-}P_2W_{18}O_{62}]^{6-}$ and $tBuC_6H_4SH$.

1.1.2 Thiolate-protected method

The clusters synthesized *via* this method can be seen as typical core-shell particles. There are two different categories based on the type of the core:

(1) Compounds with pure metal core protected by thiolate ligands, namely $[M_n(SR)_m]^q$. (M = Cu, Ag, Au; R = alkyl);

(2) Compounds which can be regarded as M_2E (M = Cu, Ag, Au; E = S, Se, Te) core surrounded by various ligands.

For the former one, Xie et al.[20] have concluded the synthetic routine and key points in detail. In this article, two essential aspects of synthesis have been pointed out. Firstly, based on Brust-Schiffrin or Brust-Schiffrin-like synthesis, if mono-dispersity is the primary pursuit, it is essential to adjust the time scale between reduction and core-etching by introducing a suitable amount of reducing agent.

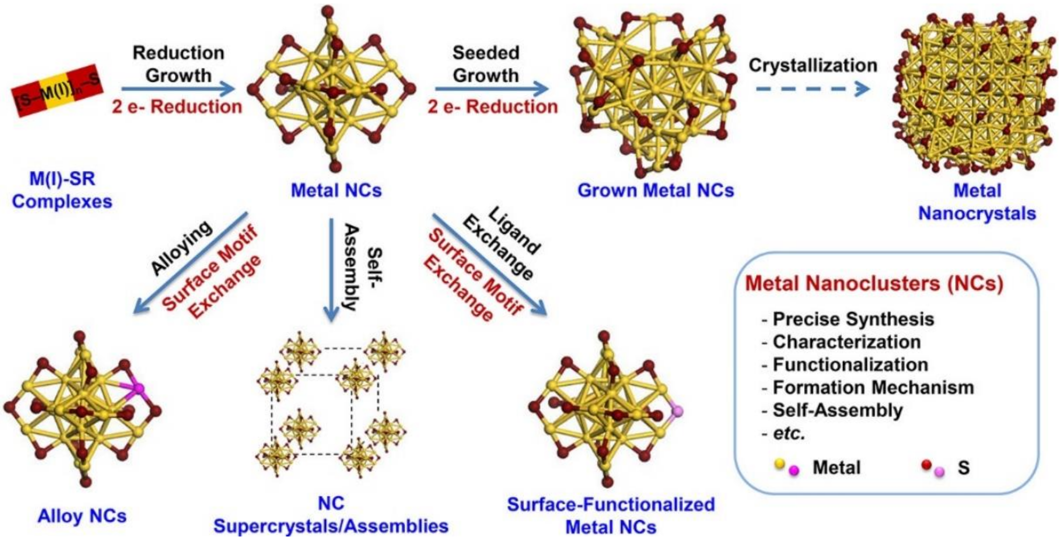

Figure 1-1 *General progress of the growth of clusters* $[Ag_x(SR)_y]$.[20]

There are a lot of crystalline compounds in this aspect, that have been published. For example, Wang et al.[21] published two surface passivated silver clusters: $[Ag_{21}(dpa)_{12}]SbF_6$ (Ag21) and $[Ag_{22}(dpa)_{12}](SbF_6)_2$ (Ag22) (dpa = dipyridylamido). These two silver clusters share the same centred icosahedral Ag_{13} core but their coordination modes of the dpa shell are different. Interestingly, Ag21 and Ag22 can reversibly interconvert in the mixture of *n*-heptane and ethanol. As increase the ratio of *n*-heptane to ethanol, Ag22 will be gradually changed to Ag21. This property may be caused by the different solubility of the two clusters in the mixed solvents. Besides, as for copper clusters, Chen et al.[22] has obtained $[Cu_6(SR)_6]^-$ (R = C_7H_4NO) with $[Na(C_3H_6O)_6]^+$ as counterion. In the anion six copper atoms are assembled in a bipyramid geometry. Each μ_3-thiolate ligand coordinates with three copper atoms, in which two of them are bridged by sulphur atoms and the third one is connected *via* the organic part. Meanwhile, this copper complex exhibits excellent performance on detection of H_2O_2 with high selectivity and sensitivity.

As for the latter one, this kind of compounds can be divided into two sub-categories. One is that the source of silylated chalcogenide participates in the synthesis process while the other is not. In terms of the crystals without silylated chalcogenide, Wang and Mak groups have published many relevant examples. For instance, in 2019, Wang et al.[23] reported a series of Ag-S clusters by taking advantage of the in-situ strategy to control the very slow release of S^{2-}. All these compounds can be described as Ag_2S cores encapsulated by AgS*t*Bu and tfa (tfa = trifluoroacetate) ligands. With growing sizes of the molecules, the geometry of obtained compounds gradually becomes close to spheres. For copper compounds, the Cu_{14} core of $[Cu_{14}(C_2B_{10}H_{10}S_2)_6(CH_3CN)_8]$[24] consists of a Cu_6^{4+} octahedron and a Cu_8^{8+} cube, in which Cu_6^{4+} is inserted into the hollow of Cu_8^{8+} *via* Cu···Cu interactions. Copper atoms on the apexes of the outer cube are coordinated by three thiolates and one solvent molecule. Interestingly, solvent molecules can be replaced by other ligands such as 4,4’-bipyridine. Therefore, by simply changing ligands one can get various discrete clusters or even frameworks using Cu_{14} as node.

Concerning the use of silylated chalcogenide, Fenske et al.[25] have conducted systematic research work. They elaborated the synthetic strategy of this kind of clusters. Firstly, MX (M = Cu, Ag; X = Cl^-, CH_3COO^-, SR^-) and phosphine ligands are put into solvents. In this step various mono- and polynuclear phosphine complexes of MX are formed. Secondly, silylated chalcogenide compounds such as $E(SiMe_3)_2$ or $RE(SiMe_3)$ (E = S, Se, Te; R = terminal or bridging organic group) were added into the reaction. These silylated ligands capture the medium species, forming giant clusters. The driving force for the formation of polynuclear copper and silver complexes is the formation of $Me_3Si–X$.

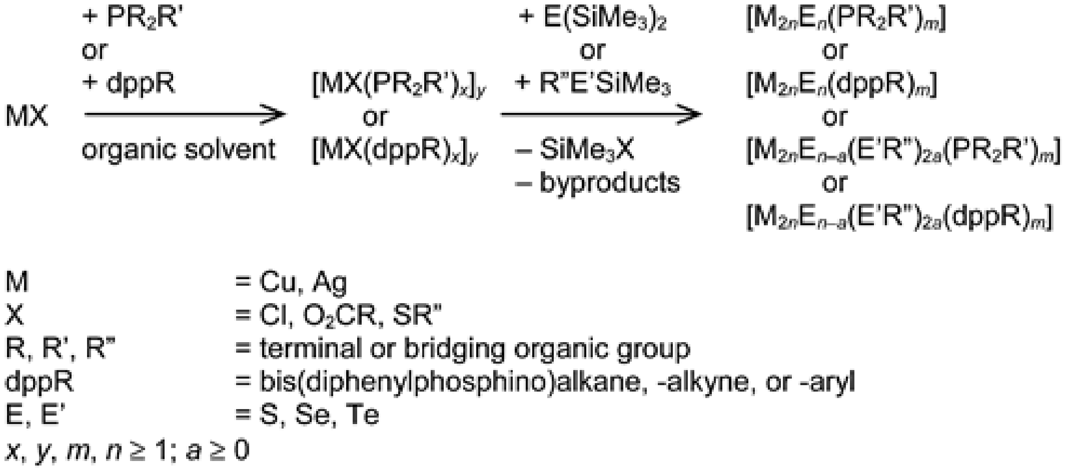

M = Cu, Ag
X = Cl, O_2CR, SR"
R, R', R" = terminal or bridging organic group
dppR = bis(diphenylphosphino)alkane, -alkyne, or -aryl
E, E' = S, Se, Te
$x, y, m, n \geq 1$; $a \geq 0$

***Figure 1-2** General synthesis route for the formation of copper and silver clusters.*[25]

Finally, the clusters are protected by phosphine ligands yielding kinetically stable molecules. The formation of the obtained compounds is influenced by the properties of MX and steric and electronic behaviour of the used phosphine ligands, the solvent and reaction temperature. Hence, based on the above routine, this class of numerous ligand-protected M_2E clusters have been published during the past years and the transition from mononuclear complexes to the bulk phase has been discussed. Besides, these compounds are proved to have potential on the application of high ionic[26] and even higher electric conductivity[27] in the solid state. To make these structures clearer, one can classify these kinds of structures based on the sizes. The clusters having ≤ 20 metal atoms are classified as low nuclear complexes; the middle nuclear clusters own 20–50 metal atoms and the large clusters have ≥ 50 metal atoms.

1.2 Structures

1.2.1 Low nuclear copper(I) thiolate complex

From a structural point of view, small copper complexes do not have a strong relationship with the bulk Cu_2S structures. Most of low nuclear complexes have discrete energy levels, presenting excellent optical or electrochemical properties. As examples temperature-dependent fluorescence and density functional theory (DFT) calculations have been widely introduced. Some of them have been applied to assemble organic light emission diodes (OLEDs).[28]

Examples of copper chalcogenide clusters are shown in **Table 1-1** and **1-2**.

A large amount of binuclear copper thiolate complex consists on a Cu_2S_2 core, possessing a butterfly-like geometry. The thiolate ligands are arranged in *cis*-[54] or *trans*-[55]conformation, either bridging two copper atoms or chelating on one copper atom. Beside coordinating with sulphur, copper atoms additionally link the other ligands such as phosphine ligands, halide, or N-heterocycle, presenting twisted triangular or tetrahedral coordination mode.[54]

Taking a specific example, $[Cu_2(P\wedge S)_2(PPh_3)_2]$[56] ($P\wedge S$ = 2-(diphenylphosphino)-benzenethiolate, PPh_3 = triphenylphosphine) has been successfully isolated by solution diffusion method and its light-emission property has been thoroughly explained. In this structure, copper atoms are tetrahedrally coordinated with two phosphorus and two sulphur atoms. $[Cu_2(p\text{-}S\text{-}C_6H_4\text{-}NMe_2)_2(dpppt)_2]$[57] (dpppt = 1,5-bis(diphenylphosphino)pentane) is also a typical Cu_2 binuclear complex with a rhombic planar core in which two tetrahedrally coordinated copper atoms are bridged by bidentate phosphine ligands and thiolates. Besides, this compound shows remarkably strong blue light-emission with the maximum wavelength at 480 nm.

Some compounds with four copper atoms consist of Cu_4S_4 eight-membered rings in which copper and sulphur atoms are arranged in stair[56] or chair[57]-like conformation. Compounds containing six to ten copper atoms display more flexible geometry: the combination of multiple membered rings[58]; octahedrons[59]; twisted hexagonal prism[60] or other more complicated structures[61], etc. For example, eight copper atoms in $[Cu_8(\mu_3\text{-}S)_4(CAAC)_4]$ (CAAC = cyclic(alkyl)(amino)carbene)[62] are divided into two groups. Four copper atoms form one plane and the adjacent two atoms are linked by one sulphur atom, giving this eight-membered ring ‘hinged’ or ‘butterfly’ geometry. The other four copper atoms coordinating with one sulphur atom link one carbene extending outside, which are trans-disposed relative to that plane.

Table 1-1 *Examples of phosphine-stabilized copper sulphur clusters*

E = S	**E = S with SR**
$[Cu_{12}S_6(PEt_3)_8]$[29]	$[Cu_{14}S(SPh)_{12}(PPh_3)_6]$[30]
$[Cu_{12}S_6(PEtPh_2)_8]$[29]	$[Cu_{136}S_{56}(SCH_2C_4H_3O)_{24}(dpppt)_{10}]$[33]
$[Cu_{20}S_{10}(PPh_3)_8]$[29]	
$[Cu_{12}S_6(P\textit{n}Pr_3)_8]$[36]	
$[Cu_{20}S_{10}(P\textit{n}Bu\textit{t}Bu_2)_8]$[36]	
$[Cu_{24}S_{12}(PMe\textit{i}Pr_2)_{12}]$[34]	
$[Cu_{28}S_{14}(P\textit{t}Bu_2Me)_{12}]$[34]	
$[Cu_{50}S_{25}(P\textit{t}Bu_2Me)_{16}]$[34]	
$[Cu_{12}S_6(dpppt)_4]$[39]	
$[Cu_{12}S_6(dppo)_4]$[39]	
$[Cu_{12}S_6(dppfc)_4]$[44]	
$[Cu_{20}S_{10}(PPh_3)_8]$[44]	
$[Cu_{20}S_{10}(P\textit{t}Bu_3)_8]$[44]	

Table 1-2 *Examples of phosphine-stabilized copper selenium clusters.*

E = Se	**E = Se with SR**	**E = Se with SeR**
$[Cu_{12}Se_6(PEtPh_2)_8]$[29]	$[Cu_{17}Se(SPh)_{15}(PPh_3)_4]$[31]	$[(PhSe)Cu(\mu\text{-}Ph_2PC{\equiv}CC{\equiv}CPPh_2)_3Cu(SePh)]$[32]
$[Cu_{31}Se_{15}(SeSiMe_3)(P\mathit{t}Bu_2Me)_{12}]$[34]	$[Cu_{20}Se(SPh)_{12}(OAc)_6(PPh_3)_4]$[31]	$[Cu_{16}Se_4(SePh)_8(dppbe)_4]$[32]
$[Cu_{48}Se_{24}(PMe_2Ph)_{20}]$[34]	$[Cu_{54}Se_8(SPh)_{30}(OAc)_8(PPh_3)_6]$[31]	$[Cu_3(SeMes)_3(dppm)]$[35]
$[Cu_{70}Se_{35}(P\mathit{t}Bu_2Me)_{21}]$[34]	$[Cu_{72}Se_{14}(SPh)_{36}(OAc)_8(PPh_3)_6]$[31]	$[Cu(dppp)_2][Cu_{25}Se_4(SePh)_{18}(dppp)_2]$[35]
$[Cu_{12}Se_6(PCy_3)_6]$[37]	$[Cu_{28}Se_6(SPh)_{16}(PPh_3)_8]$[31]	$[Cu_{38}Se_{13}(SePh)_{12}(dppb)_6]$[35]
$[Cu_{26}Se_{13}(PEt_2Ph)_{14}]$[37]	$[Cu_{36}Se_8(SPh)_{20}(PPh_3)_8]$[31]	$[Cu_{58}Se_{16}(SePh)_{24}(dppa)_6]$[35]
$[Cu_{26}Se_{13}(PCy_3)_{10}]$[37]	$[Cu_{22}Se_6(SC_6H_4OSiMe_3)_{10}(PPh_3)_8]$[38]	$[Cu_{36}Se_5(SePh)_{26}(dppa)_4]$[35]
$[Cu_{59}Se_{30}(PCy_3)_{15}]$[37]	$[Cu_{36}Se_8(SC_6H_4OSiMe_3)_{20}(PPh_3)_8]$[38]	$[Cu(dppp)_2][Cu_{25}Se_4(SePh)_{18}(dppp)_2]$[35]
$[Cu_{20}Se_{13}(PEt_3)_{12}]$[40]	$[Cu_{52}Se_{20}(SC_6H_4OSiMe_3)_{12}(PPh_3)_{11}]$[38]	$[Cu_6(SePh)_6(PPh_3)_3(4,4'\text{-}bpy)]$[41]
$[Cu_{70}Se_{35}(PEt_3)_{22}]$[40]	$[Cu_{22}Se_6(SC_6H_4NO_2)_{10}(PPh_3)_8]$[42]	$[Cu_{15}Se_3(SePh)_9(P(C_6H_4SMe)_3)_6]$[43]
$[Cu_{140}Se_{70}(PEt_2Ph)_{34}]$[40]	$[Cu_{22}Se_6(SC_6H_4Br)_{10}(PPh_3)_8]$[45]	$[Cu_{20}Se(SePh)_{12}(OAc)_6(PPh_2C_6H_4SMe)_2]$[43]
$[Cu_{29}Se_{15}(P\mathit{i}Pr_3)_{12}]$[46]	$[Cu_{28}Se_6(SC_6H_4Br)_{16}(PPh_3)_8]$[45]	$[Cu_{22}Se_6(SePh)_{10}(PPh_2C_6H_4SMe)_8]$[43]
$[Cu_{30}Se_{15}(P\mathit{i}Pr_3)_{12}]$[46]	$[Cu_{47}Se_{10}(SC_6H_4Br)_{21}(OAc)_6(PPh_3)_8]$[45]	$[Cu_{38}Se_4(SePh)_{24}(OAc)_6(PPh_2C_6H_4SMe)_4]$[43]
$[Cu_{36}Se_{18}(P\mathit{t}Bu_3)_{12}]$[46]	$[Cu_{48}Se_{24}(S\text{-}C_3H_5NS)_2(dppm)_{10}]$[47]	$[Cu_{22}Se_6(SeC_6H_4OSiMe_3)_{10}(PPh_3)_8]$[38]
$[Cu_{32}Se_{16}(PPh_3)_{12}]$[48]	$[Cu_{50}Se_{24}(S\text{-}C_3H_4NS)_2(dppm)_{10}]$[47]	$[Cu_{32}Se_7(SenBu)_{18}(P\mathit{i}Pr_3)_6]$[49]
$[Cu_{52}Se_{26}(PPh_3)_{16}]$[48]		$[Cu_{50}Se_{20}(SetBu)_{10}(P\mathit{i}Pr_3)_{10}]$[49]
$[Cu_{72}Se_{36}(PPh_3)_{20}]$[48]		$[Cu_{73}Se_{35}(SePh)_3(P\mathit{i}Pr_3)_{21}]$[49]
$[Cu_{44}Se_{22}(PEt_2Ph)_{18}]$[50]		$[Cu_{36}Se_{12}(fcSe_2)_6(P\mathit{n}Pr_2Ph)_{12}]$[51]
$[Cu_{44}Se_{22}(P\mathit{n}Bu\mathit{t}Bu_2)_{12}]$[50]		$[Cu_{93}Se_{42}(SeC_6H_4SMe)_9(PPh_3)_{18}]_2$[33]
$[Cu_{70}Se_{35}(PEt_2Ph)_{24}]$[52]		$[Cu_{96}Se_{45}(SeC_6H_4SMe)_6(PPh_3)_{18}]$[33]
$[Cu_{140}Se_{70}(PEt_3)_{34}]$[49]		
$[Cu_{140}Se_{70}(PEt_3)_{36}]$[49]		
$[Cu_{146}Se_{73}(PPh_3)_{30}]$[53]		

Clusters containing twelve copper atoms consist of the basic unit [$Cu_{12}S_6L_x$] (L = Ligands), which is the smallest known core of a variety of [$Cu_{2n}E_n$] clusters. For these compounds, there are two different stable structures known depending on the steric demand of the used phosphine ligand. For Type I structure, eight phosphorus atoms only coordinate with the copper atoms on the side edges of the S_6 octahedron. But in Type II structure, four phosphorus atoms coordinate with copper from bottom sides whereas the other four from side edges.[36] This isomeric phenomenon has also been observed in clusters with [$Cu_{20}S_{10}$] core too.[29,36]

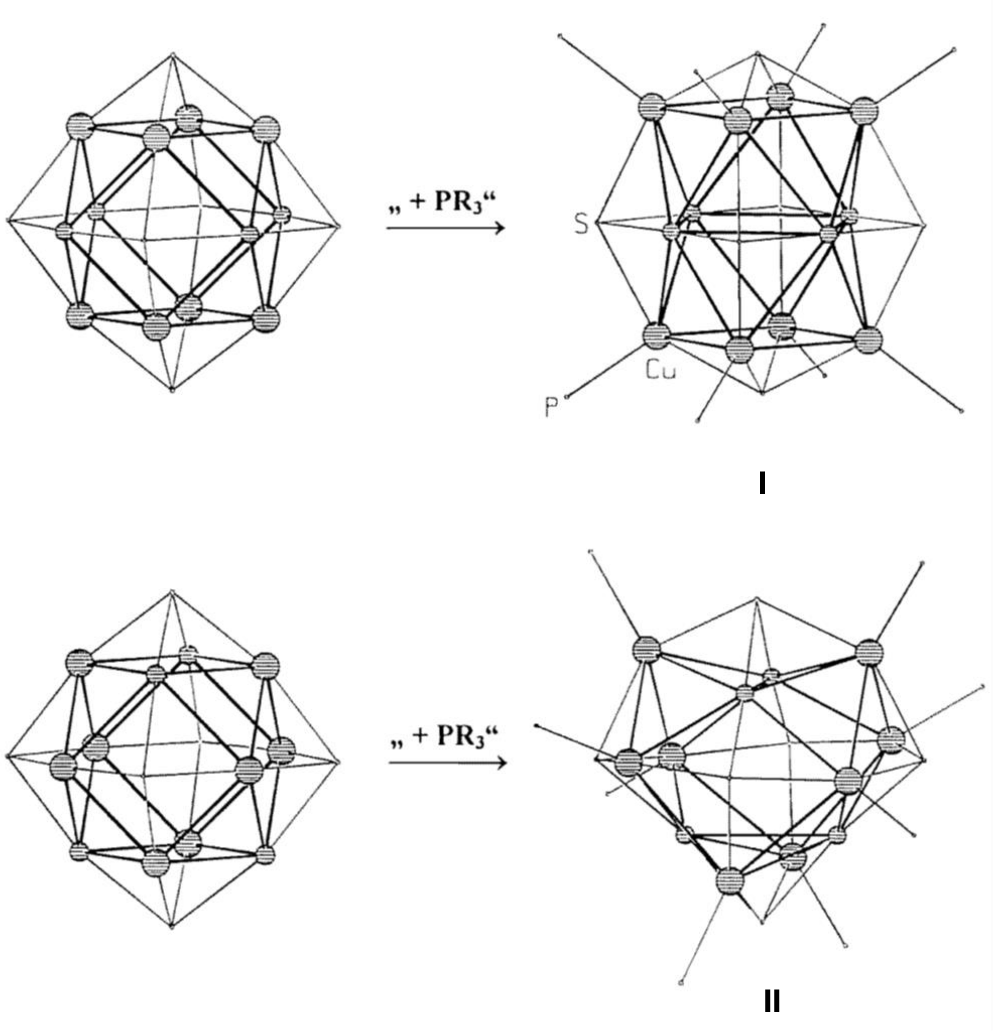

Figure 1-3 *Two different coordination mode of phosphine ligands in [$Cu_{12}S_6$] clusters.*[36]

The energy levels of these low core copper chalcogenide clusters are discrete so that they might have access to optical or photoelectrochemical properties.

Eichhöfer et al.[44] published eight copper clusters with [$Cu_{12}S_6$] or [$Cu_{20}S_{10}$] cores, including one dimer. They found that the luminescent peaks of $Cu_{12}S_6$ clusters usually reside in the range of 650–700 nm while the optical phenomena of two isomeric [$Cu_{20}S_{10}$] clusters are much different. The luminescent peak of "peanut-like" [$Cu_{20}S_{10}(PPh_3)_8$] is centred at 820 nm, whereas the oval cluster [$Cu_{20}S_{10}(P\textit{t}Bu_3)_8$] displays orange-light emission with maximum emission at 575 nm. Time-dependent DFT calculations indicate that the specifics of the ligand surface deeply effect the character of lower energy. The excited electrons transfer mainly comes from metal core to ligands dominated by core-centred transition routes.

The other two Cu_{12} clusters [$Cu_{12}S_6$(dpppt)$_4$] and [$Cu_{12}S_6$(dppo)$_4$] (dppo = bis(diphenylphosphino)octane)[39] present strong red luminescence with high quantum yield. It has been proved that solvents can influence luminescence of these clusters to some degree. After treatment of these compounds in vacuum, the solvent is removed yielding to the formation of an amorphous material. The structural collapse causes blue-shift of the maximum light emission position and broadening of the photoluminescent curves. DFT calculation indicate that the exciting electron transition of [$Cu_{12}S_6$(dpppt)$_4$] is metal to ligand, whereas in [$Cu_{12}S_6$(dppo)$_4$] the transition is core-centred.

Some copper clusters exhibit interesting electrochemical properties. For example, Corrigan et al.[63] demonstrated by cyclic voltammetry of copper clusters owning dppfc (dppfc = bis(diphenylphosphino)ferrocene) ([$Cu_{12}(\mu_4\text{-}S)_6(\mu\text{-dppfc})_4$], [$Cu_8(\mu_4\text{-}Se)_4(\mu\text{-dppfc})_3$], [$Cu_4(\mu_4\text{-}Te)(\mu_4\text{-}\eta^2\text{-}Te_2)(\mu\text{-dppfc})_2$], and [$Cu_{12}(\mu_5\text{-}Te)_4(\mu_8\text{-}\eta^2\text{-}Te_2)_2(\mu\text{-dppfc})_4$]), that the oxidation progress of these clusters is firstly on the ferrocene ligand dppfc, followed by further oxidation of copper and phosphorus atoms.

1.2.2 Middle and high nuclear copper clusters

Silylated chalcogenide sources are the ideal choice for obtaining clusters with higher nuclearity. Specific synthetic routine has been mentioned above.

In the initial stage, clusters are commonly achieved by the reaction of CuCl or CuOAc and silylated chalcogenide sources in the presence of bidentate or monodentate phosphine ligands. For example, reacting CuCl with P*i*Pr$_3$ and Se(SiMe$_3$)$_2$ in diethyl ether (Et$_2$O) leads to the formation of a mixture of [Cu$_{30-x}$Se$_{15}$(P*i*Pr$_3$)$_{12}$] (x = 0, 1).[46]

Dehnen et al.[50] synthesized two clusters with [Cu$_{44}$Se$_{22}$] core but different ligands. In terms of [Cu$_{44}$Se$_{22}$(PEt$_2$Ph)$_{18}$] (Et = ethyl), its selenium framework can be described as a deltahedron containing two selenium atoms in the centre, which can also be deconstructed as two hexagonal antiprisms linking through hexagonal faces. Whereas for [Cu$_{44}$Se$_{22}$(P*n*Bu*t*Bu$_2$)$_{12}$], there is an inversion centre. If carbon atoms and the distortion of the Cu-Se-P framework are ignored, this compound can be seen as having approximate C_{4h} symmetry. This difference is caused by the different steric requirement of the two phosphine ligands.

Chalcogenide frameworks of some middle-sized clusters exhibit layer geometry. Copper atoms in compound [Cu$_{32}$Se$_7$(Se*n*Bu)$_{18}$(P*i*Pr$_3$)$_6$][49] are inserted into the regular triple-layer selenium skeleton corresponding to hexagonal close packing (*hcp*). In analogy to [Cu$_{32}$Se$_7$(Se*n*Bu)$_{18}$(P*i*Pr$_3$)$_6$], the 24 chalcogen atoms in [Cu$_{40}$Se$_{16}$(S-C$_6$H$_4$-CN)$_8$(dppm)$_8$][64] (dppm = bis(diphenylphosphino)methan) are arranged in two parallel hexagonal layers, forming a drum-like skeleton.

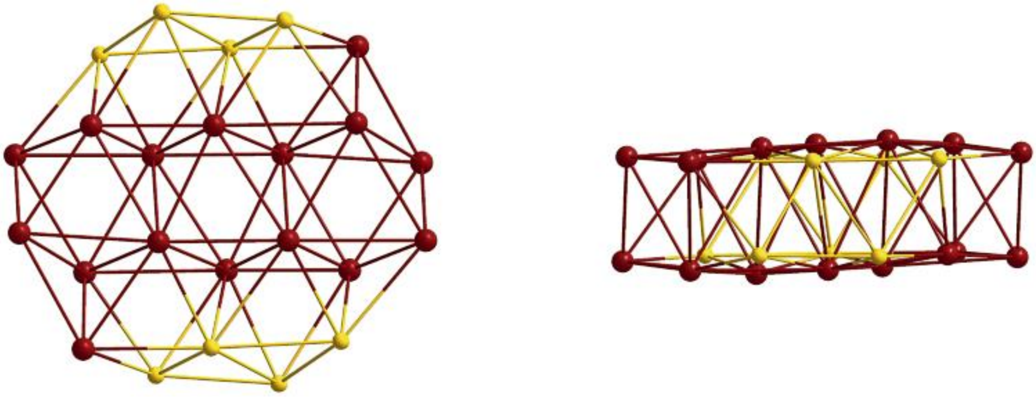

Figure 1-4 *Drum like chalcogenide framework of [Cu$_{40}$Se$_{16}$(S-C$_6$H$_4$-CN)$_8$(dppm)$_8$] in two orientations rotated by 90° (Se: red, S: yellow).*[64]

Comparing with selenium-bridged clusters, sulphur-framework compounds are less reported. An example is [Cu$_{52}$S$_{12}$(SCH$_2$C$_6$H$_4$*t*Bu)$_{28}$(PPh$_3$)$_8$][65], as the largest binary spherical cluster, which can be seen as a core-shell structure

$[(Cu_2S)_{12}@(CuSCH_2C_6H_4\textit{t}Bu)_{28}(PPh_3)_8]$. These middle-sized clusters present various geometric structures and coordination modes; there is just a weak relationship between these structures and their Cu_2S bulk counterpart.

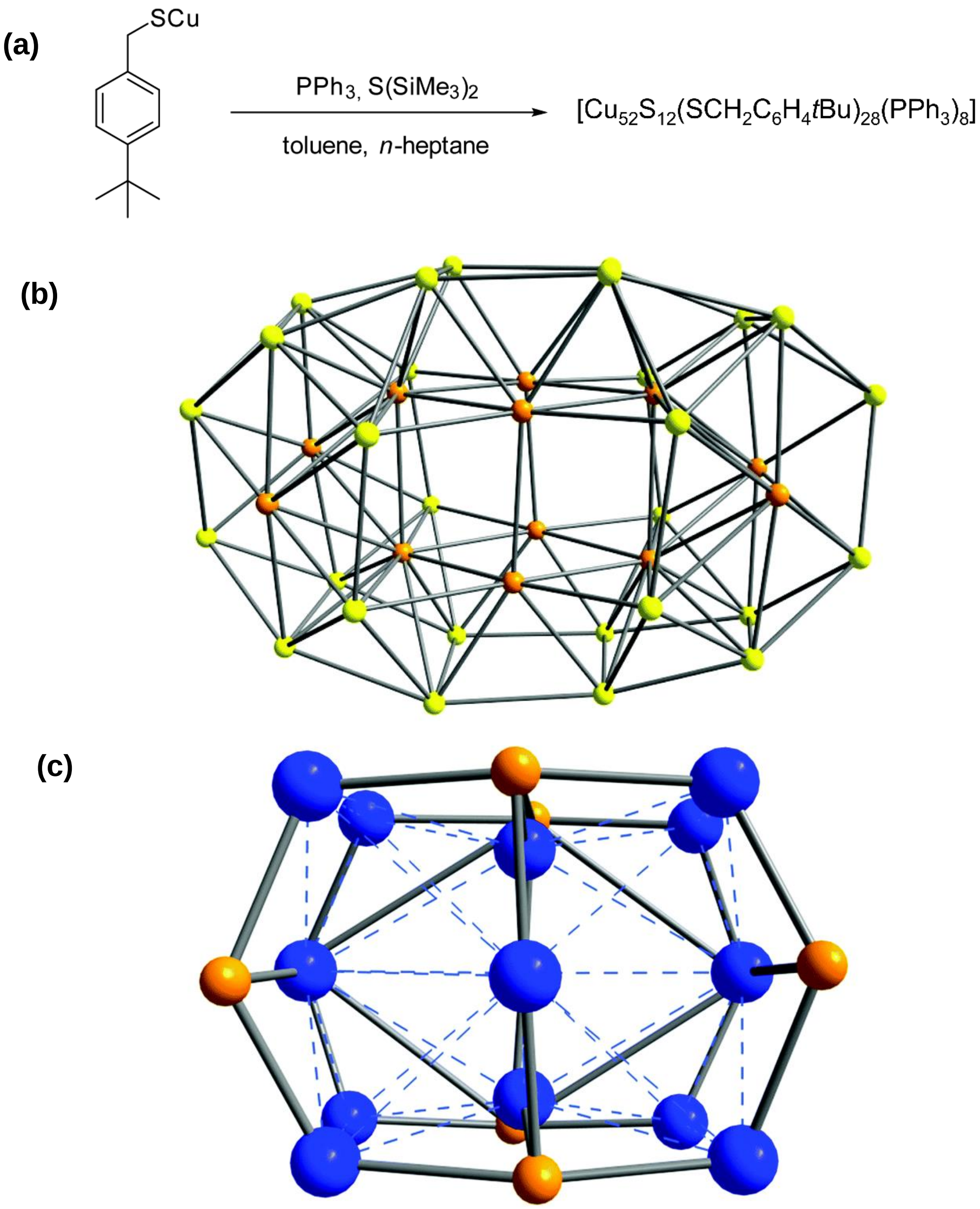

Figure 1-5 (a) *Synthesis of* $[Cu_{52}S_{12}(SCH_2C_6H_4tBu)_{28}(PPh_3)_8]$; ***(b)*** *oval sulphur sub-lattice and* ***(c)*** $[Cu_{14}S_6]$ *core with copper atoms arrangement of face centred cubic (fcc) packing of* $[Cu_{52}S_{12}(SCH_2C_6H_4tBu)_{28}(PPh_3)_8]$ *(Cu: blue,* S^{2-}*: orange, S in* $SCH_2C_6H_4tBu$*: yellow).*[65]

In larger copper clusters the copper atoms are inserted into the void of layer-type S/Se frameworks, which are close to that of bulk Cu_2E. But the features between sulphur and selenium bridged clusters are different. $[Cu_{136}S_{56}(SCH_2C_4H_3O)_{24}(dpppt)_{10}]$[33] has been proved as the largest reported Cu-S cluster till now. In this compound the sulphur atoms are arranged in a distorted face-centred cubic close packing (**Figure 1-6**). Copper atoms are embedded into this framework forming a small piece of the monoclinic mineral chalcocite (Cu_2S) low-temperature phase.

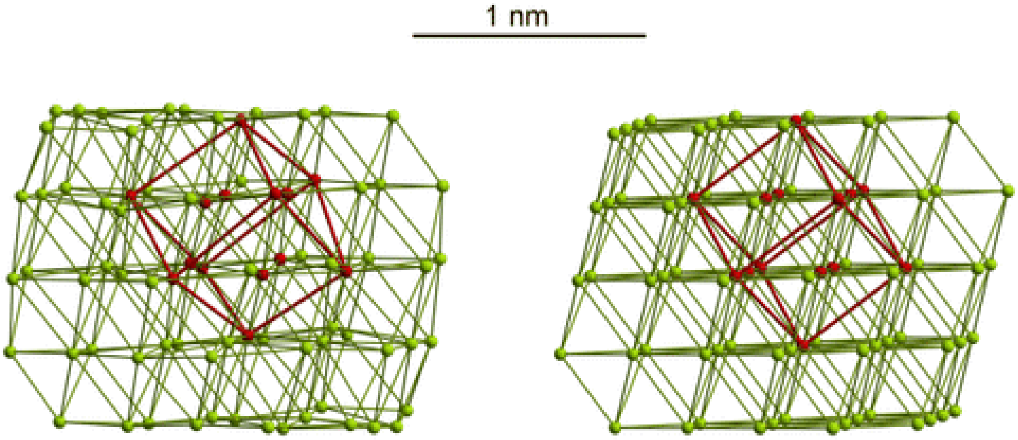

Figure 1-6 *Left: sulphur sublattice in* $[Cu_{136}S_{56}(SCH_2C_4H_3O)_{24}(dpppt)_{10}]$*, right: ideal cut-out of the fcc packing (red: fcc unit cell).*[33]

A series of giant copper selenium clusters have been reported since 1990. Their structures are based on a triangular layer selenium framework. This structural motif has been observed for the first time in $[Cu_{70}Se_{35}(PtBu_2Me)]_{21}$.[34] All the other known copper selenium clusters with less than 70 copper atoms are organized in ball-like globular structures. The largest Cu-Se cluster $[Cu_{146}Se_{73}(PPh_3)_{20}]$[53] has been published in 1993. All selenium atoms are arranged in three trigonal layers consisting of 21, 31, 21 atoms per layer forming a small part of a *hcp* structure. This arrangement of selenium atoms has not been observed in the structures of Cu_2Se minerals. 20 copper atoms on the surface are tetrahedrally coordinated by PPh_3 ligands and three selenium atoms. The remaining copper atoms are found in the tetrahedral holes of the close packed selenium structure. Other Cu-Se clusters are also found to be triangular prisms with selenium atoms in A–B–A packing (**Figure 1-7**). In addition, $[Cu_{70}Se_{35}(PtBu_2Me)]_{21}$[34] (Me = methyl), $[Cu_{73}Se_{35}(SePh)_3(PiPr_3)_{21}]$[49], $[Cu_{140}Se_{70}(PEt_3)_{34}]$[49] and $[Cu_{140}Se_{70}(PEt_3)_{36}]$[49]

can be classified into this A–B–A stacking mode, too.

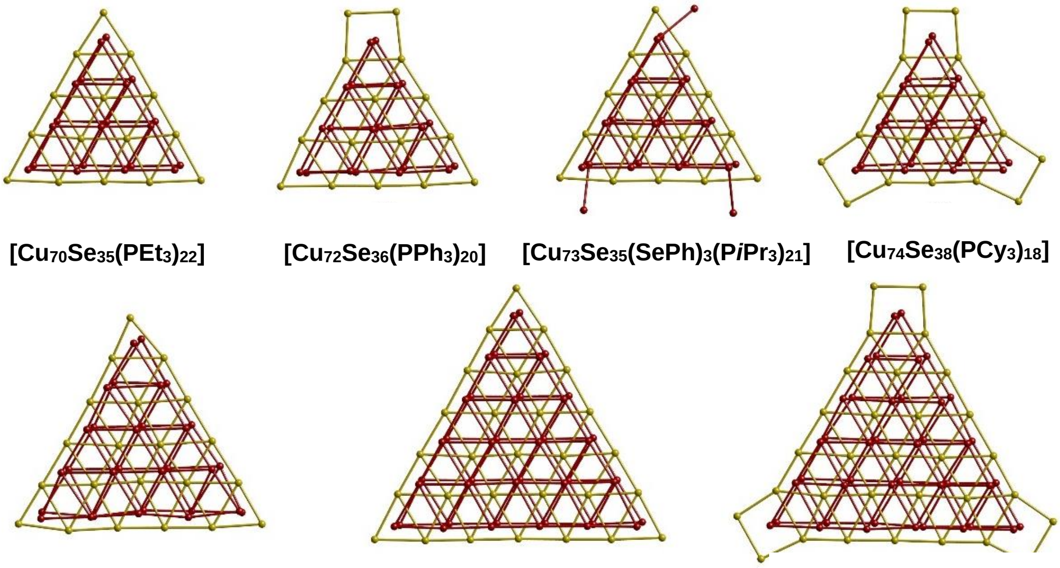

$[Cu_{70}Se_{35}(PEt_3)_{22}]$ **$[Cu_{72}Se_{36}(PPh_3)_{20}]$** **$[Cu_{73}Se_{35}(SePh)_3(P\textit{i}Pr_3)_{21}]$** **$[Cu_{74}Se_{38}(PCy_3)_{18}]$**

$[Cu_{93}Se_{42}(SeC_6H_4SMe)_9(PPh_3)_{18}]$ **$[Cu_{140}Se_{70}(PEt_3)_{36}]$** **$[Cu_{146}Se_{73}(PPh_3)_{30}]$**

Figure 1-7 *Selenium frameworks of $[Cu_{70}Se_{35}(PEt_3)_{22}]$[40], $[Cu_{72}Se_{36}(PPh_3)_{20}]$[48], $[Cu_{73}Se_{35}(SePh)_3(PiPr_3)_{21}]$[49], $[Cu_{74}Se_{38}(PCy_3)_{18}]$[66], $[Cu_{93}Se_{42}(SeC_6H_4SMe)_9(PPh_3)_{18}]$[33], $[Cu_{140}Se_{70}(PEt_3)_{36}]$[49] and $[Cu_{146}Se_{73}(PPh_3)_{30}]$[53] (Red: layers A, yellow: layer B).*

Furthermore, attributed to the reports about Cu-Se clusters, one can conclude one general rule of their possible growing process. In Cu_{70} clusters [34, 40, 52], selenium atoms are arranged in three layers owning 10, 15, 10 atoms, respectively. In $[Cu_{93}Se_{42}(SeC_6H_4SMe)_9(PPh_3)_{18}]$[33], three Se layers contain 15, 21 and 15 atoms, in $[Cu_{140}Se_{70}(PEt_3)_{36}]$[49] three selenium layers contain 21, 28 and 21 atoms, respectively.

A hypothetic growing process from a Se_{10} to a Se_{15} layer is shown in **Figure 1-8.** Firstly, two apexes of the Se_{10} layer will deform from triangle to square by addition of two selenium atoms at the vertex of the triangle. Then the other three selenium atoms take part in building the larger Se_{15} layer.

1.2.3 Silver chalcogenide clusters

Silver chalcogenide compounds are interesting because of their photophysical and thermoelectrical properties. Ag_2S can act as an effective photosensitive material and Ag_2Se is widely used in the field of fast ionic conductivity. The synthesis of ligand stabilized silver chalcogenides is not easy due to the very low solubility of bulk silver sulphide and silver selenide.

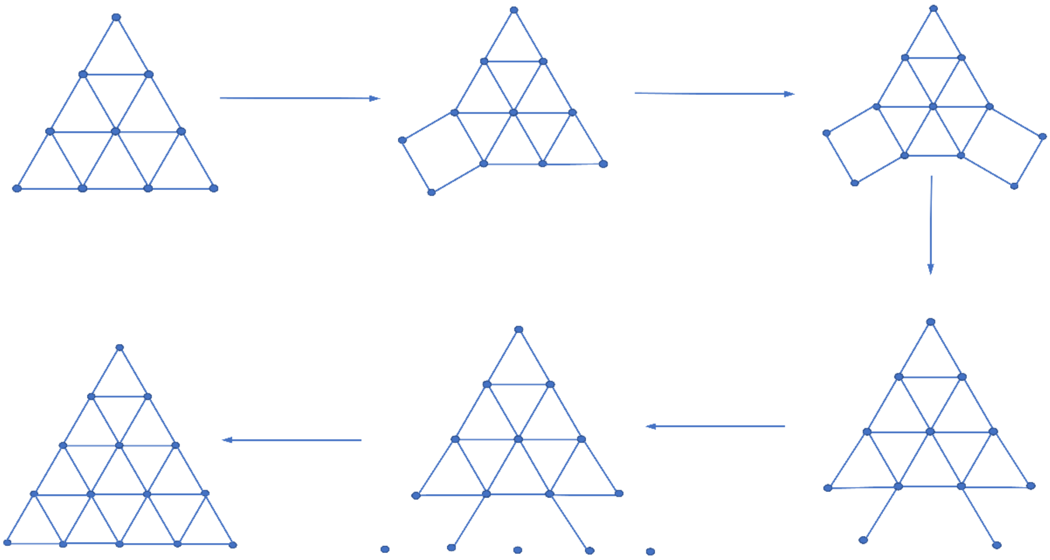

Figure 1-8 *Growing progress of the middle layer from* Se_{10} *to* Se_{15}*.*

After decades of research, several feasible approaches have been developed. Apart from the anion-templated method mentioned above, another method is the reaction of silver salts (AgCl, AgOAc, AgSR) with phosphine ligands and silylated chalcogenide sources in organic solvents. There are not many reports about crystallization of small silver thiolate clusters. Some of them are discrete complexes, the others are Ag-S cluster-based polymers. For example, Yang et al.[67] published a series of silver thiolates including discrete $[Ag_{10}(SCy)_{10}(dpph)_2]$ (Cy = cyclohexyl; dpph = 1,6-bis(diphenylphosphino)hexane), 1D-chain $[Ag_3(SMes)_3(dpph)_2]$ (Mes = mesityl) and 2D-plate honeycomb like $[Ag_3(SMes)_3(dppfc)_{1.5}]$. Corrigan et al.[68] reported several silver compounds with Ag_4S_4 eight membered rings as core ($[Ag_4(S\textit{t}Bu)_4(\textit{i}Pr_2\text{-bimy})_2]$ ($\textit{i}Pr_2$-bimy = 1,3-diisopropylbenzimidazol-2-ylidene) and $[Ag_4(S\textit{t}Bu)_4(P\textit{n}Pr_3)_2]$) (*n*Pr = normal propyl) or typical Ag_5S_6 structure ($[Ag_5(S\textit{t}Bu)_6][Ag(\textit{i}Pr_2\text{-mimy})_2]$) ($\textit{i}Pr_2$-mimy = 1,3-diisopropyl-4,5-dimethylimidazol-2-ylidene) with a Ag_5 bipyramide inserted into a S_6 prism. Although till now relevant reports about silver thiolate compounds are scarce, there are several publications. Examples are $[Ag_6(\mu\text{-dppm})_4\text{-}(\mu_3\text{-}SC_6H_4Me\text{-}$

$p)_4](PF_6)_2$[69], $[Ag_6(\mu\text{-dppm})_4(\mu_3\text{-SeC}_6H_4Cl)_4](PF_6)_2$[69], $[H_4Ag_8(2\text{-mpa})_6(PPh_3)_6]\cdot EtOH$[70] (2-$H_2$mpa = a racemic form of 2-mercaptopropionic acid) and $[(AgSCH_2CH_2NMe_2)_5\cdot 0.5H_2O]_n$.[71] The very poorly soluble silver thiolates can be dissolved in organic solvents with the help of phosphine ligands yielding to the above described oligomeric and polymeric compounds.[67] Further addition of $E(SiMe_3)_2$ or $RE(SiMe_3)$ (R = organic groups) opens the way to the synthesis of very large silver clusters with hundreds of silver atoms. Previously these compounds were prepared by the reaction of silver salts like AgOAc and AgCl, chalcogenide sources and phosphine ligands at low temperature. In contrast, higher temperature only results in the formation of amorphous Ag_2E precipitate. Hence, to simplify the synthetic progress, one can use silver thiolates to ensure that the reactions can be carried out at room temperature.

As for middle-sized silver clusters, most of them display spherical or oval core-shell structures, which is not only different from Cu/E parallel layer-like structures but also weakly structurally connected to the bulk phase counterpart.

Silver sulphide, Ag_2S, exists in three modifications. The low temperature form (< 173°C) is the monoclinic acanthite (α-Ag_2S). Between 173°C[72]and 586°C the body centred cubic argentite (β-Ag_2S)[72] is stable. Above 586°C a face centred cubic modification has been observed (δ-Ag_2S).[72] In the case of Cu/Se clusters it was found that there is a structural transition from molecular spherical structures towards cut-outs of the bulk structure when the clusters reach 70 copper atoms. An analogous structural transformation has not been found yet in the case of sulphur-bridged silver clusters.

For example, reacting silver benzoate and triphos with a mixture of $S(Ph)SiMe_3$ and $S(SiMe_3)_2$ (2:1) at –20°C in diglyme leads to the compound $[Ag_{70}S_{16}(SPh)_{34}(PhCO_2)_4(triphos)_4]$[73] (triphos = 1,1,1-tris((diphenylphosphanyl)methyl)ethane; Ph = phenyl), a spherical structure whose shell consists of SPh^- and phosphine ligands, protecting a S_{16} sulphide core. A structurally similar compound, $[Ag_{70}S_{20}(SPh)_{28}(dppm)_{10}](CF_3CO_2)_2$,[74] has been isolated from the reaction of $AgCF_3CO_2$, dppm, $S(Ph)SiMe_3$ and $S(SiMe_3)_2$ in DME (DME = dimethoxyethane) at –40°C. In this cationic cluster, twelve S^{2-} anions together with 28 SPh^{-} build up the outer egg-shaped polyhedron and the remaining eight S^{2-} compose a hexagonal bipyramid in the inner part.

The molecular structures of silver-richer compounds such as $[Ag_{123}S_{35}(S\textit{t}Bu)_{50}]$ and $[Ag_{344}S_{124}(S\textit{t}Bu)_{96}]$[75] are two core-shell spherical clusters whose chemical formula can be written as $[(Ag_{73}S_{35})@(AgS\textit{t}Bu)_{50}]$ and $[(Ag_{248}S_{124})@(AgS\textit{t}Bu)_{96}]$. These two compounds can generally be seen as a Ag_2S core protected by a silver thiolate shell. Interestingly, although phosphine ligands have been used in the synthesis the phosphines do not coordinate to the final product.

The largest clusters $[Ag_{490}S_{188}(S\textit{t}C_5H_{11})_{114}]$[76] and $[Ag_{352}S_{128}(S\textit{t}C_5H_{11})_{96}]$[76] co-crystallize from the reaction of $AgS\textit{t}C_5H_{11}$, dppbp, (dppbp = 4,4'-bis(diphenylphosphanyl)biphenyl) and $S(SiMe_3)_2$ in toluene. The structure of the Ag/S core of $[Ag_{490}S_{188}(S\textit{t}C_5H_{11})_{114}]$ can be described as a narrow-waisted cylinder with the diameter of 2.8–3.1 nm. Also $[Ag_{94}S_{34}(SAd)_{26}(dpppt)_6]$ (Ad = adamantly), $[Ag_{190}S_{58}(SCH_2fur)_{74}(dpppt)_8]$[77] (fur = furan-2-ylmethanethiol) and soluble $[Ag_{115}S_{34}(SCH_2C_6H_4\textit{t}Bu)_{47}(dpph)_6]$[78] are core-shell structures. Some Ag/S clusters synthesized *via* the other approaches present remarkable fluorescence.[23 79]

Table 1-2 *Silver chalcogenide clusters*

Silver sulphur clusters	**Silver selenium clusters with SeR ligands**	**Silver selenium clusters with SR**
$[\mathrm{Ag_6(SC_6H_4CN)_6(PPh_3)_6}]$[80]	$[\mathrm{Ag_{14}Se(SePh)_{12}(PR_3)_8}]$[81]	$[\mathrm{Ag_{40}Se_4(SC_6H_4OSiMe_3)_{32}(PPh_3)_8}]$[80]
$[\mathrm{Ag_6(SC_6H_4NO_2)_6(PPh_3)_6}]$[80]	$[\mathrm{Ag_4(Se\mathit{i}Pr)_4(dppm)_2}]$[82]	$[\mathrm{Ag_{76}Se_{13}(SC_6H_4NMe_2)_{50}(PPh_3)_{6.5}}]$[83]
$[\mathrm{Ag_8(SC_6H_4OH)_6(PEt_3)_8}](\mathrm{OAc})_2$[80]	$[\mathrm{Ag_8(SeEt)_8(dppp)}]_\infty$[82]	$[\mathrm{Ag_{88}Se_{12}(SC_6H_4NMe_2)_{63}(PPh_3)_6}]$[83]
$[\mathrm{Ag_{14}S(SC_6H_4CN)_{12}(PPh_3)_8}]$[80]	$[\mathrm{Ag_{28}Se_6(Se\mathit{n}Bu)_{16}(dppp)_4}]$[82]	
$[\mathrm{Ag_{14}S(SC_6H_4NCS)_{12}(PPh_3)_8}]$[80]	$[\mathrm{Ag_{124}Se_{57}(SeP\mathit{t}Bu_2)_4Cl_6(\mathit{t}Bu_2P(CH_2)_3P\mathit{t}Bu_2)_{12}}]$[82]	
$[\mathrm{Ag_7(SPh)_7(dppm)_3}]_\infty$[84]	$[\mathrm{Ag_{30}Se_8(Se\mathit{t}Bu)_{14}(P\mathit{n}Pr_3)_8}]$[85]	
$[\mathrm{Ag_{22}(SPh)_{10}Cl(O_2CPh)_{11}(DMF)_3}]$[68]	$[\mathrm{Ag_{30}Se_8(Se\mathit{t}Bu)_{14}(P\mathit{n}Pr_3)_8}]$[85]	
$[\mathrm{Ag_{65}S_{13}(SC_6H_4NMe_2)_{28}(dppm)_5}]$[83]	$[\mathrm{Ag_{112}Se_{32}(Se\mathit{n}Bu)_{48}(P\mathit{t}Bu_3)_{12}}]$[85]	
$(\mathrm{HNEt_3})_4[\mathrm{Ag_{50}S_7(SC_6H_4\mathit{t}Bu)_{40}}]$[86]	$[\mathrm{Ag_{114}Se_{34}(Se\mathit{n}Bu)_{46}(P\mathit{t}Bu_3)_{14}}]$[85]	
$[\mathrm{Ag_{14}S(SPh)_{12}(PPh_3)_8}]$[87]	$[\mathrm{Ag_{172}Se_{40}(Se\mathit{n}Bu)_{92}(dppp)_4}]$[85]	
$[\mathrm{Ag_{70}S_{16}(SPh)_{34}(O_2CPh)_4(triphos)_4}]$[73]		
$[\mathrm{Ag_{188}S_{94}(P\mathit{n}Pr_3)_{20}}]$[73]		
$[\mathrm{Ag_{70}S_{20}(SPh)_{28}(dppm)_{10}}](\mathrm{O_2CCF_3})_2$[74]		
$[\mathrm{Ag_{262}S_{100}(S\mathit{t}Bu)_{62}(dppb)_6}]$[74]		
$[\mathrm{Ag_{123}S_{35}(S\mathit{t}Bu)_{50}}]$[75]		
$[\mathrm{Ag_{344}S_{124}(S\mathit{t}Bu)_{96}}]$[75]		
$[\mathrm{Ag_{320}S_{130}(StBu)_{60}(dppp)_{12}}]$[76]		
$[\mathrm{Ag_{352}S_{128}(S\mathit{t}C_5H_{11})_{96}}]$[76]		
$[\mathrm{Ag_{490}S_{188}(S\mathit{t}C_5H_{11})_{114}}]$[76]		
$[\mathrm{Ag_{115}S_{34}(SCH_2C_6H_4\mathit{t}Bu)_{47}(dpph)_6}]$[78]		
$[\mathrm{Ag_{58}S_{13}(SAd)_{32}}]$[77]		
$[\mathrm{Ag_{94}S_{34}(SAd)_{26}(dpppt)_6}]$[77]		
$[\mathrm{Ag_{190}S_{58}(SCH_2Fur)_{74}(dpppt)_8}]$[77]		

Compared with Cu/Se clusters, there are only a few reports concerning Ag/Se clusters. The largest published Ag/Se cluster is [$Ag_{172}Se_{40}$(Se*n*Bu)$_{92}$(dppp)$_4$],[85] (dppp = 1,3-bis(diphenylphosphino)propane) whose structure can be described as a cut-out of the body centred cubic bulk Ag_2Se.[88] In the structure of [$Ag_{124}Se_{57}$(SeP*t*Bu$_2$)$_4$Cl$_6$(*t*Bu$_2$P(CH$_2$)$_3$P*t*Bu$_2$)$_{12}$][82] there is a central distorted Frank-Kasper polyhedron consisting of 16 selenium atoms. The surrounding shell composed of 44 Se^{2-} and four SeP*t*Bu$_2^-$ forms a distorted deltahedron. [$Ag_{88}Se_{12}(SC_6H_4NMe_2)_{63}(PPh_3)_6$][83] displays a layer-like structure whose twelve selenium atoms make up a slightly bent 3×4 hexagonal layer surrounded by 63 thiolate ligands. Further examples of silver chalcogenide clusters have been collected and classified in **Table 1-3**.

2 Aim of the project

During the past decades, a great variety of compounds have been published to explore the growing pathway from small molecules *via* clusters to binary bulk materials like Ag_2E and Cu_2E (E = S, Se). An important question is the relation between size-dependence and structural and physical properties step by step through this progress. The most important task of this thesis is expanding the richness of coinage metal chalcogenide clusters based on previous work. The thesis can be divided into three parts:

(1) Synthesis of small Cu/S binary clusters without introducing silylated chalcogenide and the investigation of their optical properties;

(2) Synthesis of Cu/Mo/S heterometallic clusters;

(3) Synthesis of smaller or larger Cu/E and Ag/E clusters with the help of silylated chalcogenide $E(SiMe_3)_2$ and exploring the relationship between the obtained structures and that of bulk materials.

3 Results and discussion

This chapter contains the synthesis and structural characterisation of about 50 new compounds. Due to the complexity of some of these compounds, a very detailed discussion of the molecular structures would exceed the scope of this work. Therefore, only the essential structural features will be discussed.

In the figures, the following colour code of the elements is used: Copper: blue, silver: purple, sulphur in thiolate SR^{-}: yellow, sulphur as S^{2-}: orange, selenium: red, phosphorus: green, carbon: grey.

3.1 Reactions of copper thiolates with phosphines

The reactions of different copper(I) thiolates such as CuSCy (Cy = cyclohexyl), CuSCp (Cp = cyclopentyl), CuSPh (Ph = phenyl) CuSAd (Ad = adamantly) and Cu(Strimethyl-benzyl) (Strimethyl-benzyl = (2,4,6-trimethyl)benzylthiol) with various phosphine ligands result in the formation of a series of low nuclear copper complexes. The abbreviation of the used phosphine ligands are written in the attachment. Metal-rich clusters are synthesized directly from the reaction of copper thiolates, phosphines and silylated chalcogenides. In all isolated compounds the formal oxidation state of copper remains +1 (d^{10} configuration).

3.1.1 Synthesis of copper clusters starting from CuSCy

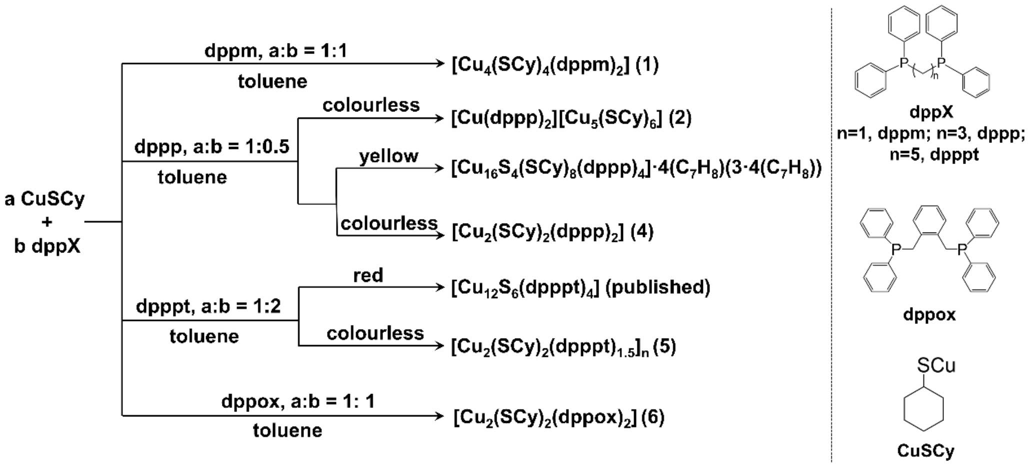

Scheme 3-1 *Synthesis of copper compounds starting from CuSCy.*

Using CuSCy yields to the formation of different compounds. Generally, all of the solid starting materials are dissolved in toluene by stirring at 80°C or room temperature. If the resulting solution is not clear, it is filtered. Crystals can either be yielded directly from to mother solution or by layering with a non-polar solvent.

Compound **1** is a tetranuclear complex whose core consists of a twisted eight-membered ring. Changing dppm by dppp yields the ionic compound **2** with a $[Cu_5(SCy)_6]^-$ anion or the mixture of **3** and **4**. Actually, the first time this reaction was conducted, the mixture **3** and **4** were obtained. However, when this reaction was repeated, compound **2** isolated. This phenomenon might be caused by the reagent $[CuSCy]_n$. For every time this reagent was obtained, the value *n* is different. This might lead to different structures.

Replacing dppp with dpppt results in the formation of two compounds. The red one is the published $[Cu_{12}S_6(dpppt)_4]$[39] and the yellow polymer is compound **5.** Using the bulky dppox (dppox = 1,2-bis(diphenylphosphinomethyl)benzene) as ligand, the binuclear **6** is obtained. More synthetic details have been mentioned in the experimental section.

3.1.1.1 $[Cu_4(SCy)_4(dppm)_2]$ (1)

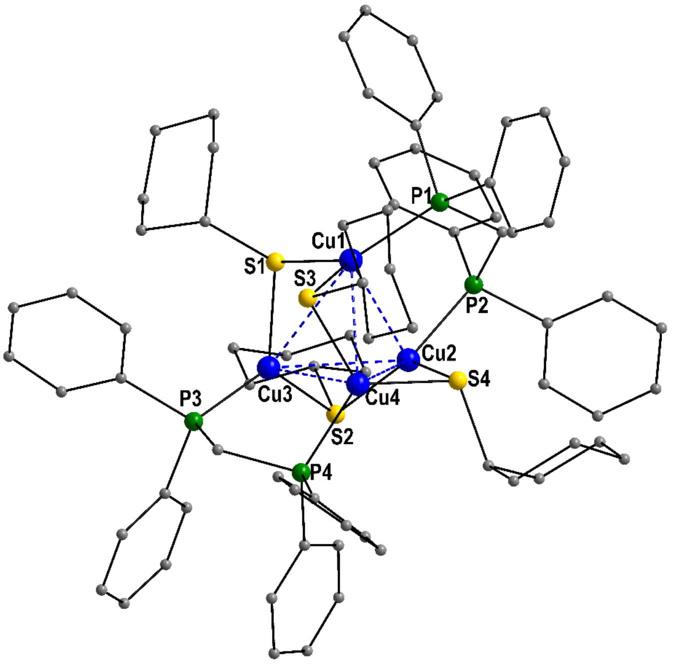

Figure 3-1 *Molecular structure of* ***1*** *in the solid state (H atoms omitted).*

Compound **1** crystallizes in the triclinic space group $P\bar{1}$ with two molecules per unit cell. The core of this structure consists of four sulphur atoms and four copper atoms, forming a twisted eight-membered ring. The four copper atoms build a distorted tetrahedron with non-bonding Cu···Cu distances from 2.763(4) Å to 3.013(4) Å. Four of the six edges of this tetrahedron are bridged by thiolate groups and the other two are bridged by dppm ligands. All copper atoms are distorted trigonal planar coordinated by two sulphur and one phosphorus atom with Cu–S bond length of 2.214(2) Å to 2.311(2) Å. The bond lengths of Cu–P range from 2.223(4) Å to 2.271(2) Å, which are in the expected range.

3.1.1.2 [Cu(dppp)$_2$][Cu$_5$(SCy)$_6$] (2)

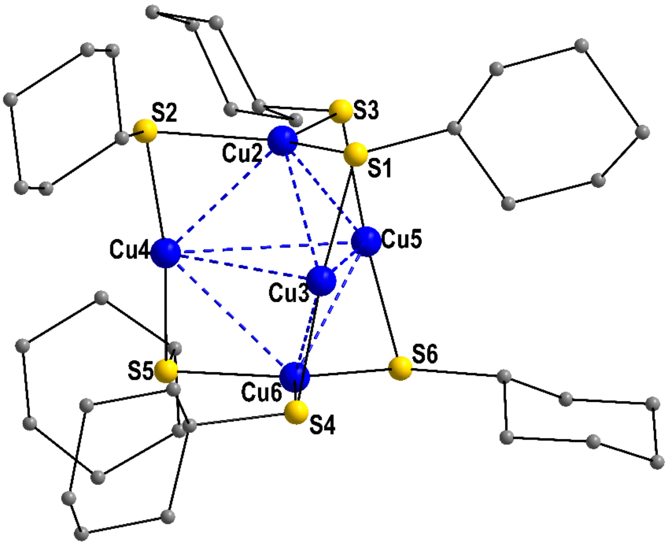

Figure 3-2 *Molecular structure of the [Cu$_5$(SCy)$_6$]$^-$ anion in* ***2*** *in the solid state (H atoms omitted).*

Compound **2** crystallizes in the triclinic space group $P\bar{1}$ with two formula units per unit cell. This compound shows an uncommon ionic structure with a [Cu$_5$(SCy)$_6$]$^-$ anion and a [Cu(dppp)$_2$]$^+$ cation. As shown in **Figure 3-2**, the five copper atoms in the anion form a distorted trigonal bipyramid in which Cu2 and Cu6 occupy the apexes and the other three copper atoms (Cu3, Cu4 and Cu5) are located on the equatorial positions. As a result of the d^{10} configuration of all copper atoms there are no bonding Cu···Cu interactions though the Cu···Cu distance vary 2.704(4) Å to 2.918(9) Å

The Cu_5 bipyramid is encapsulated into a distorted trigonal prism built by six sulphur atoms. Cu2 and Cu6 are located close to the centre of the two triangular faces built by S1, S2, S3 and S4, S5, S6, respectively. Cu3, Cu4 and Cu5 are linearly coordinated occupying the three edges of the S_6 prism. The bond lengths of Cu–S in this anion vary from 2.153(3) Å to 2.268(9) Å.

The structure of the $[Cu_5L_6]^-$ anion belongs to a known structure type, which has been widely reported during the past years. Zang et al. published a chiral structure $[K(CH_3OH)_2(18\text{-crown-6})][Cu_5(S\textit{t}Bu)_6]$.[89] Six sulphur atoms from thiolate groups locate on the vertex of a trigonal prism, where two of five copper atoms states on the central top and bottom of the triangular faces and the other three copper atoms at the middle point of side edges. In contrast to the structure of **2** this anion is less distorted, possessing D_3 symmetry with a C_3 axis through the centre of the prism. Another example are the anions in $Na[Cu_5(L)_3]$ (L = pyridine-2,6-dimethanethiolate (L1); 4-methylpyridine-2,6-dimethanethiolate (L2)).[90]

3.1.1.3 $[Cu_{16}S_4(SCy)_8(dppp)_4]\cdot 4(C_7H_8)$ ($3\cdot 4(C_7H_8)$)

Compound **3** crystallizes in the triclinic space group $P\overline{1}$ with two molecules per unit cell. The neutral **3** consists of sixteen Cu^+ ions, four S^{2-} ions, eight thiolate groups and four dppp ligands. The structure of **3** can be described as ten connected rings. Seen from **Figure 3-3(a)**, the left and right sides of this molecule consist of six eight membered rings (right: S4–Cu3–S2–Cu1–S1–Cu2–S9–Cu5–S4, S1–Cu1–S2–Cu3–S10–Cu4–S3–Cu2–S1, S9–Cu5–S4–Cu3–S10–Cu4–S3–Cu2–S9; left: S11–Cu8–S6–Cu10–S7–Cu12–S8–Cu11–S11, S8-Cu12-S7-Cu10-S12-Cu9-S5-Cu11, S12–Cu10–S6–Cu8–S11–Cu11–S5–Cu9–S12;). The top and bottom are built up by two eight-membered rings (bottom: Cu14–S11–Cu11–S5–Cu13–S9–Cu2–S3; top: S6–Cu10–S12–Cu16–S4–Cu3–S10–Cu15), which are divided into two six-membered rings *via* the connection of S–Cu–S, respectively.

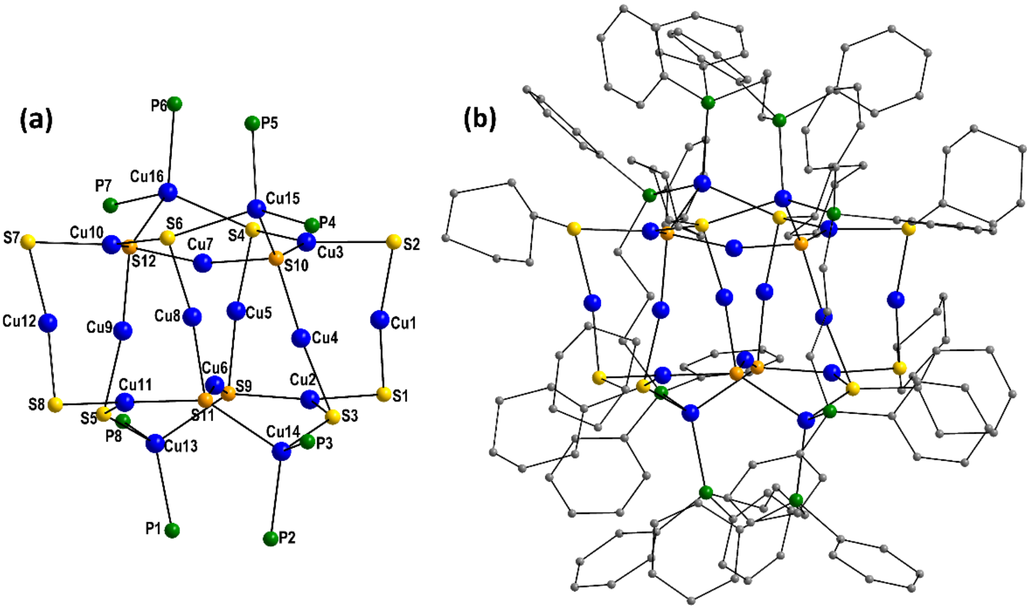

Figure 3-3 (a) *Structure of the heavy atoms core of compound **3** in the solid state; **(b)** molecular structure of **3** in the solid state in the same orientation as in **(a)** (H atoms omitted).*

Copper atoms are found in different coordination modes. Four copper atoms (Cu13, Cu14, Cu15, Cu16) are tetrahedrally coordinated by two phosphorus atoms, one S^{2-} ion and the sulphur atom of one thiolate group. Cu13 and Cu14, Cu14 and Cu15, Cu15 and Cu16, Cu16 and Cu13 are bridged by the bidentate phosphine ligands dppp, respectively (**Figure 3-3(b)**). Four copper atoms (Cu2, Cu3, Cu10, Cu11) triangularly coordinate with three sulphur atoms, one is a S^{2-} ion, the other are sulphur atoms of two thiolate groups. Cu4, Cu5, Cu8, Cu9 coordinate with one S^{2-} ion and one sulphur atom of a thiolate group. Besides, Cu1 and Cu12 coordinate with two sulphur atoms from thiolate groups.

All S^{2-} ions (S9, S10, S11, S12) present distorted tetrahedral geometry, bridging four copper atoms. Three sulphur atoms from thiolate groups (S3, S4, S5, S6) act as μ_3 bridges, the remaining four sulphur atoms (S1, S2, S7, S8) show μ_2 bridging mode. The bond lengths of Cu–S range from 2.146(3) Å to 2.430(2) Å. The Cu···Cu distances vary from 2.644(6) Å to 3.058(8) Å.

3.1.1.4 [$Cu_2(SCy)_2(dppp)_2$] (4)

Compound **4** crystallizes in the triclinic space group $P\bar{1}$ with one molecule per unit cell. There is an inversion centre located on the intersection of Cu1···Cu1' and S1···S1'. The two copper atoms tetrahedrally coordinate with two sulphur atoms and two phosphorus atoms. The μ_2-sulphur atoms bridge the two copper atoms and the copper atoms are chelated by dppp ligands. The bond lengths of Cu–S range from 2.354(4) Å to 2.391(1) Å.

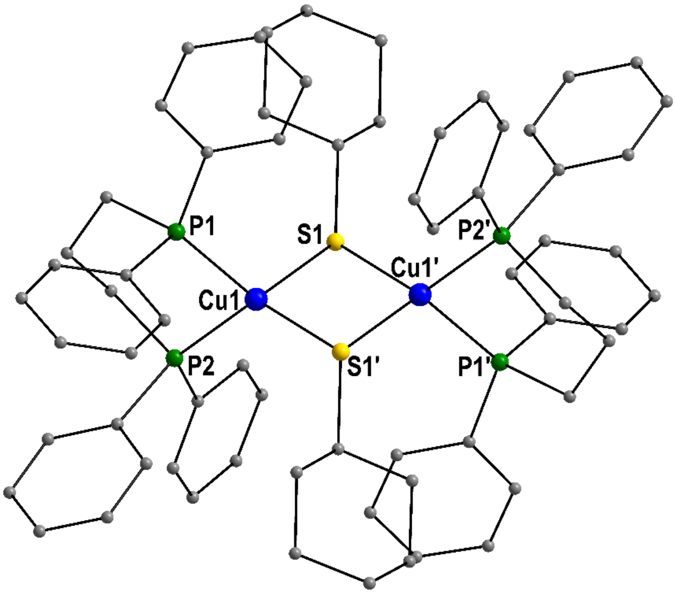

***Figure 3-4** Molecular structure of **4** in the solid state (H atoms omitted).*

3.1.1.5 [$Cu_2(SCy)_2(dpppt)_{1.5}$]$_n$ (5)

Compound **5** crystallizes in the monoclinic space group *C*2/*c* with eight formula units per unit cell. The asymmetric unit contains two copper atoms, two thiolate groups and 1.5 phosphine ligands. Cu1 and Cu2 are bridged by thiolates, forming a nearly planar Cu_2S_2 ring. The deviation from Cu1, Cu2, S1 and S2 to the mean plane is 0.029, 0.024, 0.104 and 0.069 Å, respectively. Cu1 and Cu2 present different coordination modes. Cu1 is trigonal planar coordinated by two sulphur atoms and one phosphorus atom (P1). Cu2 tetrahedrally coordinates with two sulphur atoms and two phosphorus atoms (P2 and P3). The Cu–S bond lengths ranges from 2.277(8) Å to 2.299(10) Å. The Cu1···Cu2 distance is 2.820(10) Å.

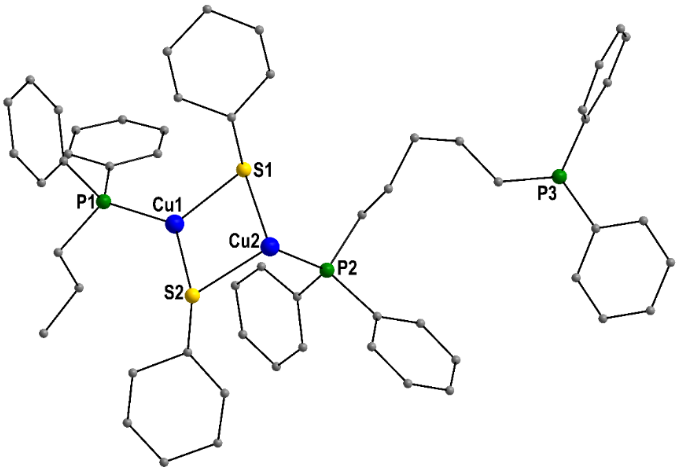

Figure 3-5 *Molecular structure of the asymmetric unit of* ***5*** *in the solid state (H atoms omitted).*

The $[Cu_2(SCy)_2]$ groups are linked by phosphine ligands forming a double chain one-dimensional band structure. **5** can be described as two parallel chains with the dpppt ligands (P2 and P3) within the chain and a further dpppt ligand (P1 and P1') connecting the chains. There is a two-fold axis through the carbon atom C27.

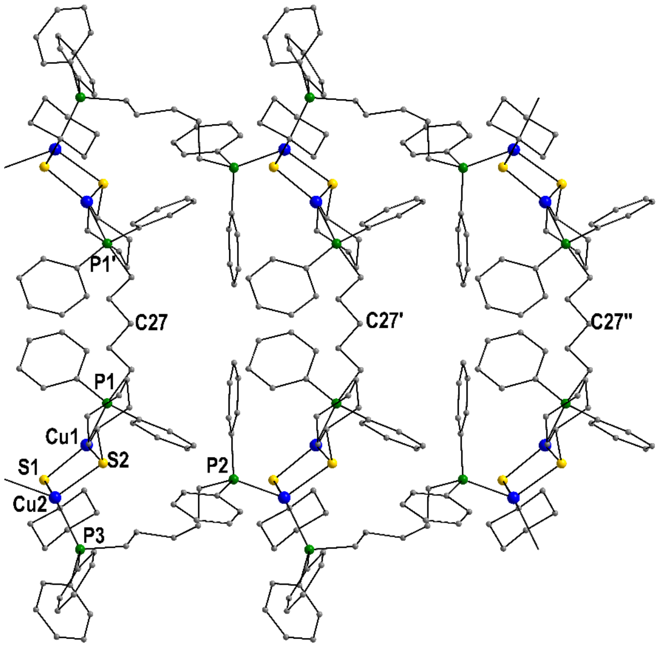

Figure 3-6 *Molecular structure of the polymeric chains in* ***5*** *in the solid state (H atoms omitted).*

3.1.1.6 [$Cu_2(SCy)_2(dppox)_2$] (6)

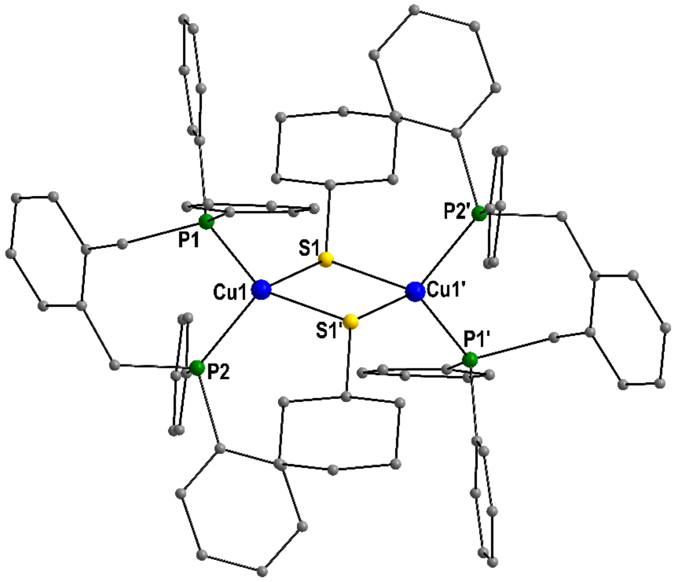

Figure 3-7 *Molecular structure of* ***6*** *in the solid state (H atoms omitted).*

Compound **6** crystallizes in the triclinic space group $P\bar{1}$ with one molecule per unit cell. The two copper atoms in the planar Cu_2S_2 ring are distorted tetrahedrally coordinated by two sulphur atoms (Cu–S: 2.333(5) Å to 2.354(4) Å) and two phosphorus atoms (average Cu–P bond lengths: 2.271(2) Å). *Trans*- and *cis*- arrangement of the bridging thiolate ligands are two typical geometries in binuclear copper complexes. In **6** the thiolate groups are in *trans*-arrangement.

An example for *cis*-orientation is [(dppe)Cu(μ_2-S-tucHcet)$_2$Cu(dppe)][54] (tucHcet = ethyl 2-thiouracil-5-carboxylate; dppe = 1,2-bis(diphenylphosphino)ethane).

3.1.2 Synthesis of copper clusters starting from CuSCp

In analogy to the compounds described above, a mixture of the starting materials CuSCp and phosphine is suspended in toluene, stirred at 80°C for at least 3 hours and then kept at 40°C overnight. On the next day, the suspension is filtered, and the solution is layered by non-polar solvent. Seen from **Scheme 3-2**, phosphines with different steric demand are used yielding compounds with structural diversity.

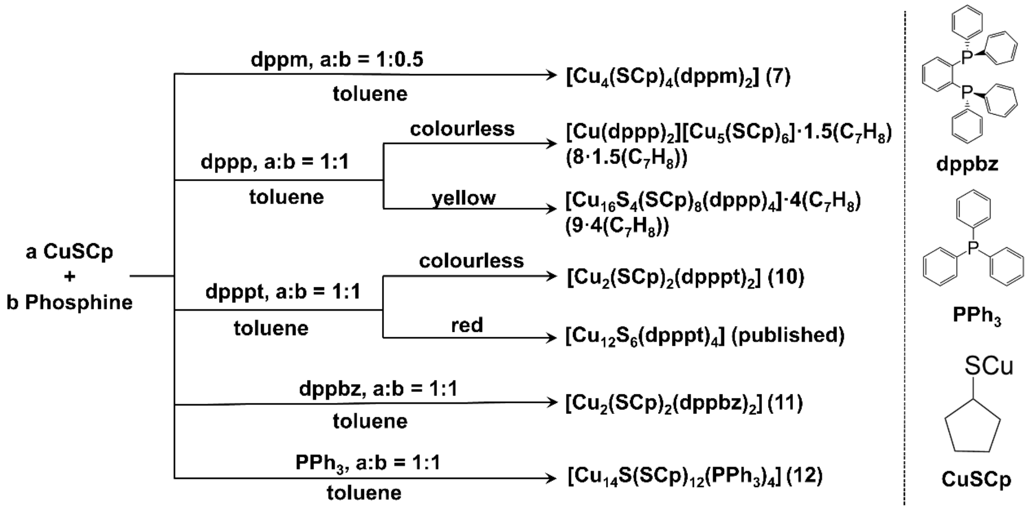

Scheme 3-2 *Synthesis of copper compounds starting from CuSCp.*

Compound **7** is a tetra-nuclear complex, with a Cu_4S_4 core in a chair-like eight-membered ring. Compound **8** and **9** co-crystallized from the same reaction. The anion in **8** is $[Cu_5(SCp)_6]^-$, which is similar to the structure of **2**. The $Cu_{16}S_{12}$ unit of compound **9** can be seen as the polyhedral configuration consisting of ten irregular eight-membered rings. Compound **10** and the published compounds $[Cu_{12}S_6(dpppt)_4]$ crystallized successively from the same reaction. Firstly, $[Cu_{12}S_6(dpppt)_4]$ isolated. Several days later, blossoms of compound **10** were observed on the inner tube of the Schlenks. Compounds **10** and **11** are two binuclear complexes, whose thiolate ligands are found in *trans*-orientation. **12** is a spherical cluster containing 14 copper atoms. More synthetic details have been mentioned in the experimental section.

3.1.2.1 [Cu4(SCp)4(dppm)2] (7)

Compound **7** crystallizes in the triclinic space group $P\overline{1}$ with one molecule per unit cell. The asymmetric unit contains two copper atoms, two thiolate ligands and one dppm ligand, so that the structure of **7** is combined by two asymmetric units *via* an inversion centre. The central Cu_4S_2 unit (Cu1, Cu2, S2 and symm. equivalents) is planar with S1 and S1’ above and below this plane. All copper atoms are distorted trigonal planar coordinated by two sulphur and one phosphorus atom. The Cu–S bond lengths are 2.212(2) Å to

2.276(7) Å. The shortest distance between copper atoms is 2.864(4) Å.

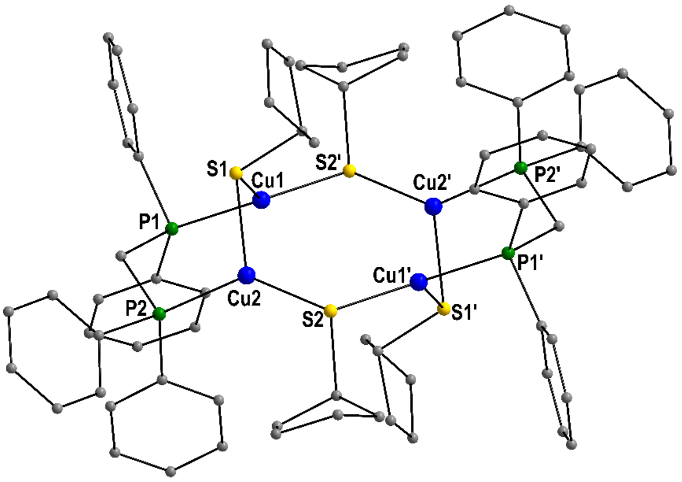

Figure 3-8 *Molecular structure of compound **7** in the solid state (H atoms omitted).*

3.1.2.2 [Cu(dppp)$_2$][Cu$_5$(SCp)$_6$]·1.5(C$_7$H$_8$) (8·1.5(C$_7$H$_8$))

Compound **8** crystallizes in the triclinic space group of $P\bar{1}$ with four formula units per unit cell. **8** is an ionic compound consisting of [Cu(dppp)$_2$]$^+$ cations and [Cu$_5$(SCp)$_6$]$^-$ anions. This structure is very similar to the previously described compound **2**. In the cations (**Figure 3-9(a)** and **(c)**) there are tetrahedrally coordinated Cu1 and Cu2 which are chelated by two dppp ligands. The Cu–P bond lengths range from 2.291(5) Å to 2.318(9) Å. In the [Cu$_5$(SCp)$_6$]$^-$ anions (**Figure 3-9(b)** and **(d)**) the five copper atoms are arranged in a distorted trigonal bipyramid in which Cu3 (Cu12) and Cu7 (Cu8) occupy the apexes and Cu4, Cu5 and Cu6 (Cu9, Cu10 and Cu11) are located at the equatorial positions. As in the structure of **2** the Cu$_5$ bipyramid is inserted into a distorted trigonal prism built from six sulphur atoms. Cu3 (Cu7) and Cu8 (Cu12) occupy the centre of the two trigonal faces and Cu4, Cu5 and Cu6 (Cu9, Cu10 and Cu11) stay on the edges of the prism. As expected, the Cu···Cu distance vary from 2.698 Å to 2.864 Å; Cu–S distances are from 2.149(1) Å to 2.266(7) Å.

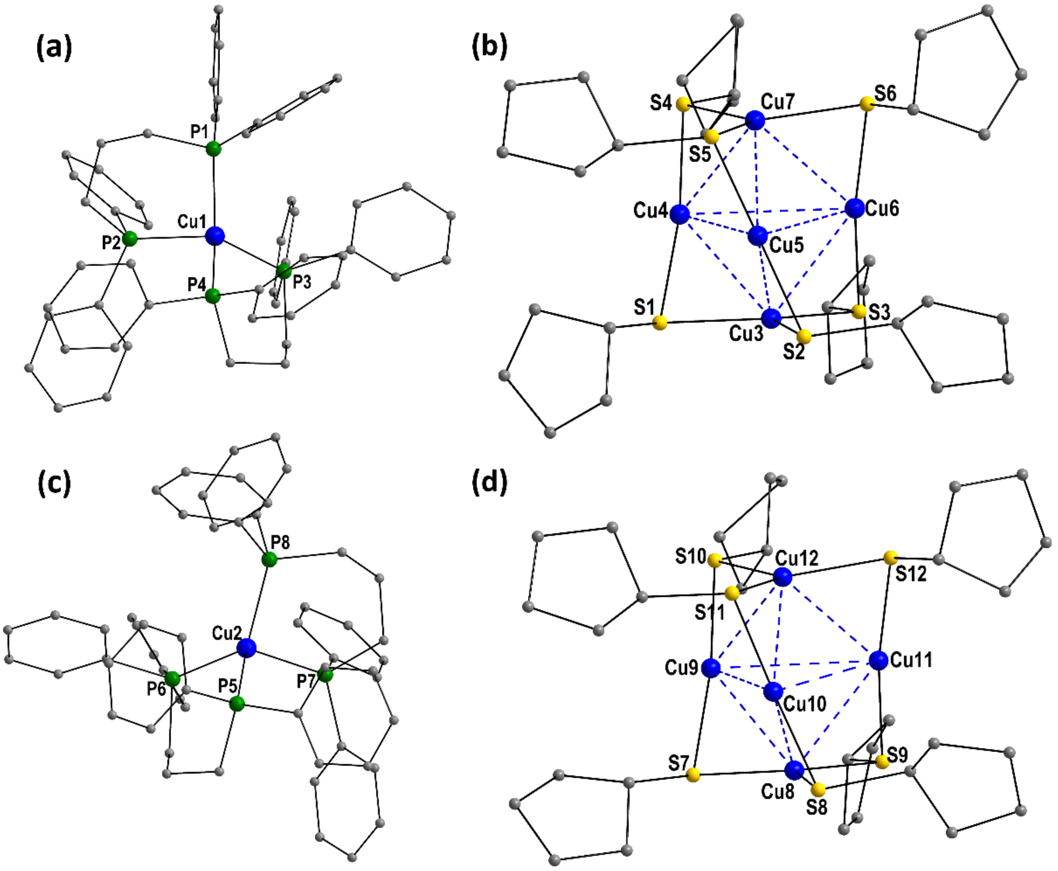

Figure 3-9 *Molecular structures of* ***(a)*** *cation* ***A*** *in* ***8****;* ***(b)*** *anion* ***A*** *in* ***8****;* ***(c)*** *cation* ***B*** *in* ***8****;* ***(d)*** *anion* ***B*** *in* ***8*** *in the solid state (H atoms omitted).*

3.1.2.3 $[Cu_{16}S_4(SCp)_8(dppp)_4]\cdot4(C_7H_8)$ ($9\cdot4(C_7H_8)$)

Compound **9** crystallizes in triclinic space group $P\bar{1}$ with two molecules per unit cell. **9** is analogous with **3**. In **9** there are eight SCp^- groups whereas in **3** one finds eight SCy^- groups. Despite of that all bonding parameters of the Cu/S/P core are the same within the standard deviation. Therefore, there is no need for a more detailed discussion of this structure.

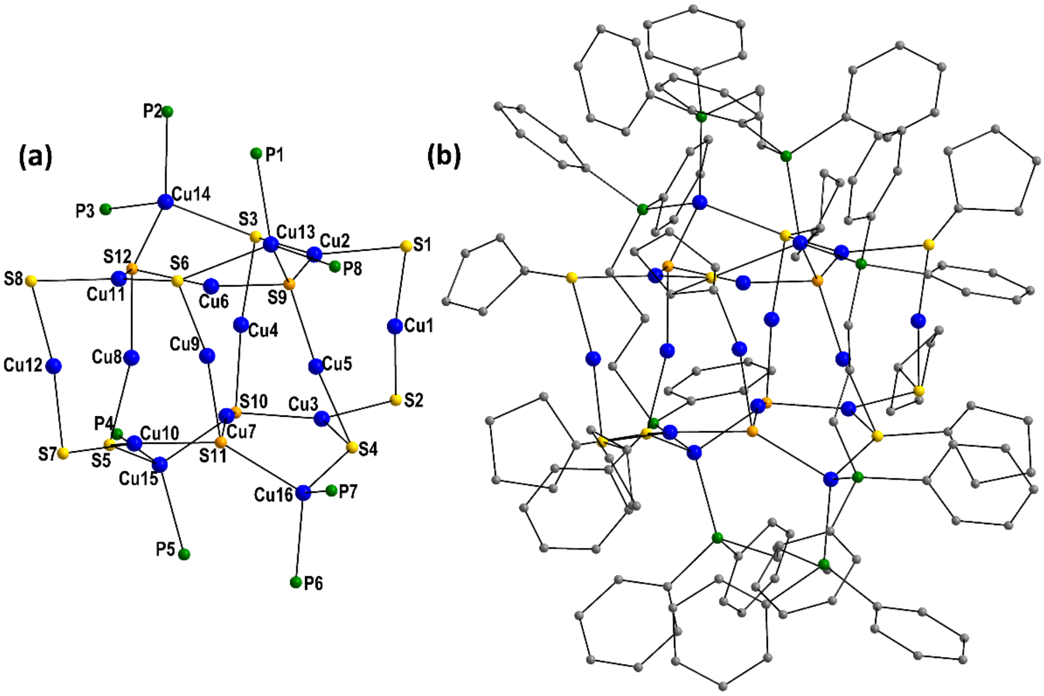

Figure 3-10 (a) *Structure of the heavy atoms core of* ***9*** *in the solid state;* ***(b)*** *molecular structure* ***9*** *in the solid state in the same orientation as in* ***(a)*** *(H atoms omitted).*

3.1.2.4 [$Cu_2(SCp)_2(dpppt)_2$] (10)

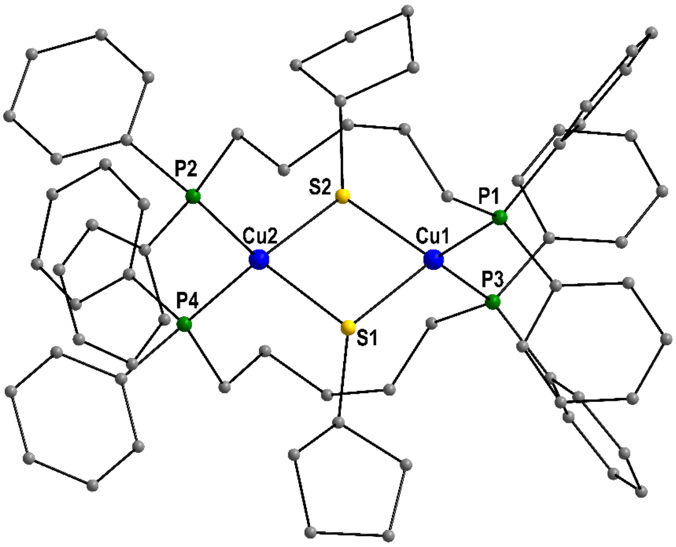

Figure 3-11 *Molecular structure of compound* ***10*** *in the solid state (H atoms omitted).*

Compound **10** crystallizes in the triclinic space group $P\overline{1}$ with two molecules per unit cell. The core of this structure is a nearly planar (torsion angle: 2.37°, 2.32°, 2.34°, 2.34°) Cu_2S_2 four-membered ring in which two thiolate ligands are presented in *trans*-orientation. The two copper atoms are distorted tetrahedrally coordinated by two sulphur atoms and two phosphorus atoms of the dpppt ligands with Cu–S bond lengths from 2.363(3) Å to 2.411(1) Å and Cu–P bond lengths from 2.286(6) Å to 2.290(1) Å.

3.1.2.5 [$Cu_2(SCp)_2(dppbz)_2$] (11)

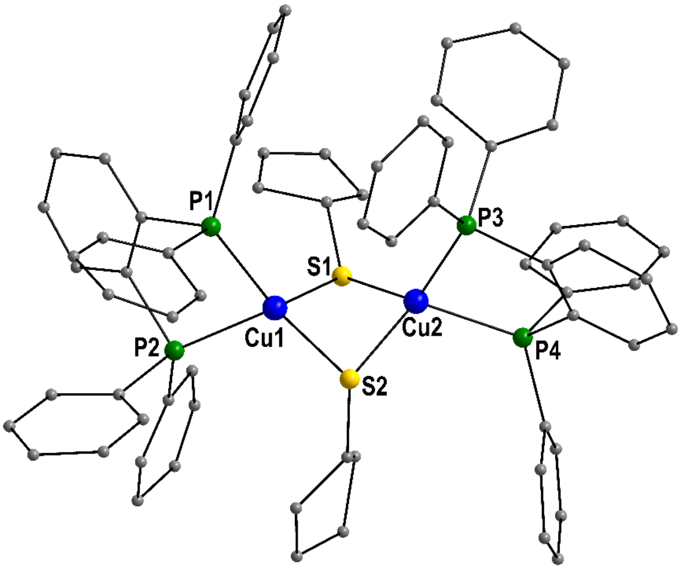

Figure 3-12 *Molecular structure of compound* ***11*** *in the solid state (H atoms omitted).*

Compound **11** crystallizes in the tetragonal space group $I\bar{4}$ with eight molecules per unit cell (**Figure 3-12**). Similar to the above-described binuclear complexes **4** and **6**, the two copper atoms are bridged by two thiolate ligands and furthermore chelated by two phosphorus atoms from the same dppbz (dppbz = 1,2-bis(diphenylphosphino)benzene) ligand, resulting in a distorted tetrahedral coordination. The Cu–S bond lengths vary from 2.335(3) Å to 2.361(3) Å and Cu–P from 2.253(3) Å to 2.306(3) Å. The Cu_2S_2 ring shows a butterfly arrangement (torsion angles: 27.3°, 27.5°, 27.2°, 27.6°) with Cp groups in *trans*-orientation.

3.1.2.6 $[Cu_{14}S(SCp)_{12}(PPh_3)_4]$ (12)

Compound **12** crystallizes in acentric hexagonal space group $P6_3$ with four molecules per unit cell and two crystallographically independent molecules (**A** and **B**). In **A** there is a 3-fold axis through P1, Cu1, S5 and Cu6, in **B** through P3, Cu7, S10 and Cu12. Since the bonding parameters of **A** and **B** are the same within the standard deviation only the structure of molecule **A** will be discussed in more detail.

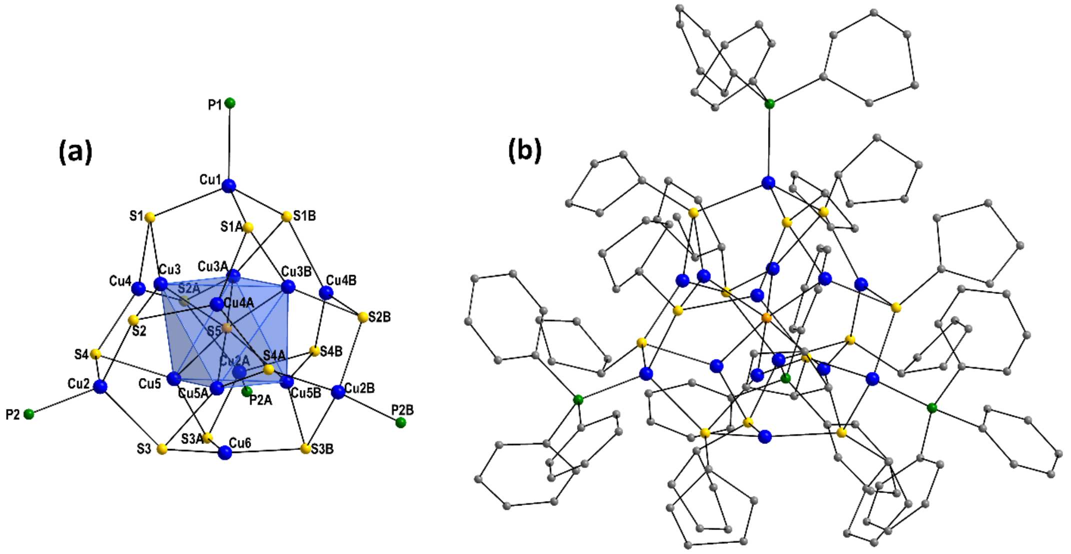

***Figure 3-13 (a)** Structure of the heavy atoms core of cluster **A** in compound **12** in the solid state; **(b)** molecular structure of cluster **A** in compound **12** in the solid state in the same orientation as in **(a)** (H atoms omitted).*

The structure can be derived from a tetrahedron, in which the four corners are occupied by four copper atoms (Cu1 and Cu2 and symm. equiv.) (symm. equiv. = symmetric equivalence). These atoms are tetrahedrally coordinated by phosphorus atoms and the sulphur atoms of three μ_3-SCp$^-$ groups. The faces of the tetrahedron are occupied by four copper atoms (Cu4 and symm. equiv. and Cu6), which are distorted trigonal planar coordinated by three sulphur atoms of SCp$^-$ groups (Cu4 bonds to S1, S2 and S4; Cu6 bonds to S3, S3A and S3B). The remaining six copper atoms (Cu3, Cu5 and symm. equiv.) in the inner part of the cluster form a distorted octahedron (the non-bonding Cu···Cu distances in the octahedron range from 3.103(0) Å to 3.490(0) Å and the distances from the central S5 to the copper atoms of the octahedron are 2.334(5) Å to 2.370(5) Å). Each of the six copper atoms is trigonally coordinated by two SCp⁻ groups and the central μ_6-S5, which is a naked sulphide ion. All other Cu–S bond lengths are in the range from 2.244(5) Å to 2.470(5) Å and Cu···Cu distances range from 2.621(4) Å to 2.671(4) Å.

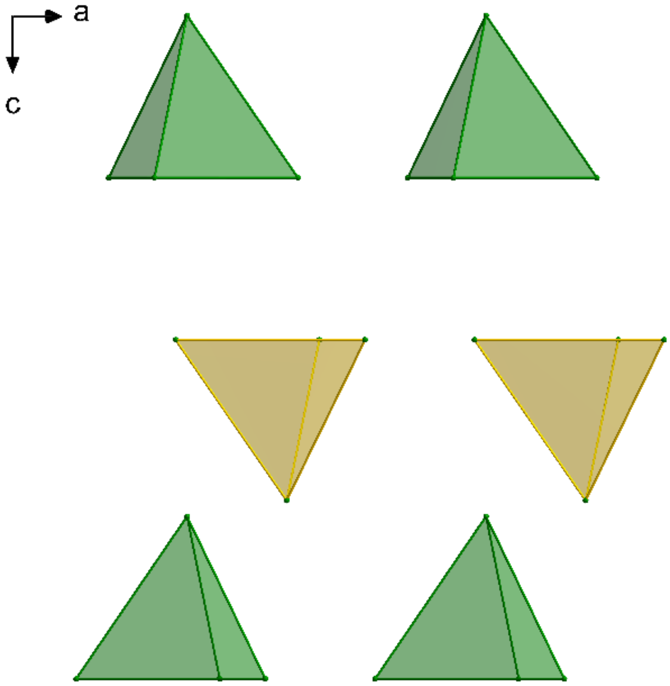

Figure 3-14 *Polyhedron representation of tetrahedral clusters in compound* ***12****, seen from axis b. Green: cluster* ***A****; Yellow: cluster* ***B****.*

Using a tetrahedron representing the packing of **12** (**Figure 3-14**) it can be seen that **A** (green) and **B** (yellow) are organized in opposite orientations alongside the *c* axis.

12 is structurally related to $[Cu_{17}Se(SPh)_{15}(PPh_3)_4]$[91]. Both of them crystallized in the space group $P6_3$. However, there are two differences. First, in **12**, the central chalcogenide atom is sulphur while this atom is replaced by selenium in $[Cu_{17}Se(SPh)_{15}(PPh_3)_4]$. The second difference can be seen on one corner of these two molecules. In **12**, three sulphur atoms (S1) of the top $CuPS_3$ group directly coordinate with the copper atoms of the central octahedron (Cu3, Cu4). In $[Cu_{17}Se(SPh)_{15}(PPh_3)_4]$, three S1 atoms are bridged *via* Cu2. Then Cu2 and Cu3 are linked by S2 atoms. In other words, compared with compound **12**, $[Cu_{17}Se(SPh)_{15}(PPh_3)_4]$ owns three more copper atoms and three more sulphur atoms extending on the top of this cluster.

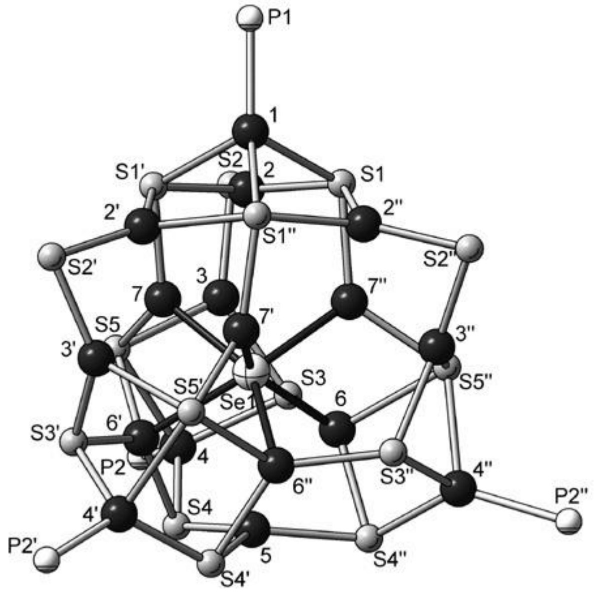

Figure 3-15 *Structure of the heavy atoms core of [$Cu_{17}Se(SPh)_{15}(PPh_3)_4$] in the solid state.*[91]

3.1.3 Synthesis of copper clusters starting from CuSPh

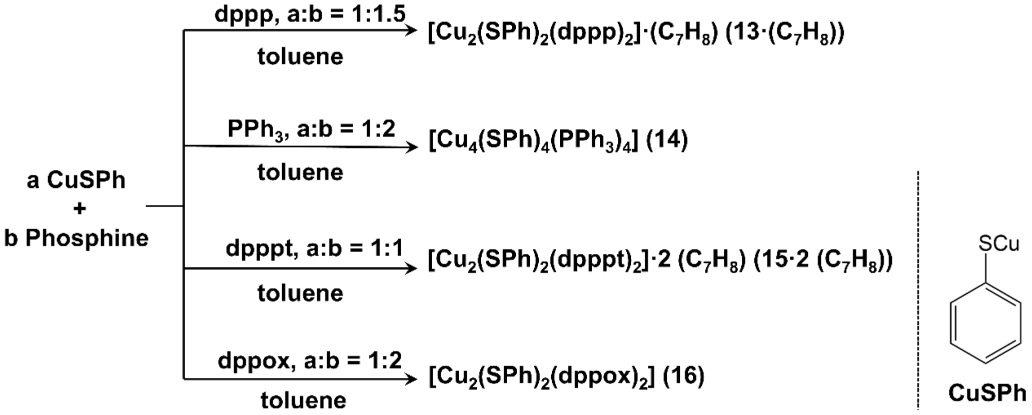

Scheme 3-3 *Synthesis of copper compounds starting from CuSPh.*

The procedures for the synthesis of these four compounds are similar (see **Scheme 3-3**). Mixtures of the starting materials are suspended in toluene and stirred at 80°C for 3 hours; then the reaction mixture is kept at 40°C overnight. On the next day, the suspension is filtered, and the solution is layered by non-polar solvent. Several days later colourless crystals are formed.

Except for tetranuclear compound **14**, the other three are typical binuclear complexes.

More synthetic details have been mentioned in the experimental section.

3.1.3.1 [$Cu_2(SPh)_2(dppp)_2$]·(C_7H_8) (13·(C_7H_8))

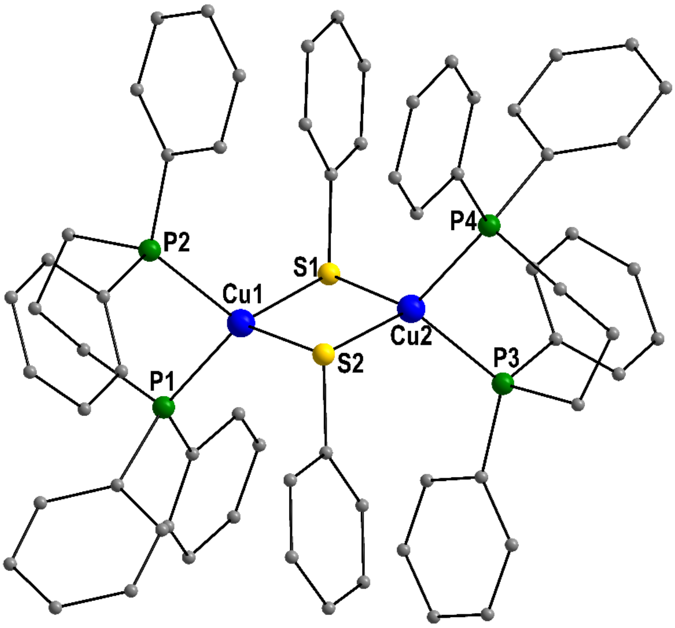

Figure 3-16 *Molecular structure of* ***13*** *in the solid state (H atoms omitted).*

Compound **13** crystallizes in the triclinic space group $P\bar{1}$ with two molecules per unit cell. Similar to compound **5**, compound **13** also has a core of a planar Cu_2S_2 four-membered ring. Cu1 and Cu2 are bridged by two *trans*-oriented thiolate groups and chelated by two phosphorus atoms from dppp ligands, presenting a distorted tetrahedral coordination with bond lengths of Cu1–S1, Cu1–S2, Cu1–P1, Cu1–P2, Cu2–S1, Cu2–S2, Cu2–P3, Cu2–P4 of 2.346(6) Å, 2.407(7) Å, 2.300(10) Å, 2.279(9) Å, 2.384(4) Å, 2.349(9) Å, 2.270(10) Å and 2.307(7) Å, respectively.

3.1.3.2 [$Cu_4(SPh)_4(PPh_3)_4$] (14)

Compound **14** crystallizes in the triclinic space group $P\bar{1}$ with three molecules per unit cell. There are two crystallographically independent molecules in **14**: one is located on an inversion centre (**Figure 3-17(a)**, molecule **A**) and the other - occupying the general position - showing a similar but distorted structure (**Figure 3-17(b)**, molecule **B**).

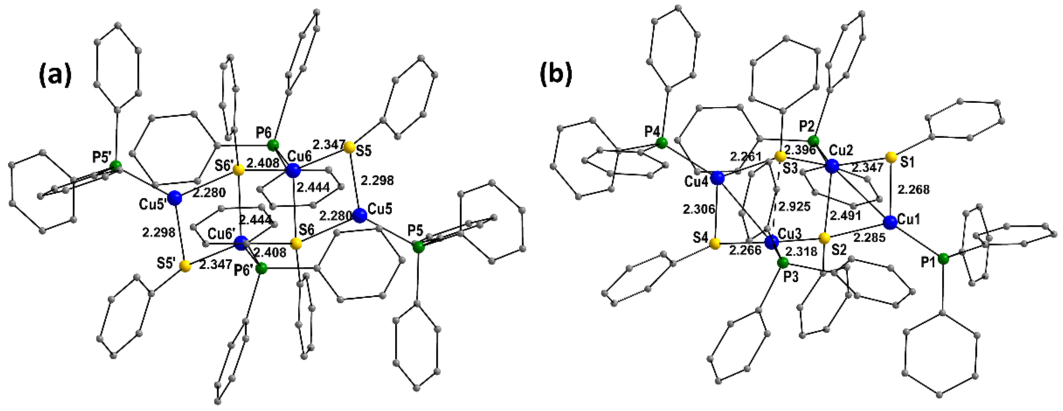

Molecule A **Molecule B**

Figure 3-17 *Two different molecular structures of **14** in the solid state (H atoms omitted).*

Molecule **A** has a core of two connected Cu$_2$S$_2$ rings (Cu5, Cu6, S5, S6 and symm. equiv.), building an approximate chair-conformation. Cu5 and Cu5' triangularly coordinate with two sulphur and one phosphorus atom and Cu6 and Cu6' tetrahedrally bond to three sulphur and one phosphorus. The Cu–S bond lengths in this molecule range from 2.280(1) Å to 2.444(5) Å.

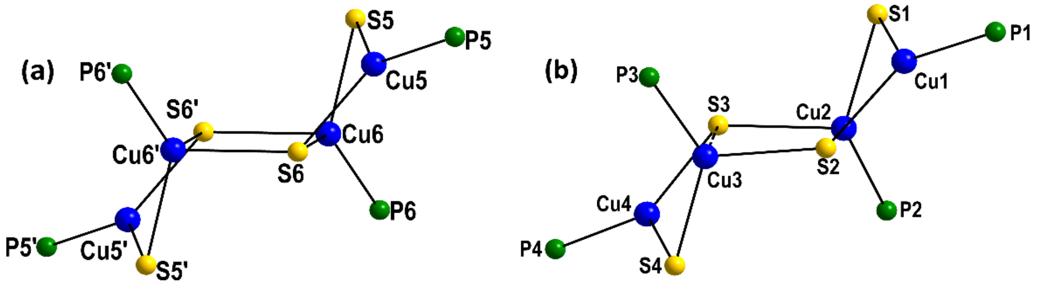

Molecule A **Molecule B**

Figure 3-18 *Chair-like conformation of the heavy atoms core of two molecules in **14** in the solid state.*

Different from molecule **A**, molecule **B** (Cu1–Cu4, S1–S4) is less symmetric. Although similar in most bond lengths, there is one eye-catching difference. In molecule **A** the bond length Cu6–S6 is with 2.444(5) Å in the range of a covalent Cu–S bond whereas in molecule **B** the Cu3–S3 distance (2.925(6) Å) can be described as a very weak Cu–S interaction. This yields in molecule **A** to a tetrahedral coordination of Cu6 and in molecule **B** to a trigonal planar coordination of Cu3. As a consequence the sulphur and phosphorus atoms coordinated to Cu3 show significant shorter bond length compared to Cu6. The other two Cu–S bond lengths in both molecules vary from 2.261(1) Å to 2.491(1) Å.

3.1.3.3 [$Cu_2(SPh)_2(dpppt)_2$]·2(C_7H_8) (15·2(C_7H_8))

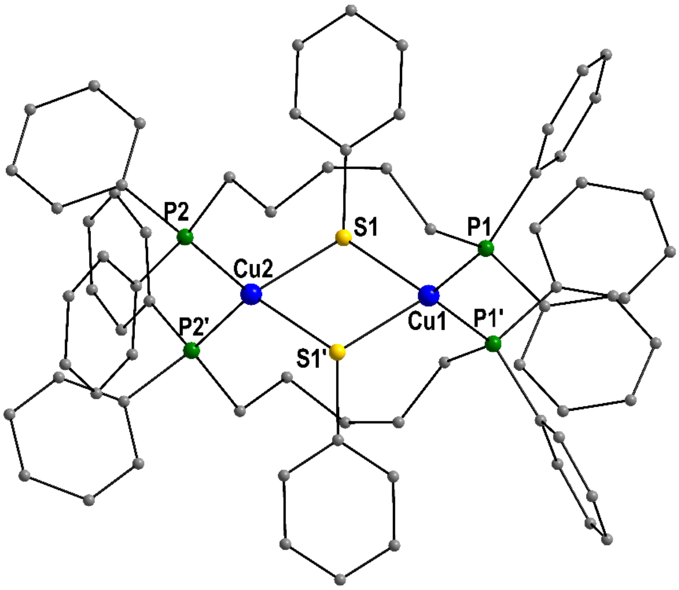

Figure 3-19 *Molecular structure of compound* ***15*** *in the solid state (H atoms omitted).*

Compound **15** crystallizes in the monoclinic space group *C*2/*c* with four molecules per unit cell. There is a 2-fold axis running through the atoms Cu1 and Cu2. The core of this binuclear complex is a planar Cu_2S_2 four-membered ring in which the thiolate groups are in *trans*-conformation. Due to the steric demand of the bulky dpppt ligands one can observe a bridging bonding mode of the phosphine ligands between the two copper atoms. The copper atoms are bridged not only by the thiolate groups but also by the two phosphine ligands, yielding to a distorted tetrahedral coordination mode with average Cu–S bond lengths of 2.393(6) Å and the average Cu–P bond lengths of 2.287(6) Å.

3.1.3.4 [$Cu_2(SPh)_2(dppox)_2$] (16)

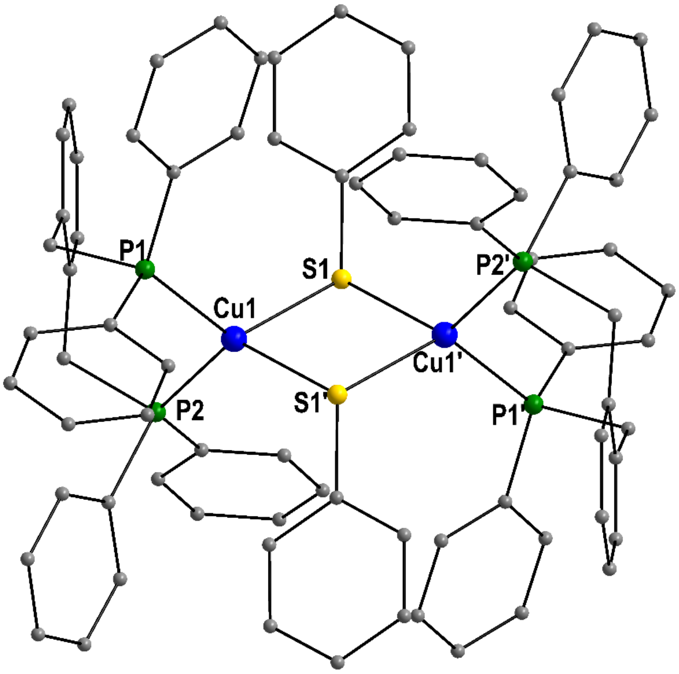

Figure 3-20 *Molecular structure of compound* ***16*** *in the solid state (H atoms omitted).*

Compound **16** crystallizes in the triclinic space group $P\bar{1}$ with one molecule per unit cell. The core of this complex consists of a planar four-membered Cu_2S_2 ring with the thiolate groups in *trans*-orientation. The copper atoms bridged by thiolates are chelated by two phosphorus atoms from the same dppox ligand with the expected Cu–S bond lengths of 2.372(2) Å and 2.364(4) Å and Cu–P distances of 2.271(1) Å to 2.274(5) Å.

3.1.4 Synthesis of copper clusters starting from CuSAd

The result of using CuSAd as starting material is very interesting. Obviously, the structures of the final products are very sensitive to the experimental conditions such as stoichiometric ratio between the starting compounds as well as reaction time. For **17** and **18**, the ratio of the starting compounds and the used phosphine are the same. **17** could be isolated after a few hours' reaction time at 80°C and layering with a non-polar solvent. Whereas **18** was yielded after a significantly longer reaction time (2 days) at 40°C. More synthetic details have been mentioned in the experimental section.

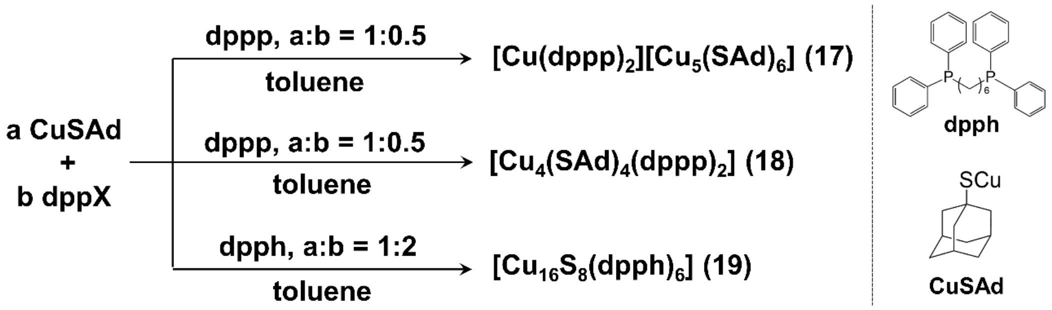

Scheme 3-4 *Synthesis of copper compounds starting from CuSAd.*

3.1.4.1 $[Cu(dppp)_2][Cu_5(SAd)_6]$ (17)

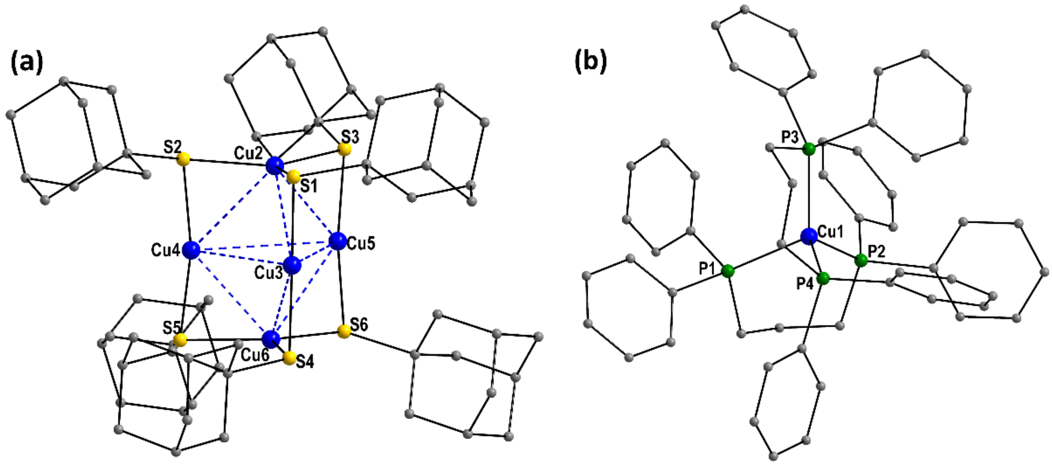

Figure 3-21 (a) *Molecular structure of the $[Cu_5(SAd)_6]^-$ anion in* ***17*** *in the solid state (H atoms omitted);* ***(b)*** *molecular structure of the $[Cu(dppp)_2]^+$ cation in* ***17*** *in the solid state (H atoms omitted).*

Compound **17** crystallizes in triclinic space group $P\overline{1}$ with two formula units per unit cell. The structure is similar to compound **2** and **8**. Also **17** is an ionic compound comprising a $[Cu_5(SAd)_6]^-$ anion and a $[Cu(dppp)_2]^+$ cation. However, due to different thiolates, there are slight deformations of the molecular structures of the pentanuclear anions. In all three cases the anion can be described as a Cu_5 trigonal bipyramid embedded into a distorted S_6 trigonal prism. As expected, the Cu–S bond lengths of the anions are similar. For compound **2**, the Cu–S bond lengths range from 2.153(3) Å to 2.268(9) Å. The Cu–S bond lengths in **17** vary from 2.160(2) Å to 2.262(3) Å. The bond angles of the equatorial copper atoms (Cu3, Cu4 and Cu5) differ from **2** to **17**. In **2**, the range of the bond angles of S–Cu3/Cu5/Cu5–S is 171.2(2)° to

173.0(1)° while this range in compound **17** becomes 164.0(1)° to 168.6(1)°. This might be a result of the bulkier adamantly groups in **17**.

3.1.4.2 [$Cu_4(SAd)_4(dppp)_2$] (18)

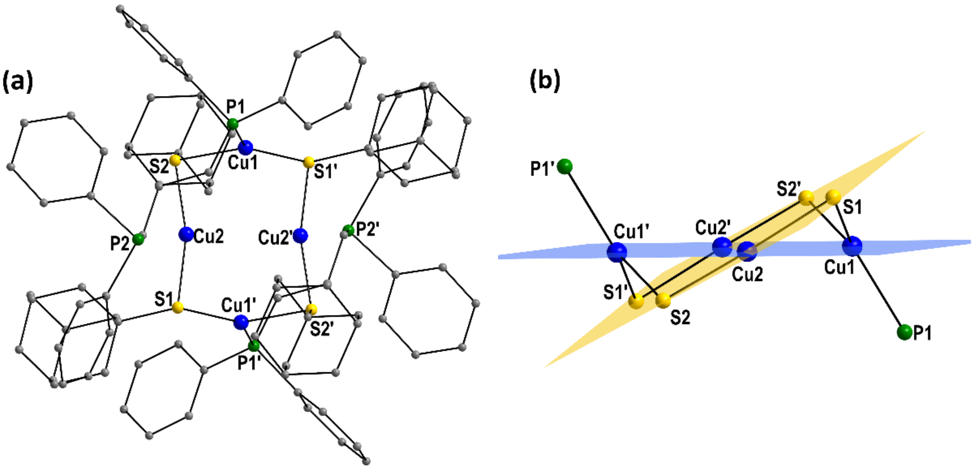

Figure 3-22 (a) *Molecular structure of compound **18** in the solid state (H atoms omitted); **(b)** mean planes of the copper and sulphur atoms in **18** in the solid state, only heavy atoms.*

Compound **18** crystallizes in the triclinic space group $P\bar{1}$ with one molecule per unit cell. Core of this molecule is an eight-membered Cu_4S_4 ring localized on a crystallographic inversion centre. One can construct two mean planes for the copper and sulphur atoms, respectively (**Figure 3-22(b)**). Cu1 and Cu1' are coordinated in a distorted trigonal fashion by S1, S2 and P1, whereas Cu2 and Cu2' are only distorted linearly coordinated by two sulphur atoms (S1 and S2). The different coordination modes can also be seen in the Cu–S distances: for the trigonal planar Cu1 the distances are Cu1–S1 2.239(9) Å and Cu1–S2 2.287(6) Å; for the double coordinated Cu2 the bond lengths are Cu2–S1 2.171(1) Å and Cu2–S2 2.160(1) Å. The Cu1–P1 distance is 2.246(5) Å. All Cu···Cu distances are in the range of 2.995(5) Å to 3.018(8) Å. The longer one is between the distorted linearly coordinated Cu2 and Cu2', which is a hint that there is definitely no attractive Cu···Cu interaction. In contrast to all compounds described previously, the dppp molecule only acts as a monodentate ligand *via* P1, whereas P2 does not coordinate to any metal atom.

3.1.4.3 [$Cu_{16}S_8(dpph)_6$] (19)

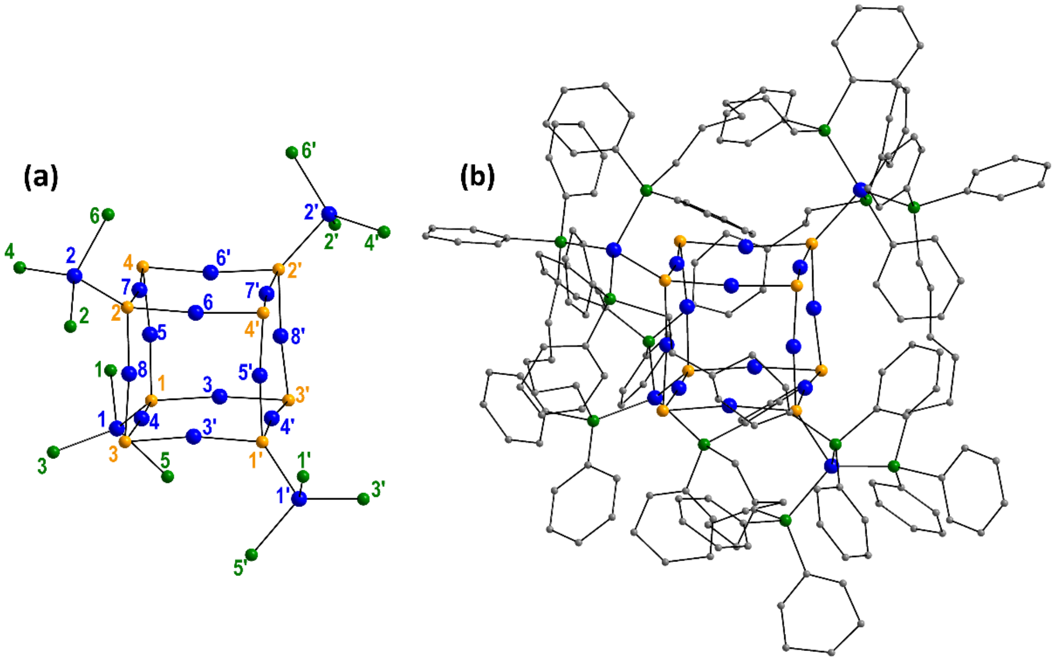

Figure 3-23 (a) *Structure of the heavy atoms core of compound* ***19*** *in the solid state;* ***(b)*** *molecular structure of* ***19*** *in the solid state in the same orientation as in* ***(a)*** *(H atoms omitted).*

Changing the phosphine ligands from dppp to dpph results in the formation of compound **19** in which all adamantly groups are lost due to a cleavage of the S–C bond in the used copper thiolate. Compound **19** crystallizes in the monoclinic acentric space group *C*2 with two molecules per unit cell. There is a two-fold axis running through the molecule. The central building block is a distorted cube built by the eight sulphide ions where all edges are occupied by twelve copper atoms (Cu3–Cu8 and symm. equiv.) in a distorted linear coordination mode. These twelve copper atoms form a distorted cube-octahedron. The bond angles S–Cu–S range from 171.0(1)° to 173.0(1)°. Four (S1, S2 and symm. equiv.) of the eight sulphur-corners act as μ_4 ligands and bind to four CuP_3 groups (Cu1, Cu2 and symm. equiv.) with the tetrahedrally coordinated copper atoms forming a tetrahedron. All edges of this tetrahedron are bridged by the six dpph ligands. The other four sulphur atoms (S3, S4 and symm. equiv.) within the $Cu_{12}S_8$ core act as μ_3 ligands. The Cu–S–Cu bond angles cover a wide range: e.g. for Cu–(μ_3-S3)–Cu the angles are 78.7(8)°, 81.4(5)° and 81.9(10)°; for Cu–(μ_4-S1)–Cu the angles range from 85.4(5)° to 91.0(2)°. As expected, the Cu–S bond lengths depend on the coordination number of the copper atoms. The Cu–S distances for the tetrahedrally coordinated copper atoms Cu1 and Cu2 are 2.381(3) Å and 2.241(1) Å, respectively; the distances for the linearly coordinated copper atoms are shorter and range between 2.141(4) Å and 2.169(4) Å.

3.1.5 Synthesis of copper clusters starting from Cu(Strimethyl-benzyl)

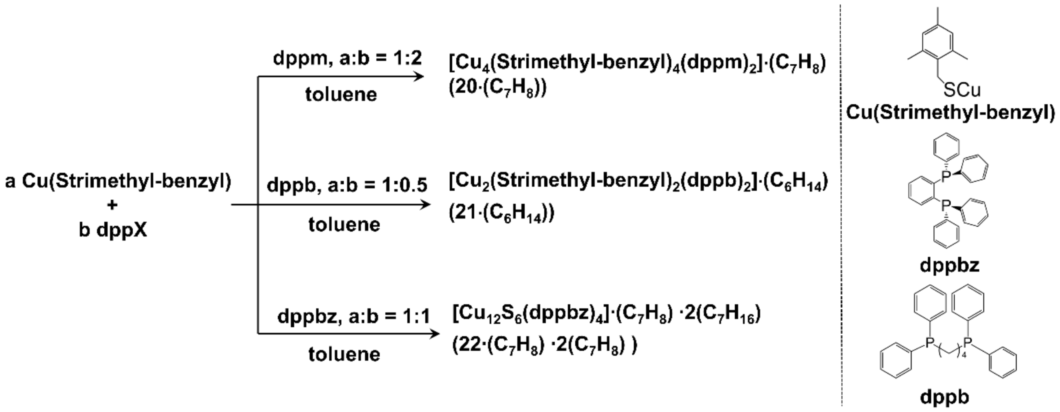

Scheme 3-5 *Synthesis of copper compounds starting from Cu(Strimethyl-benzyl).*

To investigate the influence of the steric demand of the thiolate ligands the reaction of the copper salt of 2,4,6-trimethylbenzylthiol with several bidentate phosphines has been carried out in different stoichiometric ratios in toluene. More synthetic details have been mentioned in the experimental section.

3.1.5.1 [Cu$_4$(Strimethyl-benzyl)$_4$(dppm)$_2$]·(C$_7$H$_8$) (20·(C$_7$H$_8$))

Compound **20** crystallizes in the triclinic space group $P\overline{1}$ with two molecules per unit cell. It consists of four copper atoms, four thiolate groups and two dppm ligands. The Cu$_4$S$_4$ core can be described as a Cu$_4$ tetrahedron (Cu···Cu distances 2.803(3) Å to 3.029(1) Å) where four of the six edges are capped by four μ_2 thiolate ligands. Cu1 and Cu3 are linked by S1, Cu1 and Cu4 by S4, Cu2 and Cu3 by S2 while Cu2 and Cu4 by S3. Besides, Cu1 and Cu2, Cu3 and Cu4 are bridged by dppm ligands.

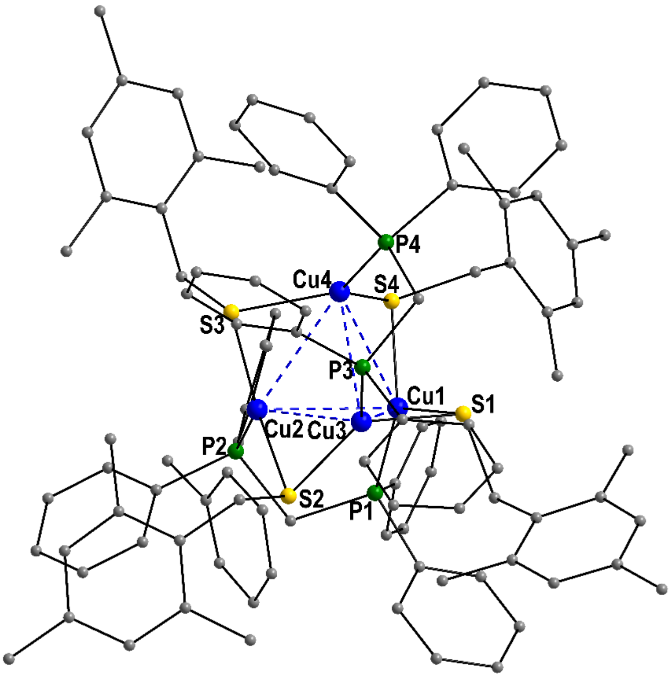

***Figure 3-24** Molecular structure of compound **20** in the solid state (H atoms omitted).*

All Cu–S bond lengths are in the expected range of 2.206(6) Å to 2.298(8) Å and the Cu–P bond lengths range from 2.244(4) Å to 2.268(9) Å.

3.1.5.2 [Cu_2(Strimethyl-benzyl)$_2$(dppb)$_2$]·(C_6H_{14}) (21·(C_6H_{14}))

Compound **21** crystallizes in the triclinic space group $P\overline{1}$ with one molecule per unit cell. **21** is located on an inversion centre, which leads to a planar Cu_2S_2 ring with the thiolate groups in *trans*-position. Both copper atoms are distorted tetrahedrally coordinated by two sulphur and two phosphorus atoms and the two dppb (dppb = 1,4-bis(diphenylphosphino)butane) ligands act as additional bridges between the two copper atoms. The bond lengths of Cu1–S1 and Cu1–S1' are 2.383(3) Å and 2.453(3) Å, respectively, the Cu–P bond lengths are 2.284(5) Å and 2.294(4) Å.

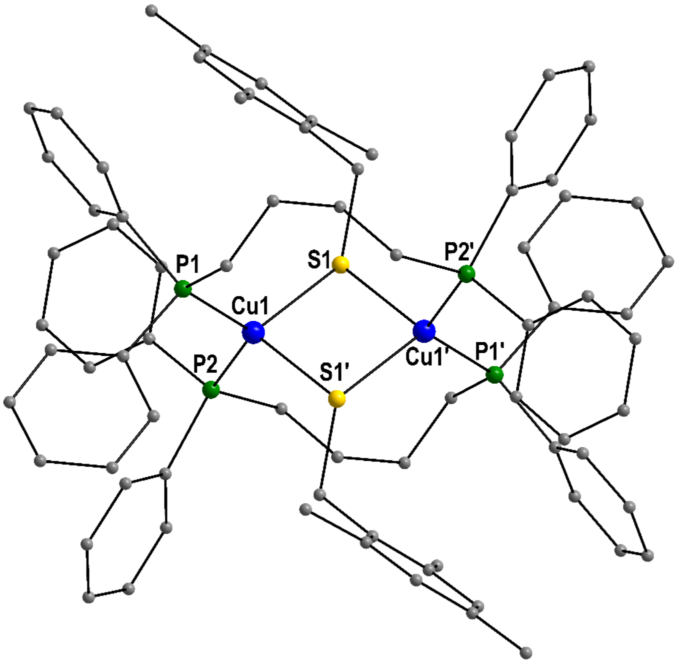

Figure 3-25 *Molecular structure of compound **20** in the solid state (H atoms omitted).*

3.1.5.3 $[Cu_{12}S_6(dppox)_4]\cdot(C_7H_8)\cdot2(C_7H_{16})$ ($22\cdot(C_7H_8)\cdot2(C_7H_{16})$)

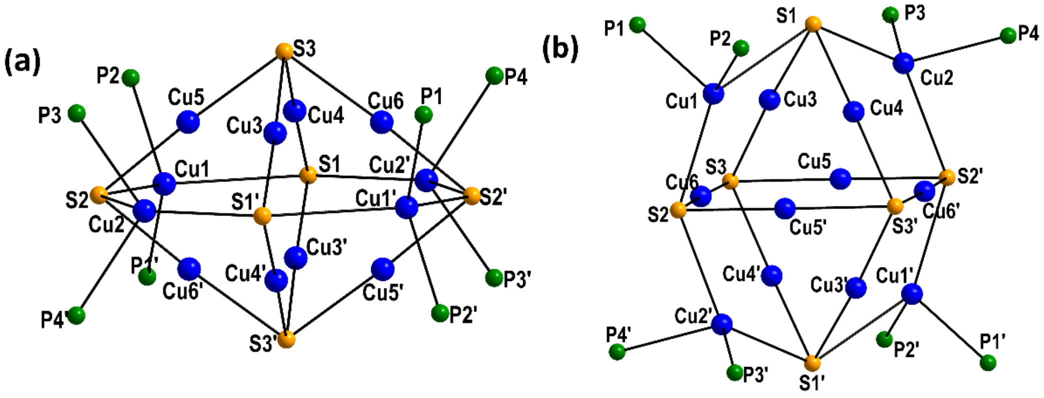

Figure 3-26 *Structure of the heavy atoms core of compound **22** in the solid state, seeing from **(a)** c and **(b)** b axis.*

Compound **22** crystallizes in the monoclinic space group $P2_1/n$ with two molecules per unit cell. **22** is localized on an inversion centre. Seen from **Figure 3-26** the central $Cu_{12}S_6$ unit can be described as a S_6 octahedron where the twelve edges are bridged by copper atoms. Four of these copper atoms (Cu1, Cu2 and symm. equiv.) are additionally coordinated by the phosphorus atoms of chelating dppox ligands, resulting in a distorted tetrahedral coordination sphere. The remaining eight copper atoms (Cu3–Cu6 and symm. equiv.) are linearly coordinated by two sulphur atoms (S–Cu–S angles between 175.2° to 176.7°).

As seen in **Figure 2-26(a),** the S_6 octahedron is strongly elongated (S1···S1' 6.894(4) Å, S2···S2' of 6.912(2) Å, S3···S3' 5.339(9) Å). The Cu–S bond lengths range from 2.478(9) Å to 2.809(10) Å for the tetrahedrally coordinated copper atoms; for the linearly coordinated copper atoms the Cu–S bonds are significantly shorter (2.142(1) Å to 2.221(2) Å). Though non-bonding the shortest Cu···Cu distances are ranging from 2.532(3) Å to 2.892(2) Å.

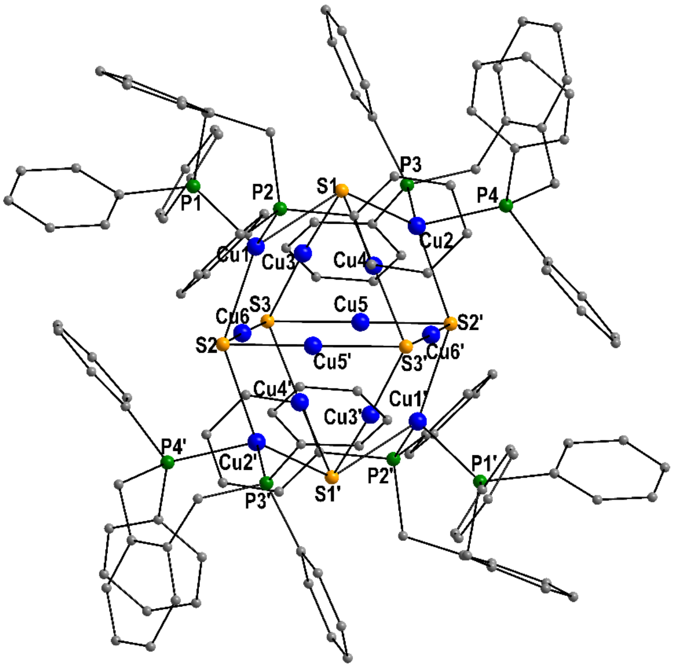

Figure 3-27 *Molecular structure of compound* ***22*** *in the solid state, seeing from b axis (H atoms omitted).*

The core of **22** is very similar to the previously described compound $[Cu_{12}S_6(PEtPh_2)_8]$.[29] In this cluster eight of the twelve copper atoms are trigonal planar coordinated by two sulphur and one phosphorus atom whereas in **22** four copper atoms are tetrahedrally coordinated.

3.2 Reactions of copper thiolates with phosphines in the presence of oxomolybdates

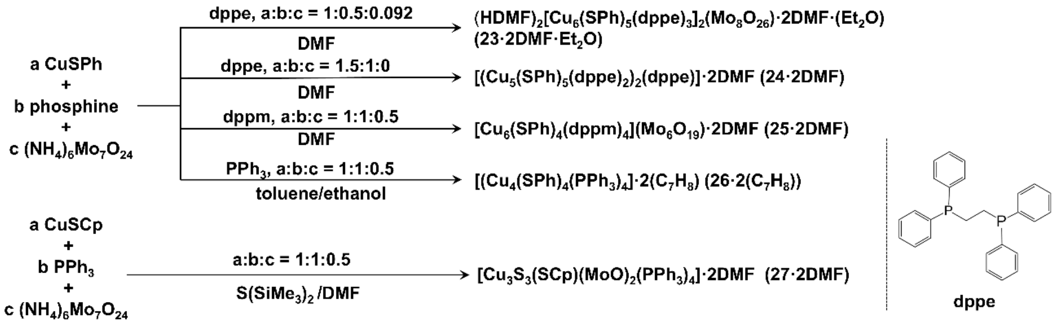

Scheme 3-6 *Synthesis of copper clusters in the presence of polyoxomolybdates.*

Polyoxometalates have been used several times for the synthesis of coordination compounds with two different metal atoms. With this synthetic procedure one could have access to more abundant structures and active coordination sites.[92]

During past decades, several Mo/W-Cu/Ag-S compounds have been synthesized, some of them are discrete clusters,[93] others are 1D[94], 2D[95] or 3D[96] cluster-node frameworks. For the discrete clusters, copper and Mo/S atoms locate in the same cations or anions or neutral molecules while the other compounds consist of copper containing cations and Mo/W oxoanions[97].

In the reactions described here, $(NH_4)_6Mo_7O_{24}$ was chosen as molybdenum source. Firstly, the reaction of CuSPh, dppe and $(NH_4)_6Mo_7O_{24}$ results in formation of **23**. In addition, for comparison the reaction was carried out without $(NH_4)_6Mo_7O_{24}$ resulting in the dimer **24**. Though present in the reaction mixture Mo atoms did not enter into the structure of **26**. More synthetic details have been mentioned in the experimental section.

3.2.1 $(HDMF)_2[Cu_6(SPh)_5(dppe)_3]_2(Mo_8O_{26})\cdot 2DMF\cdot(Et_2O)$ $(\mathbf{23}\cdot 2DMF\cdot(Et_2O))$

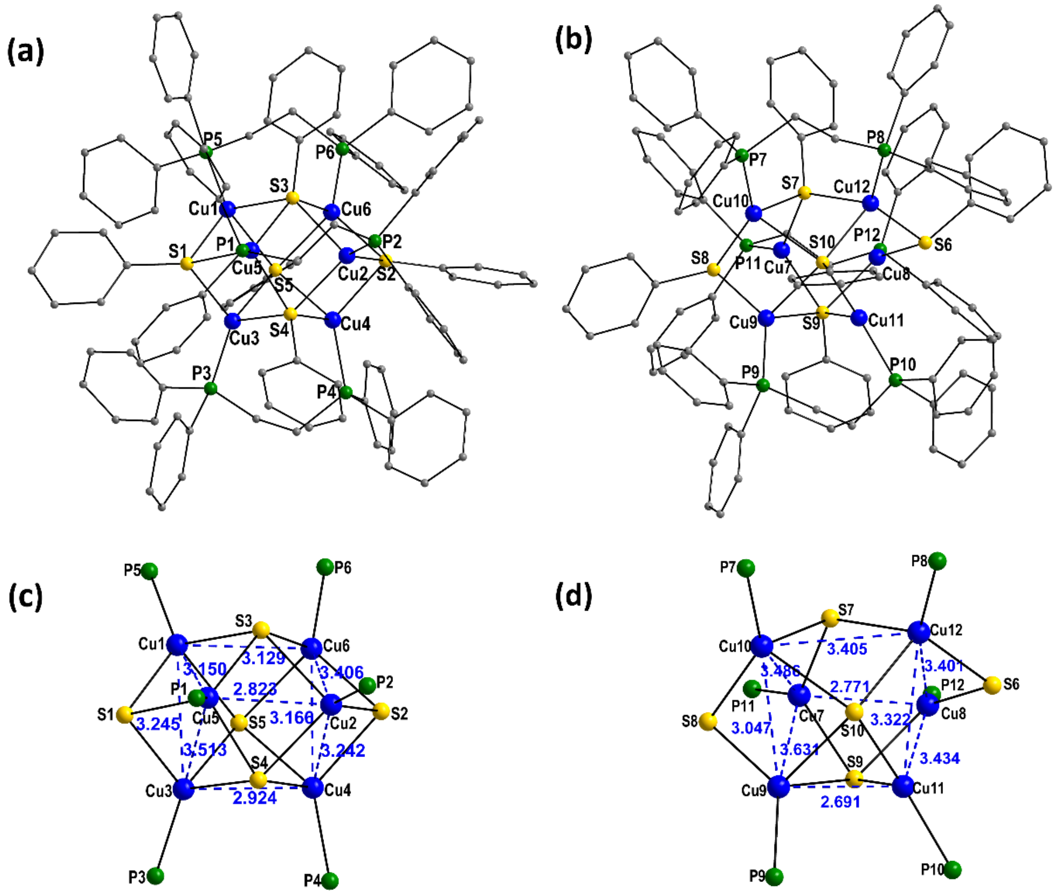

Figure 3-28 *Top: Molecular structures of the two* $[Cu_6(SPh)_5(dppe)_3]^+$ *cations A (left) and B (right) in* ***23*** *in the solid state (H atoms omitted). Bottom: structures of the heavy atoms core of the cations in* ***23*** *in the solid state in same orientation as in top images (distances in Å).*

The light-blue compound **23** crystallizes in the triclinic space group $P\overline{1}$ with two independent $[Cu_6(SPh)_5(dppe)_3]^+$ cations, one $(Mo_8O_{26})^{4-}$ anion, four DMF molecules and one Et_2O molecule in the asymmetric unit. Assuming that copper is in oxidation state +1 and the SPh ligands have a charge of –1, each $[Cu_6(SPh)_5(dppe)_3]^+$ cation should get a charge of +1. Accordingly, the $(Mo_8O_{26})^{4-}$ anion should present a charge of –2. However, in literature one can only find $(Mo_8O_{26})^{4-}$ anions, which means each $[Cu_6(SPh)_5(dppe)_3]^{2+}$ cation should have a charge of +2. This would result in a mixed valency with copper in oxidation state +1 and +2. However, quantum chemical calculations clearly show that both cations should have a singlet ground state with all copper atoms in d^{10} configuration. Hence, the most reasonable explanation could be a protonation of DMF (DMF = N,N'-dimethylformamid) in the solution, a phenomenon which has been observed very often.[98] To summarize the final composition of **23** should be $(HDMF)^{+}_{2}[Cu_6(SPh)_5(dppe)_3]^{+}_{2}(Mo_8O_{26})^{4-}$.

The structures of the two independent $[Cu_6(SPh)_5(dppe)_3]^+$ cations are similar but not identical. In both cations (**A** and **B**) one can identify two differently distorted trigonal prisms consisting of six copper atoms (Cu1–Cu6; Cu7–Cu12). In cation **A** (**Figure 3-28(a), Figure 3-28(c)**) the Cu···Cu distances within the trigonal faces (Cu1, Cu3, Cu5 and Cu2, Cu4, Cu6) are 3.150(1) Å to 3.513(4) Å; in cation **B** (Cu7, Cu9, Cu10 and Cu8, Cu11, Cu12) the Cu···Cu distances are 3.047(5) Å to 3.631(1) Å. The Cu···Cu distances between the Cu_3 faces are 2.823(2) Å to 3.128(8) Å in cation **A**, whereas the corresponding values in cation **B** are significantly different (2.691(9)°Å–3.405(6) Å). Corresponding differences are also found in the S-Cu distances in both cations. In cation **A** the sulphur atoms can clearly be classified as μ_3 (S1, S2) and μ_4 (S3, S4, S5) (**Table 3-1**) and all copper atoms show a distorted tetrahedral coordination sphere of three sulphur and one phosphorus atom.

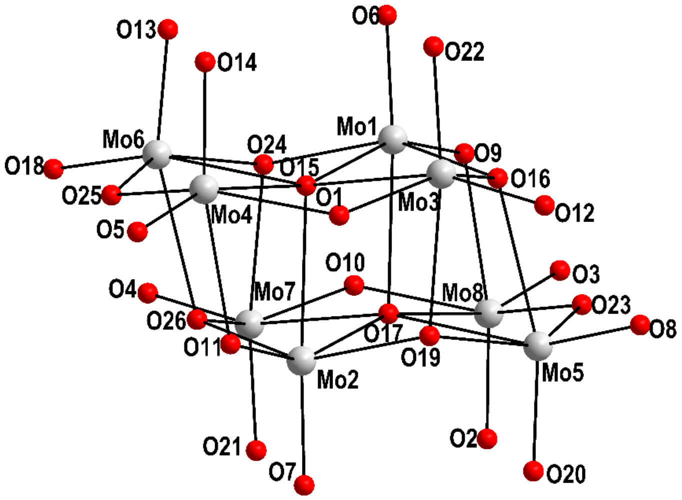

Figure 3-29 *Structure of the* $[Mo_8O_{26}]^{4-}$ *anion in* ***23*** *in the solid state.*

In contrast, the S–Cu distances in cation **B** (**Figure 3-28(b)**, **Figure 3-28(d)**) are significantly different to cation **A**. The bridging sulphur atoms can therefore be described as μ_2 (S6, S8), μ_3 (S7, S9) and μ_4 (S10) ligands (**Table 3-2**). This results in various coordination modes for the copper atoms: Cu7, Cu8, Cu9 and Cu11 show nearly trigonal planar coordination by two sulphur and one phosphorus atom, whereas Cu10 and Cu12 are distorted tetrahedrally coordinated by three sulphur and one phosphorus atom.

Table 3-1 *S–Cu distances (in Å) in cation **A**.*

μ_3–S	**μ_4–S**
S1–Cu1 2.293(4)	S3–Cu1 2.380(1)
S1–Cu3 2.415(6)	S3–Cu2 2.476(7)
S1–Cu5 2.524(5)	S3–Cu5 2.403(4)
S2–Cu2 2.374(6)	S3–Cu6 2.514(5)
S2–Cu4 2.364(5)	S4–Cu2 2.411(2)
S2–Cu6 2.349(10)	S4–Cu3 2.461(2)
	S4–Cu4 2.446(1)
	S4–Cu5 2.393(3)
	S5–Cu1 2.623(5)
	S5–Cu3 2.394(5)
	S5–Cu4 2.454(5)
	S5–Cu6 2.403(3)

First DFT calculations of the two isomers **A** and **B** demonstrate that the calculated total energy for both isomers is nearly the same and the energy barrier for the transformation from **A** to **B** or **B** to **A** is about 30 kJ/mol. This means that the two isomers are stable at room temperature in a thermal equilibrium.

Table 3-2 *S-Cu distances (in Å) in cation **B***

μ_2–S	**μ_3–S**	**μ_4–S**
S6–Cu8 2.262(3)	S7–Cu7 2.262(3)	S10–Cu9 2.466(7)
S6–Cu12 2.327(9)	S7–Cu10 2.420(1)	S10–Cu10 2.545(6)
S6–Cu11 3.120 (nonbonding)	S7–Cu12 2.426(7)	S10–Cu11 2.244(5)
S8–Cu9 2.267(8)	S7–Cu8 3.200 (nonbonding)	S10–Cu12 2.447(8)
S8–Cu10 2.296(8)	S9–Cu7 2.279(10)	
S8–Cu7 2.911 (nonbonding)	S9–Cu8 2.407(8)	
	S9–Cu11 2.285(6)	
	S9–Cu9 2.812(2)	

3.2.2 $[(Cu_5(SPh)_5(dppe)_2)_2(dppe)]\cdot 2DMF$ (24·2DMF)

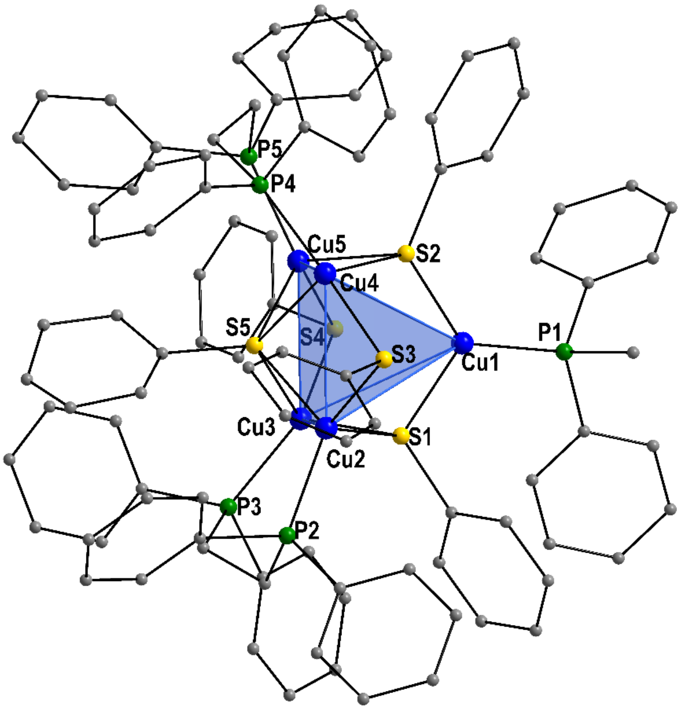

Figure 3-30 *Molecular structure of the asymmetric unit in compound* ***24*** *in the solid state, polyhedron of the* Cu_5 *square pyramid marked in blue (H atoms omitted).*

Compound **24** crystallizes in the monoclinic space group $P2_1/n$ with two molecules ($\bar{1}$ symmetry) per unit cell. Seen from **Figure 3-31**, compound **24** consists of two $[Cu_5(SPh)_5(dppe)_2]$ subunits connected *via* a dppe ligand. The Cu_5S_5 core can be described as a distorted Cu_5 square pyramid with Cu2 to Cu5 as the base and Cu1 on top. The non-bonding Cu···Cu distances are between 2.990(0) Å and 3.283(3) Å in the base and 3.505(5) Å to 4.116(1) Å to Cu1. Concerning the sulphur atoms one can identify different coordination modes: S5 is a μ_4 ligand on the base of the Cu_5 pyramid, S3 and S4 act as μ_2 ligands on two edges of the base of the pyramid whereas S1 and S2 are μ_3 bridging over two trigonal faces. The Cu–S distances range from 2.201(5) Å to 2.635(4) Å. The two edges of the base of the pyramid, which are not bridges by sulphur, are bridged by two dppe ligands; the fifth dppe ligand coordinates to Cu1 and connects the two halves of the dimer (Cu–P distances 2.193(5) Å–2.224(5) Å). This results in tetrahedral coordination for Cu2 to Cu5 and trigonal planar coordination for Cu1.

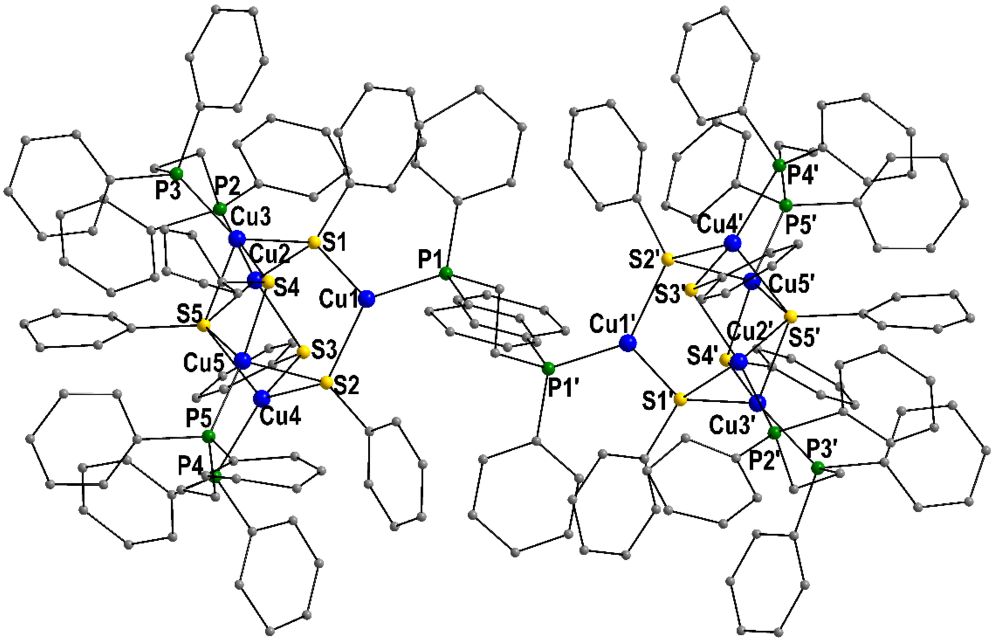

***Figure 3-31** Molecular structure of compound **24** in the solid state, illustrating dimeric feature of **24** (H atoms omitted).*

3.2.3 [$Cu_6(SPh)_4(dppm)_4$](Mo_6O_{19})·2DMF (25·2DMF)

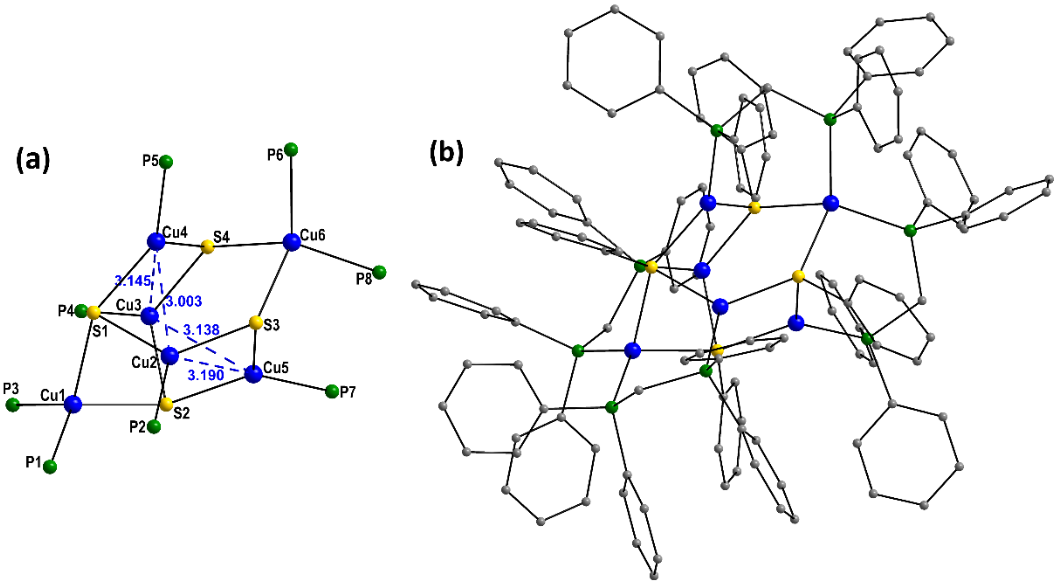

***Figure 3-32 (a)** Structure of the heavy atoms core of the [$Cu_6(SPh)_4(dppm)_4$]$^{2+}$ dication in **25** in the solid state; **(b)** molecular structure of the [$Cu_6(SPh)_4(dppm)_4$]$^{2+}$ dication in **25** in the solid state in the same orientation as in **(a)** (H atoms omitted).*

Compound **25** crystallizes in the triclinic space group $P\overline{1}$ with two formula units per unit cell. **25** is an ionic compound consisting of a $[Cu_6(SPh)_4(dppm)_4]^{2+}$ dication (**Figure 3-32**) and a $[Mo_6O_{19}]^{2-}$ dianion (**Figure 3-33**). In the unit cell there are two $[Cu_6(SPh)_4(dppm)_4]^{2+}$ dications occupying the general position and two $[Mo_6O_{19}]^{2-}$ dianions each located on an inversion centre.

The copper atoms in **25** are arranged as a Cu_4 butterfly (Cu2–Cu5), which is capped by two further copper atoms (Cu1, Cu6). The non-bonding Cu···Cu distances within the butterfly are 3.003(4) Å for Cu2–Cu4, 3.145(6) Å for Cu3–Cu4, 3.138(9) Å for Cu3–Cu5 and 3.190(1) Å for Cu2–Cu5. All sulphur atoms act as μ_3 bridges (Cu–S distances 2.230(2) Å–2.445(6) Å). Each copper atom of the butterfly motif is coordinated trigonal planar by two sulphur and one phosphorus atom. Cu1 and Cu6 are connected to the butterfly *via* S1 and S2 and S3 and S4, respectively. As a result, Cu1 and Cu6 are tetrahedrally coordinated by two sulphur and two phosphorus atoms. The shortest Cu···Cu distances are 3.250(11) Å for Cu1–Cu2, 3.330(11) Å for Cu1–Cu3, 3.252(2) Å for Cu4–Cu6 and 3.316(7) Å for Cu5–Cu6. All other distances are longer than 4 Å. The Cu–P bond lengths are from 2.222(2) Å to 2.487(3) Å.

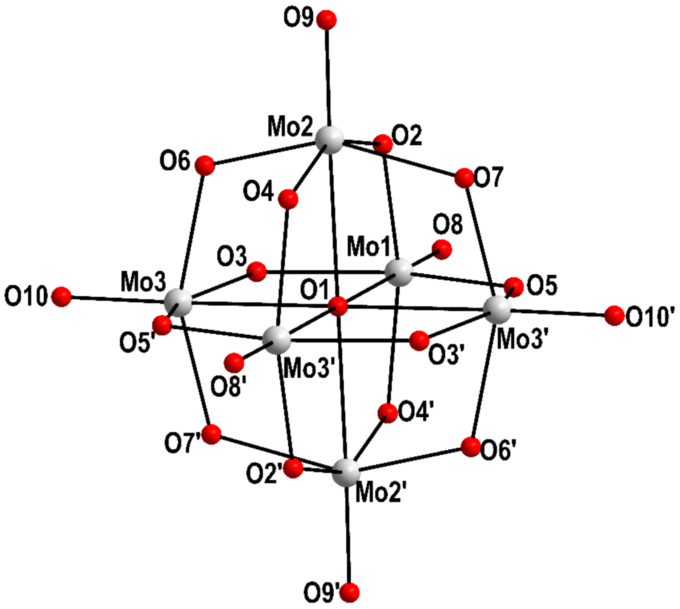

Figure 3-33. *Structure of one of $[Mo_6O_{19}]^{2+}$ dianions in **25** in the solid state.*

One of the two $[Mo_6O_{19}]^{2-}$ dianions is shown in **Figure 3-33**. The bonding parameters found in $[Mo_6O_{19}]^{2-}$ are in good agreement with those published in literature. For example, Zhou et al.[99] described a 3D organic-inorganic hybrid compound [{Cu(phen)}$_3${Cu(μ_2-ox)$_3$}{Mo$_6$O$_{19}$}] (phen = 1,10-phenanthroline, ox = oxalate). In 2005, Shivaiah et al.[97a] obtained one compound [Cu(H$_2$O)$_4$(dibenzo-24-crown-8)][Mo$_6$O$_{19}$]. In the above two anions, the Mo–O bond lengths vary from 1.674 Å to 2.325 Å, which is identical to the values found in **25** (1.679(5) Å–2.328(8) Å).

3.2.4 [Cu$_4$(SPh)$_4$(PPh$_3$)$_4$]·2(C$_7$H$_8$) (26·2(C$_7$H$_8$))

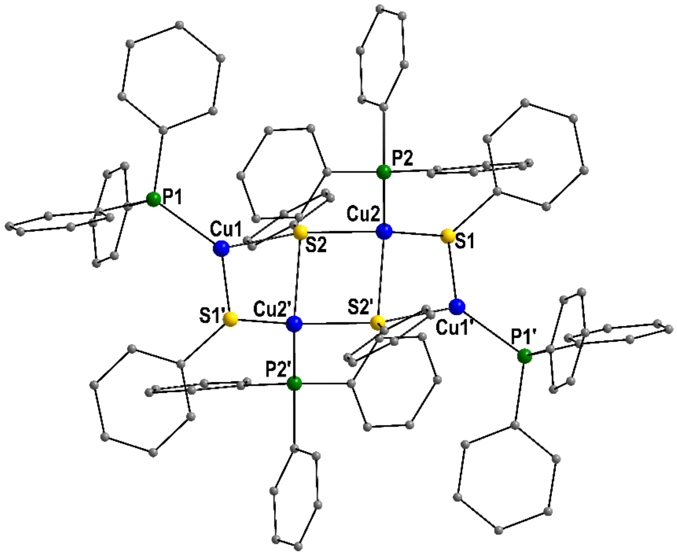

***Figure 3-34** Molecular structure of compound **26** in the solid state (H atoms omitted).*

Compound **26** crystallizes in the triclinic space group $P\bar{1}$ with one molecule per unit cell. Though present in the reaction mixture, molybdenum is not incorporated into the formed product. **26** can be seen as a ladder-like structure of three condensed Cu$_2$S$_2$ rings in a chair conformation. Due to the inversion centre the middle ring is planar whereas the two outer rings are distorted.

Cu1 and Cu1' are trigonal planar coordinated, whereas Cu2 and Cu2' show tetrahedral coordination. The Cu–S bond lengths vary from 2.276(6) Å to 2.469(9) Å; Cu–P bond lengths are 2.214(4) Å and 2.233(3) Å.

3.2.5 $[Cu_3S_3(SCp)(MoO)(PPh_3)_2]_2\cdot 2DMF$ (27·2DMF)

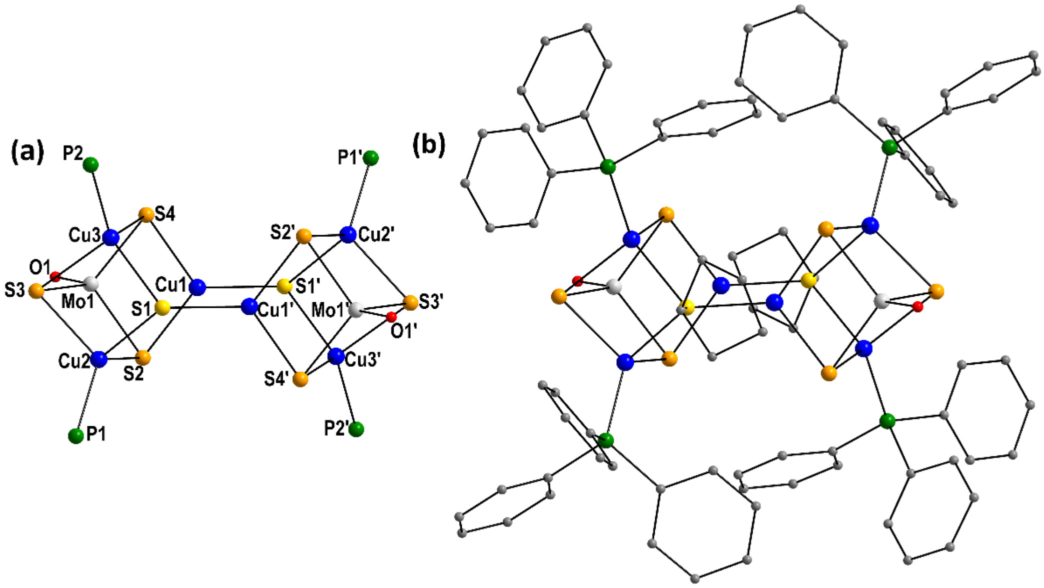

***Figure 3-35 (a)** Structure of the heavy atoms core of **27** in the solid state; **(b)** molecular structure of compound **27** in the solid state in the same orientation as in **(a)** (H atoms omitted).*

Compound **27** crystallizes in the monoclinic space group $P2_1/n$ with two molecules per unit cell. **27** is localized on an inversion centre. In this cluster one can identify six S^{2-}, two SCp^- and two O^{2-} ions. Under the assumption that copper is in the formal oxidation state +1, molybdenum shows oxidation number +6 resulting in a neutral molecule. The core of **27** can be described as two connected (*via* Cu1 and S1) $[Cu_3MoS_4]$ distorted heterocubanes. Cu2, Cu3 and Mo1 tetrahedrally coordinate with three sulphur atoms and one phosphine (for Cu) or oxygen (for Mo), respectively. The bond lengths are Cu2–S 2.301(2) Å to 2.498(8) Å, Cu3–S 2.342(2) Å to 2.394(4) Å, Mo1–S 2.251(1) Å to 2.269(9) Å and Mo1–O1 1.705(3) Å. Cu1 presents trigonal coordinating mode (Cu1–S: 2.205(5) Å–2.244(2) Å).

3.3 Reactions of CuSCp and CuSAd with $Se(SiMe_3)_2$ in the presence of various bidentate phosphines

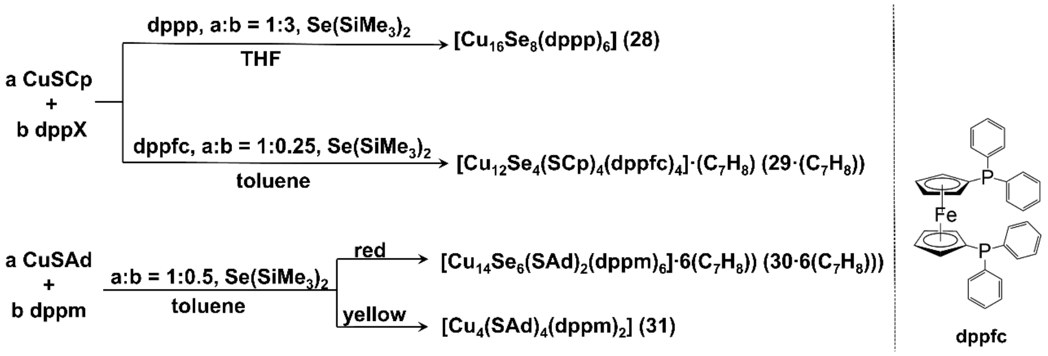

Scheme 3-7 *Synthesis of copper selenium clusters starting from CuSCp and CuSAd.*

In earlier publications the use of $Se(SiMe_3)_2$ has been described to obtain large, metal-rich clusters. However, sometimes only smaller multinuclear complexes crystallize from the reaction mixture. **28**–**31**, are synthesized at room temperature. Firstly, CuSCp and the bidentate phosphine were dissolved in THF (THF = tetrahydrofuran) or toluene and stirred for several minutes, then $Se(SiMe_3)_2$ was added and stirred overnight. On the next day, the clear solutions were layered by non-polar solvents. As a result, crystals of **28** and **29** could be isolated. An analogous reaction with CuSAd, dppm and $Se(SiMe_3)_2$ leads to a mixture of red (**30**) and yellow (**31**) crystals. More synthetic details have been mentioned in the experimental section.

3.3.1 $[Cu_{16}Se_8(dppp)_6]$ (28)

Compound **28** crystallizes in two different space groups. The monoclinic form (in $P2_1/n$) crystallizes with two THF molecules and one Et_2O molecule, whereas the triclinic form (in $P\overline{1}$) crystallizes with one molecule of Et_2O and one molecule of THF.

Despite of the solvent molecules the bonding parameters of both isomers are identical within the standard deviation. Therefore, only the structure of the monoclinic form is discussed here. **28** consists of sixteen copper atoms, eight selenium atoms and six dppp ligands yielding to a cylinder-like molecule. This can be described as two Cu_6Se_4 building blocks on top and bottom of the cluster core, connected *via* four additional copper atoms (Cu9, Cu11, Cu14, Cu15). Four dppp ligands are additionally bridging the top and bottom Cu_6Se_4 units. The other two (P3/P4 and P9/P10) are coordinated to Cu2 and Cu3 and Cu6 and Cu7 within the Cu_6Se_4 units.

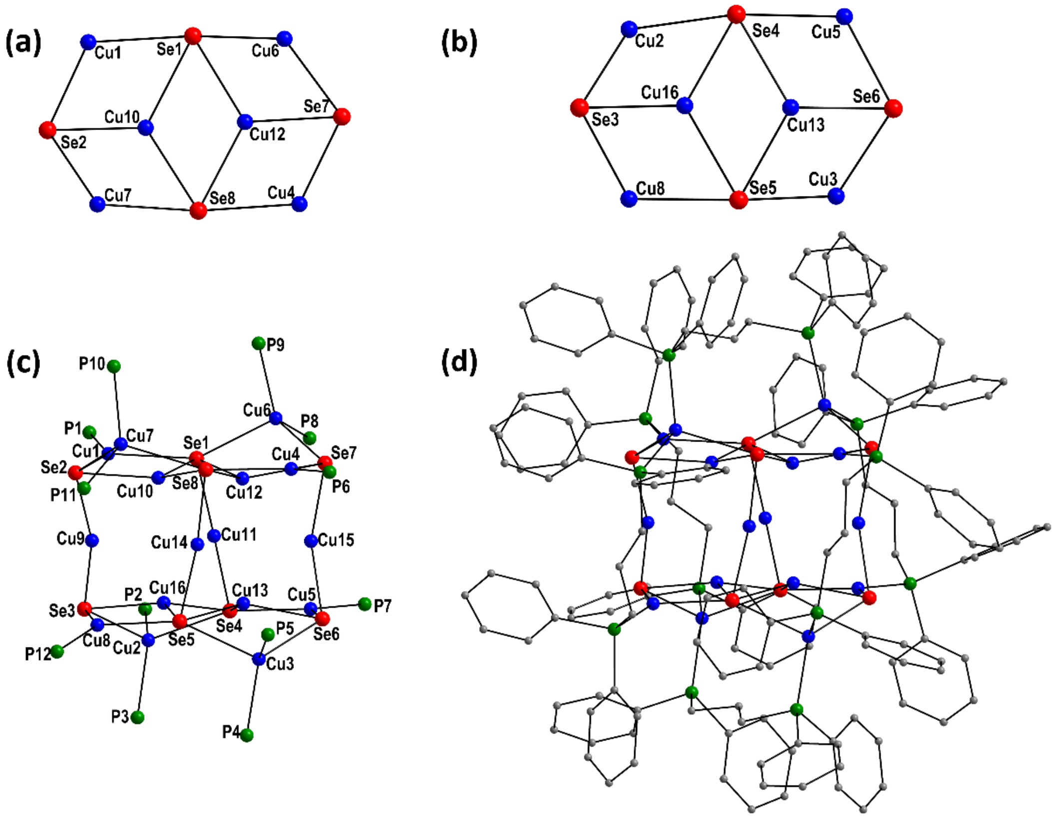

Figure 3-36 *Structure of* ***(a)*** *the top Cu/Se surface and* ***(b)*** *the bottom Cu/Se surface of* ***28*** *in the solid state;* ***(c)*** *the heavy atoms core of* ***28*** *in the solid state (consisting of building blocks* ***(a)*** *and* ***(b)*** *connected by four copper atoms);* ***(d)*** *molecular structure of* ***28*** *in the solid state in the same orientation as in* ***(c)*** *(H atoms omitted).*

The copper atoms adopt different coordination modes:

1. Cu9, Cu11, Cu14, Cu15 are coordinated linearly by two selenium atoms with bond angles Se–Cu–Se of 161.4(4)° to 164.8(4)° (Cu–Se: 2.277(7) Å to 2.297(8) Å),

2. Cu10, Cu12, Cu13, Cu16 are trigonal planar coordinated by three selenium

atoms (Cu–Se: 2.393(4) Å to 2.560(1) Å),

3. Cu1, Cu4, Cu5, Cu8 are trigonal planar coordinated by two selenium atoms and one phosphorus atom (Cu–Se: 2.364(4) Å to 2.560(10) Å, Cu–P: 2.200(1) Å to 2.216(8) Å)

4. Cu2, Cu3, Cu6, Cu7 are tetrahedrally coordinated by two selenium atoms and two phosphorus atoms (Cu–Se: 2.496(7) Å to 2.584(5) Å, Cu–P: 2.242(3) Å to 2.283(4) Å).

All copper atoms are in formal oxidation state +1 (d^{10} configuration). Therefore Cu···Cu bonding cannot be expected, though there are relatively short Cu···Cu distances from 2.451(1) Å to 2.891(2) Å.

3.3.2 [$Cu_{12}Se_4(SCp)_4(dppfc)_4$]·($C_7H_8$) (29·($C_7H_8$))

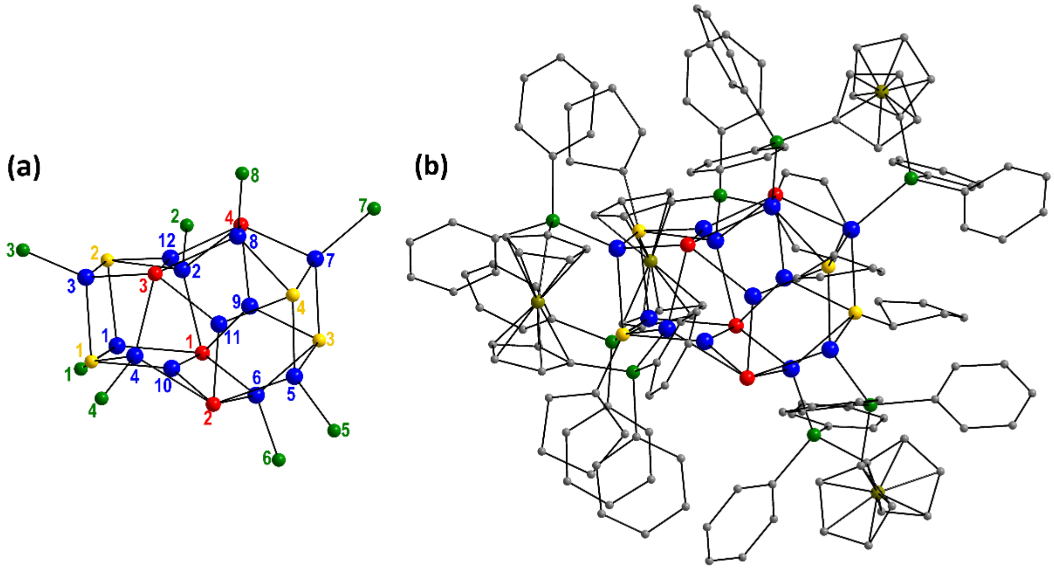

Figure 3-37 (a) *Structure of the heavy atoms core of* ***29*** *in the solid state;* ***(b)*** *molecular structure of* ***29*** *in the solid state in the same orientation as in* ***(a)*** *(H atoms omitted).*

Compound **29** crystallizes in the monoclinic space group *C*2/*c* with eight molecules per unit cell as dark brown crystals together with a red amorphous residue, which could not be analysed yet. **29** consists of twelve Cu^+ cations, four Se^{2-} anions, four SCp^- anions and four neutral dppfc ligands. The core of this neutral cluster is a cylinder in which left and right sides are capped by

Cu_2S_2 four-membered rings (Cu1, Cu3, S1, S2 and Cu5, Cu7, S3, S4). These two units are connected to the central Cu_8Se_4 building block. The copper atoms are in two different coordination modes (triangular, tetrahedral): four copper atoms (Cu2, Cu4, Cu6, Cu8) coordinate with two selenium, one sulphur and one phosphorus atom; four copper atoms (Cu1, Cu3, Cu5, Cu7) coordinate with two sulphur, one selenium and one phosphorus atom; four copper atoms (Cu9, Cu10, Cu11, Cu12) coordinate with two selenium and one sulphur atom. Cu–Se bond lengths range from 2.364(5) Å to 2.732(2) Å and Cu–S from 2.334(5) Å to 2.664(5) Å. Eight copper atoms coordinating with sulphur atoms are bridged by four dppfc ligands (Cu1 and Cu2, Cu3 and Cu4, Cu5 and Cu6, Cu7 and Cu8). The Cu···Cu distances vary from 2.574(6) Å to 2.980(10) Å.

3.3.3 $[Cu_{14}Se_6(SAd)_2(dppm)_6]\cdot 6(C_7H_8)$ ($30\cdot 6(C_7H_8)$) and $[Cu_4(SAd)_4(dppm)_2]$ (31)

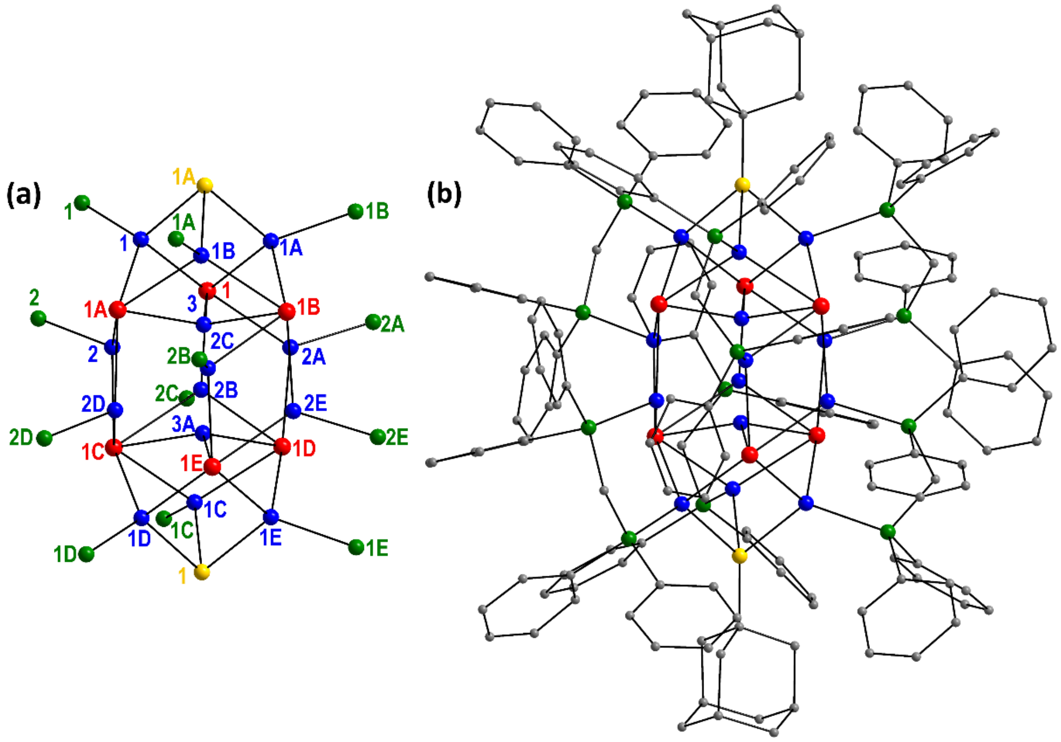

Figure 3-38 ***(a)*** *Structure of the heavy atoms core of* ***30*** *in the solid state;* ***(b)*** *molecular structure of compound* ***30*** *in the solid state in the same orientation as in* ***(a)*** *(H atoms omitted).*

Compounds **30** and **31** crystallize together from one reaction mixture. The red **30** crystallizes in the trigonal space group $R\bar{3}c$ with six molecules per unit cell. **30** consists of fourteen copper atoms, six selenium atoms, two thiolate groups and six dppm ligands with a $\bar{3}$-axis running through the atoms Cu3, Cu3A, S1 and S1A. There is a central Cu_8Se_6 substructure formed by Cu2 and Cu3 (and symm. equiv.) and the six selenium atoms (Se1 and symm. equiv.) which can be described as highly distorted interpenetrating Cu_8 and Se_6 polyhedra. This central building block in **30** is capped by two Cu_3S pyramids on top and bottom (**Figure 3-38(a)**).

Cu1 is tetrahedrally coordinated by two selenium, one sulphur and one phosphorus atom, whereas Cu2 bonds to three selenium and one phosphorus atom. Cu3 is trigonal planar coordinated by three selenium atoms. All selenium atoms are in μ_5 bridging mode. The Cu–Se bond lengths range from 2.432(3) Å to 2.884(4) Å, the Cu–S distance is 2.346(2) Å.

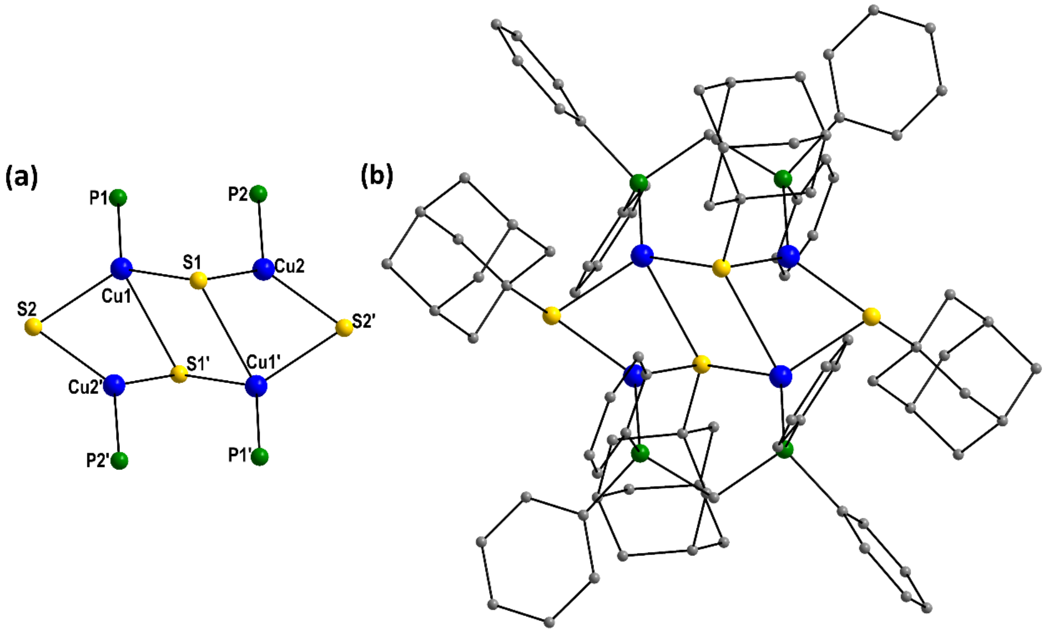

Figure 3-39 ***(a)*** *Structure of the heavy atoms core of compound* ***31*** *in the solid state;* ***(b)*** *molecular structure of compound* ***31*** *in the solid state in the same orientation as in* ***(a)*** *(H atoms omitted).*

The yellow compound **31** crystallizes in the monoclinic space group $P2_1/n$ with two molecules per unit cell. **31** consists of four copper atoms, four SAd$^-$ thiolate groups and two dppm ligands and is located on an inversion centre.

The core of this tetranuclear complex is a ladder-like Cu_4S_4 arrangement in chair configuration which is similar to **26**. Cu1 tetrahedrally coordinates with three sulphur atoms and one phosphorus atom, while Cu2 trigonally coordinates with two sulphur atoms and one phosphorus atom. S2 acts as μ_2-bridge between Cu1 and Cu2 and S1 is μ_3-bridging Cu1, Cu1' and Cu2. The Cu–S bond lengths vary from 2.264(5) Å to 2.806(6) Å and Cu–P distances range from 2.202(3) Å to 2.230(1) Å.

3.4 Reactions of copper thiolates with $E(SiMe_3)_2$ (E = S, Se) in the presence of dppp and PPh_3

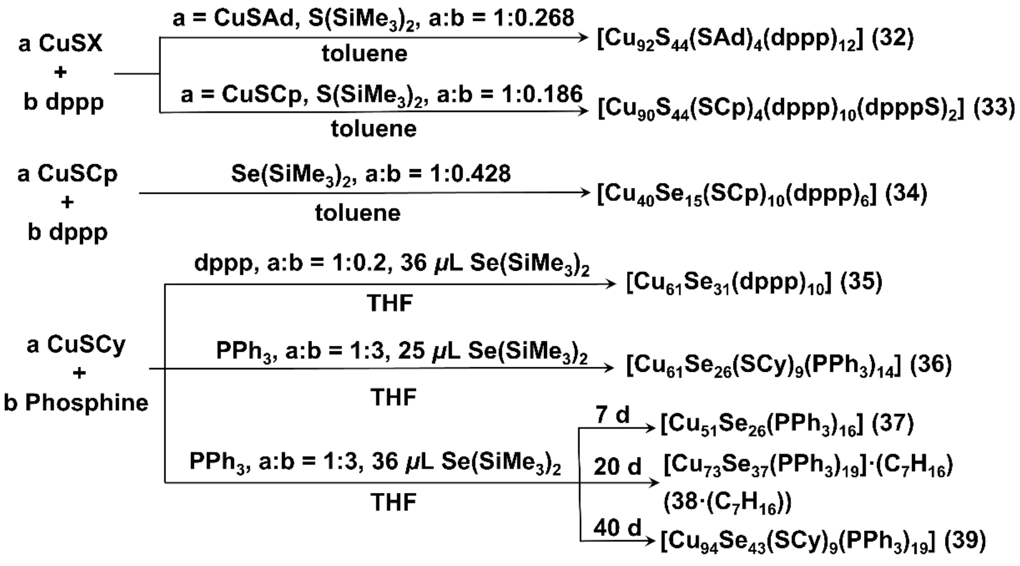

Scheme 3-8 *Synthesis of metal-rich copper chalcogenide clusters* ***32–39****.*

The reaction of CuSAd with $S(SiMe_3)_2$ in the presence of dppp leads to $[Cu_{92}S_{44}(SAd)_4(dppp)_{12}]$ (**32**) which is one of the largest Cu/S clusters published so far. When CuSAd is changed to CuSCp, $[Cu_{90}S_{44}(SCp)_4(dppp)_{12}]$ (**33**) is obtained. Furthermore, using $Se(SiMe_3)_2$ instead of $S(SiMe_3)_2$ results in middle sized cluster $[Cu_{40}Se_{15}(SCp)_{10}(dppp)_6]$ (**34**).

Using CuSCy and $Se(SiMe_3)_2$ as chalcogenide source a series of five large clusters could be isolated.

The reaction of CuSCy with dppp and $Se(SiMe_3)_2$ leads to the formation of **35**.

Using PPh_3 instead of dppp yields to four different compounds **36**–**39** depending on the reaction conditions. Simply increasing the reaction time results in different compounds **37**, **38** and **39** with increasing number of copper atoms. More synthetic details have been mentioned in the experimental section.

3.4.1 [$Cu_{92}S_{44}(SAd)_4(dppp)_{12}$] (32)

Compound **32** crystallizes in the monoclinic space group $P2_1/c$ with two molecules per unit cell. **32** is located on an inversion centre and consists of 92 copper atoms, 44 S^{2-} ions, four SAd^- groups and twelve dppp ligands. Due to the charge balance all copper atoms are in oxidation state +1.

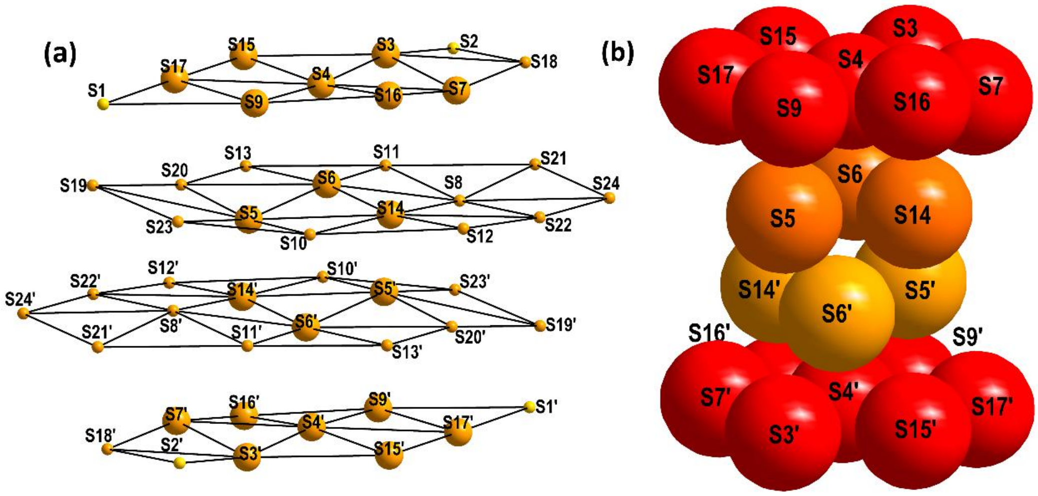

Figure 3-40 (a) *Arrangement of sulphur atoms in compound* ***32****, illustrating fcc packing (A-B-C packing atoms marked as bigger balls);* ***(b)*** *space filling model of fcc-like packing in* ***32****.*

The sulphur atoms in **32** are organized in four hexagonal layers of 10, 14, 14 and 10 atoms. This sulphur arrangement can be seen as a cut-out of a face centred cubic close packing (**Figure 3-40**) as found in some Cu_2S minerals. In **Figure 3-40(b)** a cut-out of the sulphur lattice is shown illustrating the *fcc*-like arrangement of the sulphur atoms. There is no S–S bonding interaction as the measured S⋯S distances range from 3.620 Å to 4.660 Å.

Copper atoms occupy various interstitial sites in this sulphur skeleton with different coordination modes. The copper atoms on the periphery are either coordinated trigonally by two sulphur and one phosphorus atom (Cu5, Cu23, Cu26, Cu29, Cu34 and and symm. equiv.) or tetrahedrally by three sulphur and one phosphorus atom (Cu11, Cu12, Cu13, Cu32, Cu45 and symm. equiv.). Two copper atoms (Cu40 and symm. equiv.) coordinate to two sulphur and two phosphorus atoms. The remaining copper atoms inside the sulphur framework show three different coordination spheres. There are 32 copper atoms, which are coordinated linearly by two sulphur atoms (Cu2, Cu3, Cu8, Cu9, Cu14, Cu20, Cu21, Cu24, Cu25, Cu30, Cu35, Cu38, Cu39, Cu43, Cu44, Cu46 and symm. equiv.). 34 copper atoms are surrounded trigonally by three sulphur atoms (Cu1, Cu4, Cu6, Cu7, Cu10, Cu15, Cu16, Cu18, Cu19, Cu22, Cu27, Cu28, Cu31, Cu33, Cu36, Cu37, Cu42 and symm. equiv.). The remaining four copper atoms show tetrahedral coordination by four sulphur atoms (Cu17, Cu41 and symm. equiv.). All observed Cu–S bond lengths are between 2.115(7) Å and 2.799(7) Å. The Cu···Cu distances range from 2.518(5) Å to 3.033(8) Å.

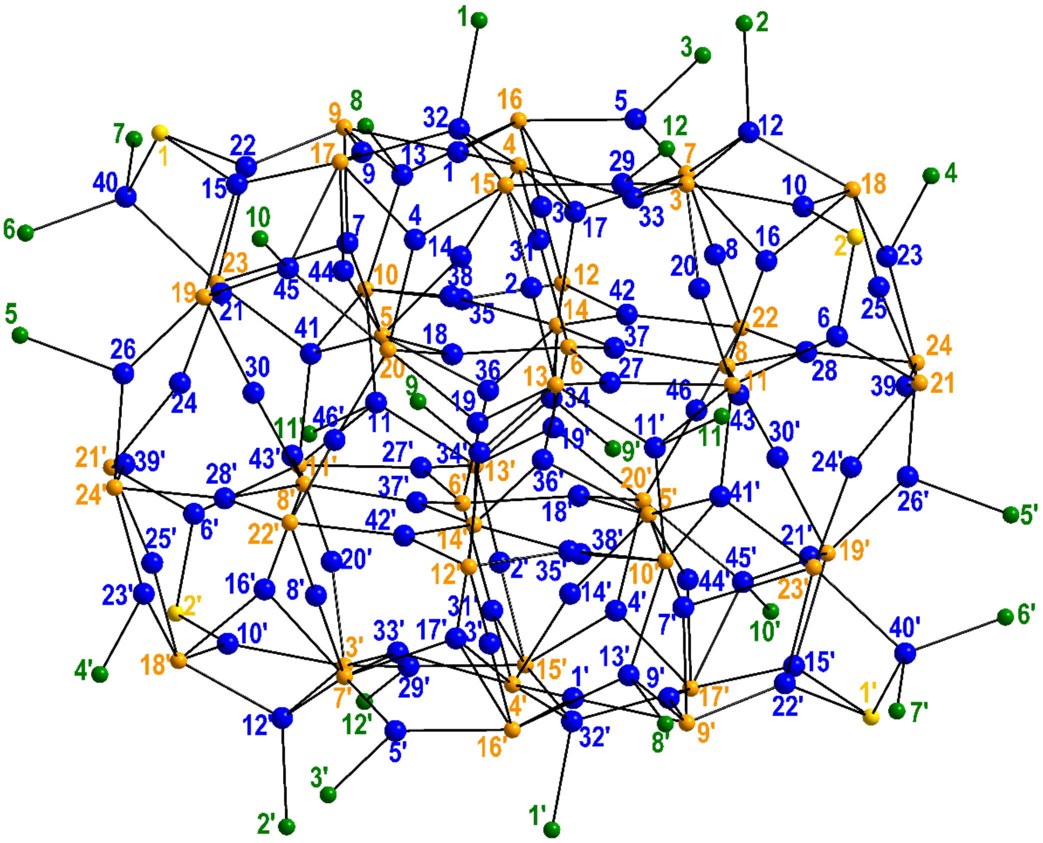

Figure 3-41 *Structure of the heavy atoms core of compound **32** in the solid state.*

The structure of **32** is related to that of [Cu$_{136}$S$_{56}$(SCH$_2$C$_4$H$_3$O)$_{24}$(dpppt)$_{10}$]

which can also be seen as a cut-out of cubic Cu_2S.[33]

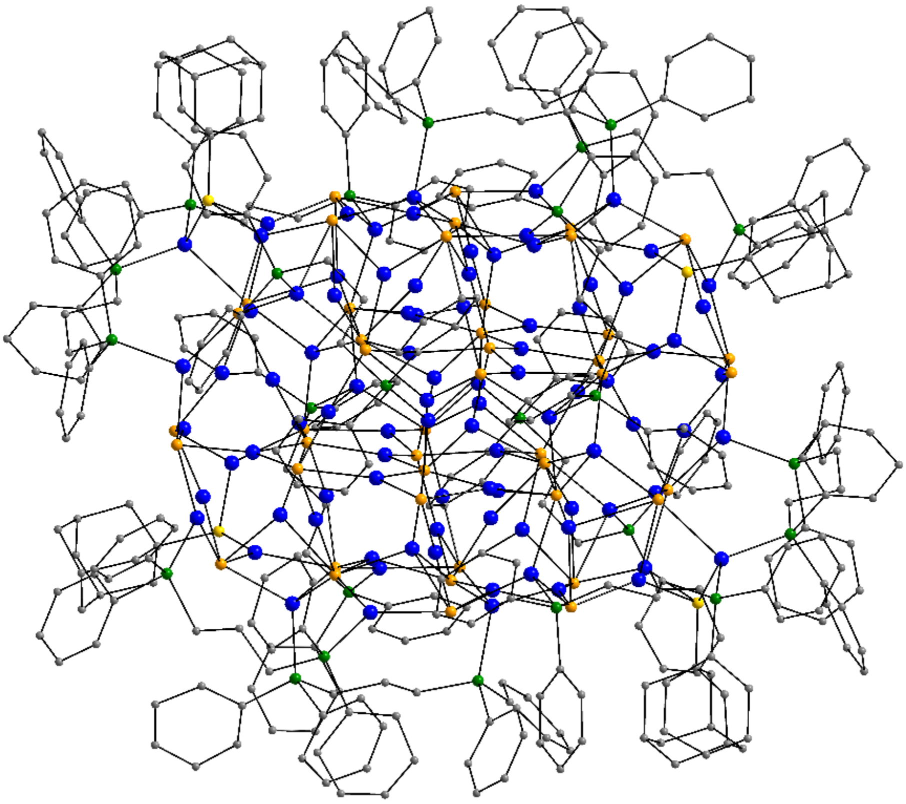

Figure 3-42 *Molecular structure of compound* ***32*** *in the solid state in the same orientation as in* ***Figure 3-41*** *(H atoms omitted).*

3.4.2 $[Cu_{90}S_{44}(SCp)_4(dppp)_{10}(dpppS)_2]$ (33)

Compound **33** crystallizes in the monoclinic space group *C*2/*c* with four molecules per unit cell. Each molecule, which is located on an inversion centre, consists of 90 copper atoms, 44 S^{2-} anions, four SCp^{-} groups, ten dppp ligands and two sulphur-oxidised dpppS ligands. The structures of **32** and **33** are strongly related to each other. The obvious difference is a result of the oxidation of two dppp ligands by sulphur. Therefore these dpppS ligands are coordinated to the cluster core only *via* one phosphorus atom. Besides, there is a difference in composition. In **33** there are only 90 copper atoms. Considering that the 44 S^{2-} anions and the four SCp^{-} groups are present the overall negative charge is 92–. Under the assumption, that all copper atoms are in oxidation state +1, there is no charge balance and **33** can be described as a non-stoichiometric compound.

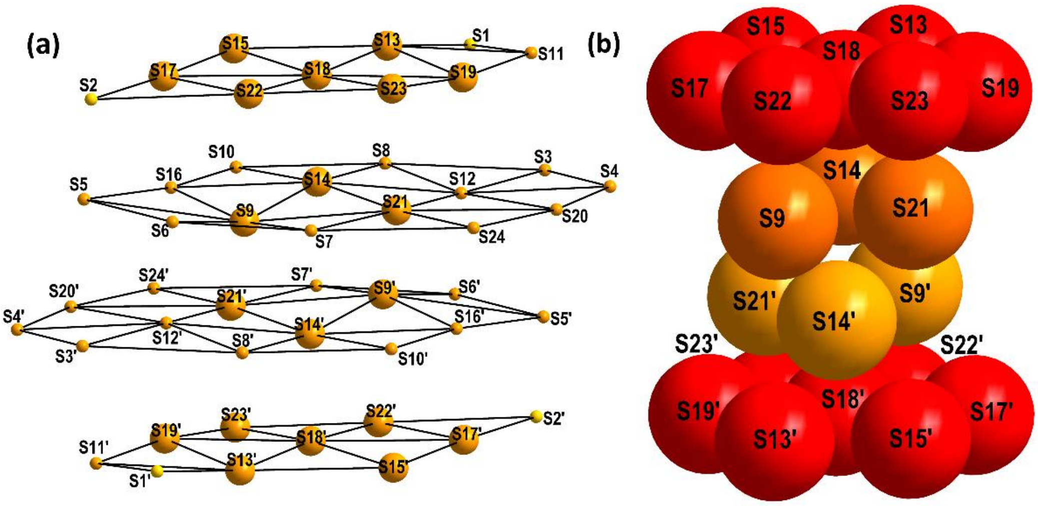

Figure 3-43 (a) *Arrangement of sulphur atoms in compound* ***33****; A-B-C packing mode in fcc lattice marked as bigger ball;* ***(b)*** *space-filling model of captured A-B-C close packing in compound* ***33****.*

Like **32**, **33** also consists of an *fcc*-like sulphur framework. The 48 sulphur atoms (44 S^{2-} and four sulphur from SCp^{-}) are arranged in a four-layer skeleton consisting of 10, 14, 14 and 10 sulphur atoms, respectively. Four sulphur atoms from SCp^{-} locate on the four apexes of this molecule. This framework can be seen as the cut-out of a *fcc* packing (**Figure 3-43**) as found in the bulk phase of Cu_2S.

Copper atoms are localized in the voids of the sulphur substructure with different coordination modes. Cu36 coordinates with one S^{2-} anion, one SCp^{-} and two phosphorus atoms (from dppp and dpppS, respectively). In addition, eight copper atoms (Cu6, Cu8, Cu9, Cu17 and symm. equiv.) are tetrahedrally coordinated with three sulphur atoms and one phosphorus atom; ten copper atoms (Cu10, Cu14, Cu16, Cu18, Cu45 and symm. equiv.) triangularly coordinate with two sulphur atoms and one phosphorus atom; 32 copper atoms (Cu12, Cu13, Cu20, Cu22, Cu24, Cu28, Cu31, Cu32, Cu33, Cu34, Cu35, Cu39, Cu41, Cu42, Cu43, Cu44 and symm. equiv.) linearly bridge two sulphur atoms; 38 copper atoms (Cu1, Cu2, Cu3, Cu4, Cu5, Cu7, Cu11, Cu15, Cu19, Cu21, Cu23, Cu25, Cu26, Cu27, Cu29, Cu30, Cu37, Cu38, Cu40 and symm. equiv.) are distorted trigonal planar connected to three sulphur atoms. The range of Cu–S bond lengths is from 2.141(9) Å to 2.803(7) Å. Cu···Cu distance vary from 2.470(6) Å to 3.056(6) Å.

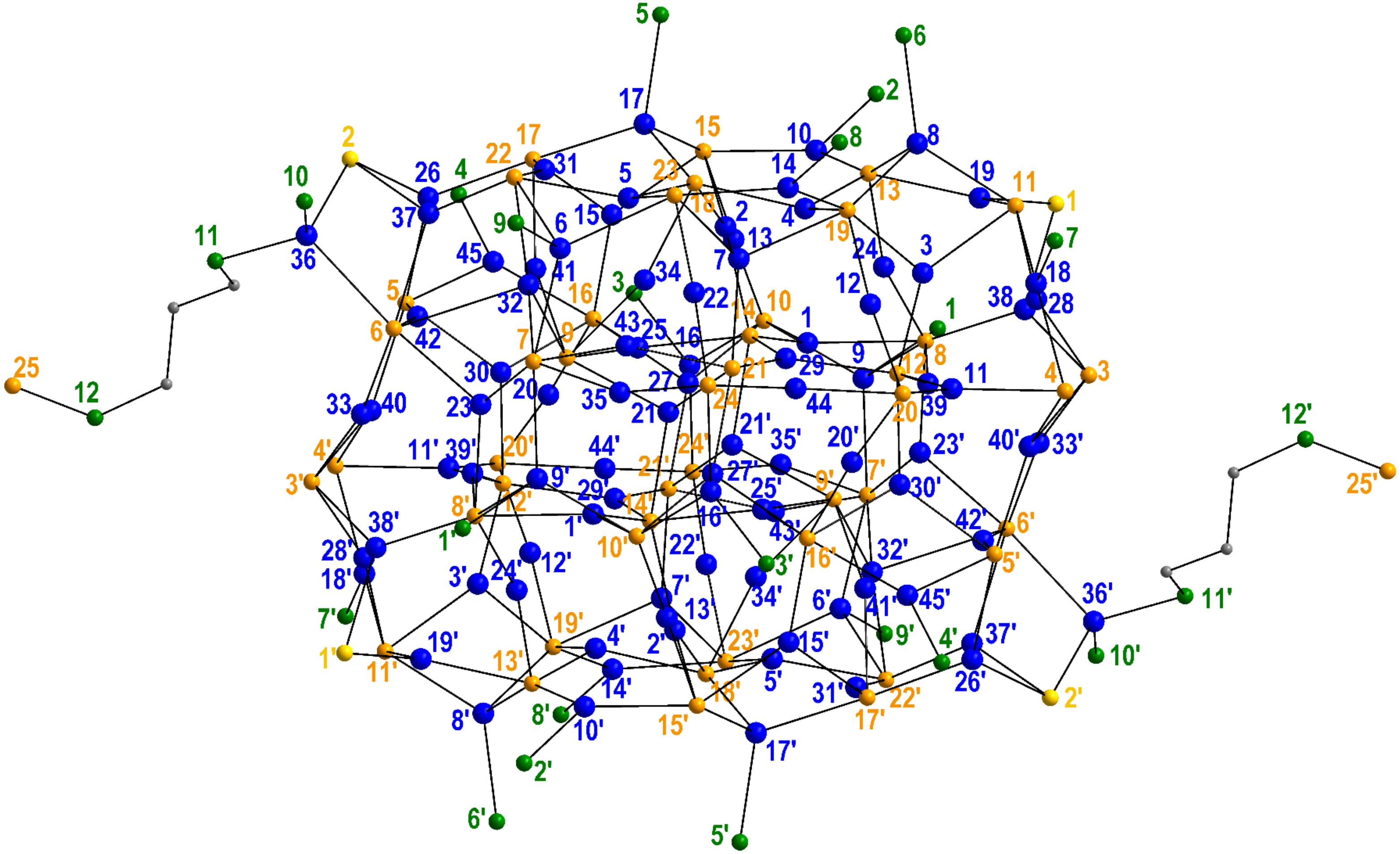

Figure 3-44 *Structure of the heavy atoms core of compound* ***33*** *in the solid state.*

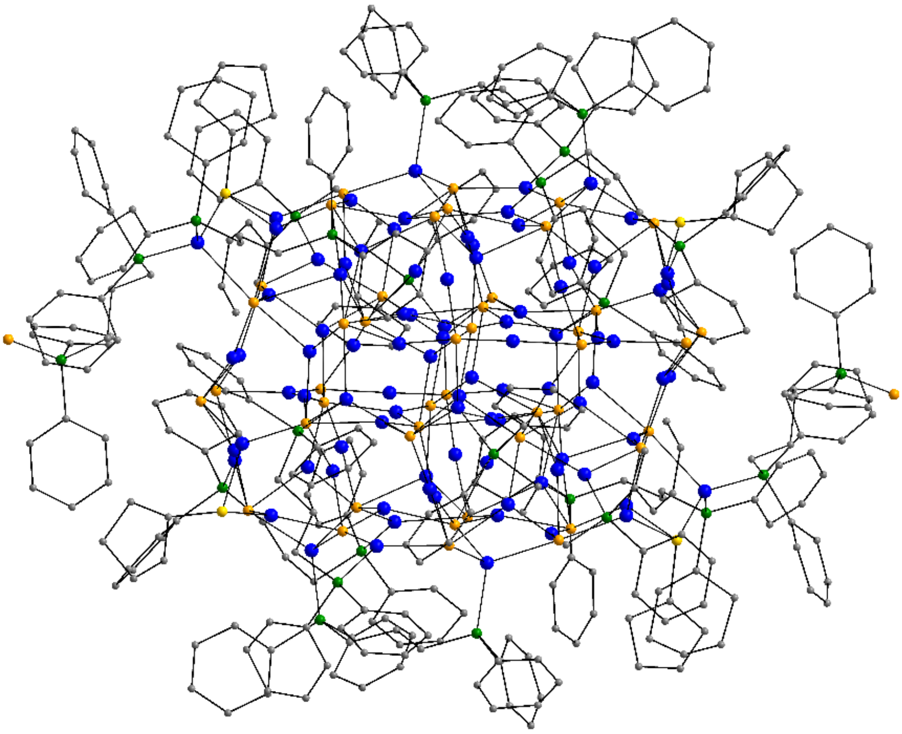

Figure 3-45 *Molecular structure of compound* ***33*** *in the solid state in the same orientation as in* ***Figure 3-44*** *(H atoms omitted).*

3.4.3 [$Cu_{40}Se_{15}(SCp)_{10}(dppp)_6$] (34)

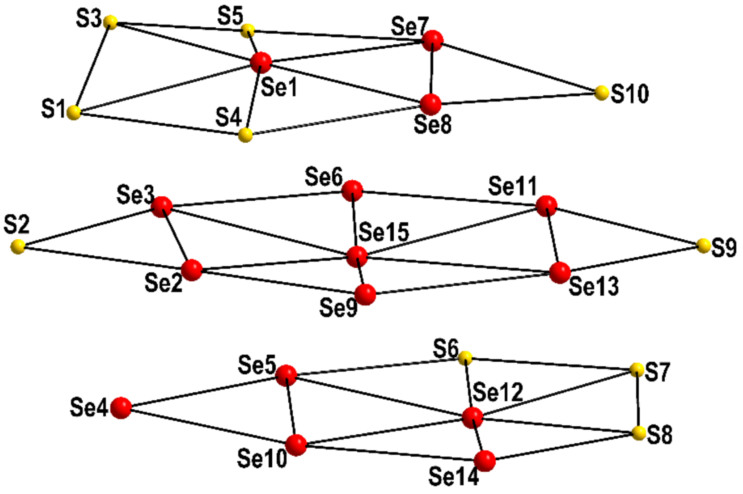

Figure 3-46 *Layer-type arrangement of chalcogen atoms in compound* ***34****.*

Compound **34** crystallizes in the monoclinic space group *P*2$_1$/*n* with four molecules per unit cell. The structure of **34** consists of 40 copper atoms, 15 selenium atoms, ten SCp$^-$ groups and six dppp ligands. The 25 chalcogen atoms in **34** are arranged in three distorted layers consisting of 8, 9 and 8 chalcogen atoms, respectively. There is no bond of neither Se–S nor S–S nor Se–Se because the range of the shortest measured distances within the layers (shown in **Figure 3-46**) of S···S, Se···S and Se···Se are 3.740 Å–4.120 Å, 3.440 Å–4.360 Å and 3.920 Å–4.740 Å, respectively.

Copper atoms show different coordination geometry in **34**. As for tetrahedral geometry, four copper atoms (Cu3, Cu5, Cu8, Cu12) coordinate with one phosphorus atom and three selenium atoms; two copper atoms (Cu23, Cu35) coordinate with four selenium atoms; three copper atoms (Cu6, Cu7, Cu11) coordinate with one phosphorus atom, one sulphur atom and two selenium atoms.

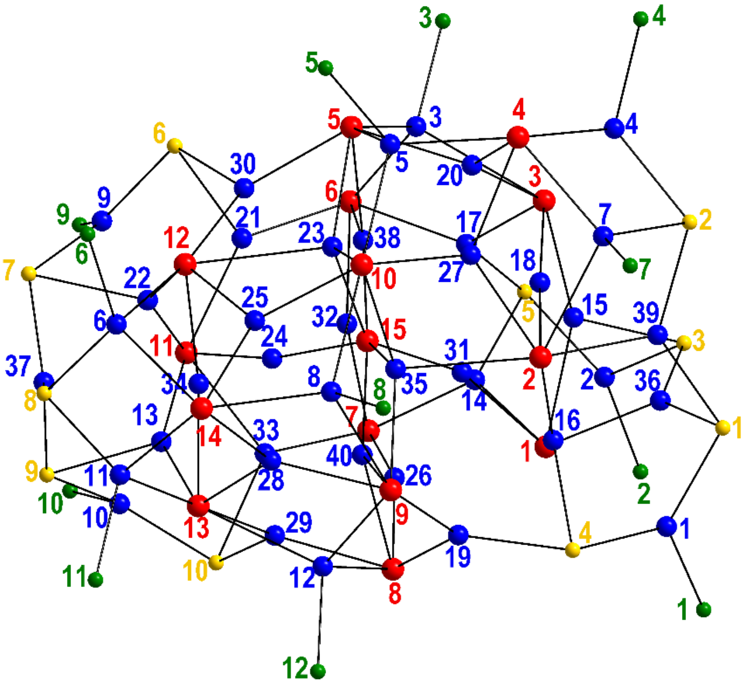

Figure 3-47 *Structure of the heavy atoms core of compound* ***34*** *in the solid state.*

Six copper atoms (Cu18, Cu24, Cu26, Cu31, Cu32, Cu34) linearly bridge two selenium atoms; Cu4 coordinates with one phosphorus atom, one sulphur atom and one selenium atom; four copper atoms (Cu1, Cu2, Cu9 and Cu10) coordinate with two sulphur atoms and one phosphorus atom; Cu37 coordinates with three sulphur atoms; Cu36 and Cu39 coordinate with two sulphur atoms and one selenium atom; six copper atoms (Cu20, Cu25, Cu27, Cu28, Cu38, Cu40) coordinate with three selenium atoms; the remaining eleven copper atoms (Cu13, Cu14, Cu15, Cu16, Cu17, Cu19, Cu21, Cu22, Cu29, Cu30, Cu33) coordinate with two selenium atoms and one sulphur atom. All Cu–Se bond lengths range from 2.153(5) Å to 2.902(3) Å and Cu–S from 2.230(5) Å to 2.386(5) Å and the Cu···Cu distances are 2.515(3) Å to 3.033(3) Å.

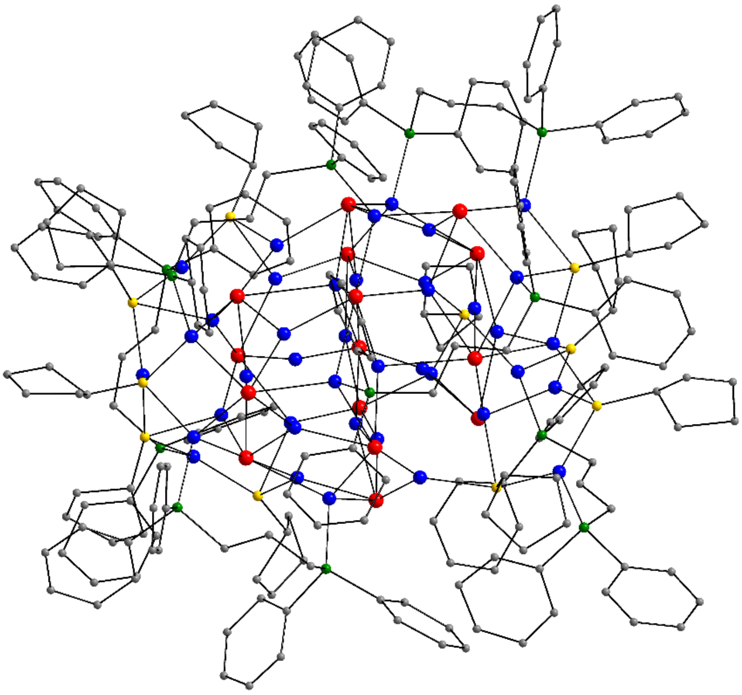

Figure 3-48 *Molecular structure of* ***34*** *in the solid state in the same orientation as in* ***Figure 3-47*** *(H atoms omitted).*

3.4.4 [$Cu_{61}Se_{31}(dppp)_{10}$] (35)

Compound **35** crystallizes in the triclinic space group $P\overline{1}$ with two molecules per unit cell. **35** consists of 61 copper atoms, 31 selenium atoms and ten dppp ligands. Counting every selenium atom as charged 2–, a stoichiometrically composed molecule should have 62 copper(I) ions. As mentioned before non-stoichiometric copper selenium clusters with a Cu:Se ratio lower than 2 have been observed several times: e.g. [$Cu_{29}Se_{15}(PiPr_3)_{12}$][46] and

$[Cu_{74}Se_{38}(PCy_3)_{18}]$[66]**.** This reflects the observation made in copper selenide minerals, where compositions of $Cu_{2-x}Se$ are common.

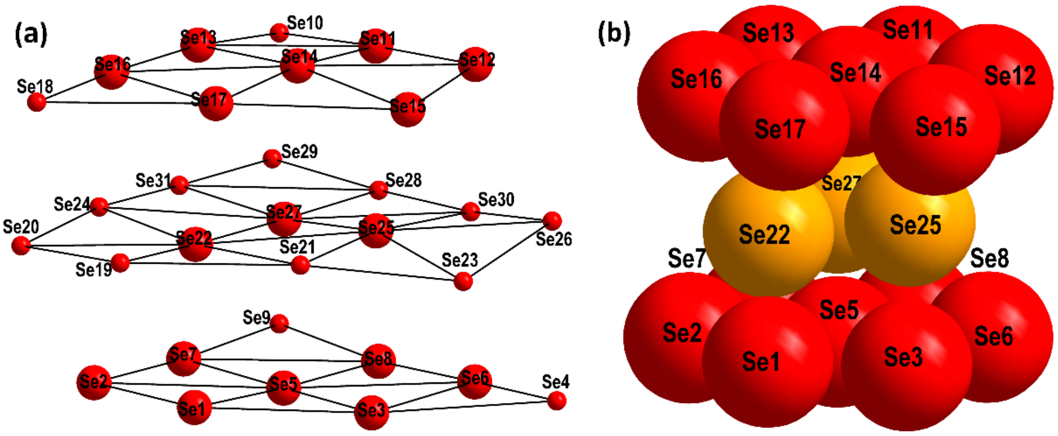

***Figure 3-49 (a)** Selenium substructure in **35**, presenting hcp mode (A-B-A packing marked as bigger balls); **(b)** space filling model of a part of the selenium substructure to demonstrate the hcp mode in **35**.*

The selenium atoms in **35** are arranged in three close packed hexagonal layers containing 9, 13 and 9 atoms, respectively (**Figure 3-49(a)**). The distances between the layers are approximately 3.45 Å and 3.59 Å. The selenium framework can be described as a cut-out of a *hcp* (A-B-A stacking, **Figure 3-49(b)**). All the measured Se···Se distances shown in **Figure 3-49(a)** within the layers range from 3.700 Å to 4.690 Å, indicating non-bonding contacts. In view of the known phosphine stabilized copper selenium clusters with less than 60 copper atoms, which form ball- or ellipsoidal-like molecules, the structure of **35** is the first example where the selenium substructure changes from spherical arrangement to a layer-like structure. A further growth of the selenium network has been observed in $[Cu_{70}Se_{35}(P\textit{t}Bu_2Me)_{21}]$[34] and $[Cu_{140}Se_{70}(PEt_3)_{34}]$[49] with 10-15-10 or 21-28-21 selenium atoms in the first, second and third layer, respectively. In summary this means that **35** is a small piece of copper selenide with a *hcp* network of selenium, which has not been observed in minerals so far.

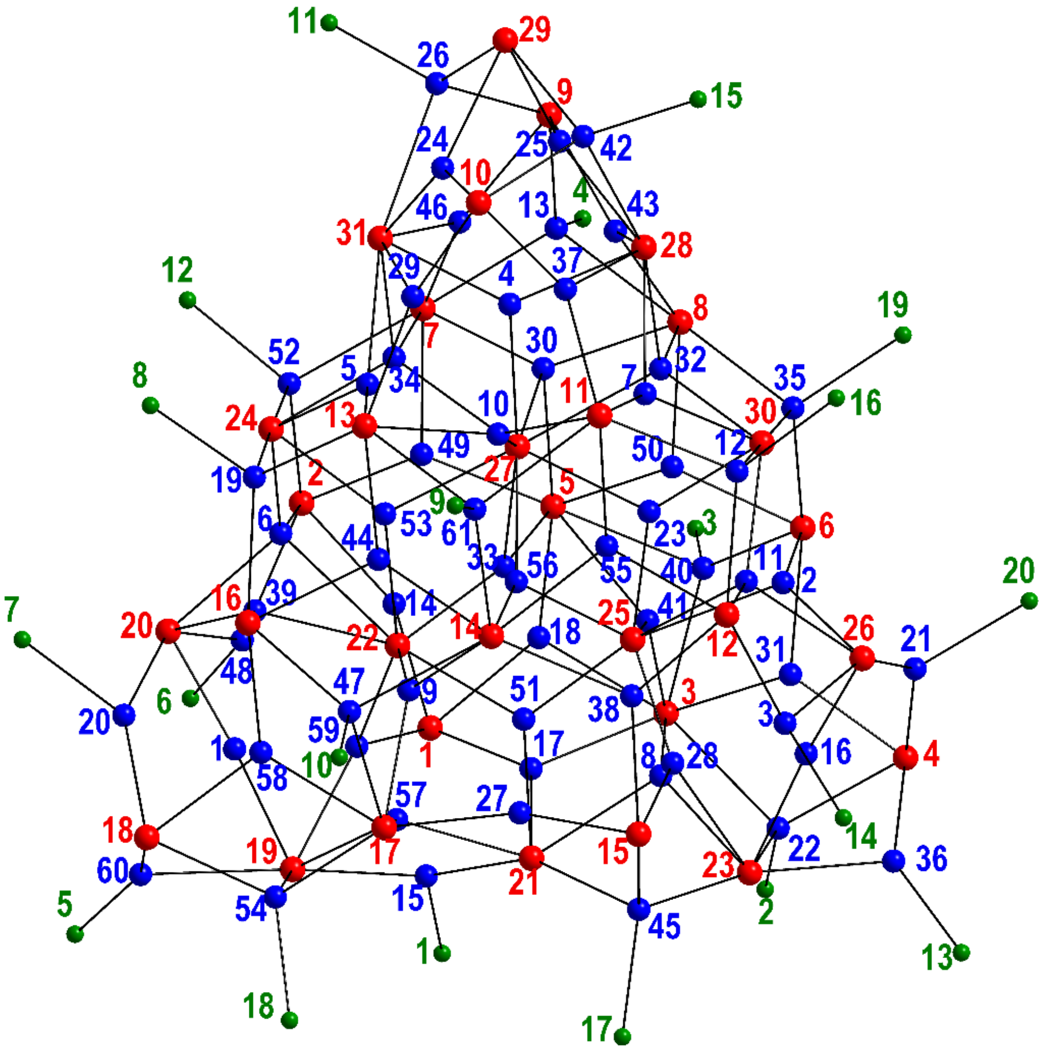

Figure 3-50 *Structure of the heavy atoms core of compound* ***35*** *in the solid state.*

As in previously described compounds, the copper atoms in **35** show various coordination modes. Copper atoms coordinating to phosphorus atoms are located on the surface of the selenium framework. They can be divided into two groups. 13 $CuPSe_3$ groups (Cu12, Cu13, Cu19, Cu22, Cu26, Cu35, Cu40, Cu42, Cu45, Cu47, Cu52, Cu54, Cu61) show tetrahedral geometry; seven $CuPSe_2$ groups are trigonal planar (Cu3, Cu15, Cu20, Cu21, Cu36, Cu48, Cu60). Inside the selenium framework one can identify three linearly coordinated copper atoms (Cu1, Cu16, Cu27) and five tetrahedrally coordinated copper atoms (Cu6, Cu11, Cu30, Cu32, Cu34). The remaining 33 copper atoms show trigonal planar coordination with three selenium atoms. Cu–Se bond lengths range from 2.200(5) Å to 2.942(3) Å.

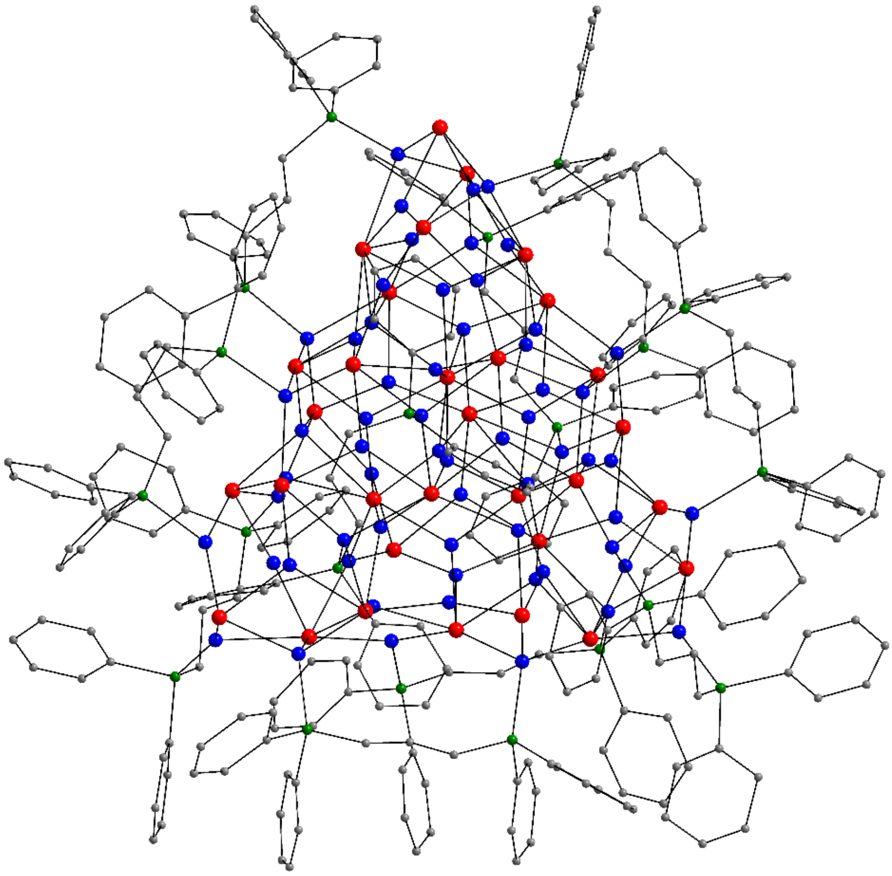

__Figure 3-51__ Molecular structure of __35__ in the solid state in the same orientation as in __Figure 3-50__ (H atoms omitted).

3.4.5 [$Cu_{61}Se_{26}(SCy)_9(PPh_3)_{14}$] (36)

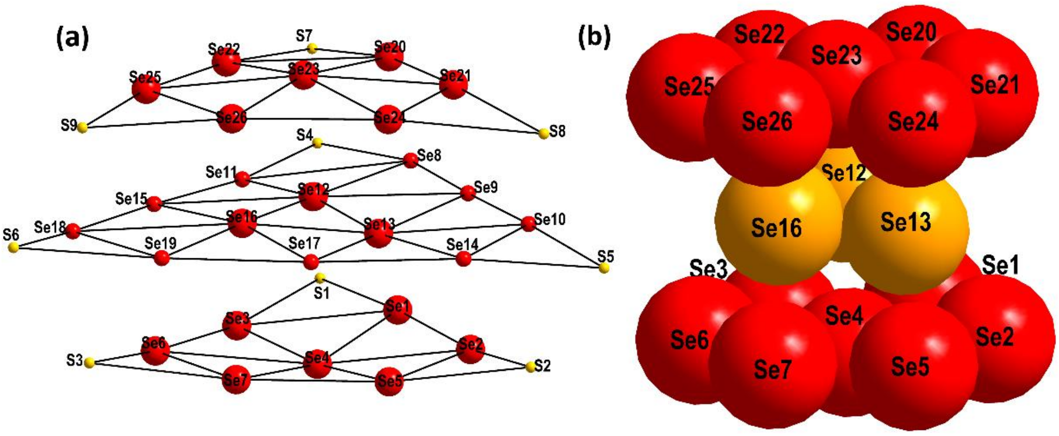

__Figure 3-52 (a)__ Chalcogen substructure in __36__ demonstrating the hcp (A-B-A packing – atoms marked as bigger balls); __(b)__ space filling cut-out of the selenium network in __36__.

Compound **36** crystallizes in the monoclinic space group $P2_1/c$ with four molecules per unit cell. The charge of 61 copper(I) ions is balanced by 26 Se^{2-} ions and nine SCy^- ligands. Similar with **35**, there is a three-layer chalcogen substructure in **36** consisting of Se_7S_3 in the first and third layer and $Se_{12}S_3$ in the middle layer. This is similar to the selenium arrangement found in $[Cu_{70}Se_{35}(PtBu_2Me)_{21}]$[34], where one finds pure selenium layers consisting of 10 selenium in the first and third layer and 15 selenium atoms in the middle layer. In **36** the corners of the chalcogen triangles are occupied by the sulphur atoms of the SCy^- groups (**Figure 3-52**).

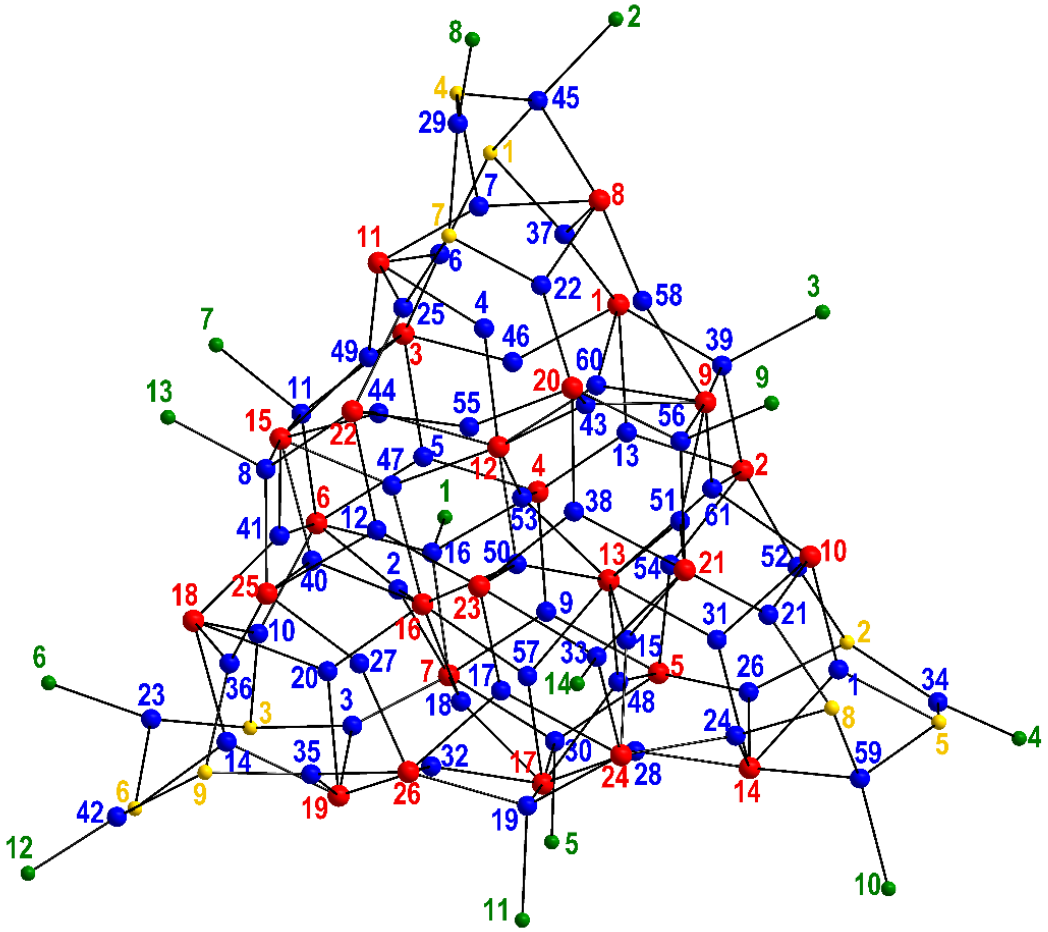

***Figure 3-53** Structure of the heavy atoms core of **36** in the solid state.*

14 copper atoms are found on the surface of the chalcogen framework. These atoms coordinate with phosphorus atoms and additionally bond to either two sulphur atoms (Cu23, Cu29, Cu34, Cu42) or three selenium atoms (Cu8, Cu11, Cu16, Cu19, Cu30, Cu33, Cu39, Cu56), whereas the remaining ones (Cu45, Cu59) coordinate with two sulphur and one selenium atom. The other

copper atoms occupy voids between the selenium layers. Similar to the structure of **35** these copper atoms show linear, trigonal planar or tetrahedral coordination. Besides, three copper atoms (Cu50, Cu51, Cu61) nearly tetrahedrally bond to four selenium atoms; six copper atoms (Cu4, Cu27, Cu46, Cu54, Cu55, Cu58) linearly link two Se atoms; 15 copper atoms (Cu1, Cu3, Cu6, Cu7, Cu10, Cu14, Cu21, Cu22, Cu24, Cu25, Cu26, Cu35, Cu36, Cu37, Cu52) triangularly connect to two selenium atoms and one sulphur atom and the remaining copper atoms coordinate with three selenium atoms. The Cu–Se bond lengths range from 2.233(4) Å to 2.922(3) Å, Cu–S distances vary from 2.234(5) Å to 2.446(5) Å.

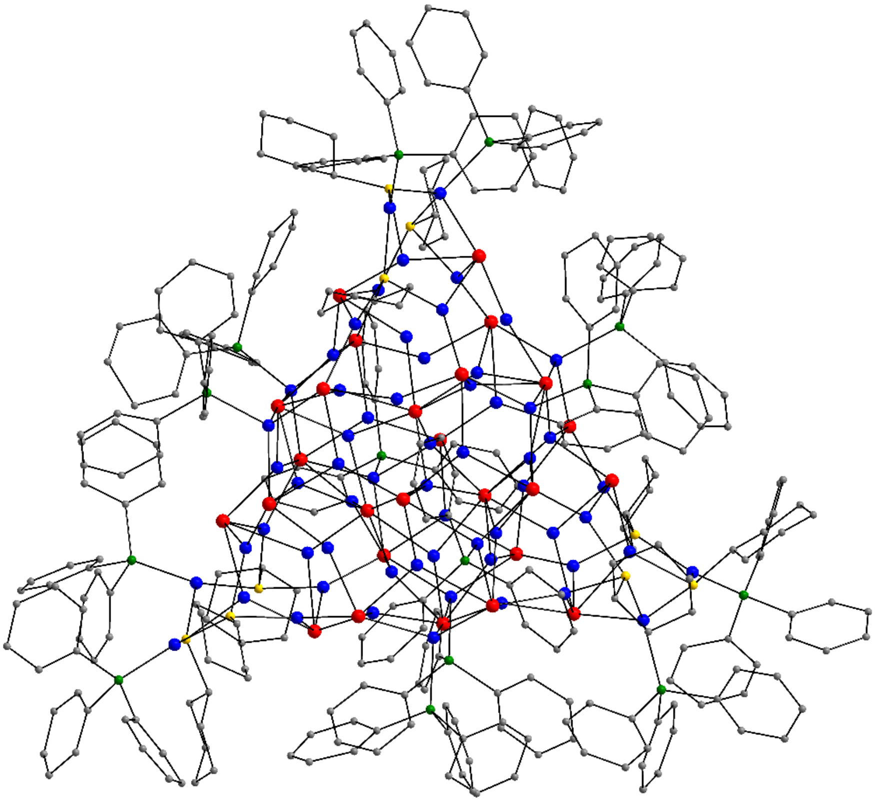

Figure 3-54 *Molecular structure of* ***36*** *in the solid state in the same orientation as in* ***Figure 3-53*** *(H atoms omitted).*

3.4.6 [$Cu_{51}Se_{26}(PPh_3)_{16}$] (37)

Compound **37** crystallizes in the triclinic space group $P\overline{1}$ with two molecules per unit cell. In contrast to the previously described structures of **35** and **36** with A-B-A stacking of chalcogen layers compound **37** shows a ball-like structure. The selenium framework of **37** (**Figure 3-55**) consists of an inner Se_3 triangle (Se7, Se16, Se24) surrounded by a deltahedron of 23 selenium atoms. The shortest Se···Se distances range from 3.810 Å to 4.900 Å.

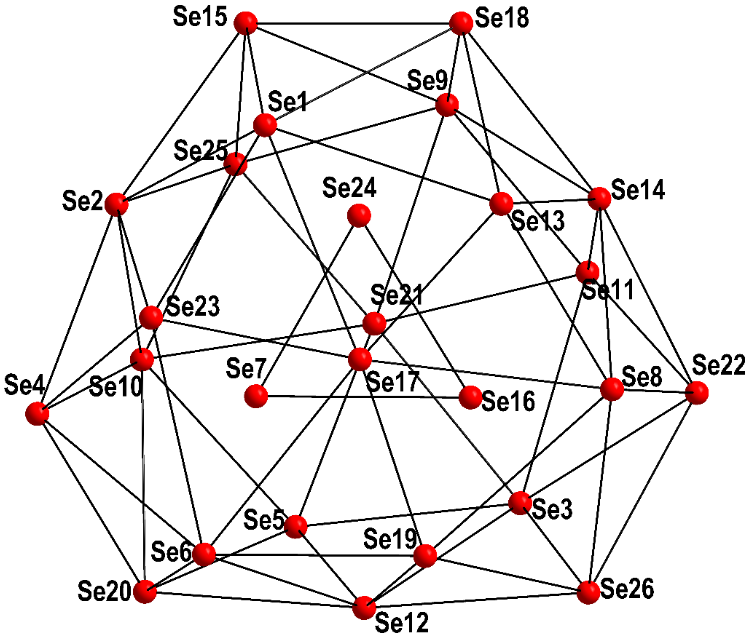

Figure 3-55 *Selenium arrangement of compound* ***37****.*

Copper atoms, which only coordinate with selenium atoms, present linear (Cu16, Cu17, Cu36, Cu46), triangular (Cu1, Cu4, Cu5, Cu7, Cu8, Cu9, Cu10, Cu11, Cu13, Cu14, Cu15, Cu22, Cu23, Cu26, Cu32, Cu33, Cu34, Cu35, Cu38, Cu39, Cu41, Cu47, Cu50) and tetrahedral (Cu25, Cu29, Cu30, Cu31, Cu40, Cu44, Cu49, Cu51) coordination mode with Cu–Se distances from 2.333 Å to 2.939 Å. Eight copper atoms (Cu2, Cu3, Cu12, Cu20, Cu28, Cu42, Cu43, Cu48) bond to two selenium atoms and one phosphine ligand present trigonal planar coordination. The remaining copper atoms (Cu6, Cu18, Cu19, Cu21, Cu24, Cu27, Cu37, Cu45) are distorted tetrahedrally coordinated by three selenium atoms and one triphenylphosphine ligand.

The structure of **37** looks like the earlier described $[Cu_{52}Se_{26}(PPh_3)_{16}]$[48]. Although these two compounds share a similar selenium framework, there are some structural differences.

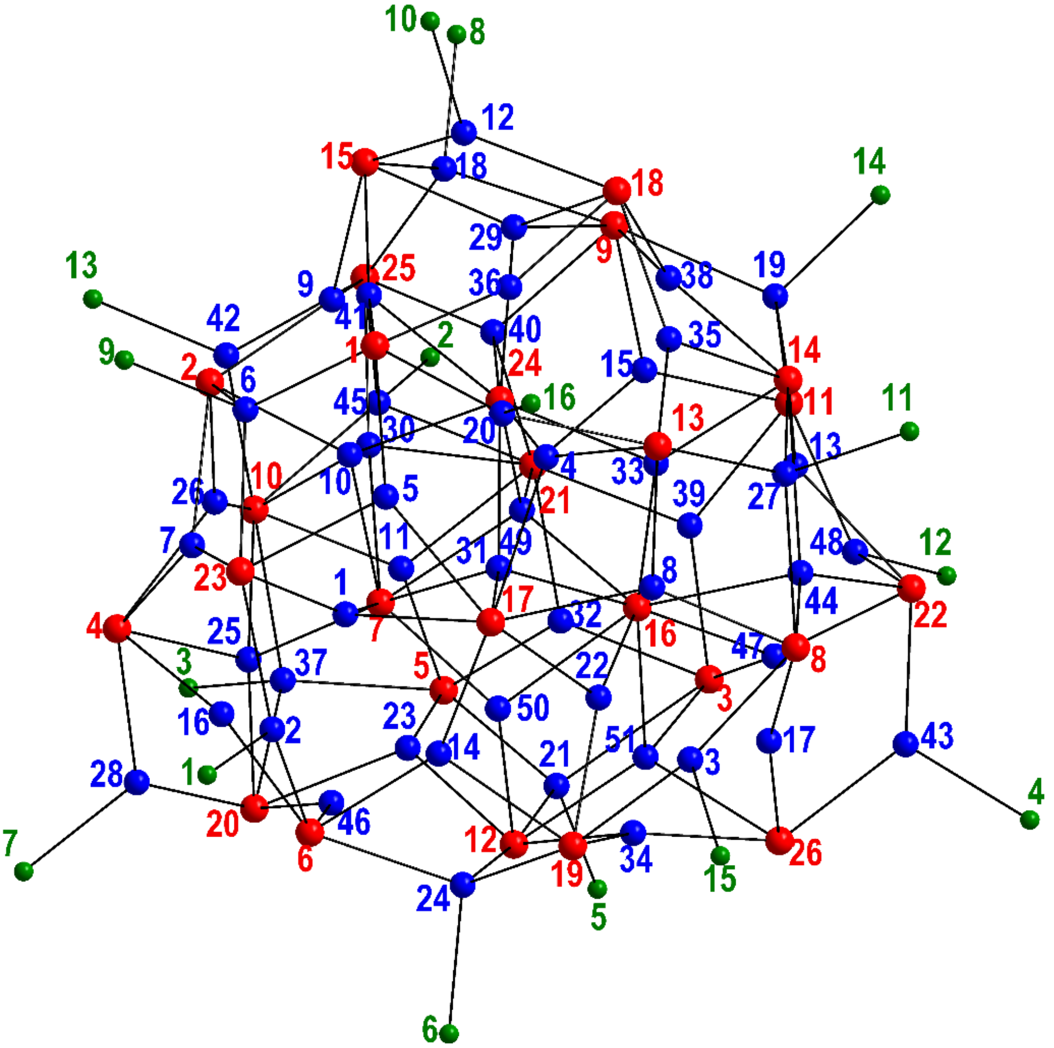

Figure 3-56 *Structure of the heavy atoms core of **37** in the solid state.*

As for the coordination modes of the copper atoms in [$Cu_{52}Se_{26}(PPh_3)_{16}$][48], 20 cooper atoms are present within the selenium polyhedron present triangular coordination mode. Eight copper atoms have a tetrahedral environment, and four copper atoms are coordinated in a linear fashion. [$Cu_{52}Se_{26}(PPh_3)_{16}$] is strictly stoichiometric with a Cu:Se ratio of 2:1, whereas in **37** there is a deficiency of copper. As mentioned before this seems to be a characteristic behaviour of phosphine protected copper selenides.

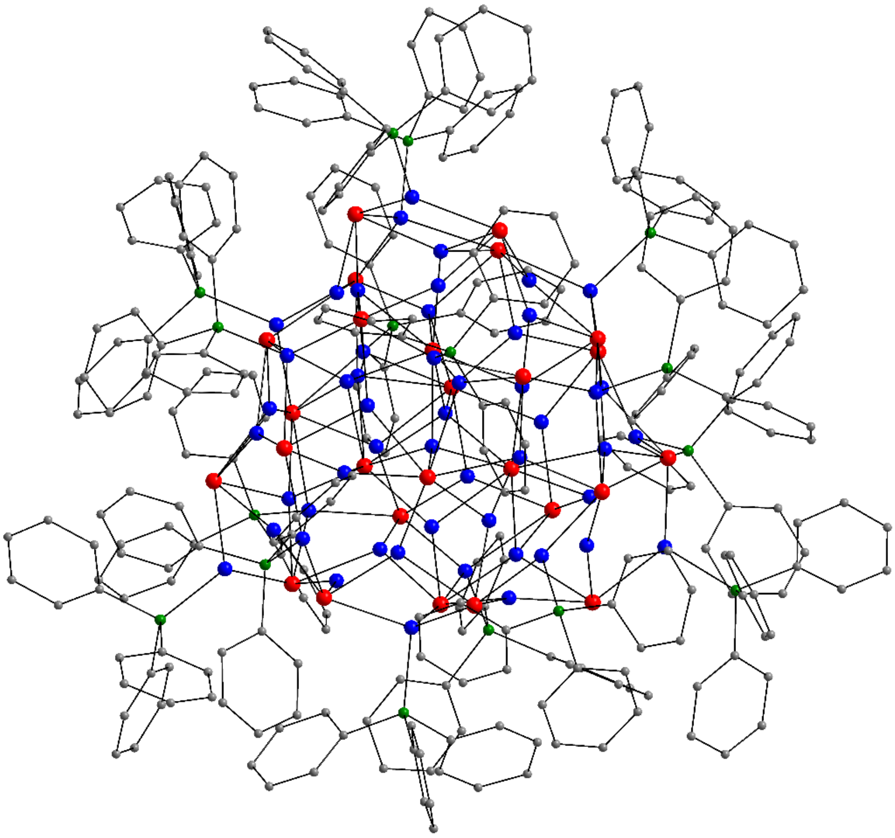

Figure 3-57 *Molecular structure of **37** in the solid state in the same orientation as in **Figure 3-56** (H atoms omitted).*

3.4.7 $[Cu_{73}Se_{37}(PPh_3)_{19}]\cdot(C_7H_{16})$ (38·(C_7H_{16}))

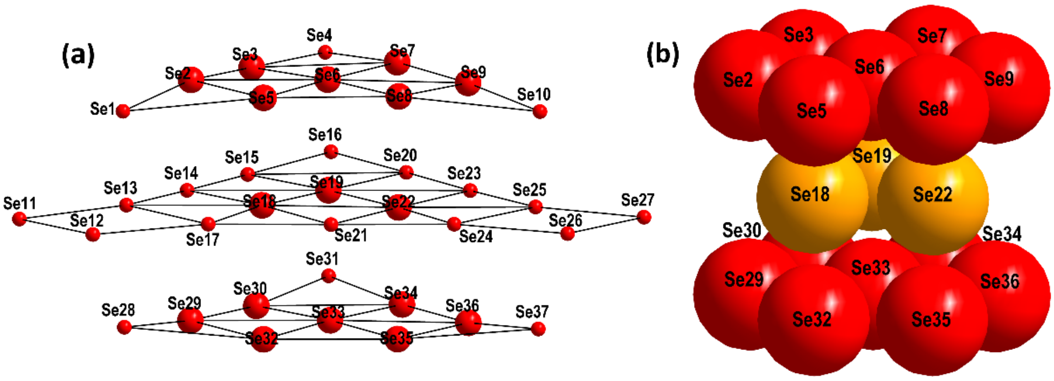

Figure 3-58 (a) *Three-layer selenium skeleton of compound **38** (A-B-A packing atoms marked as bigger balls); **(b)** space-filling model of captured hcp mode in compound **38**.*

Compound **38** crystallizes in the triclinic space group $P\overline{1}$ with two molecules per unit cell. Each molecule consists of 73 copper atoms, 37 selenium atoms and 19 PPh_3 ligands. **38** is another example where the Cu:Se ratio is less than 2:1.

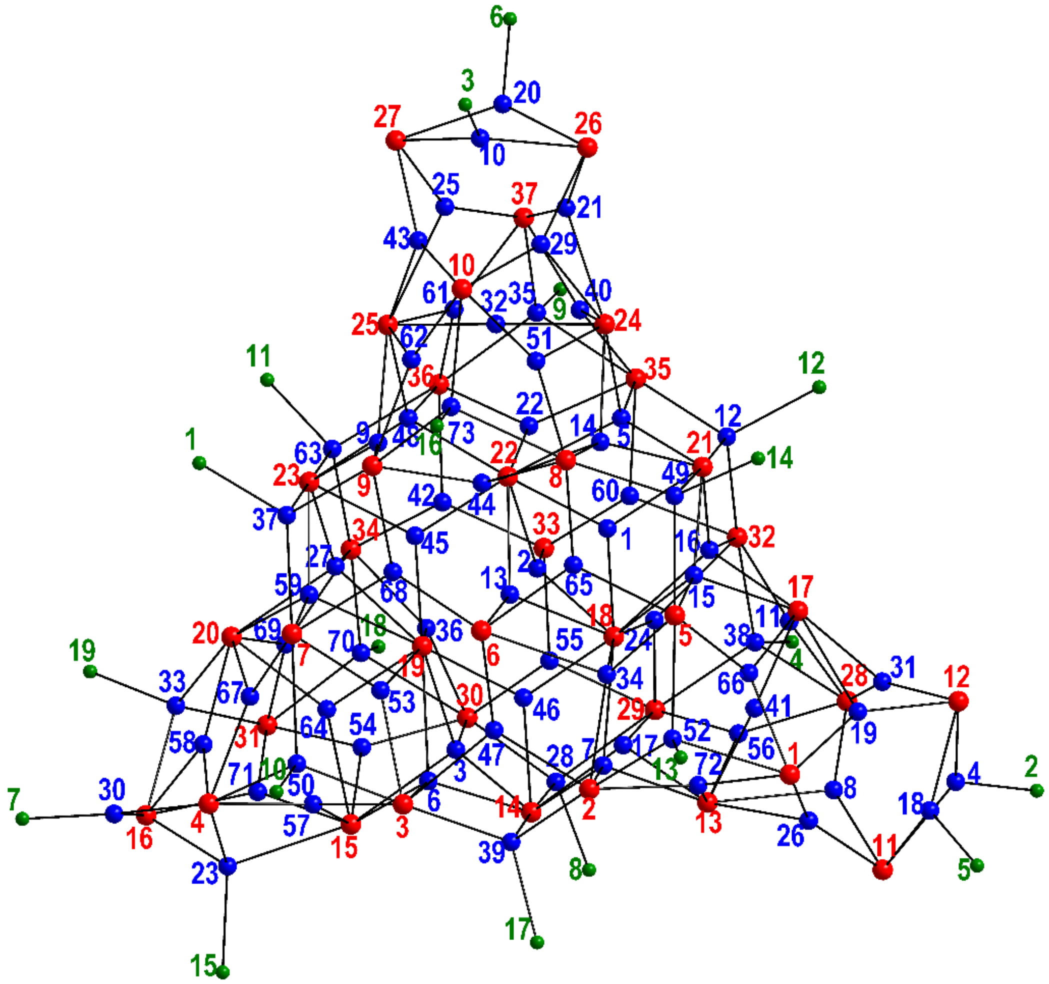

Figure 3-59 *Structure of the heavy atoms core of compound* ***38*** *in the solid state.*

Similar to **35** and **36**, compound **38** shows a layer-type structure with three selenium layers consisting of 10, 17 and 10 atoms. These layers are organized in a nearly *hcp* mode. This structural feature has also been described for $[Cu_{70}Se_{35}(PtBu_2Me)_{21}]$[34] $[Cu_{72}Se_{36}(PPh_3)_{20}]$[48] and $[Cu_{74}Se_{38}(PCy_3)_{18}]$.[66]

In these three compounds the selenium networks consist of 10, 15 and 10, 10, 16 and 10 and 10, 18 and 10 atoms, respectively. In this sense **38** is the missing link in the growing process to larger Cu/Se clusters (**Figure 3-60**).

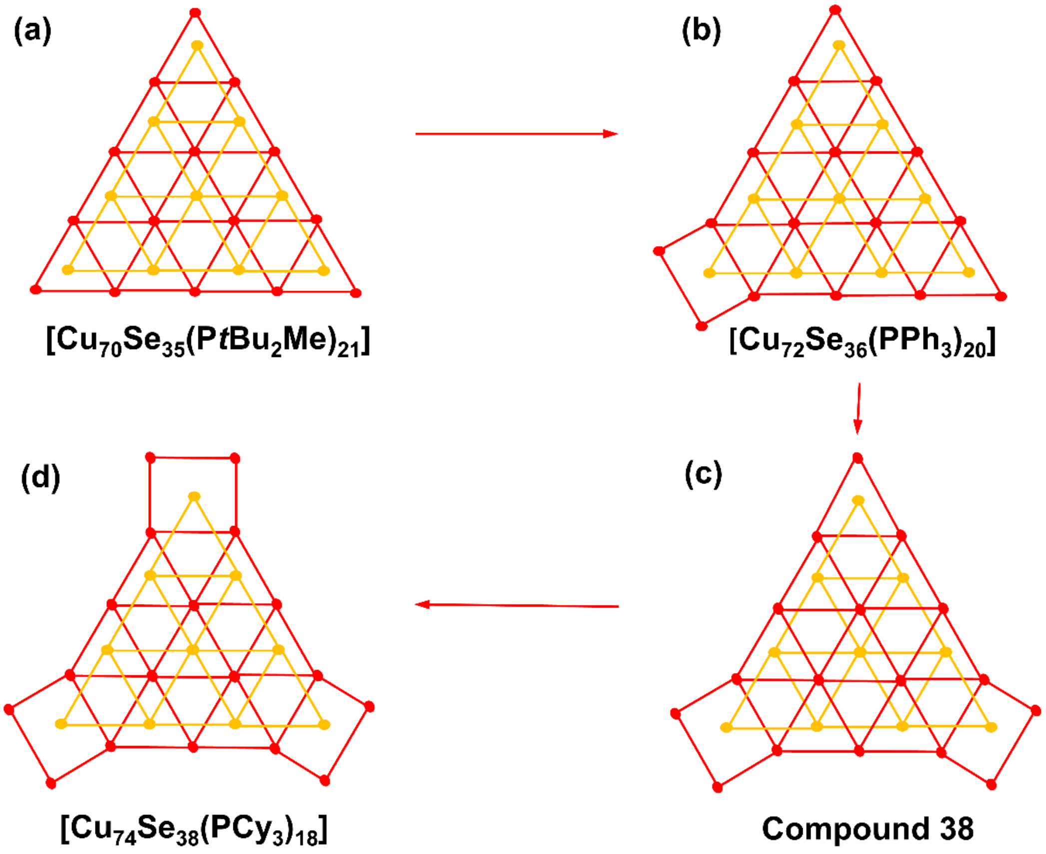

$[Cu_{70}Se_{35}(PtBu_2Me)_{21}]$

$[Cu_{72}Se_{36}(PPh_3)_{20}]$

$[Cu_{74}Se_{38}(PCy_3)_{18}]$

Compound 38

Figure 3-60 *Idealised selenium networks in* ***(a)*** *$[Cu_{70}Se_{35}(PtBu_2Me)_{21}]$[34],* ***(b)*** *$[Cu_{72}Se_{36}(PPh_3)_{20}]$[48],* ***(c)*** *compound* ***38*** *and* ***(d)*** *$[Cu_{74}Se_{38}(PCy_3)_{18}]$[66], demonstrating the growth of copper selenium clusters.*

In **38**, 19 phosphine ligands bond to copper atoms at the periphery of the Cu_{73} core with two different coordination modes: 14 copper atoms (Cu12, Cu23, Cu28, Cu33, Cu35, Cu37, Cu38, Cu39, Cu49, Cu50, Cu52, Cu63, Cu70, Cu73) tetrahedrally coordinate with three selenium atoms and one phosphorus atom, whereas five copper atoms (Cu4, Cu10, Cu18, Cu20, Cu30) trigonally bond to two selenium atoms and one phosphine ligand. The other copper atoms coordinate exclusively with selenium atoms in three types of geometries: (1) Cu32 and Cu41 linearly bridge two selenium atoms; (2) eleven copper atoms (Cu3, Cu5, Cu6, Cu7, Cu14, Cu15, Cu16, Cu27, Cu34, Cu48, Cu59) tetrahedrally coordinate with four selenium atoms; (3) the remaining copper atoms triangularly connect three selenium atoms. The Cu–Se bond lengths in **38** vary from 2.313(3) Å to 2.906(3) Å.

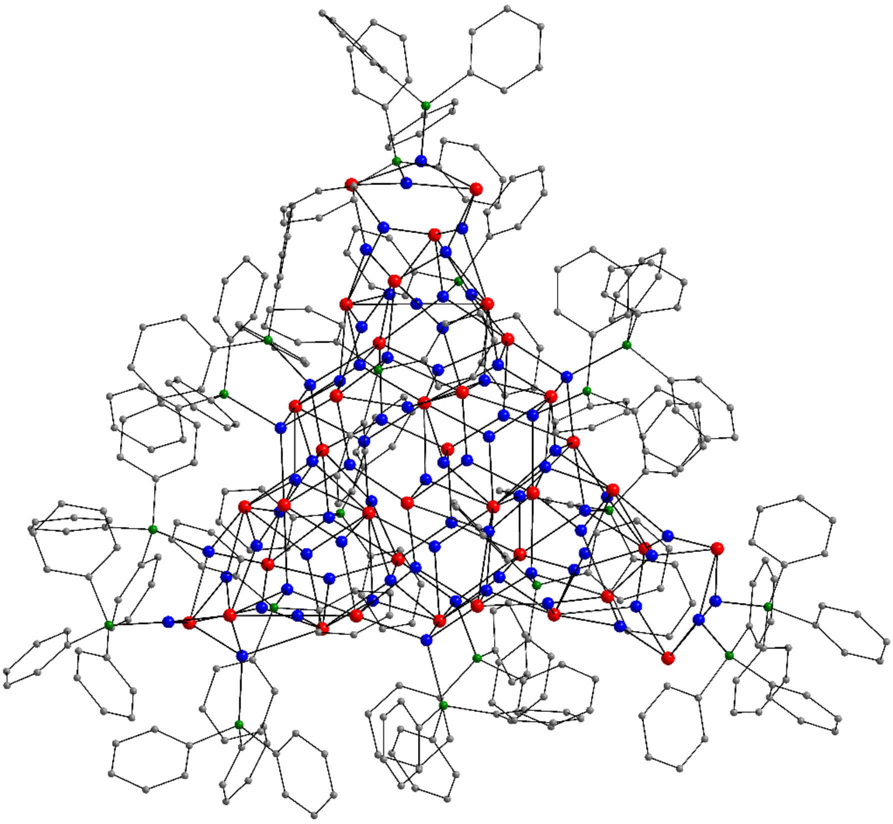

Figure 3-61 *Molecular structure of **38** in the solid state in the same orientation as in **Figure 3-60** (H atoms omitted).*

3.4.8 $[Cu_{94}Se_{43}(SCy)_9(PPh_3)_{18}]$ (39)

A further step in the growing process from small to large copper chalcogenide clusters can be seen in the structure of **39**.

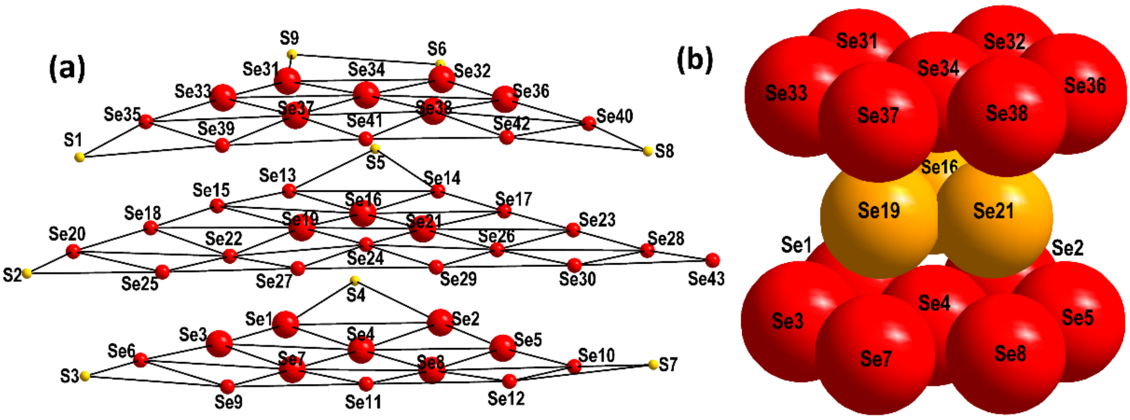

Figure 3-62 (a) *Chalcogenide framework of compound **39**, A-B-A Packing marked as bigger balls; **(b)** space-filling model of the A-B-A packing mode.*

Compound **39** crystallizes in the monoclinic space group *P*2/*c* with four molecules per unit cell. Every molecule is composed of 94 copper atoms, 43 selenium atoms, nine cyclohexyl thiolate groups and 18 PPh_3 ligands. Like the compounds described before (**35**, **36** and **38**) the chalcogen framework consisting of 43 selenium atoms and nine sulphur atoms shows a layer-like packing structure (**Figure 3-62**). Concerning the selenium network there are 12, 19 and 12 selenium atoms arranged in a *hcp* mode. In the top layer, there are four sulphur atoms occupying the corners. In the middle layer two sulphur atoms are localized on the corners. The third layer can be derived from a Se_{15} layer where the three atoms at the corners are substituted by sulphur atoms. This yields to the three layers with compositions $Se_{12}S_4$, $Se_{19}S_2$ and $Se_{12}S_3$. This build-up is strongly related to the structure of the previously published $[Cu_{93}Se_{42}(SeC_6H_4SMe)_9(PPh_3)_{18}]_2$ and $[Cu_{96}Se_{45}(SeC_6H_4SMe)_6(PPh_3)_{18}]$.[33]

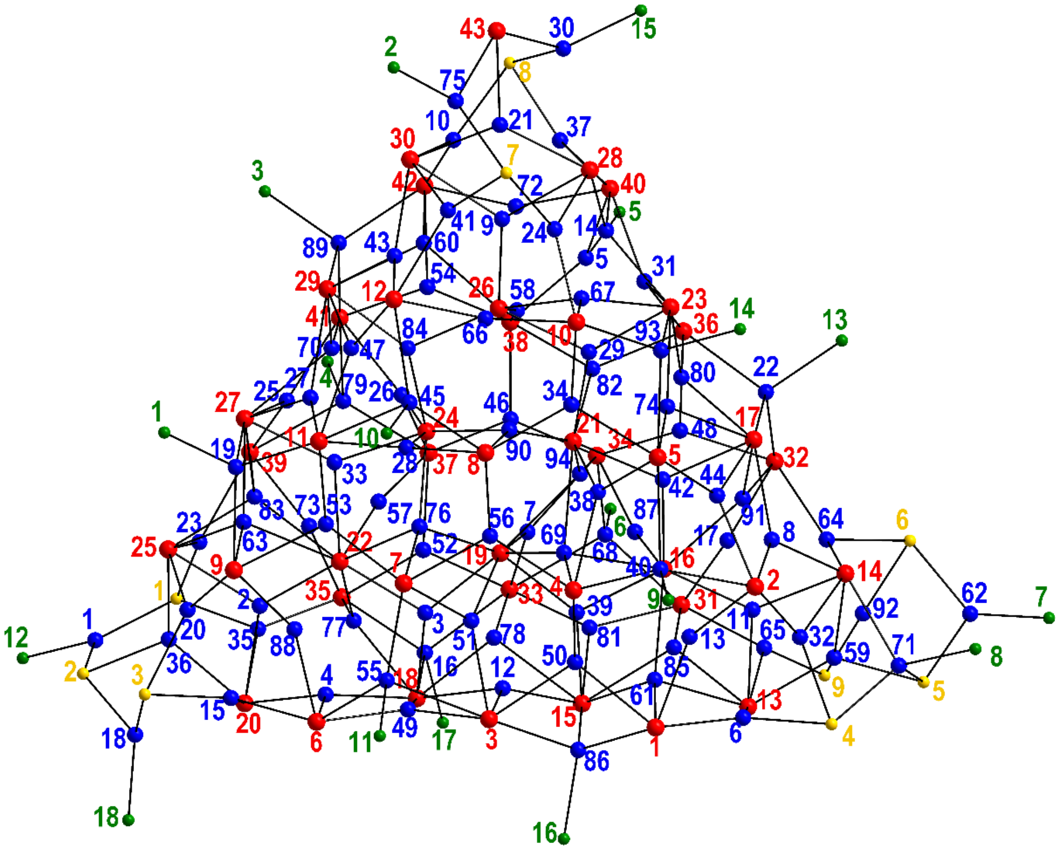

***Figure 3-63** Structure of the heavy atoms core of **39** in the solid state.*

Copper atoms in **39** present linear, triangular or tetrahedral coordination mode. 18 copper atoms coordinate with phosphorus atoms, of which three (Cu1, Cu18, Cu62) coordinate with two sulphur atoms and one phosphorus atom, Cu5 coordinates with two selenium atoms and one phosphorus atom, two (Cu30, Cu75) coordinate with one sulphur, one selenium and one phosphorus atom, one (Cu71) coordinates with two sulphur atoms, one selenium atom and one phosphorus atom and eleven atoms (Cu16, Cu19, Cu22, Cu40, Cu45, Cu55, Cu68, Cu79, Cu86, Cu89, Cu93) coordinate with three selenium atoms and one phosphorus atom.

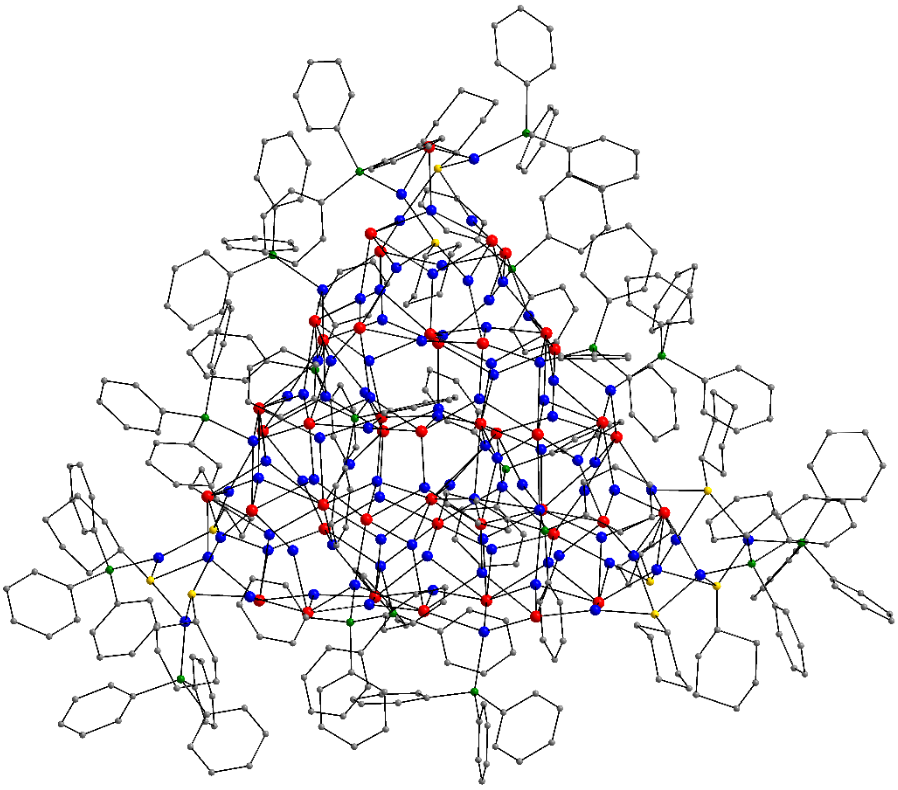

Figure 3-64 *Molecular structure of* ***39*** *in the solid state in the same orientation as in* ***Figure 3-63*** *(H atoms omitted).*

The other copper atoms only coordinate with chalcogen atoms. Cu92 linearly bridges two sulphur atoms; nine atoms (Cu13, Cu17, Cu57, Cu58, Cu66, Cu72, Cu73, Cu87, Cu88) link two selenium atoms; five atoms (Cu61, Cu63, Cu69, Cu76, Cu83) tetrahedrally coordinate with four selenium atoms; 14 atoms (Cu6, Cu10, Cu15, Cu20, Cu23, Cu24, Cu32, Cu35, Cu36, Cu37, Cu41, Cu59, Cu64, Cu65) coordinate with two selenium atoms and one sulphur atom and the remaining atoms trigonally coordinate with three selenium atoms. The Cu–Se bond lengths range from 2.161(5) Å to

2.879(5) Å and the Cu–S distances are 2.196(9) Å to 2.480(8) Å.

3.5 Reactions of silver thiolates with $E(SiMe_3)_2$ (E = S, Se) in the presence of various phosphines and $NaBPh_4$

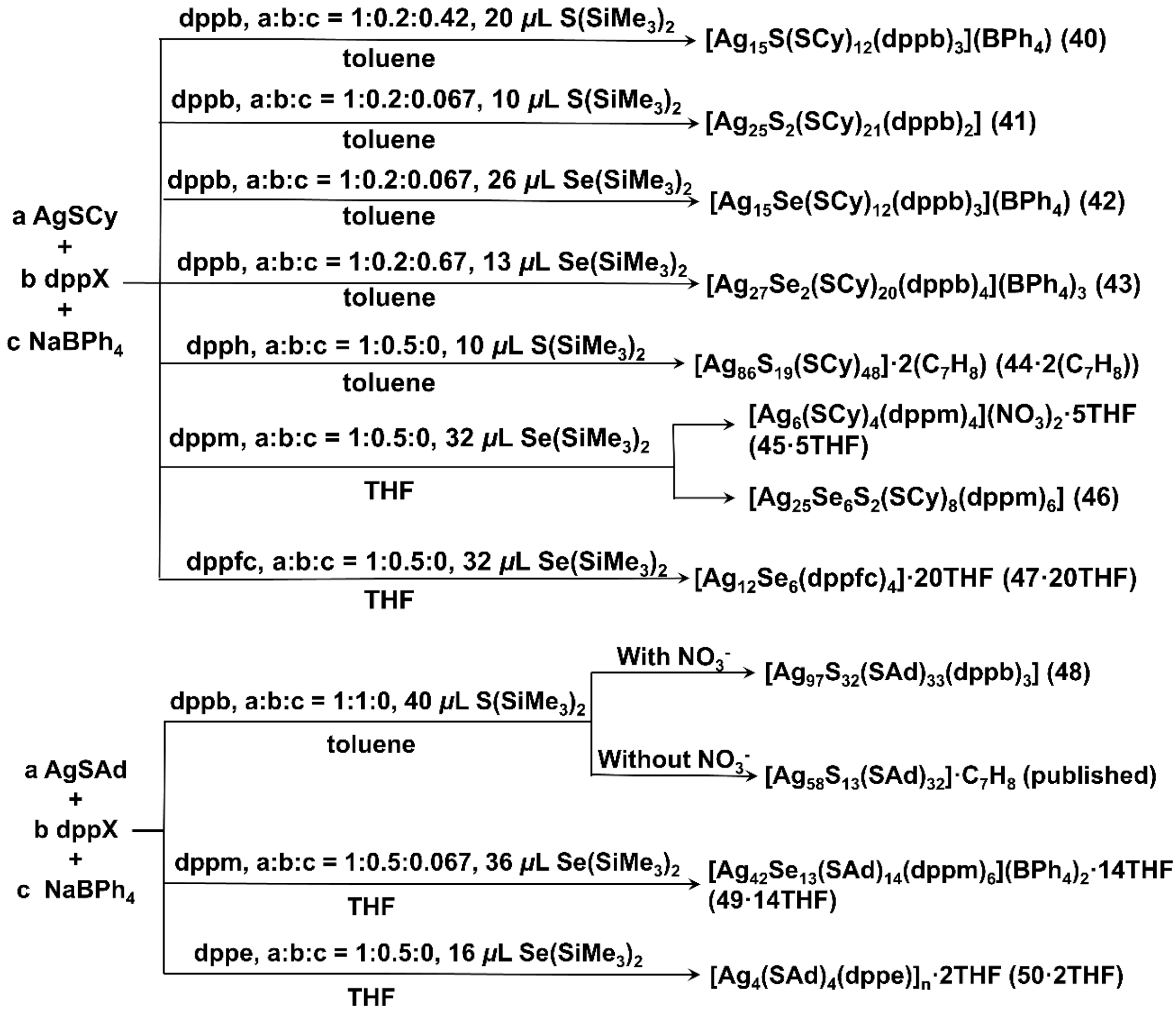

Scheme 3-9 *Synthesis of silver chalcogen clusters* ***40–50****.*

As seen in **Scheme 3-9** reactions of silver thiolates with $E(SiMe_3)_2$ (E = S, Se) in the presence of stabilizing phosphines and $NaBPh_4$ yield to the formation of various smaller and larger neutral and ionic silver chalcogen clusters.

The use of AgSCy and AgSAd results in the formation of eleven new compounds. Initially a reaction of AgSCy with dppb and $S(SiMe_3)_2$ was carried out yielding a compound with the composition $[Ag_{15}S(SCy)_{12}(dppb)_3]$, where the charge of the molecule was not clear. Concerning the charge balance in this compound the cluster should be a monocation. In the structure refinement one could not find any hint for a possible counterion. Therefore, the same reaction was made in the presence of $NaBPh_4$, which yields to the ionic compound **40**. Based on this result a series of reactions was carried out using $NaBPh_4$ as additional starting material to stabilize also other cationic cluster species.

Yellow crystal **45** and orange crystal **46** co-crystallized from the same reaction. Unfortunately, the information of the anion of **46** has not been collected.

The presence of silver nitrate plays an important role in the formation of **48**, although nitrate is not present in the structure. In the absence of silver nitrate, the reaction results in the published compound $[Ag_{58}S_{13}(SAd)_{32}]$.[77] More synthetic details have been mentioned in the experimental section.

3.5.1 $[Ag_{15}S(SCy)_{12}(dppb)_3](BPh_4)$ (40) and $[Ag_{15}Se(SCy)_{12}(dppb)_3](BPh_4)$ (42)

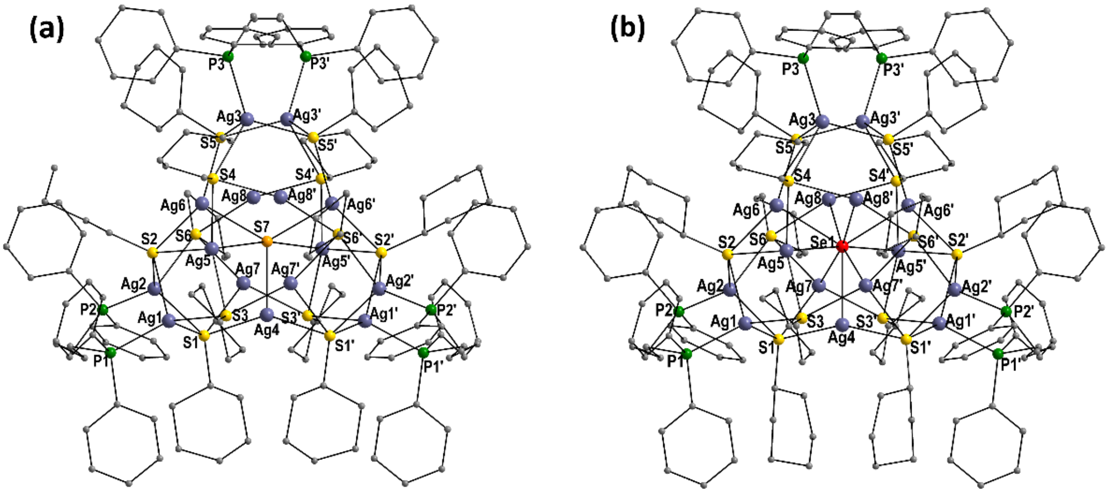

Figure 3-65 *Molecular structure of the* $[Ag_{15}E(SCy)_{12}(dppb)_3]^+$ *cation in* ***(a) 40*** *(E = S) and* ***(b) 42*** *(E = Se) in the solid state (H atoms omitted).*

Compound **40** crystallizes in the acentric orthorhombic space group $C222_1$ with four formula units per unit cell. There is a 2-fold axis running through the atoms Ag4 and S7. The ionic **40** consists of a $[Ag_{15}S(SCy)_{12}(dppb)_3]^+$ cation (**Figure 3-65(a)**) and a BPh_4^- anion. The central μ_5 sulphide ion S7 is surrounded by five silver atoms (Ag4, Ag5, Ag5', Ag6 and Ag6') with bond lengths of 2.546(5) Å to 2.912(5) Å. The other sulphur atoms of the SCy^- thiolate groups are acting as μ_3 (S3, S4, S5, S6) or μ_4 (S1, S2) bridges. Six silver atoms (Ag1, Ag2, Ag3 and symm. equiv.) are tetrahedrally coordinated by one phosphorus atom and three sulphur atoms; Ag5 tetrahedrally coordinate with four sulphur atoms; two silver atoms (Ag8 and Ag8') coordinate with two sulphur atoms linearly and five silver atoms (Ag4, Ag6, Ag7 and symm. equiv.) triangularly coordinate with three sulphur atoms. The Ag–S bond lengths vary from 2.433(3) Å to 2.866(4) Å.

Compound **42** is isostructural to **40** with the difference that the central sulphide ion in **40** is replaced by a selenide ion. This central selenium atom acts as μ_9 ligand to nine silver atoms (Ag4, Ag5, Ag6, Ag7, Ag8 and symm. equiv.) with Ag–Se distances from 2.712(3) Å to 3.043(4) Å.

3.5.2 $[Ag_{25}S_2(SCy)_{21}(dppb)_2]$ (41)

Compound **41** is the main product of the reaction of AgSCy with dppb, $NaBPh_4$ and $S(SiMe_3)_2$. The minority product in this reaction is the previously described **40**.

Compound **41** crystallizes in the monoclinic space group *C*2/*c* with eight molecules per unit cell. The spherical neutral cluster consists of 25 silver cations, two S^{2-} (S22, S23), 21 SCy^- groups and two dppb ligands. Silver atoms are found in linear, trigonal and tetrahedral coordination mode. Ag9, Ag19, Ag25 linearly bridge two sulphur atoms, in which Ag25 links the two central S^{2-} ions. Ag1, Ag2, Ag3 and Ag4 coordinate with three thiolate groups and one phosphorus atom of the dppb ligands. Ag12 and Ag13 are connected to one sulphide ion and three thiolate units. Ag20 coordinates with four thiolate groups. Five silver atoms (Ag8, Ag10, Ag15, Ag18, Ag23) bond to three thiolate groups. The remaining silver atoms coordinate with one S^{2-} and two SCy^- groups. These two atoms coordinate to three thiolate groups. The two sulphide ions (S22, S23) act as μ_7 bridges, whereas the sulphur atoms of

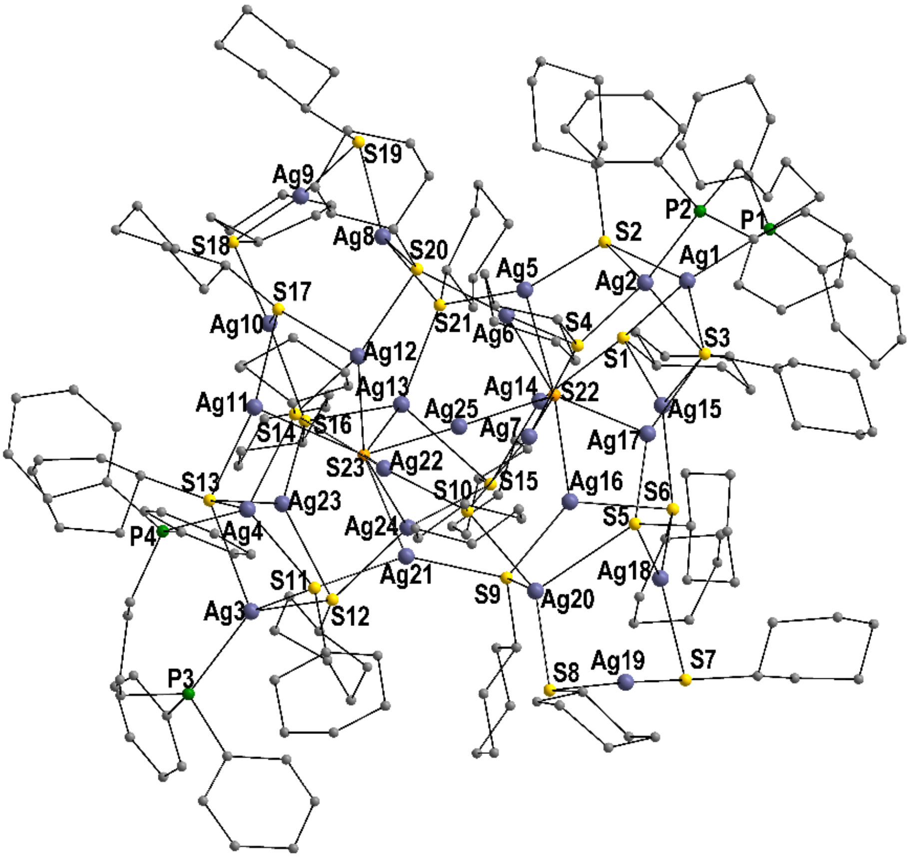

Figure 3-66 *Molecular structure of compound* ***41*** *in the solid state (H atoms omitted)*

the thiolate groups show μ_2 (S7, S8, S18, S19), μ_3 (S1, S2, S4, S5, S6, S9, S10, S11, S12, S14, S15, S16, S17, S20, S21) and μ_4 (S3, S13) bridging mode. The Ag–S bond lengths depend on the order of the sulphur bridging mode. For instance, the bond lengths of Ag–S22/23 vary from 2.353(3) Å to 2.910(3) Å. The bond lengths of Ag–S3/S13 range from 2.428(3) Å to 2.806(3) Å.

3.5.3 $[Ag_{27}Se_2(SCy)_{20}(dppb)_4](BPh_4)_3$ (43)

Compound **43** crystallizes in the triclinic space group $P\bar{1}$ with two formula units per unit cell. **43** is an ionic compound consisting of a $[Ag_{27}Se_2(SCy)_{20}(dppb)_4]^{3+}$ trication and three BPh_4^- anions. The structure of the cation is built of 27 silver atoms, two selenide anions, 20 SCy^- thiolate groups and four dppb ligands.

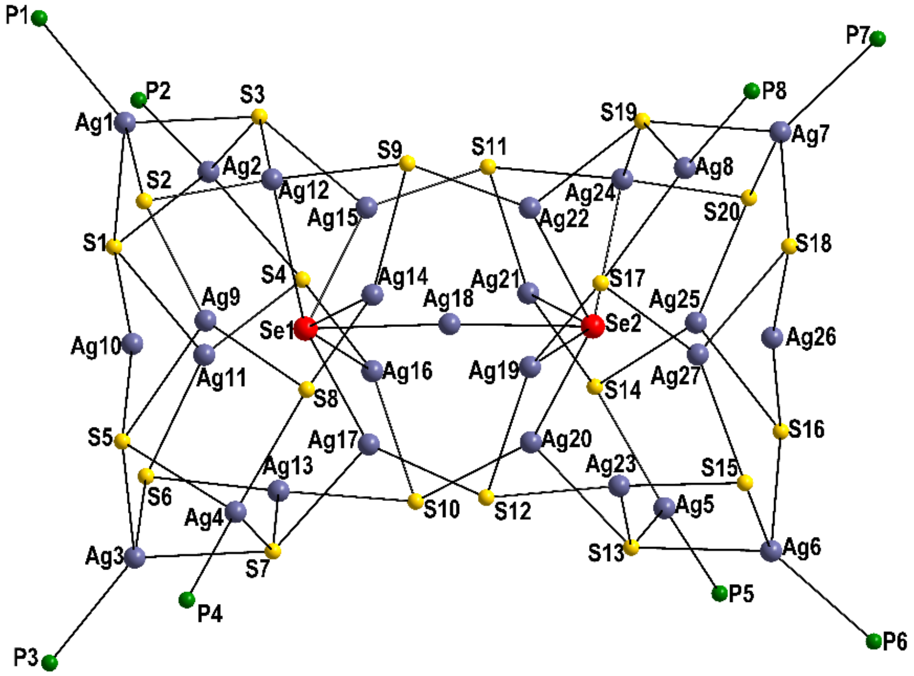

Figure 3-67 *Structure of the heavy atoms core of the* $[Ag_{27}Se_2(SCy)_{20}(dppb)_4]^{3+}$ *trication in* ***43*** *in the solid state.*

There is a central linear $AgSe_2$ unit (Ag18, Se1, Se2) surrounded by an ellipsoidal shell of silver thiolate. These two selenium atoms act as μ_6 bridges to the neighbouring silver atoms. Six sulphur atoms (S1, S3, S5, S7, S13, S19) show μ_4 bridging mode whereas the remaining sulphur atoms are μ_3. Silver atoms display different coordination modes. Six atoms (Ag1, Ag2, Ag3, Ag4, Ag6, Ag7) are tetrahedrally coordinated with three sulphur atoms and one phosphorus atom; Ag12 and Ag24 coordinate with three sulphur atoms and selenium atom; Ag10 and Ag26 linearly coordinate with two sulphur atoms; Ag5 and Ag8 coordinate with two sulphur atoms and one phosphorus atom; six atoms (Ag9, Ag11, Ag13, Ag23, Ag25, Ag27) triangularly coordinate with three sulphur atoms; Ag18 coordinate with two selenium atoms and the remaining atoms coordinate with two sulphur atoms and one selenium atom. The Ag–S bond lengths range from 2.410(2) Å to 2.923(2) Å, the Ag–Se distances range from 2.562(3) Å to 3.026(7) Å.

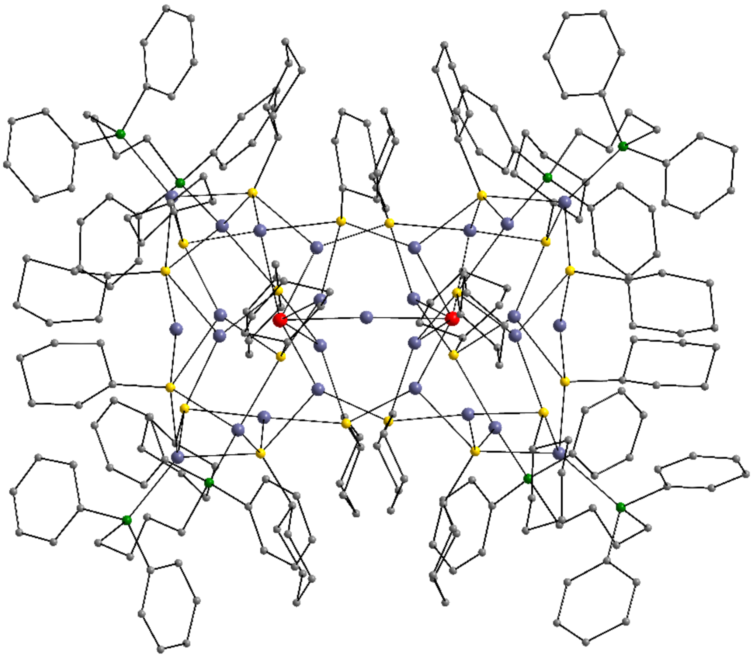

Figure 3-68 *Molecular structure of the* $[Ag_{27}Se_2(SCy)_{20}(dppb)_4]^{3+}$ *trication in* ***43*** *in the solid state in the same orientation as in* ***Figure 3-67*** *(H atoms omitted).*

3.5.4 $[Ag_{86}S_{19}(SCy)_{48}]\cdot 2(C_7H_8)$ ($44\cdot 2(C_7H_8)$)

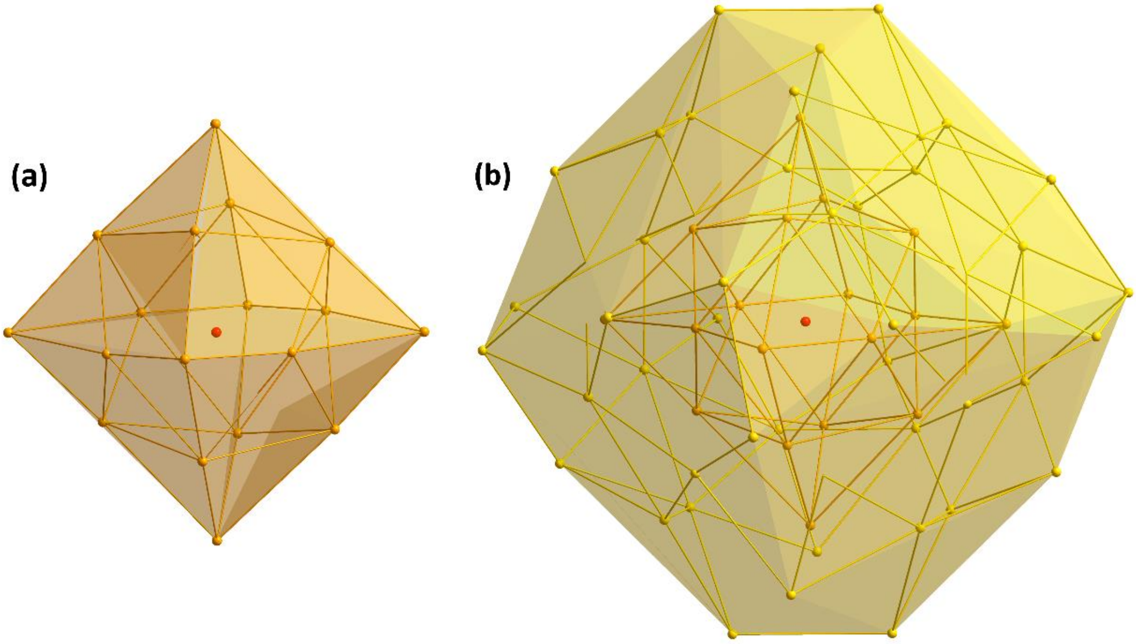

Figure 3-69 (a) *Octahedron type S@S*$_{18}$ *core in* ***44****;* ***(b)*** *spherical arrangement of the 48 sulphur atoms surrounding the S@S*$_{18}$ *octahedron in* ***44****.*

Compound **44** crystallizes in the triclinic space group $P\overline{1}$ with one molecule per unit cell. The neutral cluster **44**, which is located on an inversion centre, consist of 86 Ag$^+$ ions, 19 S^{2-} sulphide ions and 48 SAd$^-$ thiolate groups. Similar to compound **48**, **44** can be described as a core-shell structure with the molecular formula [(Ag$_2$S)$_{19}$@(AgSCy)$_{48}$].

The diameter of the (Ag$_2$S)$_{19}$ core is approximately 1.82 nm. If the AgSCy shell is taken into consideration, this value increases to about 3 nm. Although present in the reaction mixture the phosphine dpph is not incorporated into the ligand shell. Nevertheless it is necessary for the formation of **44**, which is not formed in the absence of dpph.

The sulphide framework of the (Ag$_2$S)$_{19}$ core can be seen as a S@S$_{18}$ octahedron in which S34 occupies the centre of this polyhedron (see **Figure 3-69(a)**). This S@S$_{18}$ octahedron is surrounded by a spherical shell of the 48 sulphur atoms of the SCy$^-$ ligands.

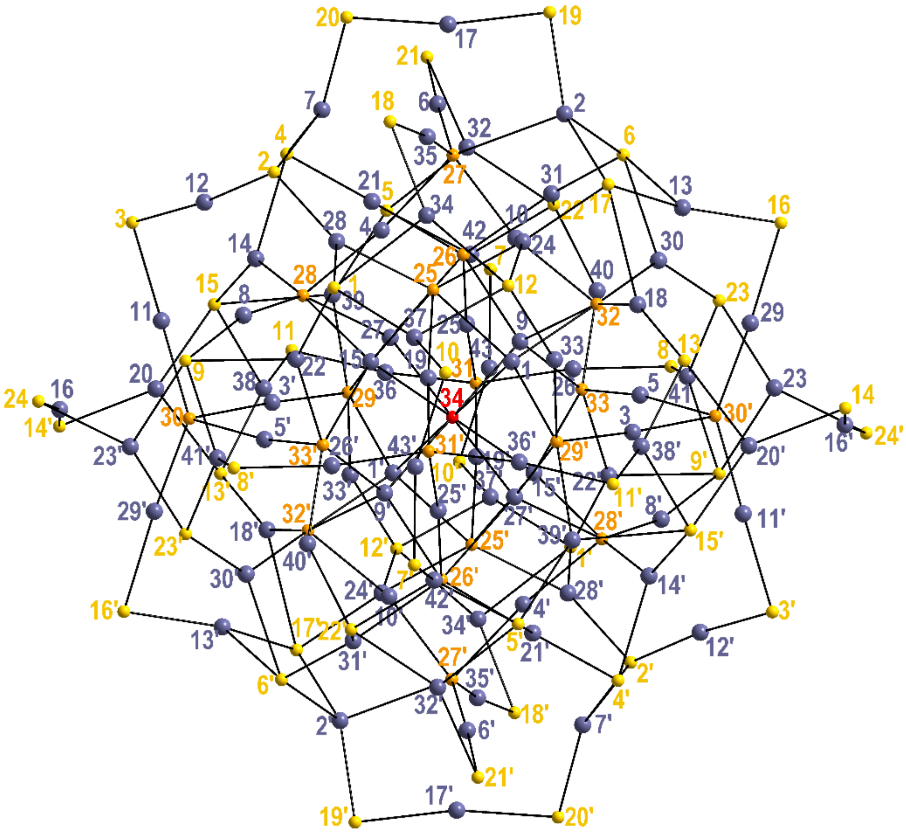

Figure 3-70 *Structure of the heavy atoms core of compound* ***44*** *in the solid state, central S34 marked in red.*

All silver atoms are inserted inside the sulphur framework. Eight silver atoms (Ag1, Ag9, Ag15, Ag27 and symm. equiv.) are located in the S@S18 core surrounding the central S34 in form of a distorted cube. The bond lengths of them range from 2.621(2) Å to 2.734(5) Å.

Further twelve silver atoms (Ag3, Ag4, Ag5, Ag10, Ag19, Ag25 and symm. equiv.) stay on the edge of the octahedral core, linearly coordinated by two sulphur atoms with bond lengths of 2.402(4) Å to 2.941(4) Å. The remaining silver atoms act as connectors of the core and the shell, presenting linear (Ag6, Ag8, Ag11, Ag12, Ag16, Ag17, Ag26, Ag29, Ag33, Ag35, Ag36, Ag40, Ag43 and symm. equiv.) or trigonal (Ag7, Ag13, Ag14, Ag18, Ag20, Ag21, Ag22, Ag23, Ag24, Ag28, Ag30, Ag31, Ag32, Ag34, Ag37, Ag38, Ag39, Ag40, Ag41, Ag42 and symm. equiv.) or tetrahedral (Ag2 and symm. equiv.) coordination mode.

Due to the observed Ag⋯Ag distances from 2.927(2) Å to 3.367(2) Å there is no hint for any attractive d^{10}–d^{10} interactions.

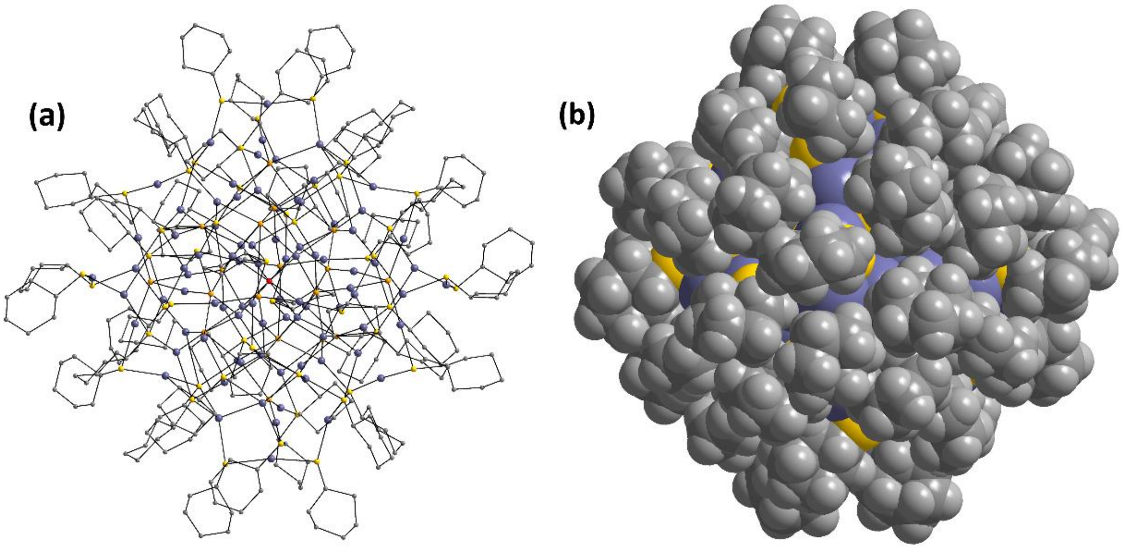

Figure 3-71 (a) *Molecular structure of* ***44*** *in the solid state in the same orientation as in* ***Figure 3-70*** *(H atoms omitted, central S34 marked in red);* ***(b)*** *space-filling model of compound* ***44*** *in the solid state.*

3.5.5 [$Ag_6(SCy)_4(dppm)_4](NO_3)_2$·5THF (45·5THF)

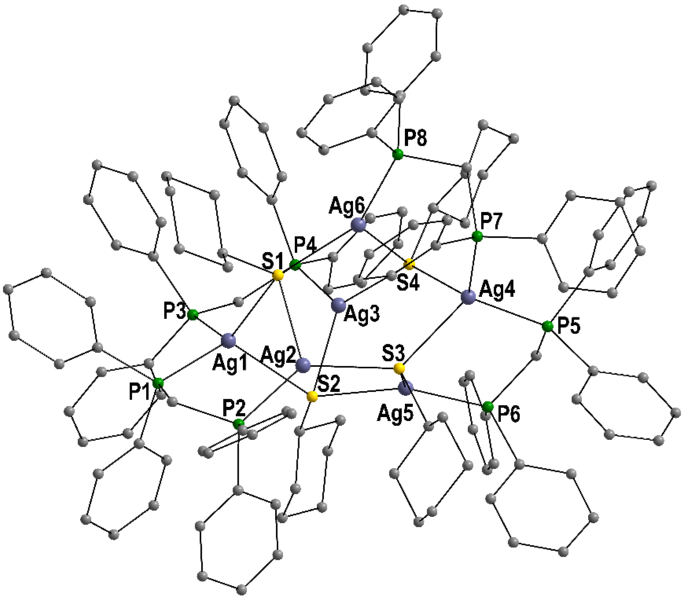

Figure 3-72 *Molecular structure of the $[Ag_6(SCy)_4(dppm)_4]^{2+}$ dication in* ***45*** *in the solid state (H atoms omitted).*

As shown in **Scheme 3-9** the reaction of AgSCy, dppm and $Se(SiMe_3)_2$ yields to the formation of a mixture of two components: $[Ag_6(SCy)_4(dppm)_4](NO_3)_2$ (**45**) and $[Ag_{25}Se_6S_2(SCy)_8(dppm)_6]$ (**46**).

The ionic compound **45** crystallizes in the monoclinic space group $P2_1/c$ with four formula units per unit cell. Due to the composition the charge of the cation is 2+. The two nitrate anions could be localized in the final Fourier synthesis.

The silver atoms in **45** are in two different coordination modes. Ag1 and Ag4 are tetrahedrally coordinate by two sulphur and two phosphorus atoms; the other silver atoms triangularly coordinate with two sulphur and one phosphorus atom. All sulphur atoms exhibit μ_3 bridging mode. Ag–S bond lengths in this structure vary from 2.478(9) Å to 2.704(4) Å. Ag–P bond lengths range from 2.389(9) Å to 2.553(3) Å.

A possible explanation for the presence of the nitrate counter anions could be an impurity of $AgNO_3$ in the used AgSCy, which has been synthesized by the reaction of $AgNO_3$ with cyclohexyl thiol.

3.5.6 $[Ag_{25}Se_6S_2(SCy)_8(dppm)_6]$ (46)

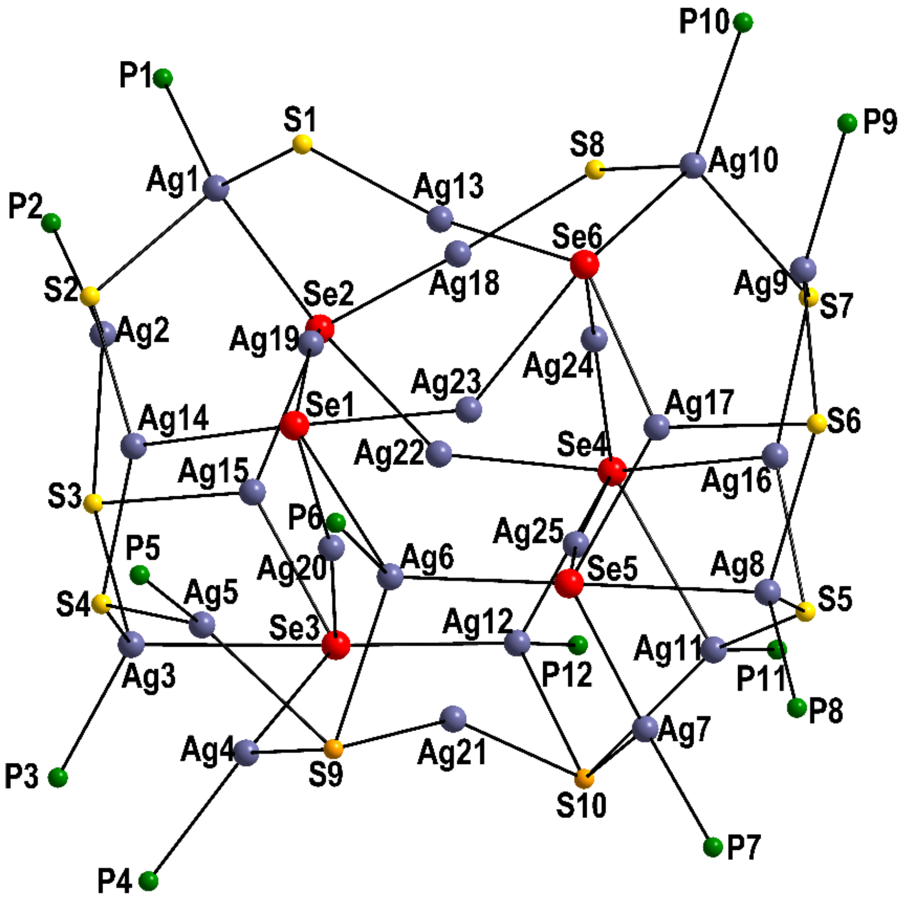

Figure 3-73 *Structure of the heavy atoms core of **46** in the solid state.*

Compound **46** crystallizes in the triclinic space group of $P\bar{1}$ with two molecules per unit cell. Compound **46** yields from a reaction of AgSCy, dppm and $Se(SiMe_3)_2$ and consists of 25 Ag^+ cations, six Se^{2-} (Se1–Se6), two S^{2-} (S9, S10), eight SCy^- (S1–S8) and six dppm ligands. Most likely this cluster should be a monocation. Unfortunately, a counter anion could not be identified in the structure refinement, which is maybe a result of a disordered nitrate anion. Such a nitrate anion could origin from impurities in the used AgSCy. An analogous reaction in the presence of $NaBPh_4$ does not yield to the formation of $[Ag_{25}Se_6S_2(SCy)_8(dppm)_6](BPh_4)$, instead $[Ag_{27}Se_2(SCy)_{20}(dppb)_4](BPh_4)_3$ (**43**) is formed.

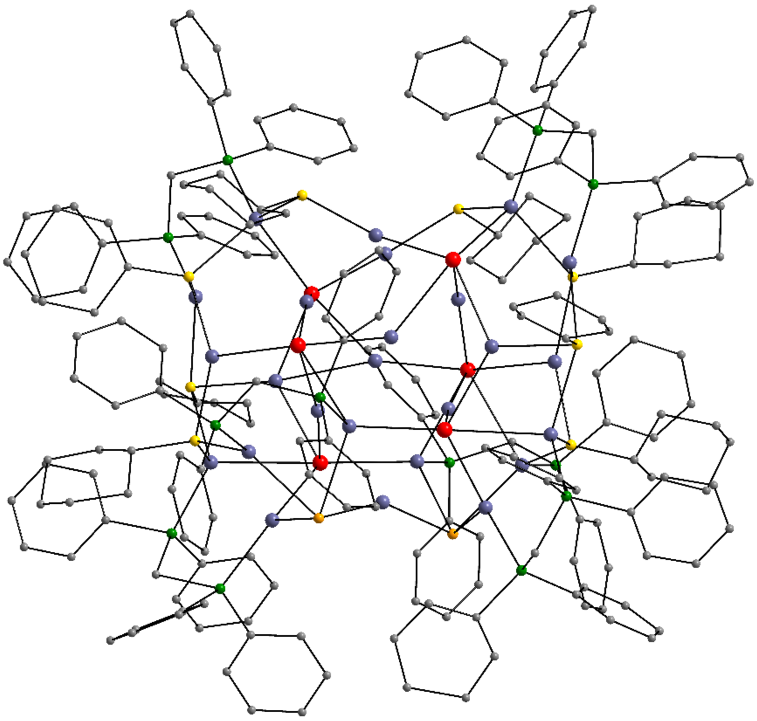

***Figure 3-74** Molecular structure of **46** in the solid state in the same orientation as in **Figure 3-73** (H atoms omitted).*

In **46** the silver atoms are found in three coordination modes: linear, triangular and tetrahedral. Ag1, Ag3, Ag8, Ag10 and Ag11 coordinate with one selenium, two sulphur and one phosphorus atom; Ag6 and Ag12 coordinate with two selenium, one sulphur and one phosphorus atom. These silver atoms present tetrahedral geometry with Ag–Se bond lengths of 2.852(2) Å to 3.065(7) Å and Ag–S bond lengths of 2.534(4) Å to 2.783(3) Å.

Nine silver atoms exhibit trigonal geometry: Ag2, Ag5 and Ag9 bond to two sulphur and one phosphorus atom, while Ag4 and Ag7 coordinate with one selenium, one sulphur and one phosphorus atom. Ag14, Ag15, Ag16 and Ag17 are surrounded by three chalcogen atoms in a trigonal planar coordination mode. The Ag–S bond lengths range from 2.374(3) Å to 2.771(4) Å and Ag–Se from 2.481(1) Å to 3.095(7) Å.

3.5.7 $[Ag_{12}Se_6(dppfc)_4]\cdot 20THF$ (47·20THF)

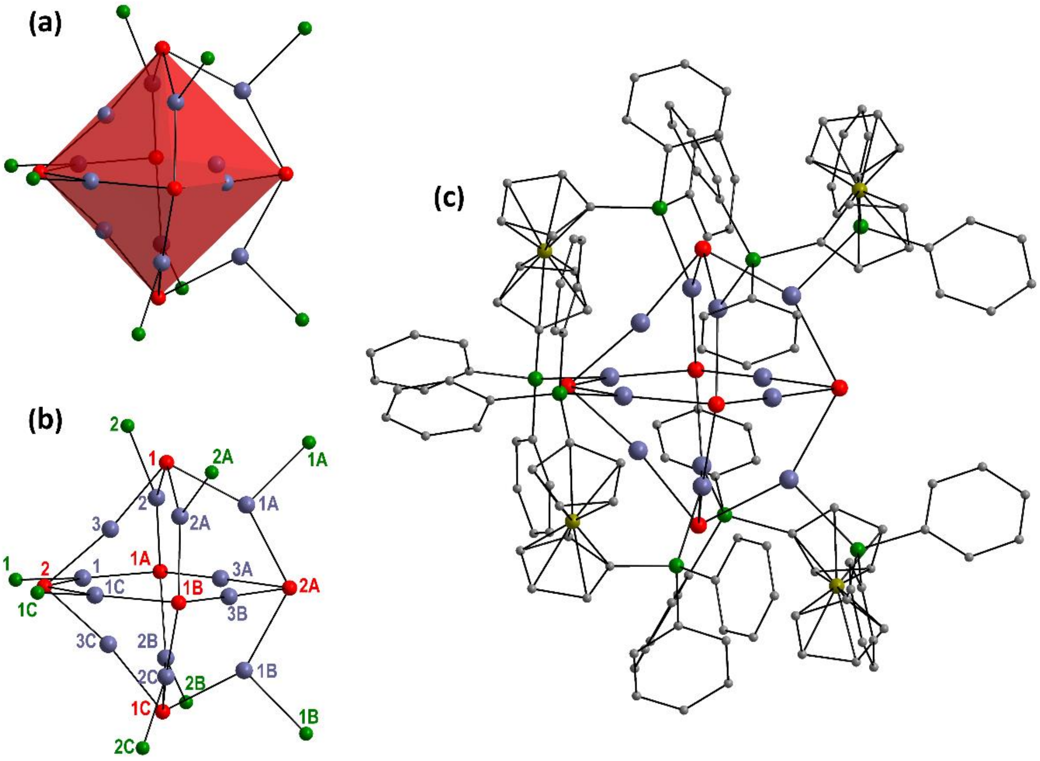

Figure 3-75 (a) *Se octahedron in the heavy atoms core of* ***47*** *in the solid state;* ***(b)*** *the heavy atoms core of compound* ***47****;* ***(c)*** *molecular structure of* ***47*** *in the solid state in the same orientation as in* ***(a)*** *(H atoms omitted).*

Compound **47** crystallizes in the tetragonal space group *I*4$_1$/*a* with four molecules per unit cells. **47** consists of twelve silver atoms, six selenium atoms and four dppfc ligands. There is a $\bar{4}$-axis running through the atoms Se2 and Se2A. The structure can be derived from a distorted Se_6 octahedron, where the twelve edges are capped by the twelve silver atoms. Eight silver atoms (Ag1, Ag2 and symm. equiv.) are trigonal planar coordinated by two selenium atoms and one phosphorus atom of the dppfc ligands. The four silver atoms (Ag3 and symm. equiv.) show linear coordination mode by two selenium atoms. Ag–Se bond lengths are 2.480(1) Å to 2.681(1) Å; Ag–P bond lengths range from 2.505(5) Å to 2.520(1) Å.

3.5.8 $[Ag_{97}S_{32}(SAd)_{33}(dppb)_3]$ (48)

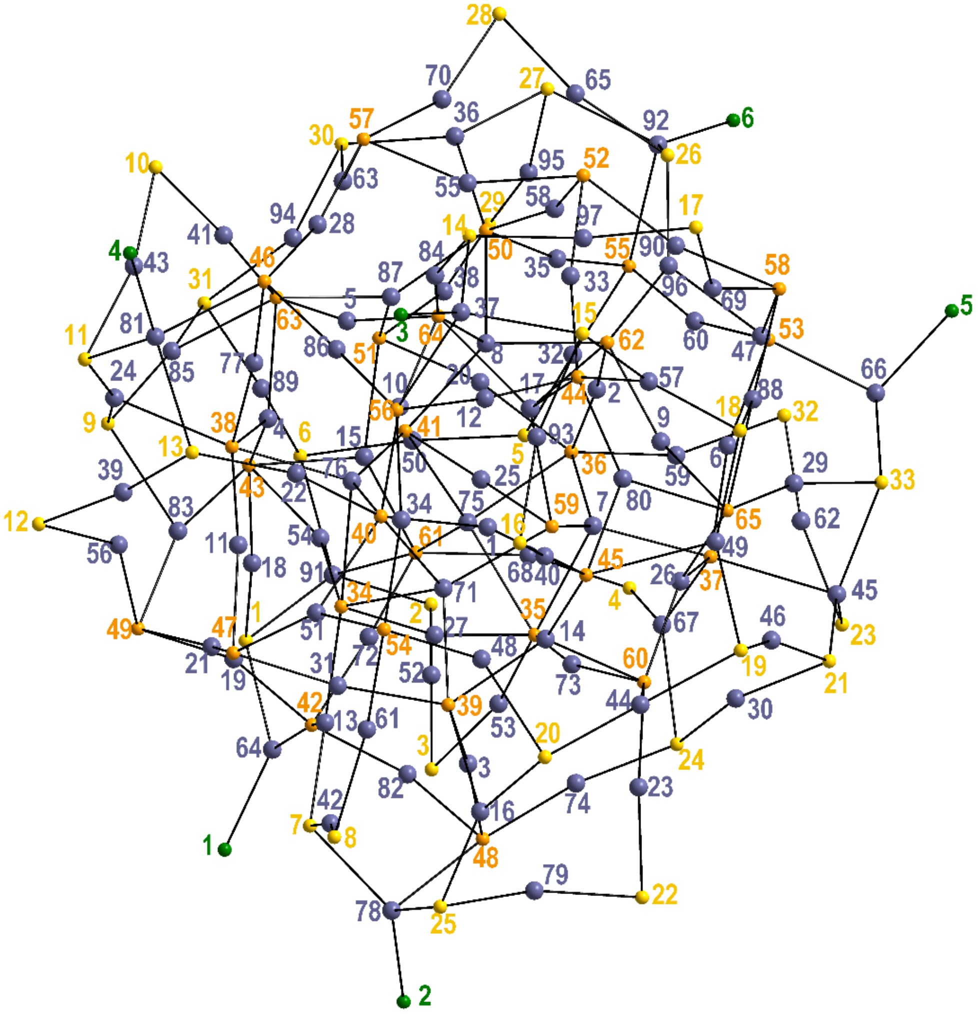

Figure 3-76 *Structure of the heavy atoms core of compound* ***48*** *in the solid state.*

Compound **48** crystallizes in the triclinic space group $P\overline{1}$ with two formula units per unit cell. The spherical molecule consists of 97 Ag^+, 32 S^{2-}, 33 SAd^- and three dppb ligands and can be described as a core-shell structure with the composition $[(Ag_2S)_{32}@(AgSAd)_{33}(dppb)_3]$ where the $(Ag_2S)_{32}$ core is surrounded by a $(AgSAd)_{33}(dppb)_3$ shell. The diameter of the central Ag_2S core is approximately 1.5 nm. Including the AgSAd shell the diameter is about 1.8 nm, together with the organic groups and the phosphine ligands diameter increases to approximately 3.0 nm. Concerning the $(Ag_2S)_{32}$ core there is no obvious structural similarity to bulk binary Ag_2S, neither monoclinic α-Ag_2S (acanthite, bcc), nor β-Ag_2S (argentite, bcc), nor γ-Ag_2S (fcc) (bcc = body-centred cubic).

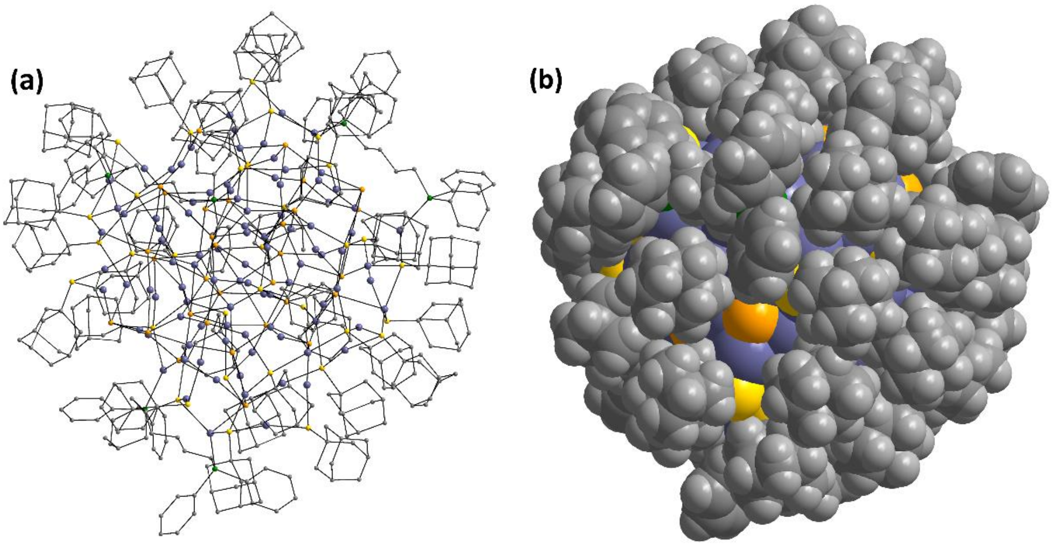

Figure 3-77(a) *Molecular structure of compound* ***48*** *in the solid state in the same orientation as in* ***Figure 3-76*** *(H atoms omitted);* ***(b)*** *space filling model of compound* ***48*** *in the solid state.*

Core-shell structures are known from other Ag/S clusters. For example, in 2002, $[Ag_{188}S_{94}(PR_3)_{30}]$[73] was published. The sulphur framework in this structure consists of three sulphur shells containing 10, 34 and 50 atoms. Another example is $[Ag_{70}S_{20}(SPh)_{28}(dppm)_{10}](CF_3CO_2)_2$[74]. There is a structural relation between **48** and the earlier described $[Ag_{94}S_{34}(SAd)_{26}(dpppt)_6]$[77] (i.e. $[(Ag_2S)_{34}@(AgSAd)_{26}(dpppt)_6]$) which has been synthesized under similar conditions from AgSAd, $S(SiMe_3)_2$ and dpppt. A reason for the formation of **48** is perhaps the different sterical demand of the used stabilizing phosphine ligands and more likely the addition of a small amount of silver nitrate. Although similar in structure the composition of the core-shell structure of $[(Ag_2S)_{34}@(AgSAd)_{26}(dpppt)_6]$ is different to **48**. Both compounds can be seen as intermediates in the growing process from small complexes to clusters of various sizes and finally the bulk silver sulphide.

As usual, in **48**, the silver atoms are found in linear, trigonal or tetrahedral coordination modes. The Ag–S bond lengths for the tetrahedrally coordination one ranges from 2.403(9) Å to 2.953(6) Å, while the trigonally coordinated silver atoms show Ag–S distances from 2.212(7) Å to 2.968(5) Å. The shortest Ag···Ag distance is 2.757(4) Å.

3.5.9 $[Ag_{42}Se_{13}(SAd)_{14}(dppm)_6](BPh_4)_2\cdot 14THF$ (49·14THF)

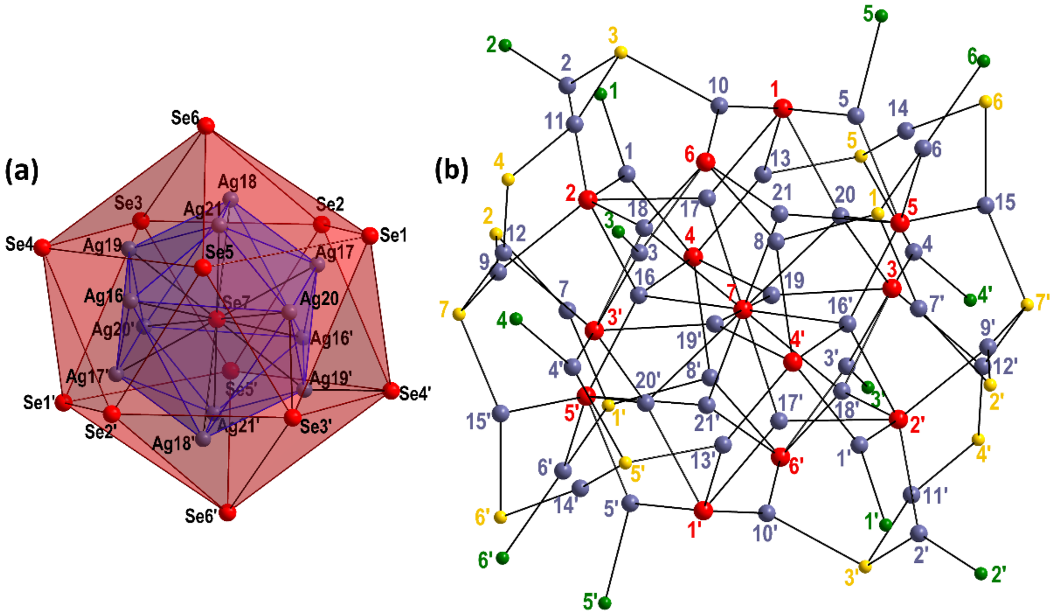

Figure 3-78 (a) *Se@Ag₁₂@Se₁₂ fragment in the centre of* ***49*** *in the solid state;* ***(b)*** *the heavy atoms core of the dication* $[Ag_{42}Se_{13}(SAd)_{14}(dppm)_6]^{2+}$ *in* ***49*** *in the solid state.*

Compound **49** crystallizes in the monoclinic space group $P2_1/n$ with two formula units per unit cell. The dication in **49**, which is localised on an inversion centre (Se7), consists of 42 Ag^+ ions, 13 Se^{2-} ions, 14 SAd^- and three dppm ligands. The charge is balanced by two BPh_4^- anions. The structure of the dication can also be seen as a core-shell particle of the composition $[\{Ag_2(Ag_2Se)_{13}\}@(AgSAd)_{14}(dppm)_6]^{2+}$, where the 13 selenium atoms are found in the inner part of the molecule as a centred icosahedron (**Figure 3-78(a)**). This $\{Ag_2(Ag_2Se)_{13}\}$ core is surrounded by a shell composed of AgSAd and dppm ligands.

Twelve Ag^+ ions (Ag16, Ag17, Ag18, Ag19, Ag20, Ag21 and symm. equiv.) are located in the inner part of the Se_{13} core, building a highly distorted icosahedron (non-bonding Ag···Ag distances are ranging from 2.908 Å to 3.972 Å). This part of the cluster can be written as $Se@Ag_{12}@Se_{12}$ (**Figure 3-77(a)**). The twelve selenium atoms act as connectors to the outer sphere created by the remaining silver atoms, the SAd^- groups and the dppm ligands. Ag2, Ag4 and Ag6 and symm. equiv. having the coordination number three are bonded to one selenium, one sulphur and one phosphorus atom; Ag1, Ag3 and Ag5 and symm. equiv. are coordinated with two selenium atoms and one phosphorus atom; Ag7, Ag9, Ag12, Ag14, Ag15 (and symm. equiv.) with two sulphur atoms and one selenium atom and Ag8, Ag10 and Ag13 (and symm. equiv.) with two selenium atoms and one sulphur atoms. All these silver atoms present trigonal planar coordination geometry, except for Ag11 which is linearly surrounded by two sulphur atoms. The Ag–S bond lengths vary from 2.390(1) Å to 2.519(1) Å. Due to the larger ionic radius of Se compared to that of S, the Ag–Se bonds length are longer and range from 2.609(9) Å to 3.082(2) Å. Except for the central μ_{12}-Se7 and the μ_5-Se6 all other selenium atoms act as μ_6 ligands.

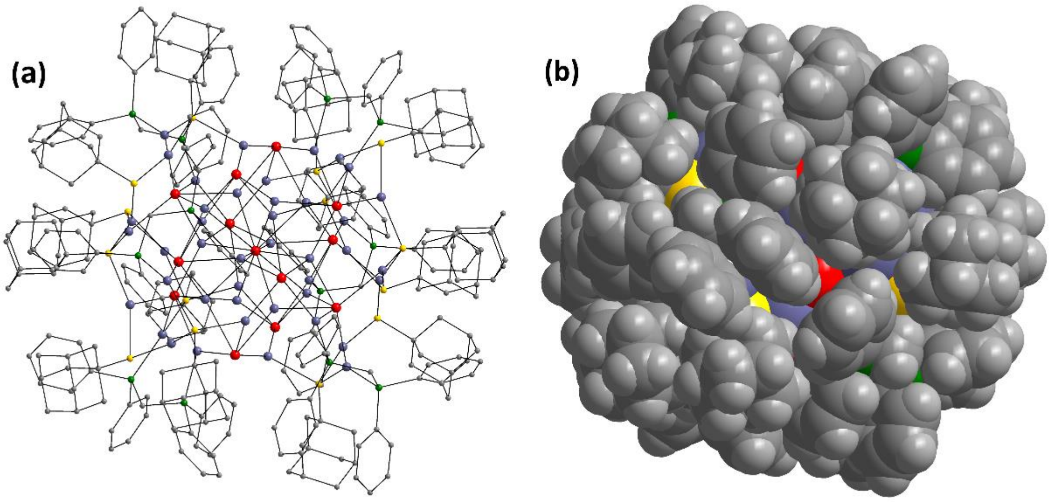

Figure 3-79 (a) *Molecular structure of the* $[Ag_{42}Se_{13}(SAd)_{14}(dppm)_6]^{2+}$ *dication in* ***49*** *in the solid state in the same orientation as in* ***Figure 3-78(b)*** *(H atoms omitted);* ***(b)*** *space-filling model of the dication in* ***49*** *in the solid state.*

Similar silver selenium clusters $[Ag_{114}Se_{34}(SenBu)_{46}(PtBu_3)_{14}]$ and $[Ag_{172}Se_{40}(SenBu)_{92}(dppp)_4]$[85] have been reported. These two compounds with cubic body-centred selenium skeletons are related to the structure of bulk phase Ag_2Se.

3.5.10 $[Ag_4(SAd)_4(dppe)]_n\cdot 2THF$ (50·2THF)

Compound **50** crystallizes in the triclinic space group $P\overline{1}$ with two formula units per unit cell. **50** is a coordination polymer where $Ag_4(SAd)_4$ units are connected *via* bridging dppe ligands. There are two crystallographically independent polymer chains.

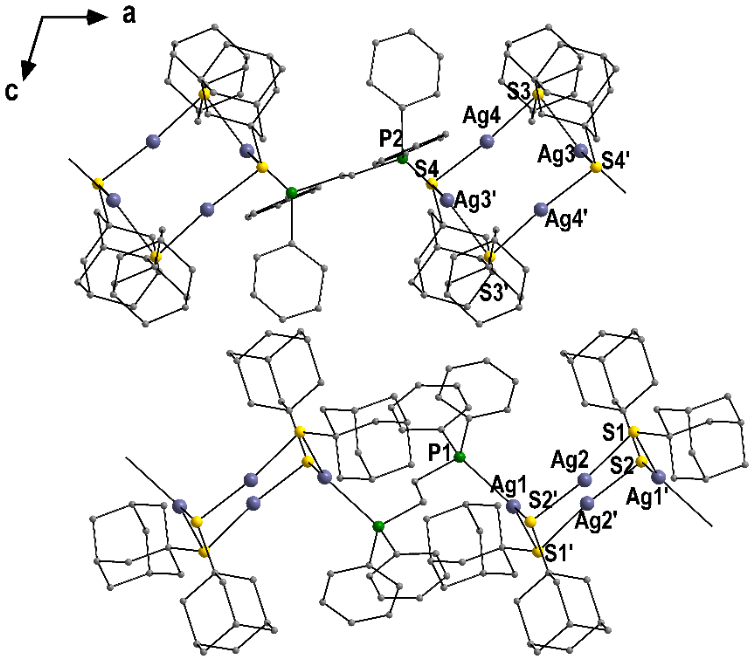

Figure 3-80 *Molecular structure of the polymeric chains in* ***50*** *in the solid state (H atoms omitted).*

Ag1 and Ag3 (and symm. equiv.) are trigonally coordinated with two sulphur atoms and one phosphorus atom. Ag2 and Ag4 (and symm. equiv.) are linearly bonded to two sulphur atoms. The Ag–S bond lengths vary from 2.349(11) Å to 2.518(9) Å and that of the Ag–P bonds are 2.446(7) Å and 2.468(9) Å, respectively.

3.6 Optical properties of selected small copper clusters

Inspired by various publications reporting small copper clusters with significant luminescence,[110] the nine clusters, namely compound **1**, **2**, **6**, **7**, **10**, **13**, **15**, **17**, **18**, which are easily obtained as pure phase were chosen to investigate their respective photoluminescence. In addition, the three compounds (**15**, **17**, **18**) with strong luminescence were investigated for their photoluminescent lifetime and quantum yields at different temperatures.

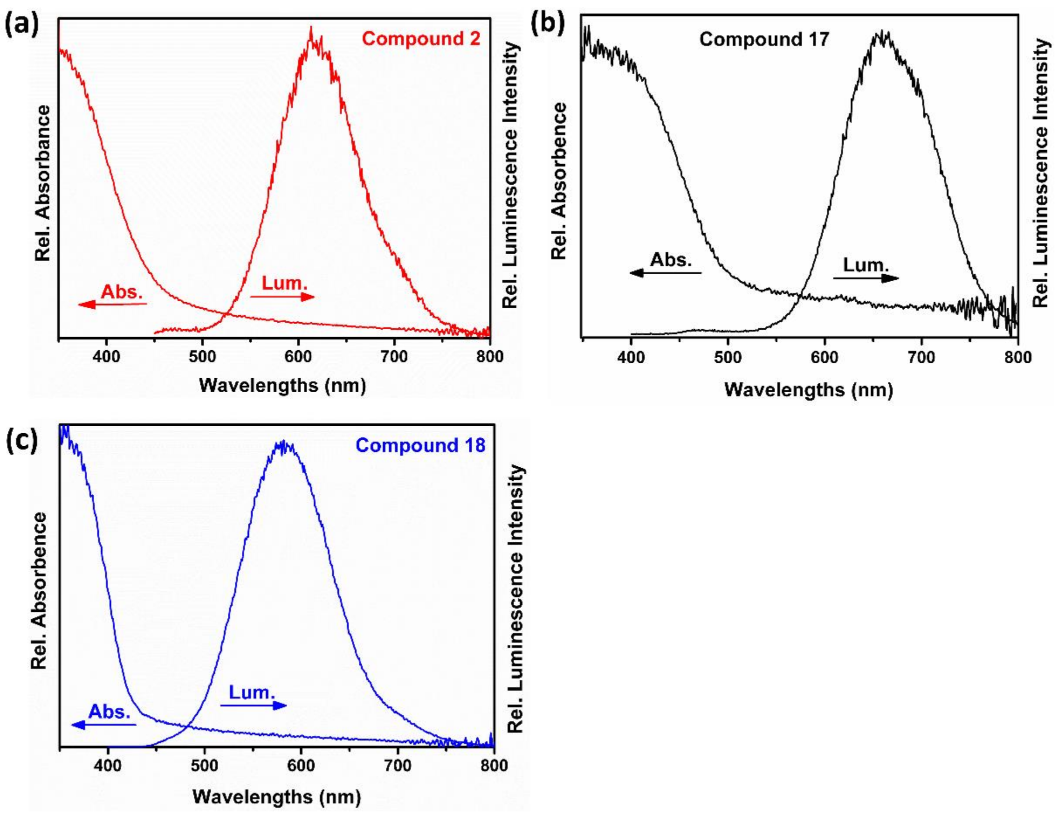

Figure 3-81 *Solid-state absorption (left) and normalized luminescence (right; λ_{ex} = 360 nm) spectra of compounds* ***(a) 2****,* ***(b) 17****,* ***(c) 18****.*

Figure 3-81 displays the UV-Vis absorption and the emission spectra of $[Cu(dppp)_2][Cu_5(SCy)_6]$ (**2**), $[Cu(dppp)_2][Cu_5(SAd)_6]$ (**17**) and $[Cu_4(SAd)_4(dppp)_2]$ (**18**) in solid state at room temperature. The estimated band gaps are 2.94 eV (458 nm) for **2**, 2.63 eV (502 nm) for **17** and 3.02 eV (427 nm) for **18**, respectively, and the maximum light emissions of **2**, **17**, **18** are at 617 nm, 666 nm and 582 nm, respectively. Firstly, a comparison of the spectra of **2** and **17**, which both contain the same $[Cu(dppp)_2]^+$ moiety and similar $[Cu_5(SR)_6]^-$ groups, shows a redshift of the absorption edge by changing from SAd^- to SCy^-. Also the emission spectrum of **17** is red-shifted compared to **2**. It can be speculated that SAd^- has a stronger electron-donating ability. Together with small changes of the bonding parameters of the two cluster anions, this leads to the shift of absorption edge and luminescence wavelength. Although sharing the same thiolate groups (SAd^-), **17** and **18** have different structures and therefore show different light emission curves. Many publications pointed out that the light-emission of low-nuclear d^{10} compounds is typically due to a ligand-to-metal charge transfer (LMCT) transition.[100]

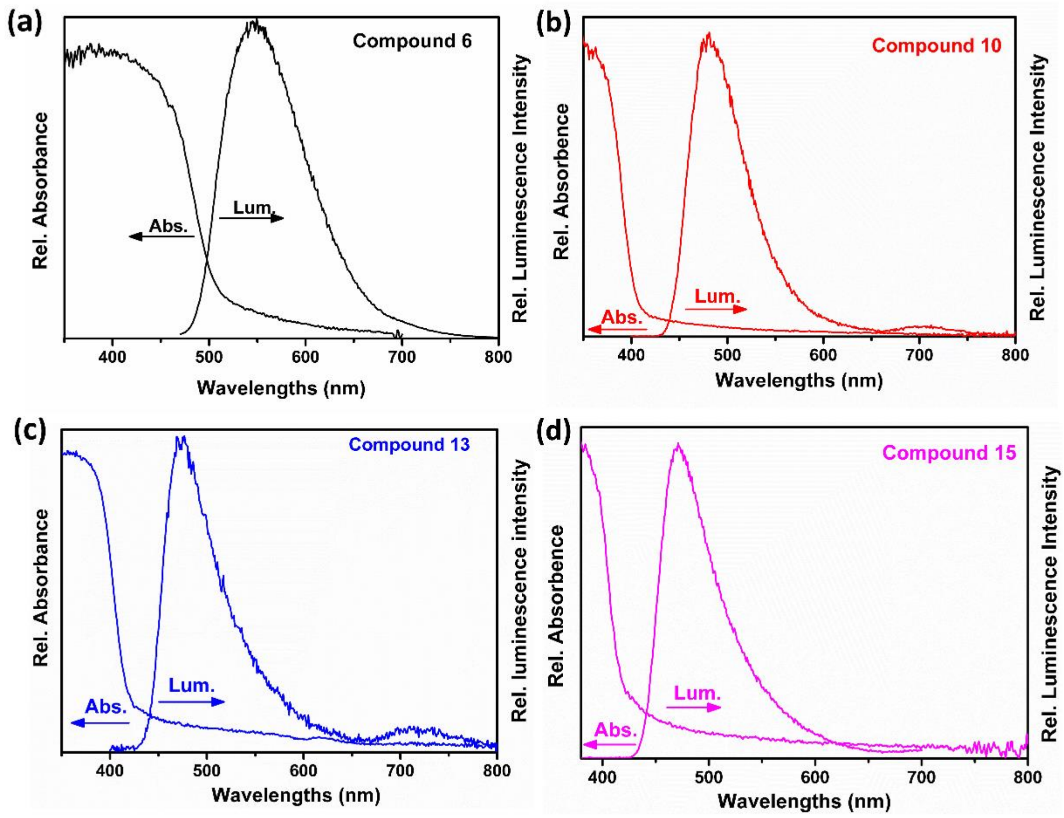

***Figure 3-82** Solid-state absorption (left) and normalized luminescence (right; λ_{ex} = 360 nm) spectra of compound **(a) 6**, **(b) 10, (c) 13, (d) 15**.*

As seen from **Figure 3-82**, the binuclear complexes $[Cu_2(SCp)_2(dpppt)_2]$ (**10**) $[Cu_2(SPh)_2(dppp)_2]$ (**13**) and $[Cu_2(SPh)_2(dpppt)_2]$ (**15**) have similar absorption and emission spectra. Calculated from the slopes of absorption spectra, the band gaps are 2.85 eV (448 nm) for **10**, 3.02 eV (420 nm) for **13** and 3.02 eV (422 nm) for **15**, respectively, whereas the maximum light emissions of **10**, **13**,

15 are located at 482 nm, 477 nm and 472 nm. In [$Cu_2(SCy)_2(dppox)_2$] (**6**) the absorption edge and the maximum of the emission are 514 nm and 549 nm, respectively, presenting a large red shift compared to the other binuclear compounds **10**, **13** and **15**. This might be caused by the different phosphine ligands.

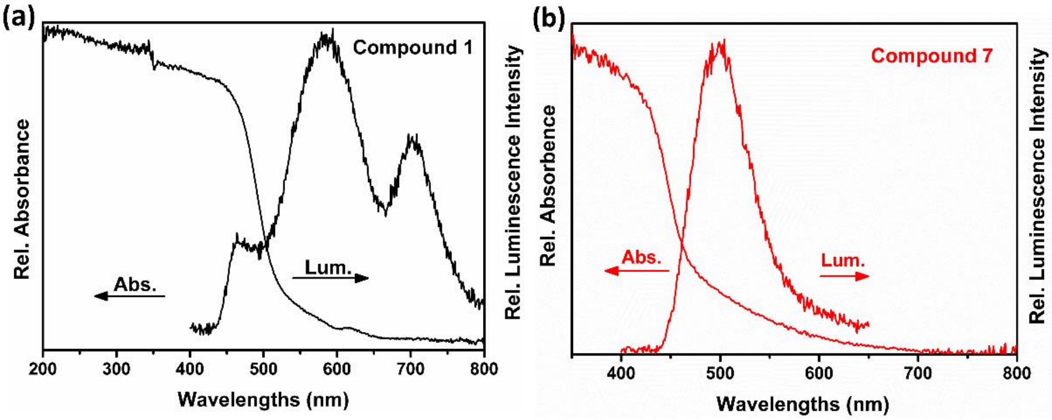

Figure 3-83 *Solid-state absorption (left) and normalized luminescenc (right; λ_{ex} = 360 nm) spectra of* ***(a) 1*** *and* ***(b) 7****.*

Compared to the above binuclear complexes, the two tetranuclear clusters [$Cu_4(SCy)_4(dppm)_2$] (**1**) and [$Cu_4(SCp)_4(dppm)_2$] (**7**) show different optical properties. A reason for that could be the different bonding situation. In **1** the copper atoms form a Cu_4 tetrahedron where four edges are capped by SCy^- groups. In **7**, a Cu_4S_4 eight-membered ring is present, which leads to completely different Cu-Cu distances. Interestingly, compound **1** presents dual emission with two maxima at 594 nm and 697 nm. The red shift of the absorption edge and the maximum of the light emission from **7** to **1** can be related to the stronger electron-donating ability of SCy^- relative to SCp^-.

Table 3-3 summarizes the optical data of the compounds discussed above. Apart from the ligands, the λ_{em} of these compounds is influenced by the nuclearity of the complexes.[101] As seen from **Table 3-3**, the maxima of the light emissions change from ionic (617 nm for **2**, 666 nm for **17**) to tetranuclear (495 nm for **7**, 582 nm for **18**, 594 nm and 697 nm for **1**), and to binuclear compounds (472 nm for **15**, 477 nm for **13**, 482 nm for **10** and 549 nm for **6**). It is obvious that there are some rough correlations with the sizes of these complexes: ionic clusters (6.15 Å for **2**, 5.89 Å for **17**) > tetranuclear clusters (5.76 Å for **18**, 5.76 Å for **7**, 5.36 Å for **1**) > binuclear clusters (3.56 Å for **15**, 3.65 Å for **13**, 3.41 Å for **10** and 3.34 Å for **6**). This trend shows the size-dependent optical property among these compounds. The ladder-like compound **1** is an exception, despite of the smaller size, its maximum luminescence is close to those of the ionic clusters **2** and **17**.

***Table 3-3** Wavelengths of the absorption edge and corresponding HOMO-LUMO gap energies, emission maxima, Stokes shift of compounds **1**, **2**, **6**, **7**, **10**, **13**, **15**, **17** and **18** and emission lifetimes at different temperatures and quantum yields at room temperature of **15**, **17** and **18**.*

	Absorption edge (nm)	**HOMO – LUMO gap (eV)**	**Emission maximum (nm)**	**Stokes shift (nm)**	**lifetime**	**lifetime**	**Quantum yield (295 K)**
					295 K	**5 K**	
1	524	2.50	594, 697	70, 173			
2	458	2.94	617	159			
6	514	2.50	549	35			
7	481	2.67	495	14			
8	448	2.85	482	34			
13	420	3.02	477	57			
15	422	3.02	472	50	1.12 μs	389 μs	3.4%
17	502	2.63	666	164	39 μs	77 μs	30%
18	427	3.02	582	155	28 μs	150 μs	22%

The luminescence intensity at different temperatures and the PL lifetime of **15**, **17**, **18** have also been measured. As seen from **Table 3-3**, the lifetimes of **15**, **17** and **18** are 1.12 μs, 39 μs and 28 μs at room temperature respectively. This means that the luminescence of **17** and **18** can be addressed as phosphorescence. The lifetimes of **17** and **18** moderately increase at lower temperature (5 K). In contrast, the emission lifetime of **15** increases drastically from 1.12 μs to 389 μs by changing the temperature from 295 K to 5 K. At low temperatures, the emission of **15** is phosphorescence, whereas at room temperature it might originates from TADF (TADF = thermally activated delayed fluorescence).[56] This effect deserves further investigation. The quantum yields of **15**, **17** and **18** at room temperature are 3.4%, 30%, 22% respectively.

With temperature increasing from 5 K to 295 K, there are several differences for the optical properties of these three compounds: the average lifetime and intensity of light-emission are decreased to a large degree, which may be caused by the increased non-radiative relaxation of the emitting excited triplet state at higher temperature.[23] For **15**, the position of the maximum emission shows a blueshift, whereas for compound **18**, no obvious change can be observed. Generally, the blueshift with increasing temperature might be the result of increasing Cu⋯Cu interactions in the core,[102] which broadens the energy gap between the metal-centred transition to a certain extent. But molecule interactions and structural change in the excited state might have an opposite effect.[103] However, there are no actual Cu⋯Cu interactions in the ground state in these compounds. Changing of the emission of **15** from phosphorescence at low temperature to TADF (with a smaller Stokes shift) at room temperature, as proposed above from the lifetime data, may be a simple reason for the emission blueshift with increasing temperature. The phosphorescence of compound **17** also shows a blueshift at higher temperatures. In this case, it might relate to the change in Cu⋯Cu interactions in the Cu_5 trigonal bipyramid core of **17**, which is similar to some other multinuclear clusters described in literature.[102]

4 Experimental section

4.1 Synthetic Methods

All reactions were carried out under an inert atmosphere of dry nitrogen using standard Schlenk technique.

4.2 Solvents

Solvents were dried and distilled before use. Toluene, THF and Et_2O were refluxed and dried over sodium/benzophenone. *n*-Pentane, *n*-hexane and *n*-heptane were dried over lithium aluminium hydride.DMF was pre-dried over magnesium sulphate and stored over molecular sieves (200 mesh) . Ethanol was used without drying.

4.3 Instruments used for characterization

Infrared spectra (IR) of all the compounds were recorded on a *Nicolet iS50 FTIR* (Fourier-transform infrared) spectrometer with ATR (attenuated total reflection) technology. The following abbreviations used in this thesis are: very strong (vs), strong (s), medium (m), weak (w), very weak (vw).

Elemental analyses (EA) were performed on an *Elementar vario Micro cube*. For elemental analyses the samples were dried under vacuum to obtain solvent-free products. Only in a few cases, proper elemental analysis was obtain. The reason for the problem with many analyses is the difficulty in the observation of analytically pure products, since in in the majority cases, a mixture of several components was formed. It was possible to select crystals under the microscope for optical spectroscopic analyses (i.e. Ultraviolet Visible spectroscopy (UV-Vis) or IR) and X-ray diffraction analysis. But in many cases, the yielded amount of product was not enough for a reasonable elemental analysis and further spectroscopic characterization (i.e. NMR). Moreover, the extremely poor solubility of the majority of products excluded NMR spectroscopy as well.

UV-Vis absorption spectra were obtained by a *CARY 5000* UV-vis-NIR (near infrared) spectrometer. Solid-state spectra were measured as a suspension of crystalline powder in mineral oil between two quartz plates with a *Labsphere* integration sphere. The absorption edges were determined by laying the tangent line through the inflection point of the first increase of the curve. The intersection point of the tangent with the abscissa was considered as wavelength of the HOMO-LUMO gaps.

Photoluminescence measurements were performed using the same sample-preparation method as for UV-vis on a *Varian Cary Eclipse* spectrometer.

4.4 Synthesis

All phosphine ligands (dppm, dppe, dppp, dppb, dpppt, dpph, dppox, dppfc, PPh_3) were commercially purchased without further purification. Silver thiolates[104], copper thiolates[105] and $E(SiMe_3)_2$ (E = S, Se)[106] were synthesized based on the literature.

4.4.1 $S(SiMe_3)_2$

Under a nitrogen atmosphere, 2.32 g (0.101 mol) sodium, 0.06 g (0.0047 mol) naphthalene, 1.6 g sulphur (0.05 mol) and approx. 100 mL THF were put into a 250 mL flask with a stirrer. The suspension was refluxed for 4 hours. After cooling to 0°C, 22.5 mL (0.2 mol) Me_3SiCl were added dropwise to the solution within 45 minutes. The reaction was stirred at 0°C for 2 hours, then at room temperature overnight. Finally, the solution was refluxed for 2 hours. Then the mixture was filtered and the residue washed with THF for three times and two times with Et_2O. Most of the solvent was removed in vacuum. Finally, the product was collected at 66°C-69°C under a reduced pressure of 15 Torr with the yield of 84% (based on sodium).

4.4.2 Silver thiolates

For the synthesis of silver thiolates always the same procedure was used. As an example, the synthesis of AgSCy is described in detail.

Under a nitrogen atmosphere, 2.6 mL (20 mmol) cyclohexanethiol (HSCy) was dissolved in 20 mL acetonitrile, then 2.8 mL triethylamine was dropped into the solution. After about ten minutes, a solution of 3.4 g (20 mmol) silver nitrate in 15 mL acetonitrile was added dropwise yielding in the precipitation of a yellow solid. The suspension was stirred for 1 hour. Then it was filtered and the solid was washed with acetonitrile for three times and Et_2O for two times. Finally, the silver thiolate was dried under vacuum (yield: 84% (based on silver)).

4.4.3 Copper thiolates

For the synthesis of copper thiolates always the same procedure was used. As an example, the synthesis of CuSCy is described in detail.

$CuSO_4 \cdot 5H_2O$ (6.26 g, 25 mmol) was added to an ice-cold mixture of 25 mL conc. aq. NH_3 and 100 mL H_2O forming a blue coloured solution. Over a period of 45 minutes, solid $NH_2OH \cdot HCl$ (3.89 g, 56 mmol) was added. Stirring overnight at 25°C yielded a colourless solution. On the next day, a solution of cyclohexanethiol (3 g) in 125 mL ethanol was dropped in slowly and a pale-yellow solid formed immediately. After stirring for half an hour, the solid product was collected *via* filtration and was washed with H_2O, ethanol and Et_2O. Finally, the product was dried under vacuum (yield: 67% (based on copper)).

4.4.4 $[Cu_4(SCy)_4(dppm)_2]$ (1)

A mixture of CuSCy (0.1075 g, 0.6 mmol) and dppm (0.2294 g, 0.6 mmol) in 1 mL toluene was stirred at room temperature for about 1 hour yielding a clear solution. Then the Schlenk tube was put into an oven with 40°C. Two days later, light yellow crystals of **1** formed. Yield: 15% (based on copper).

However, if the solution was stirred at room temperature for 1 hour and layered with 2 mL *n*-heptane, **1**$\cdot \frac{1}{2}(C_7H_8) \cdot \frac{1}{2}(C_7H_{16})$ formed. The later one's crystallographical data was put into the attachment.

Elemental analysis based on $[C_{74}H_{88}Cu_4P_4S_4]$ (1483.83 g/mol)

Calculated: C 59.90% H 5.98% S 8.64%

Found: C 58.10% H 5.57% S 8.50%

IR (ATR): 412(vw), 436(vw), 451(vw), 471(w), 479(w), 501(w), 511(w), 617(vw), 653(w), 691(s), 710(w), 717(w), 732(m), 768(w), 780(w), 817(vw), 855(vw), 886(vw), 917(vw), 996(w), 1026(vw), 1098(w), 1137(vw), 1157(vw), 1191(vw), 1254(vw), 1293(vw), 1355(vw), 1432(m), 1456(vw), 1484(w), 1573(vw), 1585(w), 1901(vw), 1967(vw), 2145(vw), 2178(vw), 2845(w), 2914(s), 3003(vw), 3047(w) cm^{-1}.

4.4.5 [Cu(dppp)$_2$][Cu$_5$(SCy)$_6$] (2), [Cu$_{16}$S$_4$(SCy)$_8$(dppp)$_4$]·4(C$_7$H$_8$) (3·4(C$_7$H$_8$)) and [Cu$_2$(SCy)$_2$(dppp)$_2$] (4)

A suspension of CuSCy (0.1072 g, 0.6 mmol) and dppp (0.1241 g, 0.3 mmol) in 10 mL toluene was stirred at 80°C for 2 hours and then filtered. The filtrate was kept at 40°C overnight. On the next day, the solution was layered with 20 mL *n*-heptane. Three days later a mixture of light yellow (**3**·4(C$_7$H$_8$)) and yellow (**4**) needle-like crystals formed. In a second experiment one could only obtain pure compound **2** (yield: 25% (based on copper)). Since it was impossible to select pure crystals of **3** and **4** only the results for **2** are presented here.

2 Elemental analyses based on [$C_{90}H_{118}Cu_6P_4S_6$] (1897.32 g/mol)

Calculated: C 56.97% H 6.27% S 10.14%

Found: C 56.65% H 6.22% S 9.99%

IR (ATR): 413(vw), 436(vw), 452(vw), 471(w), 480(w), 501(w), 511(w), 617(vw), 653(w), 692(s), 710(w), 717(w), 732(m), 768(w), 780(w), 817(vw), 855(vw), 886(vw), 918(vw), 996(vw), 1027(vw), 1098(w), 1137(vw), 1157(vw), 1191(vw), 1254(w), 1293(vw), 1355(vw), 1432(s), 1456(vw), 1484(vw), 1573(vw), 1585(vw), 1901(vw), 1967(vw), 2145(vw), 2178(vw), 2845(m), 2914(s), 3003(vw), 3047(vw) cm^{-1}.

4.4.6 [$Cu_2(SCy)_2(dpppt)_{1.5}]_n$ (5)

A mixture of CuSCy (0.0536 g, 0.3 mmol) and dpppt (0.2640 g, 0.6 mmol) in 6 mL toluene was stirred at room temperature for 1 hour, yielding a clear solution. The solution was layered with 12 mL *n*-heptane. Three days later a mixture of light yellow (**5**) and red crystals of [$Cu_{12}S_6$(dpppt)$_4$][39] formed. Due to the mixed crystals the EA and IR analysis of compound **5** was not carried out.

4.4.7 [$Cu_2(SCy)_2(dppox)_2$] (6)

A mixture of CuSCy (0.0523 g, 0.3 mmol) and dppox (0.1440 g, 0.3 mmol) in 5 mL toluene was stirred at room temperature for 1 hour. After two days at 40°C the suspension was filtered and layered with 10 mL *n*-heptane. Several days later yellow, plate-like crystals of **6** formed (yield: 15% (based on copper)).

Elemental analysis based on [$C_{76}H_{78}Cu_2P_4S_2$] (1306.46 g/mol)

Calculated:	C 69.86%	H 6.02%	S 4.91%
Found:	C 67.44%	H 5.25%	S 4.80%

IR (ATR): 419(vw), 440(w), 478(m), 493(m), 505(m), 618(vw), 663(m), 691(s), 739(s), 760(w), 818(vw), 842(vw), 881(vw), 913(vw), 995(w), 1027(w), 1069(vw), 1090(w), 1157(vw), 1191(vw), 1254(vw), 1329(vw), 1432(s), 1444(m), 1480(m), 1570(vw), 1584(w), 1963(vw), 2168(vw), 2846(m), 2919(m), 3047(w) cm^{-1}.

4.4.8 [$Cu_4(SCp)_4(dppm)_2$] (7)

A suspension of CuSCp (0.0971 g, 0.6 mmol) and dppm (0.1141 g, 0.3 mmol) in 10 mL toluene was stirred at 80°C for 3 hours and then filtered. The filtrate was kept at 40°C overnight and on the next day it was layered with 20 mL *n*-heptane. Three days later yellow, needle-like crystals of **7** formed (yield: 15% (based on copper)).

Elemental analysis based on [$C_{70}H_{80}Cu_4P_4S_4$] (1427.62 g/mol)

Calculated: C 58.89% H 5.65% S 8.98%

Found: C 56.94% H 5.52% S 8.90%

IR (ATR): 418(vw), 439(vw), 470(w), 504(w), 517(m), 691(s), 715(m), 735(s), 777(m), 825(vw), 914(vw), 933(vw), 966(vw), 998(vw), 1026(w), 1038(w), 1067(vw), 1098(w), 1122(vw), 1157(vw), 1183(vw), 1227(vw), 1251(vw), 1295(w), 1307(w), 1340(vw), 1361(w), 1432(s), 1481(m), 1584(w), 1805(vw), 1884(vw), 1980(vw), 2050(vw), 2166(vw), 2844(m), 2862(m), 2895(m), 3047(w), 3339(vw) cm^{-1}.

4.4.9 [$Cu(dppp)_2$][$Cu_5(SCp)_6$]·1.5(C_7H_8) (8·1.5(C_7H_8)) and [$Cu_{16}S_4(SCp)_8(dppp)_4$]·4($C_7H_8$) (9·4($C_7H_8$))

A mixture of CuSCp (0.0988 g, 0.6 mmol) and dppp (0.2475 g, 0.6 mmol) in 10 mL toluene was stirred at 80°C for 3 hours and then filtered. The solution was kept at 40°C overnight and then layered with 20 mL *n*-heptane. Three days later colourless block-like crystals (**8**·1.5(C_7H_8)) and yellow needle crystals (**9**·4(C_7H_8)) formed. Due to the mixed crystals the EA and IR of compound **8** and **9** was not carried out.

4.4.10 [$Cu_2(SCp)_2(dpppt)_2$] (10)

A mixture of CuSCp (0.0988 g, 0.6 mmol) and dpppt (0.2643 g, 0.6 mmol) in 5 mL toluene was stirred at 80°C for 3 hours. Then the suspension was filtered and the filtrate was kept at 40°C overnight. On the next day, the solution was layered with 10 mL *n*-heptane. Three days later a few red, block-like crystals of [$Cu_{12}S_6(dpppt)_4$][39] formed. After a further week additionally light yellow, block-like crystals of **10** formed (yield of **10** separated under the microscope: 10% (based on copper)).

Elemental analysis based on [$C_{68}H_{78}Cu_2P_4S_2$] (1210.38 g/mol)

Calculated: C 67.47% H 6.49% S 5.30%

Found: C 66.73% H 6.26% S 5.24%

IR (ATR): 422(vw), 445(w), 478(m), 508(m), 690(s), 723(m), 737(m), 846(vw), 878(vw), 917(vw), 972(vw), 1000(w), 1016(w), 1026(w), 1053(vw), 1068(w), 1097(m), 1153(w), 1217(w), 1307(w), 1414(w), 1432(m), 1451(w), 1481(m), 1567(vw), 1586(w), 1807(vw), 1890(vw), 1949(vw), 1979(vw), 2050(vw), 2166(vw), 2323(vw), 2820(w), 2855(m), 2934(m), 3050(w), 3072(vw) cm^{-1}.

4.4.11 $[Cu_2(SCp)_2(dppbz)_2]$ (11)

A mixture of CuSCp (0.0988 g, 0.6 mmol) and dppbz (0.2630 g, 0.6 mmol) in 10 mL toluene was stirred at 80°C for 3 hours. Then the suspension was filtered and the filtrate was kept at 40°C overnight. On the next day the solution was layered with 20 mL *n*-heptane. In the first experiment yellow, needle-like crystals of **11** formed (yield: 34% (based on copper)).

11 Elemental analysis based on $[C_{70}H_{66}Cu_2P_4S_2]$ (1222.30 g/mol)

Calculated: C 68.78% H 5.44% S 5.25%

Found: C 68.57% H 5.27% S 4.73%

IR (ATR): 446(m), 487(s), 502(s), 617(vw), 689(s), 737(s), 769(s), 861(m), 945(vw), 964(vw), 999(vw), 1027(m), 1045(vw), 1060(vw), 1093(m), 1156(vw), 1182(vw), 1229(vw), 1275(vw), 1305(vw), 1328(vw), 1410(vw), 1432(s), 1481(m), 1492(vw), 1571(vw), 1584(vw), 1953(vw), 1962(vw), 1977(vw), 1994(vw), 2011(vw), 2025(vw), 2034(vw), 2062(vw), 2124(vw), 2151(vw), 2165(vw), 2180(vw), 2187(vw), 2856(vw), 2943(vw), 3053(vw), 3140(vw) cm^{-1}.

4.4.12 $[Cu_{14}S(SCp)_{12}(PPh_3)_4]$ (12)

CuSCp (0.0485 g, 0.3 mmol) and PPh_3 (0.0778 g, 0.3 mmol) were suspended in 5 mL toluene and stirred at room temperature for 30 minutes. Then the solution was heated to 40°C for two days. Finally, the solution was layered with 10 mL *n*-heptane. Three days later yellow, block-like crystals of **12** formed (yield: 19% (based on copper)).

Elemental analysis based on [$C_{132}H_{168}Cu_{14}P_4S_{13}$] (3184.87 g/mol)

Calculated: C 49.78% H 5.32% S 13.09%

Found: C 46.19% H 4.61% S 12.40%

IR (ATR): 432(vw), 502(s), 541(vw), 618(vw), 694(s) 742(s), 800(vw), 851(vw), 895(vw), 933(vw), 997(vw), 1028(vw), 1092(m), 1157(vw), 1226(m), 1261(vw), 1310(vw), 1434(s), 1479(m), 1570(vw), 1585(vw), 1828(vw), 1904(vw), 1953(vw), 1971(vw), 1986(vw), 2001(vw), 2011(vw), 2030(vw), 2036(vw), 2043(vw), 2062(vw), 2081(vw), 2124(vw), 2145(vw), 2161(vw), 2173(vw), 2185(vw), 2213(vw), 2221(vw), 2861(m), 2947(s), 3051(w) cm^{-1}.

4.4.13 $[Cu_2(SPh)_2(dppp)_2]\cdot(C_7H_8)$ (13·(C_7H_8))

A mixture of CuSPh (0.1036 g, 0.6 mmol) and dppp (0.3093 g, 0.75 mmol) in 10 mL toluene was stirred at 80°C for 3 hours and then filtered. The filtrate was kept at 40°C overnight. On the next day, the solution was layered with 20 mL *n*-heptane. One week later colourless crystals of **13**·(C_7H_8) formed (yield: 13% (based on copper)).

Elemental analysis based on [$C_{66}H_{62}Cu_2P_4S_2$] (1170.31 g/mol)

Calculated: C 67.73% H 5.34% S 5.48%

Found: C 66.91% H 5.33% S 4.51%

IR (ATR): 410(w), 441(vw), 464(w), 476(w), 507(w), 517(w), 642(w), 690(s), 736(m), 796(vw), 825(w), 849(vw), 964(w), 998(w), 1022(m), 1080(m), 1095(m), 1159(w), 1189(vw), 1267(w), 1309(w), 1328(vw), 1432(s), 1467(m), 1481(m), 1495(w), 1570(m), 1582(vw), 1820(vw), 1891(vw), 1979(vw), 2050(vw), 2166(vw), 2323(vw), 2860(vw), 2899(vw), 2928(vw), 3045(w) cm^{-1}.

4.4.14 [$Cu_4(SPh)_4(PPh_3)_4$] (14)

CuSPh (0.1035 g, 0.6 mmol) and PPh_3 (0.3148 g, 1.2 mmol) were suspended in 10 mL toluene and stirred at 80°C for 2 hours. Then the suspension was heated for a few minutes up to the boiling point. The mixture was filtered and the filtrate was kept at 40°C overnight. On the next day the solution was layered with 20 mL *n*-heptane, yielding light-yellow crystals of **14** after a few days (yield: 54% (based on copper)).

Elemental analysis based on [$C_{96}H_{80}Cu_4P_4S_4$] (1739.88 g/mol)

Calculated:	C 66.27%	H 4.63%	S 7.37%
Found:	C 67.34%	H 4.50%	S 6.58%

IR (ATR): 427(vw), 478(m), 489(vw), 506(s), 519(s), 617(vw), 688(s), 730(s), 802(vw), 846(vw), 915(vw), 970(vw), 996(w), 1021(m), 1080(m), 1093(m), 1122(vw), 1159(vw), 1179(w), 1262(vw), 1308(vw), 1328(vw), 1432(s), 1469(s), 1478(m), 1493(m), 1572(s), 1602(vw), 1896(vw), 1952(vw), 1970(vw), 1985(vw), 2008(vw), 2026(vw), 2042(vw), 2096(vw), 2155(vw), 2162(vw), 2210(vw), 2982(vw), 3049(m) cm^{-1}.

4.4.15 [$Cu_2(SPh)_2(dpppt)_2$]·2(C_7H_8) (15·2(C_7H_8))

A mixture of CuSPh (0.1048 g, 0.6 mmol) and dpppt (0.2651 g, 0.6 mmol) in 10 mL toluene was stirred at room temperature for 10 minutes, forming a yellow suspension. Then the mixture was heated to the boiling point until all solids were dissolved. The reaction was stirred for additional 15 minutes and the Schlenk tube was then stored for one week at room temperature. During that period **15**·2(C_7H_8) was formed as colourless, block-like crystals (yield: 85% (based on copper)).

Elemental analysis based on [$C_{70}H_{70}Cu_2P_4S_2$] (1226.42 g/mol)

Calculated: C 68.55% H 5.75% S 5.23%

Found: C 69.42% H 5.90% S 4.55%

IR (ATR): 420(vw), 445(w), 464(w), 475(m), 512(m), 690(s), 727(s), 851(vw), 886(w), 923(vw), 975(vw), 998(w), 1019(w), 1054(w), 1080(m), 1097(m), 1155(w), 1201(vw), 1244(vw), 1265(vw), 1309(vw), 1331(vw), 1408(w), 1431(s), 1448(m), 1466(m), 1482(m), 1494(m), 1572(m), 1584(m), 1603(vw), 1979(vw), 2113(vw), 2161(vw), 2323(vw), 2850(w), 2917(w), 2948(w), 2984(w), 3002(w), 3020(w), 3049(w) cm^{-1}.

4.4.16 [$Cu_2(SPh)_2(dppox)_2$] (16)

CuSPh (0.1035 g, 0.6 mmol) and dppox (0.5694 g, 1.2 mmol) were suspended in 10 mL toluene and stirred at 80°C for 3 hours. After filtration the reaction mixture was kept at 40°C overnight. Two days later at room temperature yellow, block-like crystals of **16** formed (yield: 23% (based on copper)).

Elemental analysis based on [$C_{76}H_{66}Cu_2P_4S_2$] (1294.36 g/mol)

Calculated: C 70.46% H 5.10% S 4.94%

Found: C 70.73% H 4.80% S 4.25%

IR (ATR) 412(vw), 439(vw), 475(vw), 482(vw), 502(vw), 560(vw), 611(vw), 689(s), 732(s), 739(vw), 769(vw), 811(vw) 825(vw), 859(vw), 859(vw), 916(vw), 970(vw), 997(vw), 1021(m), 1041(vw), 1087(m), 1122(vw), 1158(vw), 1179(vw), 1268(vw), 1309(vw), 1330(vw), 1378(vw), 1433(s), 1468(vw), 1480(vw), 1572(vw), 1604(vw), 1810(vw), 1951(vw), 1981(vw), 2011(m), 2023(m), 2042(s), 2049(vw), 2124(vw), 2150(vw), 2156(vw), 2169(vw), 2181(vw), 2194(vw), 2266(vw), 2911(vw), 2945(vw), 3048(m) cm^{-1}.

4.4.17 [Cu(dppp)$_2$][Cu$_5$(SAd)$_6$] (17)

A suspension of CuSAd (0.1361 g, 0.6 mmol) and dppp (0.1239 g, 0.3 mmol) in 5 mL toluene was stirred at 80°C for 3 hours. Then the mixture was filtered and the filtrate was kept at 40°C overnight. Finally, the solution was layered with 2 mL ethanol and 10 mL *n*-heptane. Three days later two kinds of yellow crystals were formed: block-like crystals of **17** and needle-like crystals with the composition **17**·(C_7H_{16}) (yield: 25% (based on copper)).

Elemental analysis based on [$C_{114}H_{142}Cu_6P_4S_6$] (2209.75 g/mol)

Calculated: C 61.91% H 6.48% S 8.71%

Found: C 60.77% H 6.16% S 8.31%

IR (ATR): 408(vw), 489(w), 511(m), 645(w), 693(s), 738(s), 797(vw), 826(w), 966(w), 999(vw), 1037(m), 1096(m), 1160(vw), 1178(vw), 1251(vw), 1295(m), 1308(w), 1340(w), 1432(s), 1448(m), 1469(w), 1482(w), 1571(vw), 1979(vw), 2031(vw), 2050(vw), 2162(vw), 2672(vw), 2844(s), 2895(s), 3050(vw), 3339(vw) cm^{-1}.

4.4.18 [Cu$_4$(SAd)$_4$(dppp)$_2$] (18)

A mixture of CuSAd (0.1385 g, 0.6 mmol) and dppp (0.1233 g, 0.3 mmol) in 5 mL toluene was stirred at 80°C for 3 hours. Then the suspension was filtered and the filtrate was heated to 40°C for 2 days. After cooling to room temperature colourless, block-like crystals of **18** formed (yield: 25% (based on copper)).

Elemental analysis based on [$C_{94}H_{112}Cu_4P_4S_4$] (1748.10 g/mol)

Calculated: C 64.58% H 6.46% S 7.34%

Found: C 62.30% H 5.92% S 7.19%

IR (ATR): 410(vw), 442(vw), 460(vw), 480(w), 512(m), 649(w), 689(m), 737(m), 769(vw), 808(vw), 826(vw), 935(vw), 961(w), 999(w), 1036(m), 1069(vw), 1096(w), 1160(vw), 1179(vw), 1250(vw), 1295(w), 1340(w), 1431(m), 1481(w), 1586(vw), 1653(vw), 1806(vw), 1889(w), 1970(vw), 1980(vw), 2023(vw), 2049(vw), 2069(vw), 2113(vw), 2164(vw), 2285(vw), 2324(vw), 2843(s), 2896(vs), 2980(w), 3042(vw) cm^{-1}.

4.4.19 [$Cu_{16}S_8(dpph)_6$] (19)

A mixture of CuSAd (0.1385 g, 0.6 mmol) and dpph (0.5450 g, 1.2 mmol) in 10 mL toluene was stirred at 80°C for 3 hours. Then the suspension was filtered and the filtrate was kept at 40°C overnight. On the next day, the solution was layered with 20 mL *n*-heptane. One week later light yellow, block-like crystals of **19** formed (yield: 32% (based on copper)).

4.4.20 [Cu_4(Strimethyl-benzyl)$_4$(dppm)$_2$]·(C_7H_8) (20·(C_7H_8))

A mixture of Cu(Strimethyl-benzyl) (0.137 g, 0.6 mmol) and dppm (0.462 g, 1.2 mmol) in 10 mL toluene was stirred at 80°C for 3 hours. Then the suspension was filtered and the filtrate was kept at 40°C overnight. On the next day, the solution was layered with 2 mL toluene and 20 mL *n*-heptane. Three days later yellow, needle-like crystals of **20**·(C_7H_8) formed (yield: 10% (based on copper)).

Elemental analysis based on [$C_{90}H_{96}Cu_4P_4S_4$] (1684.06 g/mol)

Calculated:	C 64.19%	H 5.75%	S 7.62%
Found:	C 62.72%	H 5.18%	S 7.30%

IR (ATR): 427(vw), 473(m), 503(w), 516(m), 557(vw), 617(vw), 665(w), 689(s), 717(w) 734(s), 781(w), 849(w), 939(vw), 964(vw), 999(vw), 1025(vw), 1094(vw), 1157(vw), 1199(vw), 1219(vw), 1260(vw), 1309(vw), 1327(vw), 1358(vw), 1372(vw), 1433(s), 1480(m), 1574(vw), 1585(vw), 1612(vw), 1805(vw), 1953(vw), 1962(vw), 1976(vw), 1983(vw), 2015(vw), 2024(vw), 2030(vw), 2041(vw), 2055(vw), 2083(vw), 2125(vw), 2152(vw), 2162(vw), 2181(vw), 2191(vw), 2211(vw), 2233(vw), 2253(vw), 2267(vw), 2725(vw), 2851(vw), 2911(vw) cm^{-1}.

4.4.21 [Cu_2(Strimethyl-benzyl)$_2$(dppb)$_2$]·(C_6H_{14}) (21·(C_6H_{14}))

A mixture of Cu(Strimethyl-benzyl) (0.0692 g, 0.3 mmol) and dppb (0.0642 g, 0.15 mmol) in 5 mL toluene was stirred at room temperature for 30 minutes. Then the reaction was kept at 80°C overnight. Finally, the suspension was filtered and the filtrate was layered with 10 mL *n*-hexane. Three days later colourless, block-like crystals of **21**·(C_6H_{14}) formed (yield: 10% (based on copper)).

IR (ATR): 420(vw), 443(w), 466(w), 483(w), 504(m), 618(vw), 641(vw), 692(s), 732(s), 769(vw), 783(vw), 811(vw), 826(vw), 847(w), 885(w), 940(vw), 999(vw), 1027(w), 1089(m), 1151(vw), 1185(vw), 1213(vw), 1277(vw), 1308(vw), 1371(vw), 1432(s), 1468(m), 1481(s), 1572(w), 1668(vw), 1811(vw), 1893(vw), 1958(vw), 1970(vw), 1979(vw), 1990(vw), 2000(vw), 2013(w), 2035(vw), 2053(vw), 2110(vw), 2138(vw), 2154(vw), 2167(vw), 2180(vw), 2191(vw), 2201(vw), 2209(vw), 2228(vw), 2680(vw), 2851(w), 2918(w), 3048(w), 3140(vw) cm^{-1}.

4.4.22 [$Cu_{12}S_6$(dppox)$_4$]·(C_7H_8)·2(C_7H_{16}) (22·(C_7H_8)·2(C_7H_{16}))

Cu(Strimethyl-benzyl) (0.0686 g, 0.3 mmol) and dppox (0.1421 g, 0.3 mmol) were suspended in 5 mL toluene and stirred at room temperature for 1 hour. Then the reaction mixture was kept at 40°C for two days. Finally, the suspension was filtered and the filtrate was layered with 10 mL *n*-heptane. Three days later light yellow, needle-like crystal of **22**·(C_7H_8)·2(C_7H_{16}) formed (yield: 32% (based on copper)). The same product could also be obtained by an analogous reaction of CuSAd and dppox.

4.4.23 (HDMF)$_2$[Cu_6(SPh)$_5$(dppe)$_3$]$_2$(Mo_8O_{26})·2DMF·(Et_2O) (23·2DMF·(Et_2O))

A mixture of CuSPh (0.0264 g, 0.15 mmol), dppe (0.0304 g, 0.075 mmol) and $(NH_4)_6Mo_7O_{24}$ (0.0172 g, 0.014 mmol) in 5 mL DMF was stirred at 90°C for

3 hours. Then the Schlenk tube was kept at 80°C overnight. Finally, the suspension was filtered and the filtrate was layered by 3 mL ethanol and 10 mL Et_2O. Three weeks later light blue, block-like crystal of **23**·2DMF·(Et_2O) formed (yield: 10% (based on copper)).

Elemental analysis based on [$C_{222}H_{210}Cu_{12}P_{12}S_{10}Mo_8O_{28}N_2$] (5576.44 g/mol)

Calculated: C 47.82% H 3.80% S 5.75%

Found: C 45.87% H 4.07% S 5.00%

IR (ATR): 410(vw), 476(vw), 510(w), 554(vw), 614(vw), 689(w), 737(w), 839(w), 906(m), 937(m), 998(vw), 1021(w), 1079(w), 1096(m), 1157(vw), 1190(vw), 1254(vw), 1308(vw), 1331(vw), 1384(w), 1433(s), 1471(w), 1482(w), 1574(m), 1661(s), 1713(vw), 1818(vw), 1940(vw), 1949(vw), 1976(vw), 1997(vw), 2025(vw), 2034(vw), 2041(vw), 2060(vw), 2069(vw), 2081(vw), 2104(vw), 2137(vw), 2153(vw), 2162(vw), 2172(vw), 2188(vw), 2198(vw), 2206(vw), 2221(vw), 2268(vw), 2423(vw), 2779(vw), 2846(vw), 2921(w), 3050(w), 3171(vw), 3521(vw), 3765(vw) cm^{-1}.

4.4.24 [$(Cu_5(SPh)_5(dppe)_2)_2$(dppe)]·2DMF (24·2DMF)

CuSPh (0.0380 g, 0.225 mmol) and dppe (0.0598 g, 0.15 mmol) were suspended in 10 mL DMF and stirred at 80°C for 3 hours. Then the solution was kept at 80°C overnight. On the next day, the volume was decreased to approx. 5 mL in vacuum and the solution was layered with 2 mL ethanol and 10 mL *n*-heptane. One week later light pink, rhombohedral-like crystals of **24**·2DMF were formed (yield: 5% (based on copper)).

Elemental analysis based on [$C_{190}H_{170}Cu_{10}P_{10}S_{10}$] (3719.22 g/mol)

Calculated: C 61.36% H 4.61% S 8.62%

Found: C 60.04% H 4.70% S 7.73%

IR (ATR): 423(vw), 475(w), 511(w), 616(vw), 689(s), 735(m), 751(w), 821(vw), 998(vw), 1020(w), 1079(m), 1093(w), 1385(w), 1432(m), 1470(m), 1482(w), 1573(m), 1660(s), 1770(vw), 1932(vw), 1952(vw), 1967(vw), 1978(vw), 2016(vw), 2030(vw), 2056(vw), 2135(vw), 2159(vw), 2174(vw), 2183(vw), 2204(vw), 2218(vw), 3047(w) cm^{-1}.

4.4.25 [$Cu_6(SPh)_4(dppm)_4$](Mo_6O_{19})·2DMF (25·2DMF)

A mixture of CuSPh (0.0522 g, 0.3 mmol), dppm (0.1159 g, 0.3 mmol) and $(NH_4)_6Mo_7O_{24}$ (0.1861 g, 0.15 mmol) in 20 mL DMF was stirred at 80°C for 3 hours. Then the suspension was kept at 80°C overnight. On the next day, the reaction mixture was filtered, the volume of the filtrate was reduced to 5 mL in vacuum and finally layered with 3 mL ethanol and 10 mL *n*-heptane. One week later yellow, needle-like crystals of **25**·2DMF crystallized (yield: 19% (based on copper)).

Elemental analysis based on [$C_{124}H_{108}Cu_6P_8S_4Mo_6O_{19}$] (3235.14 g/mol)

Calculated:	C 46.04%	H 3.36%	S 3.96%
Found:	C 52.84%	H 3.65%	S 4.09%

IR (ATR): 437(vw), 475(w), 513(m), 571(vw), 689(s), 733(s), 797(m), 950(s), 999(w), 1022(w), 1093(m), 1157(vw), 1186(vw), 1254(vw), 1307(vw), 1384(w), 1432(s), 1472(w), 1481(m), 1573(w), 1668(s), 1726(vw), 1809(vw), 1936(vw), 1948(vw), 1971(vw), 1986(vw), 2010(vw), 2017(vw), 2029(vw), 2052(vw), 2141(vw), 2163(vw), 2171(vw), 2180(vw), 2222(vw), 2235(vw), 2671(vw), 2843(vw), 2896(w), 3049(w), 3233(vw), 3558(vw) cm^{-1}

4.4.26 [$Cu_4(SPh)_4(PPh_3)_4$]·2(C_7H_8) (26·2(C_7H_8))

A mixture of CuSPh (0.0515 g, 0.3 mmol) and PPh_3 (0.0790 g, 0.3 mmol) in 5 mL toluene was stirred overnight. This solution was mixed with a solution of $(MH_4)_6Mo_7O_{24}$ (0.1860 g, 0.15 mmol) in 5 mL ethanol. The resulting mixture was stirred for an additionally 3 hours. Finally, the suspension was filtered, and within one week colourless, block-like crystals of **26**·2(C_7H_8) formed (yield:

less than 5% (based on copper)).

Elemental analysis based on [$C_{96}H_{80}Cu_4P_4S_4$] (1740.00 g/mol)

Calculated: C 66.27% H 4.63% S 7.37%

Found: C 67.98% H 4.68% S 6.56%

IR (ATR): 421(w), 466(w), 472(vw), 489(w), 505(m), 518(w), 617(vw), 687(s), 730(s), 801(vw), 846(vw), 890(vw), 970(vw), 996(vw), 1021(w), 1080(m), 1094(m), 1159(vw), 1179(vw), 1263(vw), 1289(vw), 1308(vw), 1329(vw), 1432(s), 1470(s), 1479(m), 1493(w), 1572(s), 1602(vw), 1812(vw), 1897(vw), 1952(vw), 1967(vw), 1976(vw), 1990(vw), 2005(vw), 2025(vw), 2050(vw), 2159(vw), 2183(vw), 2203(vw), 2217(vw), 2987(vw), 3048(w) cm^{-1}.

4.4.27 [$Cu_3S_3(SCp)(MoO)(PPh_3)_2]_2\cdot 2DMF$ (27·2DMF)

A mixture of CuSCp (0.0481 g, 0.3 mmol), PPh_3 (0.0784 g, 0.3 mmol) and $(NH_4)_6Mo_7O_{24}$ (0.1858 g, 0.15 mmol) in 20 mL DMF was stirred at room temperature for several minutes. Then 50 μL $S(SiMe_3)_2$ was added into the suspension and stirred overnight, yielding a clear solution. On the next day, the volume of the solution was reduced to 5 mL in vacuum. Two weeks later red, block-like crystals **27**·2DMF formed (yield: less than 5% (based on copper)).

Elemental analysis based on [$C_{82}H_{78}Cu_6Mo_2O_2P_4S_8$] (2049.06 g/mol)

Calculated: C 48.06% H 3.84% S 12.52%

Found: C 47.74% H 4.19% S 11.31%

IR (ATR): 441(w), 490(w), 504(w), 521(m), 617(vw), 659(vw), 691(s), 705(w), 739(w), 798(vw), 849(vw), 866(vw), 901(w), 957(vw), 996(vw), 1026(vw), 1069(vw), 1093(m), 1160(vw), 1180(vw), 1229(vw), 1258(vw), 1307(vw), 1329(vw), 1385(vw), 1433(s), 1479(w), 1503(vw), 1542(vw), 1585(vw), 1671(s), 1811(vw), 1904(vw), 1957(vw), 1975(vw), 1987(vw), 1996(vw), 2006(vw), 2019(vw), 2034(vw), 2041(vw), 2048(vw), 2061(vw), 2069(vw), 2080(vw), 2105(vw), 2137(vw), 2149(vw), 2159(vw), 2172(vw), 2189(vw), 2211(vw), 2219(vw), 2257(vw), 2580(vw), 2679(vw), 2851(vw), 2922(vw), 3055(vw), 3071(vw), 3244(vw), 3328(vw), 3582(vw) cm^{-1}.

4.4.28 [$Cu_{16}Se_8(dppp)_6$] (28)

A mixture of CuSCp (0.0504 g, 0.3 mmol) and dppp (0.3720 g, 0.9 mmol) in 4 mL THF was stirred for 5 minutes. Then 36 *µ*L $Se(SiMe_3)_2$ were added and the suspension was stirred overnight at room temperature, yielding a clear solution. This was layered with 8 mL Et_2O. One week later a mixture of two different brown, plate-like crystals formed, a monoclinic and a triclinic form of **28** (yield: 15% (based on copper)).

IR (ATR): 418(w), 478(w), 508(m), 545(vw), 616(vw), 666(w), 688(s), 736(s), 822(w), 909(vw), 947(w), 998(vw), 1026(w), 1068(w), 1096(m), 1156(vw), 1184(vw), 1230(vw), 1274(vw), 1307(vw), 1329(vw), 1402(w), 1431(s), 1480(s), 1570(vw), 1585(w), 1665(vw), 1808(vw), 1884(vw), 1964(vw), 1976(vw), 1995(vw), 2013(vw), 2029(vw) , 2053(vw), 2128(vw), 2143(vw), 2180(vw), 2188(vw), 2199(vw), 2206(vw), 2255(vw), 2923(vw), 3045(w), 3141(vw) cm^{-1}.

4.4.29 [$Cu_{12}Se_4(SCp)_4(dppfc)_4$]·($C_7H_8$) (29·($C_7H_8$))

CuSCp (0.0822 g, 0.5 mmol) and dppfc (0.1364 g, 0.123 mmol) were suspended in 5 mL toluene and stirred at room temperature for 5 minutes. Then 40 *µ*L $Se(SiMe_3)_2$ were added. The mixture was stirred overnight, yielding a clear solution. On the next day, the solution was layered with 1 mL ethanol and 8 mL Et_2O. Three days later dark brown, block-like crystals **29**·(C_7H_8) formed (yield: less than 5% (based on copper)) together with some red amorphous residue.

4.4.30 [$Cu_{14}Se_6(SAd)_2(dppm)_6$]·6($C_7H_8$) (**30**·6($C_7H_8$)) and [$Cu_4(SAd)_4(dppm)_2$] (31)

A mixture of CuSAd (0.0822 g, 0.5 mmol) and dppm (0.096 g, 0.25 mmol) in 5 mL toluene was stirred at room temperature for 5 minutes. Then 36 μL $Se(SiMe_3)_2$ were added and stirred overnight yielding a clear solution. On the next day, the solution was layered with 8 mL Et_2O. Three days later reddish orange, rhombohedral crystals of **30**·6(C_7H_8) (yield: 14% (based on copper)) and yellow, block-like crystals of **31** co-crystallized. Crystals of **30** were selected by hand under microscope.

30 IR (ATR): 407(vw), 440(vw), 472(w), 511(m), 547(vw), 617(vw), 686(m), 713(vw), 732(m), 777(m), 837(vw), 913(vw), 962(vw), 998(vw), 1026(w), 1094(m), 1156(vw), 1186(vw), 1226(vw), 1275(vw), 1307(vw), 1358(vw), 1432(s), 1481(m), 1571(vw), 1585(vw), 1613(vw), 1680(vw), 1805(vw), 1888(vw), 1933(vw), 1941(vw), 1967(vw), 1982(vw), 1994(vw), 2033(vw), 2116(vw), 2128(vw), 2142(vw), 2154(vw), 2171(vw), 2180(vw), 2195(vw), 2240(vw), 2858(vw), 2939(vw), 3046(vw) cm^{-1}.

4.4.31 [$Cu_{92}S_{44}(SAd)_4(dppp)_{12}$] (32)

A mixture of CuSAd (0.1152 g, 0.5 mmol) and dppp (0.0525 g, 0.134 mmol) in 3.75 mL toluene was stirred for about 10 minutes. Then 75 μL $S(SiMe_3)_2$ were dropped into this suspension. The mixture was stirred overnight. One week later dark red, rhombohedral crystals of **32** formed (yield: less than 5% (based on copper)).

Elemental analysis based on [$C_{364}H_{372}Cu_{92}P_{24}S_{48}$] (12874.43 g/mol)

Calculated:	C 33.95%	H 2.91%	S 11.95%
Found:	C 36.14%	H 3.05%	S 9.00%

IR (ATR): 405(vw), 418(vw), 440(vw), 483(vw), 507(w), 554(vw), 596(vw), 625(vw), 639(vw), 689(w), 715(vw), 739(w), 821(vw), 950(vw), 981(w), 1034(vw), 1068(vw), 1095(vw), 1150(vw), 1231(w), 1308(vw), 1370(vw), 1432(w), 1481(vw), 1569(vw), 1585(vw), 1640(vw), 1731(w), 1813(vw), 1882(vw), 1951(vw), 1970(vw), 1981.07(vw), 1994(vw), 2007(vw), 2016(vw), 2052(vw), 2063(vw), 2089(vw), 2131(vw), 2147(vw), 2154(vw), 2165(vw), 2173(vw), 2181(vw), 2198(vw), 2206(vw), 2216(vw), 2226(vw), 2238(vw), 2256(vw), 2274(vw), 2841(vw), 2896(vw), 3044(vw) cm^{-1}.

4.4.32 [$Cu_{90}S_{44}(SCp)_4(dppp)_{10}(dpppS)_2$] (33)

CuSCp (0.0752 g, 0.456 mmol) and dppp (0.0353 g, 0.0856 mmol) were suspended in 7.5 mL toluene and stirred for about 10 minutes. Then 50 μL $S(SiMe_3)_2$ were dropped into this suspension. The mixture was stirred overnight, yielding a clear solution. One week later dark red, plate crystals of **33** formed (yield: less than 5% (based on copper)).

4.4.33 [$Cu_{40}Se_{15}(SCp)_{10}(dppp)_6$] (34)

CuSCp (0.0824 g, 0.5 mmol) and dppp (0.0889 g, 0.0215 mmol) were suspended in 5 mL toluene and stirred for about 10 minutes. Then 51 μL $Se(SiMe_3)_2$ were dropped into this suspension. The mixture was stirred overnight, yielding a clear solution. On the next day the solution was layered with 8 mL Et_2O. One week later dark red, needle crystals of **34** formed (yield: 30% (based on copper)).

EA analysis based on [$C_{212}H_{246}Cu_{40}P_{12}S_{10}Se_{15}$] (7212.31 g/mol)

Calculated: C 35.30% H 3.44% S 4.45%

Found: C 38.32% H 3.64% S 4.05%

IR (ATR): 426(vw), 480(vw), 508(m), 544(vw), 617(vw), 666(m), 688(s), 735(s), 823(w), 940(w), 998(vw), 1026(vw), 1069(vw), 1095(m), 1156(vw), 1183(vw), 1228(vw), 1274(vw), 1306(vw), 1432(s), 1480(m), 1570(vw), 1585(vw), 1665(vw), 1810(vw), 1880(vw), 1965(vw), 1980(vw), 1994(vw), 2012(vw), 2028(vw), 2044(vw), 2075(vw), 2126(vw), 2153(vw), 2162(vw), 2173(vw), 2180(vw), 2198(vw), 2245(vw), 2931(vw), 3045(vw) cm^{-1}.

4.4.34 [$Cu_{61}Se_{31}(dppp)_{10}$] (35)

A mixture of CuSCy (0.0532 g, 0.3 mmol) and dppp (0.0247 g, 0.06 mmol) in 4 mL THF was stirred for about 10 minutes. Then 36 μL $Se(SiMe_3)_2$ were dropped into this suspension. The mixture was stirred overnight yielding a clear solution, which was layered with 1 mL ethanol and 8 mL Et_2O. Two weeks later black, needle-like crystals of **35** formed (yield: 55% (based on copper)).

Elemental analysis based on [$C_{270}H_{260}Cu_{61}P_{20}Se_{31}$] (10447.86 g/mol)

Calculated: C 31.04% H 2.51%

Found: C 30.07% H 2.70%

IR (ATR): 413(vw), 483(w), 505(m), 616(w), 686(m), 713(vw), 735(w), 796(vw), 947(w), 997(vw), 1025(vw), 1067(vw), 1093(w), 1155(vw), 1182(vw), 1259(vw), 1304(vw), 1431(w), 1479(vw), 1569(vw), 1584(vw), 1878(vw), 2084(vw), 2324(vw), 2917(vw), 3042(vw) cm^{-1}.

4.4.35 [$Cu_{61}Se_{26}(SCy)_9(PPh_3)_{14}$] (36)

CuSCy (0.0526 g, 0.3 mmol) and PPh_3 (0.2341 g, 0.9 mmol) were suspended in 4 mL THF and stirred for about 10 minutes. Then 25 μL $Se(SiMe_3)_2$ were dropped into this suspension. The mixture was stirred overnight, and the clear solution was layered with 1 mL ethanol and 8 mL Et_2O. Two weeks later brown, needle-like crystals of **36** formed (yield: 5% (based on copper)).

IR (ATR): 409(w), 429(vw), 438(vw), 484(vw), 519(w), 546(vw), 618(vw), 688(s), 737(s), 800(s), 913(s), 951(vw), 995(w), 1026(vw), 1070(vw), 1093(w), 1156(vw), 1182(vw), 1257(w), 1308(vw), 1328(vw), 1432(m), 1478(w), 1571(w), 1585(w), 1657(vw), 1815(vw), 1889(vw), 1949(vw), 1976(vw), 1988(vw), 1997(vw), 2023(vw), 2039(vw) 2055(vw), 2089(vw), 2117(vw), 2151(vw), 2181(vw), 2199(vw), 2225(vw), 2276(vw), 2843(w), 2911(vw), 2949(vw), 3071(vw), 3161(vw), 3271(vw), 3317(vw), 3381(vw), 3414(vw), 3513(w), 3636(vw) cm^{-1}.

4.4.36 [$Cu_{51}Se_{26}(PPh_3)_{16}$] (37)

A mixture of CuSCy (0.0541 g, 0.3 mmol) and PPh_3 (0.2387 g, 0.9 mmol) in 4 mL THF was stirred for about 10 minutes. Then 36 μL $Se(SiMe_3)_2$ were dropped into this suspension. The mixture was stirred overnight and the resulting clear solution was layered with 1 mL ethanol and 8 mL Et_2O. One week later brown, block-like crystals of **37** formed (yield: 5% (based on copper)).

IR (ATR): 422(vw), 514(m), 538(w), 563(vw), 616(vw), 666(w), 687(w), 718(vw), 739(w), 840(vw), 913(vw), 996(vw), 1025(vw), 1068(vw), 1092(w), 1117(vw), 1154(vw), 1180(vw), 1306(vw), 1431(m), 1476(w), 1569(vw), 1584(vw), 1969(vw), 2092(vw), 2314(vw), 3043(vw) cm^{-1}.

4.4.37 [$Cu_{73}Se_{37}(PPh_3)_{19}$]·($C_7H_{16}$) (38·($C_7H_{16}$))

A mixture of CuSCy (0.0539 g, 0.3 mmol) and PPh_3 (0.2364 g, 0.9 mmol) in 4 mL THF was stirred for about 10 minutes. Then 36 μL $Se(SiMe_3)_2$ were dropped into this suspension. The mixture was stirred overnight and the resulting clear solution was layered with 1 mL ethanol and 8 mL Et_2O. Three weeks later brown, plate-like crystals of **38**·(C_7H_{16}) formed (yield: 20% (based on copper)).

Elemental analysis based on [$C_{342}H_{285}Cu_{73}P_{19}Se_{37}$] (12543.79 g/mol)

Calculated: C 32.75% H 2.29%

Found: C 29.57% H 2.45%

IR (ATR): 421(vw), 435(vw), 458(vw), 482(vw), 502(vw), 519(vw), 538(w), 563(vw), 616(vw), 639(vw), 666(vw), 687(w), 719(vw), 738(w), 794(w), 870(vw), 956(vw), 982(vw), 1090(vw), 1151(vw), 1198(vw), 1230(vw), 1258(vw), 1305(vw), 1431(w), 1476(vw), 1568(vw), 1583(vw), 1763(vw), 1953(vw), 1970(vw), 1980(vw), 2000(vw), 2007(vw), 2024(vw), 2039(vw), 2067(vw), 2150(vw), 2156(vw), 2164(vw), 2186(vw), 2206(vw), 2215(vw), 2235(vw), 2962(vw) cm^{-1}

4.4.38 $[Cu_{94}Se_{43}(SCy)_9(PPh_3)_{18}]$ (39)

A mixture of CuSCy (0.0539 g, 0.3 mmol) and PPh_3 (0.2369 g, 0.9 mmol) in 4 mL THF was stirred for about 10 minutes. Then 36 μL $Se(SiMe_3)_2$ were dropped into this suspension. The mixture was stirred overnight, and the resulting clear solution was layered with 1 mL ethanol and 8 mL Et_2O. Six weeks later brown, plate-like crystals of **39** formed (yield: 5% (based on copper)).

4.4.39 $[Ag_{15}S(SCy)_{12}(dppb)_3](BPh_4)$ (40)

AgSCy (0.1154 g, 0.5 mmol), dppb (0.0431 g, 0.1 mmol) and $NaBPh_4$ (0.072 g, 0.21 mmol) were suspended in 10 mL toluene and stirred for about 10 minutes. Then 20 μL $S(SiMe_3)_2$ were added into the reaction and the mixture was stirred at room temperature overnight. On the next day, the suspension was heated to the boiling point and filtered. The filtrate was layered with 20 mL *n*-heptane. One week later a few pink, block-like crystals of **41** formed together with pink crystals of **40** (yield: 15% (based on silver)).

Elemental analysis based on $[C_{180}H_{236}Ag_{15}BP_6S_{13}]$ (4631.13 g/mol)

Calculated: C 46.68% H 5.14% S 9.00%

Found: C 46.60% H 4.86% S 8.25%

IR (ATR): 439(vw), 476(vw), 509(m), 611(w), 691(s), 729(s), 791(vw), 816(vw), 842(vw), 884(vw), 914(vw), 994(m), 1027(vw), 1070(vw), 1097(w), 1192(w), 1255(w), 1292(vw), 1330(vw), 1434(s), 1444(w), 1459(vw), 1481(w), 1495(vw), 1580(vw), 1665(vw), 1756(vw), 1809(vw), 1883(vw), 1946(vw), 1956(vw), 1965(vw), 1987(vw), 1995(vw), 2012(vw), 2025(vw), 2034(vw), 2045(vw), 2053(vw), 2063(vw), 2087(vw), 2180(vw), 2188(vw), 2205(vw), 2218(vw), 2229(vw), 2255(vw), 2329(vw), 2653(vw), 2845(w), 2920(s), 2982(vw), 2999(vw), 3053(w) cm^{-1}.

4.4.40 [$Ag_{25}S_2(SCy)_{21}(dppb)_2$] (41)

A mixture of AgSCy (0.1133 g, 0.5 mmol), dppb (0.0416 g, 0.1 mmol) and $NaBPh_4$ (0.0127 g, 0.033 mmol) in 10 mL toluene was stirred for about 10 minutes. Then 10 μL $S(SiMe_3)_2$ was added into the reaction and stirred at room temperature overnight. On the next day, the suspension was heated to the boiling point and filtered. The filtrate was layered with 20 mL *n*-heptane. One week later yellow, block-like crystals of pure **41** formed (yield: 30% (based on silver)).

Elemental analysis based on [$C_{182}H_{287}Ag_{25}P_4S_{23}$] (6033.11 g/mol)

Calculated: C 36.23% H 4.79% S 12.22%

Found: C 37.71% H 4.50% S 11.15%

IR (ATR): 439(vw), 508(w), 692(m), 729(m), 816(w), 851(vw), 883(w), 993(s), 1026(vw), 1069(vw), 1113(w), 1191(m), 1253(m), 1292(vw), 1329(vw), 1434(s), 1443(s), 1481(vw), 1586(vw), 1961(vw), 2001(vw), 2025(vw), 2053(vw), 2067(vw), 2125(vw), 2146(vw), 2158(vw), 2169(vw), 2181(vw), 2188(vw), 2207(vw), 2239(vw), 2649(vw), 2845(s), 2916(s), 3053(vw) cm^{-1}.

4.4.41 [$Ag_{15}Se(SCy)_{12}(dppb)_3$]($BPh_4$) (42)

AgSCy (0.1108 g, 0.5 mmol), dppb (0.0447 g, 0.1 mmol) and $NaBPh_4$ (0.0114 g, 0.033 mmol) were suspended in 5 mL toluene. Then the temperature was decreased to –40°C. After stirring for 15 minutes, 26 μL $Se(SiMe_3)_2$ were added. The mixture was stirred for 2 hours until the solution became clear. Then this solution was put into a fridge at –20°C for one week, at 0°C for one more week and finally at room temperature for a third week. The solution was then layered with 20 mL *n*-heptane. One week later light yellow, block crystals of **42** formed (yield: 10% (based on silver)).

Elemental analysis based on [$C_{180}H_{236}Ag_{15}BP_6S_{12}Se$] (4678.03 g/mol)

Calculated: C 46.21% H 5.08% S 8.22%

Found: C 42.47% H 4.65% S 8.20%

IR (ATR): 438(w), 478(w), 506(w), 617(vw), 660(w), 694(s), 734(m), 800(w), 817(w), 850(vw), 884(vw), 914(vw), 993(m), 1025(vw), 1097(w), 1113(w), 1192(s), 1256(w), 1293(vw), 1332(vw), 1434(s), 1481(w), 1540(vw), 1573(vw), 1643(vw), 1722(vw), 1819(vw), 1904(vw), 1956(vw), 1978(vw), 1988(vw), 2019(vw), 2040(vw), 2080(vw), 2149(vw), 2161(vw), 2179(vw), 2189(vw), 2199(vw), 2218(vw), 2262(vw), 2654(vw), 2849(s), 2919(s), 3048(w), 3253(vw), 3362(vw), 3645(vw) cm^{-1}.

4.4.42 [$Ag_{27}Se_2(SCy)_{20}(dppb)_4$]($(BPh_4)_3$) (43)

A mixture of AgSCy (0.112 g, 0.5 mmol) and dppb (0.042 g, 0.1 mmol) and $NaBPh_4$ (0.114 g, 0.33 mmol) in 5 mL toluene was stirred at –40°C for 15 minutes. Then 13 μL $Se(SiMe_3)_2$ were added. The mixture was stirred for 2 hours, yielding a clear solution. It was put into a fridge at –20°C for one week, at 0°C for one more week and at room temperature for a third week. One week later yellow, plate crystals of **43** formed (yield: 24% (based on silver)).

Elemental analysis based on [$C_{304}H_{392}Ag_{27}B_3P_8S_{20}Se_2$] (8037.95 g/mol)

Calculated: C 45.42% H 4.92% S 7.98%

Found: C 44.89% H 4.70% S 8.04%

IR (ATR): 418(vw), 479(vw), 506 (w), 612 (vw), 693(s), 729(s), 741(m), 786(vw), 817(w), 842(vw), 885(vw), 993(m), 1026(vw), 1096(m), 1111(m), 1191(s), 1254(m), 1292(vw), 1330(w), 1380(vw), 1434(s), 1480(m), 1579(vw), 1810(vw), 1887(vw), 1957(vw), 1977(vw), 2007(vw), 2018(vw), 2033(vw), 2041(vw), 2079(vw), 2110(vw), 2139(vw), 2149(vw), 2160(vw), 2199(vw), 2220(vw), 2263(vw), 2649(vw), 2845(s), 2916(s), 2979(vw), 3052(m), 3143(vw), 3265(vw), 3349(vw) cm^{-1}.

4.4.43 $[Ag_{86}S_{19}(SCy)_{48}]\cdot 2(C_7H_8)$ ($44\cdot 2(C_7H_8)$)

A mixture of AgSCy (0.112 g, 0.5 mmol) and dpph (0.114 g, 0.25 mmol) in 20 mL toluene was stirred for 15 minutes, forming a clear solution. 10 μL $S(SiMe_3)_2$ were then added and the solution was stirred for 2 hours. Three days later dark red, block crystals of **44**·$2(C_7H_8)$ formed (yield: 10% (based on silver)).

Elemental analysis based on $[C_{288}H_{528}Ag_{86}S_{67}]$ (15415.91 g/mol)

Calculated: C 22.44% H 3.45% S 13.94%

Found: C 22.91% H 3.15% S 13.48%

IR (ATR): 436(vw), 463(vw), 510(vw), 559(vw), 693(w), 725(m), 814(m), 854(w), 882(w), 915(vw), 992(w), 1027(vw), 1113(vw), 1191(m), 1254(m), 1293(vw), 1330(w), 1442(m), 1495(vw), 1604(vw), 1969(vw), 1989(vw), 2036(vw), 2178(vw), 2661(m), 2844(s), 2913(s), 3086(vw) cm^{-1}.

4.4.44 $[Ag_6(SCy)_4(dppm)_4](NO_3)_2\cdot 5THF$ ($45\cdot 5THF$) and $[Ag_{25}Se_6S_2(SCy)_8(dppm)_6]$ (46)

A mixture of AgSCy (0.1122 g, 0.5 mmol) and dppm (0.0971 g, 0.25 mmol) in 10 mL THF was stirred at –40°C for 15 minutes. Then 32 μL $Se(SiMe_3)_2$ were added. The mixture was stirred for 2 hours, yielding a clear solution. Finally, this solution was kept in a fridge at –20°C for one week, at 0°C for one more week and at room temperature for a third week. One week later colourless, needle-like crystals of **45**·5THF (yield: 10% (based on silver)) formed together with orange, needle-like crystals of **46** (yield: less than 5% (based on silver)).

45 Elemental analyses based on [$C_{124}H_{132}Ag_6P_8S_4N_2O_6$] (2769.64 g/mol)

Calculated: C 53.77% H 4.80% S 4.63% N 1.01%

Found: C 52.13% H 4.66% S 4.31% N 1.25%

IR (ATR): 417(vw), 442(vw), 472(w), 512(w), 616(vw), 689(s), 714(vw), 734(m), 774(vw), 816(vw), 828(vw), 885(vw), 914(vw), 996(w), 1025(vw), 1095(m), 1158(vw), 1190(vw), 1262(w), 1328(s), 1434(s), 1482(m), 1572(vw), 1585(vw), 1632(vw), 1894(vw), 1933(vw), 1952(vw), 1969(vw), 1978(vw), 1998(vw), 2012(vw), 2024(vw), 2030(vw), 2039(vw), 2050(vw), 2056(vw), 2087(vw), 2122(vw), 2150(vw), 2166(vw), 2183(vw), 2193(vw), 2204(vw) 2217(vw), 2846(w), 2924(w), 3051(vw) cm^{-1}.

4.4.45 [$Ag_{12}Se_6(dppfc)_4$]·20THF (47·20THF)

AgSCy (0.1092 g, 0.5 mmol) and dppfc (0.2691 g, 0.25 mmol) were suspended in 10 mL THF and stirred for 10 minutes. Then the temperature was decreased to –40°C. After stirring for 15 minutes, 32 μL $Se(SiMe_3)_2$ were added. The mixture was stirred for 2 hours, yielding a clear solution. Finally, this solution was put into a fridge at –20°C for one week, at 0°C for one more week and at room temperature for a third week. The light yellow, block-like crystals of **47**·20THF formed (yield: 5% (based on silver)). These crystals co-crystallize with some black amorphous residue.

4.4.46 [$Ag_{97}S_{32}(SAd)_{33}(dppb)_3$] (48)

A mixture of AgSAd (0.1374 g, 0.5 mmol), dppb (0.2134 g, 0.5 mmol) and a small amount of $AgNO_3$ (5 mg) in 40 mL toluene was stirred at 0°C for 10 minutes. Then 40 μL $S(SiMe_3)_2$ were added and the suspension was stirred at 0°C for 2 hours. The mixture was stirred at room temperature for additional half an hour yielding a clean solution. Finally, the solution was layered by 80 mL *n*-heptane. One week later orange, plate-like crystals of **48** formed (yield: 30% (based on silver)).

Elemental analysis based on [$C_{414}H_{579}Ag_{97}P_6S_{65}$] (18288.85 g/mol)

Calculated: C 27.19% H 3.19% S 11.40%

Found: C 29.61% H 3.15% S 10.47%

IR (ATR): 406(vw), 415(vw), 446(w), 477(w), 510(vw), 618(vw), 692(s), 738(s), 807(w), 824(w), 883(vw), 927(vw), 962(vw), 976(vw), 999(vw), 1034(s), 1097(m), 1157(vw), 1176(vw), 1250(vw), 1295(m), 1307(vw), 1339(vw), 1377(vw), 1433(s), 1482(w), 1572(vw), 1586(vw), 1822(vw), 1897(vw), 1954(vw), 1974(vw), 1982(vw), 1996(vw), 2007(vw), 2021(vw), 2028(vw), 2037(vw), 2101(vw), 2114(vw), 2150(vw), 2180(vw), 2201(vw), 2225(vw), 2248(vw), 2324(vw), 2567(vw), 2651(vw), 2672(vw), 2843(s), 2894(s), 3050(vw), 3420(vw) cm^{-1}.

4.4.47 [$Ag_{42}Se_{13}(SAd)_{14}(dppm)_6$]($BPh_4$)$_2$·14THF (49·14THF)

A mixture of AgSAd (0.1364 g, 0.5 mmol), dppm (0.0983 g, 0.25 mmol) and $NaBPh_4$ (0.0114 g, 0.033 mmol) in 5 mL THF was stirred at –40°C for 15 minutes. Then 36 μL $Se(SiMe_3)_2$ were added. The mixture was stirred for 2 hours, yielding a clear solution. Finally, this solution was put into a fridge at –20°C for one week, at 0°C for one more week and at room temperature for the third week. One week later dark red, rhombohedral crystals of **49**·14THF formed (yield: 65% (based on silver)).

Elemental analysis based on [$C_{338}H_{382}Ag_{42}P_{12}S_{14}Se_{13}B_2$] (10843.80 g/mol)

Calculated: C 37.44% H 3.55% S 4.14%

Found: C 36.26% H 3.05% S 3.67%

IR (ATR): 414(vw), 423(vw), 440(vw), 466(vw), 497(vw), 513(w), 611(w), 685(m), 718(vw), 733(m), 782(w), 807(vw), 834(vw), 913(vw), 957(vw), 975(vw), 998(vw), 1034(m), 1097(w), 1158(vw), 1177(vw), 1248(w), 1293(m), 1306(vw), 1340(w), 1361(vw), 1434(m), 1447(vw), 1481(w), 1576(vw), 1671(vw), 1807(vw), 1903(vw), 1936(vw), 1954(vw), 1970(vw), 1977(vw), 1985(vw), 2002(vw), 2009(vw), 2018(vw), 2030(vw), 2038(vw), 2045(vw), 2057(vw), 2076(vw), 2136(vw), 2145(vw), 2160(vw), 2171(vw), 2190(vw), 2201(vw), 2208(vw), 2240(vw), 2323(vw), 2671(vw), 2843(vw), 2895(m), 3052(vw), 3398(vw) cm^{-1}.

4.4.48 $[Ag_4(SAd)_4(dppe)]_n\cdot 2THF$ (50·2THF)

AgSAd (0.1385 g, 0.5 mmol) and dppe (0.0992 g, 0.25 mmol) were suspended in 10 mL THF and stirred for about 10 minutes. Then the temperature of this suspension was decreased to –40°C. After stirring for 15 minutes, 16 *µ*L $Se(SiMe_3)_2$ were added. The mixture was stirred for 2 hours, yielding a clear solution. Finally, this solution was put into a fridge at –20°C for one week, at 0°C for one more week and at room temperature for a third week. One week later light yellow, needle-like crystals of **50**·2THF formed (yield: less than 5% (based on silver)).

5 Crystallographic data of the compounds

5.1 Data collection and refinement

Suitable crystals were covered in polyfluorether oil and mounted on a *MiTeGen Loop*. The crystal was transferred directly to the cold stream of nitrogen of a *STOE StadiVari* diffractometer, with a Ga radiation source from *EXCILIUM* ($\lambda(\mathrm{Ga}K_{\alpha})$ = 1.34143 Å) and an *Eiger4M Dectris* detector.

All structures were solved using the programs *SHELXS* or *SHELXT*[107] and Olex*2*.[108] The remaining non-hydrogen atoms were located from successive difference Fourier map calculations. The refinements were carried out by using full-matrix least-squares techniques on F_o^2 by using the program *SHELXL*.[107] The H-atoms were introduced into the geometrically calculated positions (*SHELXL* procedures) and refined riding on the corresponding parent atoms. In each case, the locations of the largest peaks in the final difference Fourier map calculations, as well as the magnitude of the residual electron densities, were of no chemical significance.

Some of the measured compounds crystalize with disordered solvent molecules. Especially for the huge cluster molecules the voids are large and are often about 20% of the cell volume. In these voids the solvent molecules are organized like in a liquid state and often could not be identified in the final refinements. To calculate the voids and correct the data sets the program *PLATON* (*SQUEZZE*) or the “solvent mask” in the program Olex*2* were used.

The program *Diamond 3*[109] was used to visualize the molecular structures.

A summary of the crystal data, data collection and refinement details for all compounds are given in the following section.

5.2 $[Cu_4(SCy)_4(dppm)_2]$ (1)

Compound	**1**	**1**·½(C_7H_8)·½(C_7H_{16})
Empirical formula	$C_{74}H_{88}Cu_4P_4S_4$	$C_{81}H_{100}Cu_4P_4S_4$
Formula mass	1483.72	1579.88
Temperature/K	150	150.15
Crystal system	monoclinic	triclinic
Space group	$P2_1/n$	$P\bar{1}$
a/Å	11.3785(4)	12.8163(4)
b/Å	27.5336(11)	13.1922(4)
c/Å	23.0910(8)	24.4178(7)
α/°	90	101.457(2)
β/°	100.975(3)	90.518(2)
γ/°	90	108.817(2)
V/Å^3	7101.9(5)	3818.0(2)
Z	4	2
ρ_{calc}/g·cm^{-3}	1.388	1.374
μ/mm^{-1}	7.855	7.327
F(000)	3088.0	1652.0
Crystal size/mm^3	0.18 × 0.16 × 0.14	0.24 × 0.22 × 0.21
Radiation	GaK_α (λ = 1.34143)	GaK_α (λ = 1.34143)
2Θ range for data collection/°	5.586 to 115.188	6.302 to 125
Index ranges	$-14 \le h \le 7$, $-34 \le k \le 33$, $-28 \le l \le 28$	$-16 \le h \le 16$, $-17 \le k \le 11$, $-32 \le l \le 32$
Reflections collected	36130	41745
Independent reflections	14324 (R_{int} = 0.0498, R_{sigma} = 0.0789)	17853 (R_{int} = 0.0315, R_{sigma} = 0.0347)
Indep. refl. with ($I \ge 2\sigma(I)$)		14372
Data/restraints/parameters	14324/0/775	17853/11/814
Goodness-of-fit on F^2	1.019	1.047
Final R indexes ($I \ge 2\sigma(I)$)	R_1 = 0.0786, wR_2 = 0.2016	R_1 = 0.0544, wR_2 = 0.1350
Final R indexes (all data)	R_1 = 0.1428, wR_2 = 0.2361	R_1 = 0.0721, wR_2 = 0.1510
Largest diff. peak/hole/e Å^{-3}	2.06/-0.58	0.78/-0.87

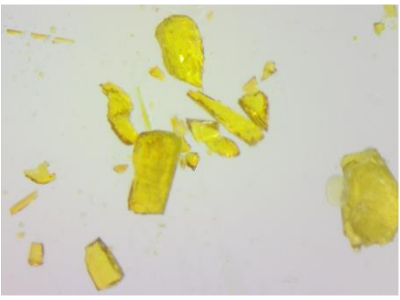

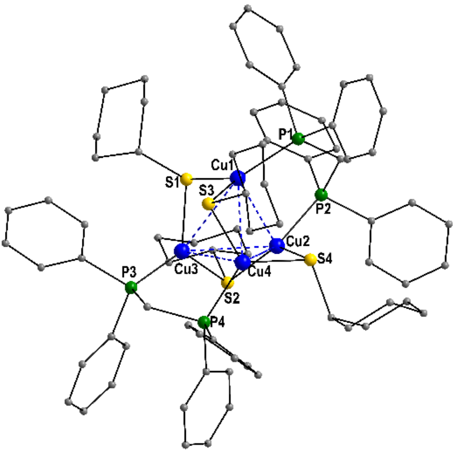

5.3 [Cu(dppp)$_2$][Cu$_5$(SCy)$_6$] (2)

Compound	**2**
Empirical formula	$C_{90}H_{118}Cu_6P_4S_6$
Formula mass	1897.32
Temperature/K	150.0
Crystal system	triclinic
Space group	$P\overline{1}$
a/Å	14.3608(4)
b/Å	14.5809(4)
c/Å	22.3962(6)
α/°	101.800(2)
β/°	95.770(2)
γ/°	101.275(2)
V/Å^3	4453.4(2)
Z	2
ρ_{calc}/g·cm^{-3}	1.415
μ/mm^{-1}	9.113
F(000)	1976.0
Crystal size/mm^3	0.14 × 0.03 × 0.02
Radiation	GaK_α (λ = 1.34143)
2Θ range for data collection/°	6.108 to 124.998
Index ranges	$-18 \leq h \leq 13$, $-19 \leq k \leq 15$, $-28 \leq l \leq 29$
Reflections collected	52418
Independent reflections	20552 (R_{int} = 0.0771, R_{sigma} = 0.1074)
Data/restraints/parameters	20552/1/945
Goodness-of-fit on F^2	1.004
Final R indexes($I \geq 2\sigma(I)$)	R_1 = 0.0511, wR_2 = 0.1071
Final R indexes (all data)	R_1 = 0.1156, wR_2 = 0.1256
Largest diff. peak/hole/e Å^{-3}	0.71/-0.51

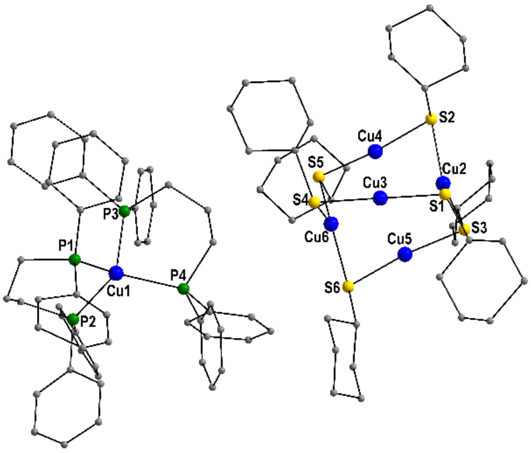

5.4 $[Cu_{16}S_4(SCy)_8(dppp)_4]\cdot4(C_7H_8)$ ($\mathbf{3}\cdot4(C_7H_8)$)

Compound	**3**·4(C_7H_8)
Empirical formula	$C_{184}H_{224}Cu_{16}P_8S_{12}$
Formula mass	4084.74
Temperature/K	180.15
Crystal system	triclinic
Space group	$P\bar{1}$
a/Å	18.5749(8)
b/Å	20.0767(13)
c/Å	24.9231(15)
α/°	100.610(5)
β/°	94.869(4)
γ/°	94.865(4)
V/Å^3	9054.5(9)
Z	2
ρ_{calc}/g·cm^{-3}	1.498
μ/mm^{-1}	11.442
F(000)	4208.0
Crystal size/mm^3	0.23 × 0.21 × 0.2
Radiation	GaK_α (λ = 1.34143)
2Θ range for data collection/°	6.012 to 100.196
Index ranges	$-10 \le h \le 21$, $-22 \le k \le 22$, $-28 \le l \le 28$
Reflections collected	54403
Independent reflections	27122 (R_{int} = 0.0421, R_{sigma} = 0.0737)
Data/restraints/parameters	27122/18/1767
Goodness-of-fit on F^2	1.062
Final R indexes ($I \ge 2\sigma(I)$)	R_1 = 0.0697, wR_2 = 0.1710
Final R indexes (all data)	R_1 = 0.1298, wR_2 = 0.1904
Largest diff. peak/hole/e Å^{-3}	0.89/-0.73

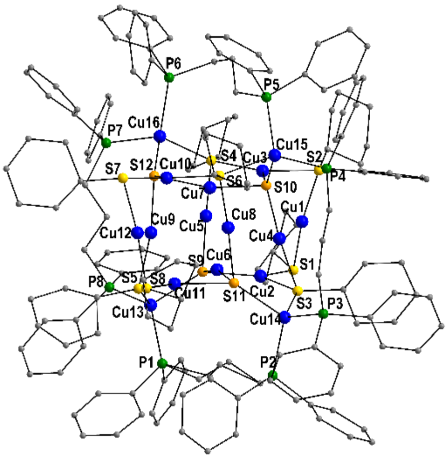

5.5 [$Cu_2(SCy)_2(dppp)_2$] (4)

Compound	**4**
Empirical formula	$C_{66}H_{74}Cu_2P_4S_2$
Formula mass	1182.33
Temperature/K	180.15
Crystal system	triclinic
Space group	$P\bar{1}$
a/Å	10.7120(3)
b/Å	12.1102(4)
c/Å	12.5574(4)
α/°	112.994(2)
β/°	97.744(2)
γ/°	91.913(2)
V/Å^3	1479.27(8)
Z	1
ρ_{calc}/g·cm^{-3}	1.327
μ/mm^{-1}	5.170
F(000)	620.0
Crystal size/mm^3	0.21 × 0.2 × 0.19
Radiation	GaK_α (λ = 1.34143)
2Θ range for data collection/°	6.74 to 124.984
Index ranges	$-14 \le h \le 14$, $-15 \le k \le 15$, $-7 \le l \le 16$
Reflections collected	22730
Independent reflections	7022 (R_{int} = 0.0157, R_{sigma} = 0.0118)
Data/restraints/parameters	7022/0/334
Goodness-of-fit on F^2	1.046
Final R indexes ($I \ge 2\sigma(I)$)	R_1 = 0.0432, wR_2 = 0.1170
Final R indexes (all data)	R_1 = 0.0463, wR_2 = 0.1203
Largest diff. peak/hole/e Å^{-3}	0.82/-0.47

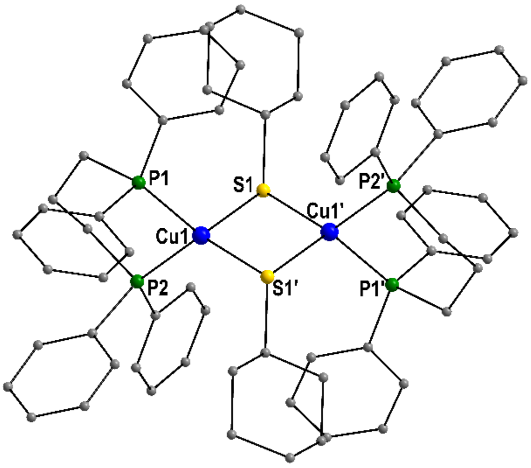

5.6 $[Cu_2(SCy)_2(dpppt)_{1.5}]_n$ (5)

Compound	**5**
Empirical formula	$C_{55.5}H_{67}Cu_2P_3S_2$
Formula mass	1018.20
Temperature/K	150.15
Crystal system	monoclinic
Space group	*C*2/*c*
a/Å	46.7684(14)
b/Å	9.0099(2)
c/Å	27.6714(8)
α/°	90
β/°	117.777(2)
γ/°	90
V/Å^3	10316.5(5)
Z	8
ρ_{calc}/g·cm^{-3}	1.311
μ/mm^{-1}	5.687
F(000)	4280.0
Crystal size/mm^3	0.27 × 0.06 × 0.04
Radiation	GaK_α (λ = 1.34143)
2*Θ* range for data collection/°	8.666 to 118.354
Index ranges	$-59 \le h \le 55$, $-11 \le k \le 6$, $-33 \le l \le 35$
Reflections collected	47608
Independent reflections	11086 (R_{int} = 0.0712, R_{sigma} = 0.0638)
Indep. refl. with ($I \ge 2\sigma(I)$)	6096
Data/restraints/parameters	11086/0/564
Goodness-of-fit on F^2	1.022
Final *R* indexes ($I \ge 2\sigma(I)$)	R_1 = 0.0722, wR_2 = 0.1934
Final *R* indexes (all data)	R_1 = 0.1346, wR_2 = 0.2267
Largest diff. peak/hole/e Å^{-3}	0.54/-0.32

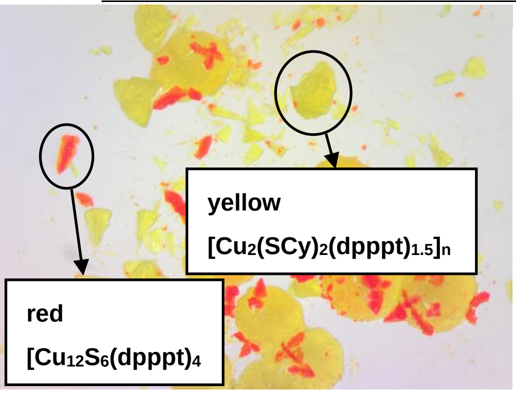

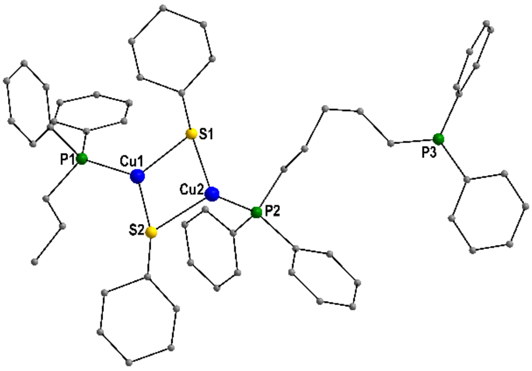

5.7 [$Cu_2(SCy)_2(dppox)_2$] (6)

Compound	**6**
Empirical formula	$C_{76}H_{78}Cu_2P_4S_2$
Formula mass	1306.46
Temperature/K	150
Crystal system	triclinic
Space group	$P\bar{1}$
a/Å	12.2677(5)
b/Å	12.5010(4)
c/Å	12.5648(4)
α/°	114.954(3)
β/°	102.348(3)
γ/°	103.902(3)
V/Å^3	1583.36(11)
Z	1
ρ_{calc}/g·cm^{-3}	1.370
μ/mm^{-1}	4.866
F(000)	684.0
Crystal size/mm^3	0.23 × 0.22 × 0.18
Radiation	GaK_α (λ = 1.34143)
2Θ range for data collection/°	6.916 to 125.072
Index ranges	$-16 \leq h \leq 6$, $-16 \leq k \leq 16$, $-14 \leq l \leq 16$
Reflections collected	19990
Independent reflections	7527 (R_{int} = 0.0202, R_{sigma} = 0.0196)
Indep. refl. with ($I \geq 2\sigma(I)$)	6909
Data/restraints/parameters	7527/0/535
Goodness-of-fit on F^2	1.041
Final R indexes ($I \geq 2\sigma(I)$)	R_1 = 0.0378, wR_2 = 0.0970
Final R indexes (all data)	R_1 = 0.0421, wR_2 = 0.1002
Largest diff. peak/hole/e Å^{-3}	0.80/-0.55

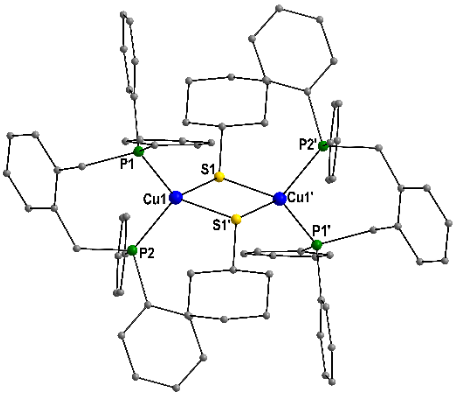

5.8 [$Cu_4(SCp)_4(dppm)_2$] (7)

Compound	**7**
Empirical formula	$C_{70}H_{80}Cu_4P_4S_4$
Formula mass	1427.62
Temperature/K	170.15
Crystal system	triclinic
Space group	$P\bar{1}$
a/Å	10.6377(5)
b/Å	12.0234(7)
c/Å	13.8435(8)
α/°	94.231(5)
β/°	109.116(4)
γ/°	102.298(4)
V/Å^3	1614.70(16)
Z	1
ρ_{calc}/g·cm^{-3}	1.468
μ/mm^{-1}	8.622
F(000)	740.0
Crystal size/mm^3	0.19 × 0.18 × 0.17
Radiation	GaK_α (λ = 1.34143)
2Θ range for data collection/°	5.95 to 125.262
Index ranges	$-14 \leq h \leq 13$, $-5 \leq k \leq 15$, $-18 \leq l \leq 18$
Reflections collected	18123
Independent reflections	7584 (R_{int} = 0.0369, R_{sigma} = 0.0329)
Indep. refl. with ($I \geq 2\sigma(I)$)	6028
Data/restraints/parameters	7584/0/370
Goodness-of-fit on F^2	1.083
Final R indexes ($I \geq 2\sigma(I)$)	R_1 = 0.0541, wR_2 = 0.1452
Final R indexes (all data)	R_1 = 0.0688, wR_2 = 0.1592
Largest diff. peak/hole/e Å^{-3}	0.59/-0.43

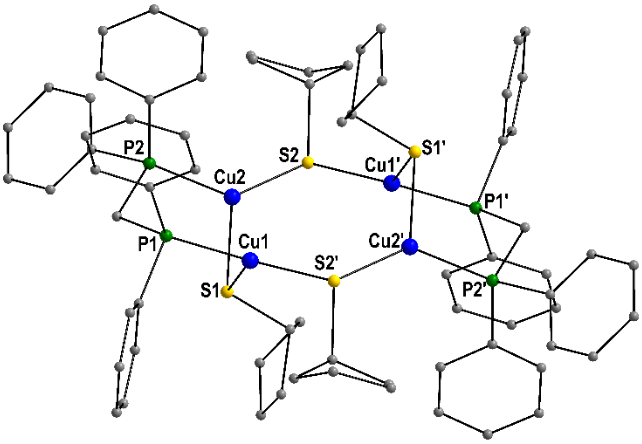

5.9 $[Cu(dppp)_2][Cu_5(SCp)_6]\cdot 1.5(C_7H_8)$ ($\mathbf{8}\cdot 1.5(C_7H_8)$)

Compound	**8**·1.5(C_7H_8)
Empirical formula	$C_{94.5}H_{118}Cu_6P_4S_6$
Formula mass	1951.36
Temperature/K	170.15
Crystal system	triclinic
Space group	$P\overline{1}$
a/Å	14.5979(2)
b/Å	24.3671(3)
c/Å	28.2669(3)
α/°	68.9040(10)
β/°	79.7290(10)
γ/°	85.6800(10)
V/Å^3	9229.9(2)
Z	4
ρ_{calc}/g·cm^{-3}	1.404
μ/mm^{-1}	8.805
F(000)	4060.0
Crystal size/mm^3	0.2 × 0.15 × 0.1
Radiation	GaK_α (λ = 1.34143)
2Θ range for data collection/°	6.354 to 125.086
Index ranges	$-19 \leq h \leq 15$, $-31 \leq k \leq 32$, $-30 \leq l \leq 37$
Reflections collected	99464
Independent reflections	42587 (R_{int} = 0.0304, R_{sigma} = 0.0340)
Indep. refl. with ($I \geq 2\sigma(I)$)	28852
Data/restraints/parameters	42587/0/1877
Goodness-of-fit on F^2	1.019
Final R indexes ($I \geq 2\sigma(I)$)	R_1 = 0.0593, wR_2 = 0.1544
Final R indexes (all data)	R_1 = 0.0936, wR_2 = 0.1774
Largest diff. peak/hole/e Å^{-3}	0.89/-0.61

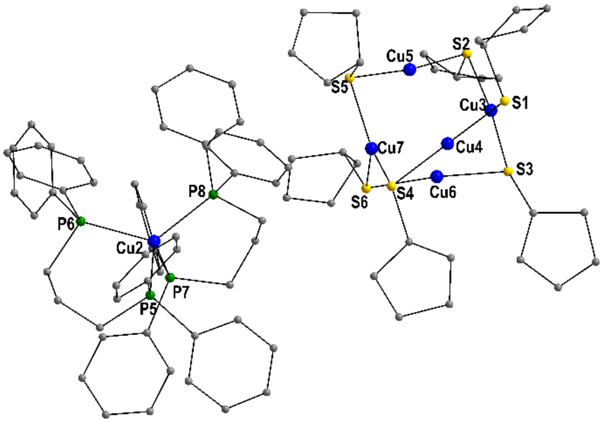

5.10 $[Cu_{16}S_4(SCp)_8(dppp)_4]\cdot4(C_7H_8)$ (**9**$\cdot4(C_7H_8)$)

Compound	**9**$\cdot4(C_7H_8)$
Empirical formula	$C_{176}H_{208}Cu_{16}P_8S_{12}$
Formula mass	3972.53
Temperature/K	180.15
Crystal system	triclinic
Space group	$P\overline{1}$
a/Å	18.7020(4)
b/Å	20.0176(4)
c/Å	23.2928(4)
α/°	92.146(2)
β/°	97.354(2)
γ/°	96.259(2)
V/Å^3	8585.1(3)
Z	2
ρ_{calc}/g·cm^{-3}	1.537
μ/mm^{-1}	12.059
F(000)	4080.0
Crystal size/mm^3	0.12 × 0.03 × 0.02
Radiation	GaK_α (λ = 1.34143)
2Θ range for data collection/°	4.172 to 120.124
Index ranges	$-24 \leq h \leq 24$, $-25 \leq k \leq 13$, $-30 \leq l \leq 29$
Reflections collected	91543
Independent reflections	37393 (R_{int} = 0.0509, R_{sigma} = 0.0632)
Indep. refl. with ($I \geq 2\sigma(I)$)	22594
Data/restraints/parameters	37393/18/1740
Goodness-of-fit on F^2	1.018
Final R indexes ($I \geq 2\sigma(I)$)	R_1 = 0.0694, wR_2 = 0.1679
Final R indexes (all data)	R_1 = 0.1234, wR_2 = 0.1954
Largest diff. peak/hole / e Å^{-3}	0.86/-0.52

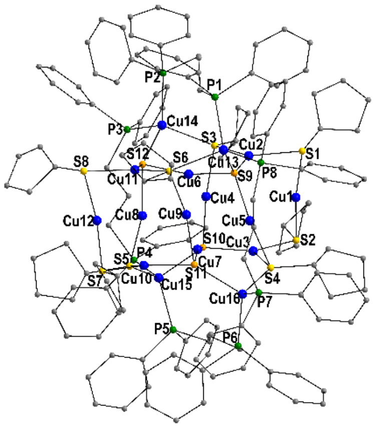

5.11 [$Cu_2(SCp)_2(dpppt)_2$] (10)

Compound	**10**
Empirical formula	$C_{68}H_{78}Cu_2P_4S_2$
Formula mass	1210.38
Temperature/K	170.15
Crystal system	triclinic
Space group	$P\bar{1}$
a/Å	14.0899(3)
b/Å	14.7426(3)
c/Å	16.1767(4)
α/°	115.389(2)
β/°	93.543(2)
γ/°	90.976(2)
V/Å^3	3026.38(13)
Z	2
ρ_{calc}/g·cm^{-3}	1.328
μ/mm^{-1}	5.061
F(000)	1272.0
Crystal size/mm^3	0.23 × 0.22 × 0.2
Radiation	GaK_α (λ = 1.34143)
2Θ range for data collection/°	5.276 to 125.054
Index ranges	$-18 \leq h \leq 16$, $-19 \leq k \leq 18$, $-21 \leq l \leq 19$
Reflections collected	34084
Independent reflections	13982 (R_{int} = 0.0144, R_{sigma} = 0.0125)
Indep. refl. with ($I \geq 2\sigma(I)$)	12721
Data/restraints/parameters	13982/0/685
Goodness-of-fit on F^2	1.019
Final R indexes ($I \geq 2\sigma(I)$)	R_1 = 0.0367, wR_2 = 0.0993
Final R indexes (all data)	R_1 = 0.0411, wR_2 = 0.1029
Largest diff. peak/hole/e Å^{-3}	1.27/-0.48

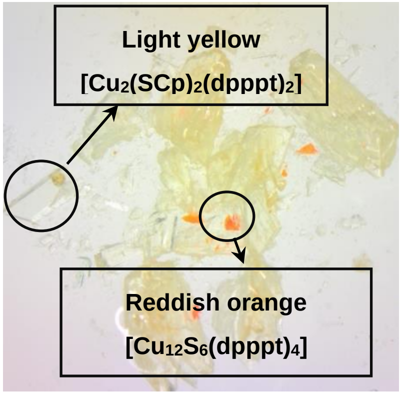

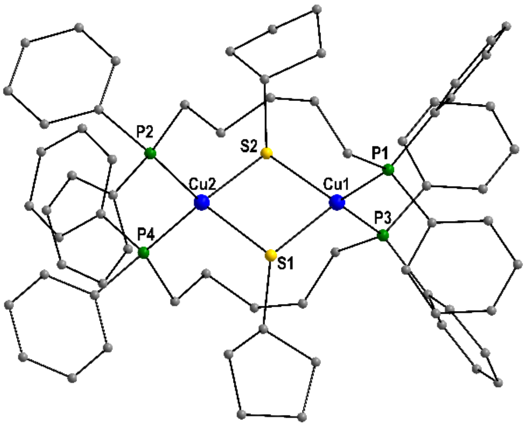

5.12 $[Cu_2(SCp)_2(dppbz)_2]$ (11)

Compound	**11**
Empirical formula	$C_{70}H_{66}Cu_2P_4S_2$
Formula mass	1222.30
Temperature/K	180.15
Crystal system	tetragonal
Space group	$I\bar{4}$
a/Å	32.1432(7)
b/Å	32.1432(7)
c/Å	15.0692(2)
α/°	90
β/°	90
γ/°	90
V/Å^3	15569.3(7)
Z	8
ρ_{calc}/g·cm^{-3}	1.043
μ/mm^{-1}	3.941
F(000)	5088.0
Crystal size/mm^3	0.24 × 0.04 × 0.03
Radiation	GaK_α (λ = 1.34143)
2Θ range for data collection/°	4.784 to 100.408
Index ranges	$-36 \le h \le 36$, $-36 \le k \le 36$, $-17 \le l \le 6$
Reflections collected	98076
Independent reflections	12181 (R_{int} = 0.0773, R_{sigma} = 0.0390)
Indep. refl. with ($I \ge 2\sigma(I)$)	9504
Data/restraints/parameters	12181/0/695
Goodness-of-fit on F^2	1.078
Final R indexes ($I \ge 2\sigma(I)$)	R_1 = 0.0767, wR_2 = 0.2052
Final R indexes (all data)	R_1 = 0.0948, wR_2 = 0.2203
Largest diff. peak/hole/e Å^{-3}	0.55/-0.34
Flack parameter	0.034(8)

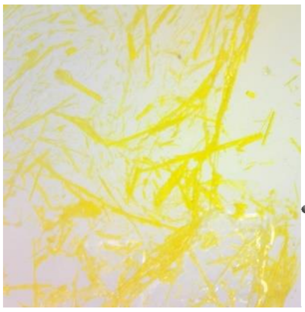

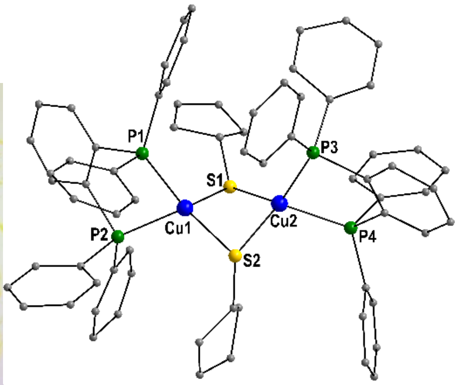

5.13 [$Cu_{14}S(SCp)_{12}(PPh_3)_4$] (12)

Compound	**12**
Empirical formula	$C_{132}H_{168}Cu_{14}P_4S_{13}$
Formula mass	3184.87
Temperature/K	150
Crystal system	hexagonal
Space group	$P6_3$
a/Å	17.8205(3)
b/Å	17.8205(3)
c/Å	51.7269(10)
α/°	90
β/°	90
γ/°	120
V/Å^3	14226.1(6)
Z	4
ρ_{calc}/g·cm^{-3}	1.487
μ/mm^{-1}	12.714
F(000)	6536.0
Crystal size/mm^3	0.18 × 0.17 × 0.16
Radiation	GaK_α (λ = 1.34143)
2Θ range for data collection/°	4.982 to 109.998
Index ranges	$-21 \leq h \leq 21$, $-18 \leq k \leq 21$, $-62 \leq l \leq 63$
Reflections collected	115813
Independent reflections	18090 (R_{int} = 0.0645, R_{sigma} = 0.0325)
Indep. refl. with ($I \geq 2\sigma(I)$)	12550
Data/restraints/parameters	18090/18/974
Goodness-of-fit on F^2	1.067
Final R indexes ($I \geq 2\sigma(I)$)	R_1 = 0.0848, wR_2 = 0.2359
Final R indexes (all data)	R_1 = 0.1161, wR_2 = 0.2581
Largest diff. peak/hole/e Å^{-3}	0.38/-0.52
Flack parameter	0.490(9)

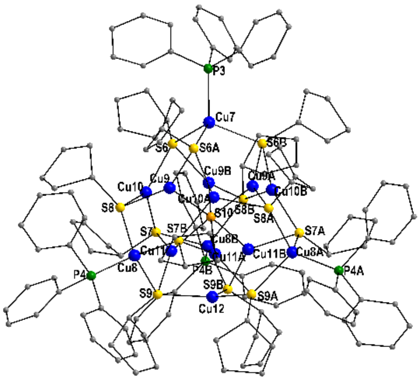

5.14 $[Cu_2(SPh)_2(dppp)_2]\cdot(C_7H_8)$ ($\mathbf{13}\cdot(C_7H_8)$)

Compound	**13**·(C_7H_8)
Empirical formula	$C_{73}H_{70}Cu_2P_4S_2$
Formula mass	1262.37
Temperature/K	180.15
Crystal system	triclinic
Space group	$P\overline{1}$
a/Å	9.9144(3)
b/Å	14.4926(4)
c/Å	23.3744(8)
α/°	83.732(3)
β/°	85.269(3)
γ/°	70.232(2)
V/Å^3	3138.02(17)
Z	2
ρ_{calc}/g·cm^{-3}	1.336
μ/mm^{-1}	4.899
F(000)	1316.0
Crystal size/mm^3	0.22 × 0.21 × 0.2
Radiation	GaK_α (λ = 1.34143)
2Θ range for data collection/°	5.658 to 124.992
Index ranges	$-10 \leq h \leq 13$, $-16 \leq k \leq 19$, $-21 \leq l \leq 30$
Reflections collected	49049
Independent reflections	14825 (R_{int} = 0.0142, R_{sigma} = 0.0121)
Data/restraints/parameters	14825/0/701
Goodness-of-fit on F^2	1.035
Final R indexes ($I \geq 2\sigma(I)$)	R_1 = 0.0341, wR_2 = 0.0895
Final R indexes (all data)	R_1 = 0.0392, wR_2 = 0.0929
Largest diff. peak/hole/e Å^{-3}	1.02/-0.59

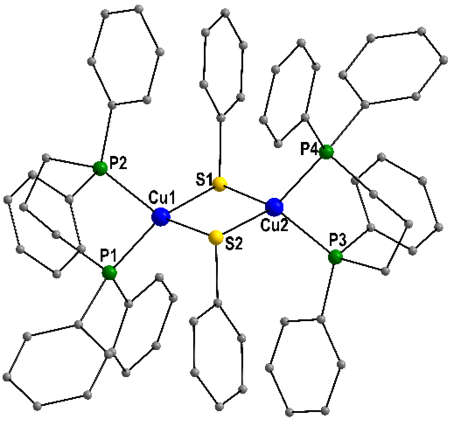

5.15 $[Cu_4(SPh)_4(PPh_3)_4]$(14)

Compound	**14**
Empirical formula	$C_{96}H_{80}Cu_4P_4S_4$
Formula mass	1739.88
Temperature/K	180.15
Crystal system	triclinic
Space group	$P\overline{1}$
a/Å	15.9926(6)
b/Å	20.4797(10)
c/Å	21.6788(9)
α/°	66.277(3)
β/°	77.427(3)
γ/°	72.016(4)
V/Å^3	6147.0(5)
Z	3
ρ_{calc}/g·cm^{-3}	1.410
μ/mm^{-1}	6.868
F(000)	2688.0
Crystal size/mm^3	0.25 × 0.24 × 0.23
Radiation	GaK_α (λ = 1.34143)
2Θ range for data collection/°	5.084 to 125.008
Index ranges	$-21 \le h \le 20$, $-17 \le k \le 27$, $-28 \le l \le 28$
Reflections collected	73570
Independent reflections	28482 (R_{int} = 0.0501, R_{sigma} = 0.0848)
Indep. refl. with ($I \ge 2\sigma(I)$)	15942
Data/restraints/parameters	28482/0/1459
Goodness-of-fit on F^2	0.920
Final R indexes ($I \ge 2\sigma(I)$)	R_1 = 0.0443, wR_2 = 0.0831
Final R indexes (all data)	R_1 = 0.1053, wR_2 = 0.0966
Largest diff. peak/hole/e Å^{-3}	0.90/-0.54

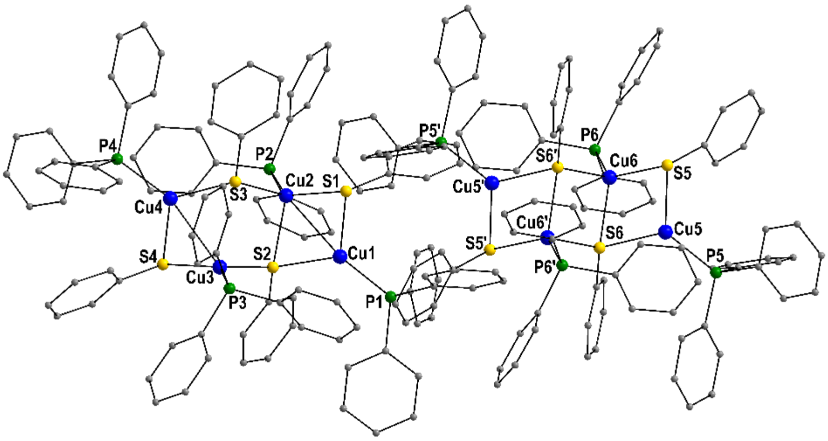

5.16 $[Cu_2(SPh)_2(dpppt)_2]\cdot 2(C_7H_8)$ ($15\cdot 2(C_7H_8)$)

Compound	**15**·2(C_7H_8)
Empirical formula	$C_{84}H_{86}Cu_2P_4S_2$
Formula mass	1410.60
Temperature/K	150.15
Crystal system	monoclinic
Space group	*C*2/*c*
a/Å	23.4910(6)
b/Å	14.9526(5)
c/Å	20.7321(5)
α/°	90
β/°	98.090(2)
γ/°	90
V/Å^3	7209.7(4)
Z	4
ρ_{calc}/g·cm^{-3}	1.300
μ/mm^{-1}	4.301
F(000)	2960.0
Crystal size/mm^3	0.29 × 0.27 × 0.26
Radiation	GaK_α (λ = 1.34143)
2Θ range for data collection/°	6.114 to 119.998
Index ranges	$-30 \leq h \leq 30$, $-14 \leq k \leq 19$, $-26 \leq l \leq 9$
Reflections collected	20670
Independent reflections	7794 (R_{int} = 0.0189, R_{sigma} = 0.0198)
Indep. refl. with ($I \geq 2\sigma(I)$)	6646
Data/restraints/parameters	7794/0/417
Goodness-of-fit on F^2	1.062
Final *R* indexes ($I \geq 2\sigma(I)$)	R_1 = 0.0407, wR_2 = 0.1052
Final *R* indexes (all data)	R_1 = 0.0504, wR_2 = 0.1095
Largest diff. peak/hole/e Å^{-3}	0.93/-0.42

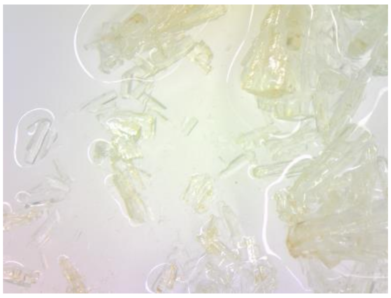

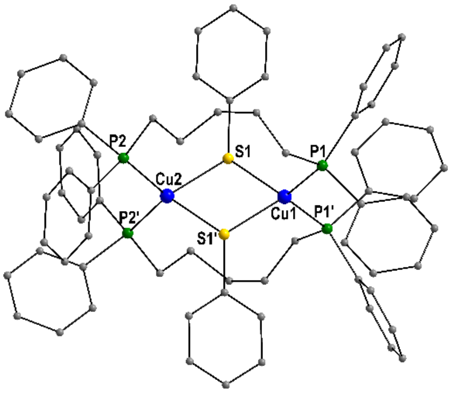

5.17 [$Cu_2(SPh)_2(dppox)_2$] (16)

Compound	**16**
Empirical formula	$C_{76}H_{66}S_2P_4Cu_2$
Formula mass	1294.36
Temperature/K	180.15
Crystal system	triclinic
Space group	$P\bar{1}$
a/Å	11.3953(3)
b/Å	13.2591(4)
c/Å	13.3091(3)
α/°	107.129(2)
β/°	112.635(2)
γ/°	106.296(2)
V/Å^3	1586.93(8)
Z	1
ρ_{calc}/g·cm^{-3}	1.354
μ/mm^{-1}	4.855
F(000)	672.0
Crystal size/mm^3	0.1 × 0.09 × 0.05
Radiation	GaK_α (λ = 1.34143)
2Θ range for data collection/°	6.784 to 123.982
Index ranges	$-14 \leq h \leq 7$, $-17 \leq k \leq 17$, $-14 \leq l \leq 17$
Reflections collected	19461
Independent reflections	7363 (R_{int} = 0.0222, R_{sigma} = 0.0316)
Indep. refl. with ($I \geq 2\sigma(I)$)	6052
Data/restraints/parameters	7363/0/379
Goodness-of-fit on F^2	1.051
Final R indexes ($I \geq 2\sigma(I)$)	R_1 = 0.0314, wR_2 = 0.0715
Final R indexes (all data)	R_1 = 0.0438, wR_2 = 0.0756
Largest diff. peak/hole / e Å^{-3}	0.28/-0.30

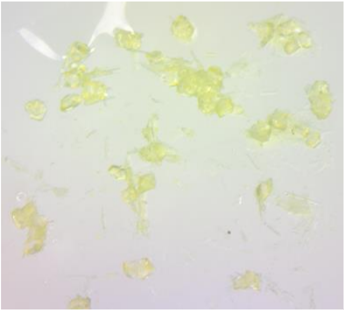

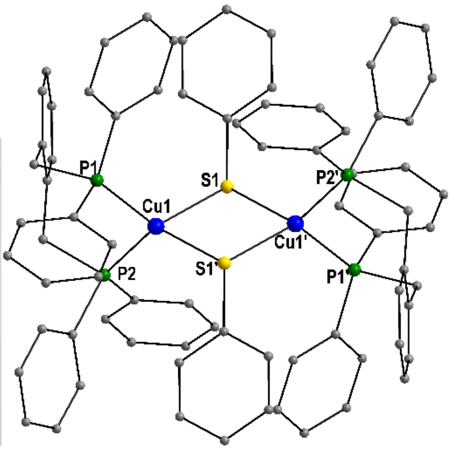

5.18 [Cu(dppp)$_2$][Cu$_5$(SAd)$_6$] (17)

Compound	**17**	**17**·(C$_7$H$_{16}$)
Empirical formula	$C_{114}H_{142}Cu_6P_4S_6$	$C_{121}H_{158}Cu_6P_4S_6$
Formula mass	2209.75	2309.94
Temperature/K	150	150.0
Crystal system	triclinic	triclinic
Space group	$P\overline{1}$	$P\overline{1}$
a/Å	14.6463(11)	18.1411(6)
b/Å	18.2647(17)	19.5636(7)
c/Å	23.123(2)	19.6124(7)
α/°	75.262(7)	111.899(3)
β/°	75.256(7)	105.409(3)
γ/°	89.706(7)	92.780(3)
V/Å^3	5773.3(9)	6140.8(4)
Z	2	2
ρ_{calc}/g·cm^{-3}	1.271	1.249
μ/mm^{-1}	7.078	6.668
F(000)	2312.0	2428.0
Crystal size/mm^3	0.17 × 0.16 × 0.15	0.12 × 0.03 × 0.02
Radiation	GaK_α (λ = 1.34143)	GaK_α (λ = 1.34143)
2Θ range for data collection/°	4.856 to 114.996	4.294 to 119.996
Index ranges	$-18 \le h \le 8$, $-22 \le k \le 22$, $-29 \le l \le 29$	$-23 \le h \le 23$, $-25 \le k \le 8$, $-25 \le l \le 25$
Reflections collected	62406	67167
Independent reflections	23144 (R_{int} = 0.0798, R_{sigma} = 0.1153)	27010 (R_{int} = 0.0840, R_{sigma} = 0.0986)
Data/restraints/parameters	23144/0/1171	27010/0/1202
Goodness-of-fit on F^2	0.893	1.052
Final R indexes ($I \ge 2\sigma(I)$)	R_1 = 0.0548, wR_2 = 0.1080	R_1 = 0.0874, wR_2 = 0.2361
Final R indexes (all data)	R_1 = 0.1236, wR_2 = 0.1211	R_1 = 0.1408, wR_2 = 0.2583
Largest diff. peak/hole/e Å^{-3}	0.49/-0.40	0.99/-0.85

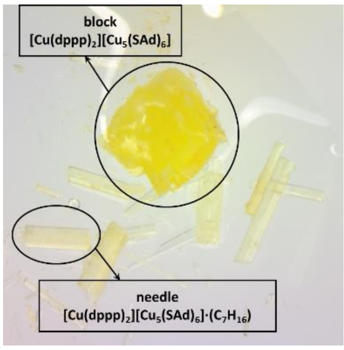

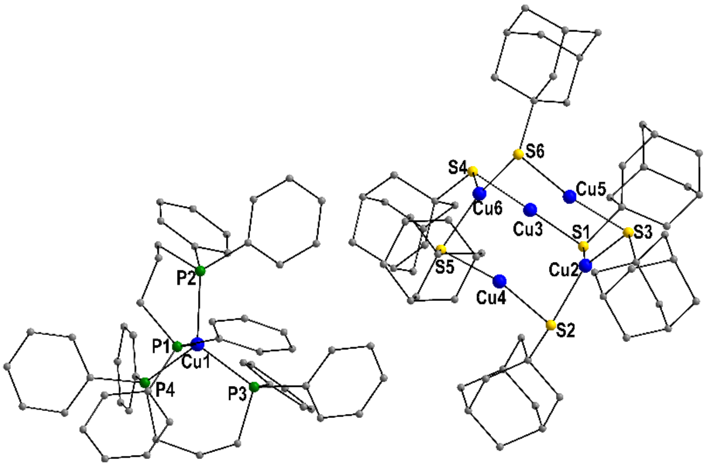

5.19 [$Cu_4(SAd)_4(dppp)_2$] (18)

Compound	**18**
Empirical formula	$C_{94}H_{112}Cu_4P_4S_4$
Formula mass	1748.11
Temperature/K	150
Crystal system	triclinic
Space group	$P\overline{1}$
a/Å	10.9432(3)
b/Å	13.7537(4)
c/Å	15.2578(5)
α/°	111.718(2)
β/°	96.306(3)
γ/°	100.608(3)
V/Å^3	2056.76(11)
Z	1
ρ_{calc}/g·cm^{-3}	1.411
μ/mm^{-1}	6.837
F(000)	916.0
Crystal size/mm^3	0.16 × 0.14 × 0.12
Radiation	GaK_α (λ = 1.34143)
2Θ range for data collection/°	5.53 to 124.996
Index ranges	$-6 \leq h \leq 14$, $-18 \leq k \leq 16$, $-20 \leq l \leq 19$
Reflections collected	23181
Independent reflections	9661 (R_{int} = 0.0192, R_{sigma} = 0.0197)
Data/restraints/parameters	9661/0/478
Goodness-of-fit on F^2	1.031
Final R indexes ($I \geq 2\sigma(I)$)	R_1 = 0.0332, wR_2 = 0.0833
Final R indexes (all data)	R_1 = 0.0387, wR_2 = 0.0881
Largest diff. peak/hole/e Å^{-3}	0.84/-0.53

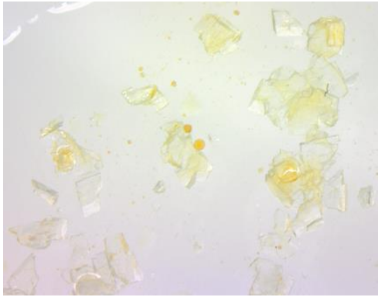

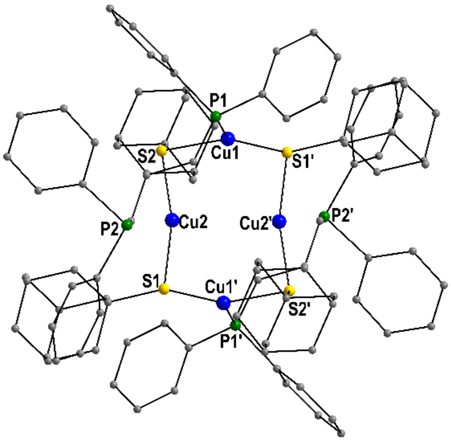

5.20 [$Cu_{16}S_8(dpph)_6$] (19)

Compound	**19**
Empirical formula	$C_{180}H_{192}Cu_{16}P_{12}S_8$
Formula mass	3998.07
Temperature/K	130
Crystal system	monoclinic
Space group	*C*2
a/Å	33.5511(12)
b/Å	17.4770(3)
c/Å	24.6517(10)
α/°	90
β/°	136.153(2)
γ/°	90
V/Å^3	10013.5(6)
Z	2
ρ_{calc}/g·cm^{-3}	1.326
μ/mm^{-1}	10.286
F(000)	4084.0
Crystal size/mm^3	0.2 × 0.18 × 0.16
Radiation	GaK_α (λ = 1.34143)
2*Θ* range for data collection/°	41.292 to 100.02
Index ranges	$-23 \le h \le 38, -19 \le k \le 17, -28 \le l \le 20$
Reflections collected	19555
Independent reflections	10371 (R_{int} = 0.0452, R_{sigma} = 0.0757)
Data/restraints/parameters	10371/36/934
Goodness-of-fit on F^2	1.010
Final *R* indexes ($I \ge 2\sigma(I)$)	R_1 = 0.0569, wR_2 = 0.1126
Final *R* indexes (all data)	R_1 = 0.1064, wR_2 = 0.1332
Largest diff. peak/hole/e Å^{-3}	0.26/-0.18
Flack parameter	-0.028(5)

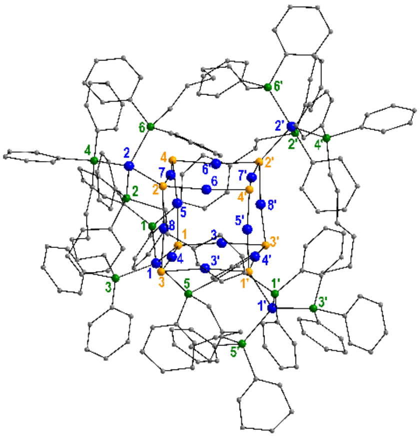

5.21 [Cu_4(Strimethyl-benzyl)$_4$(dppm)$_2$]·(C_7H_8) (20·(C_7H_8))

Compound	**20**·(C_7H_8)
Empirical formula	$C_{97}H_{104}Cu_4P_4S_4$
Formula mass	1776.08
Temperature/K	150.15
Crystal system	triclinic
Space group	$P\overline{1}$
a/Å	14.2963(7)
b/Å	14.4138(5)
c/Å	22.9825(8)
α/°	90.627(3)
β/°	94.548(3)
γ/°	112.021(3)
V/Å^3	4372.3(3)
Z	2
ρ_{calc}/g·cm^{-3}	1.349
μ/mm^{-1}	6.440
F(000)	1852.0
Crystal size/mm^3	0.23 × 0.04 × 0.03
Radiation	GaK_α (λ = 1.34143)
2Θ range for data collection/°	5.76 to 124.994
Index ranges	$-6 \le h \le 18$, $-19 \le k \le 17$, $-30 \le l \le 30$
Reflections collected	50041
Independent reflections	20237 (R_{int} = 0.0241, R_{sigma} = 0.0330)
Indep. refl. with ($I \ge 2\sigma(I)$)	15590
Data/restraints/parameters	20237/0/994
Goodness-of-fit on F^2	1.021
Final R indexes ($I \ge 2\sigma(I)$)	R_1 = 0.0358, wR_2 = 0.0805
Final R indexes (all data)	R_1 = 0.0553, wR_2 = 0.0855
Largest diff. peak/hole/e Å^{-3}	0.33/-0.29

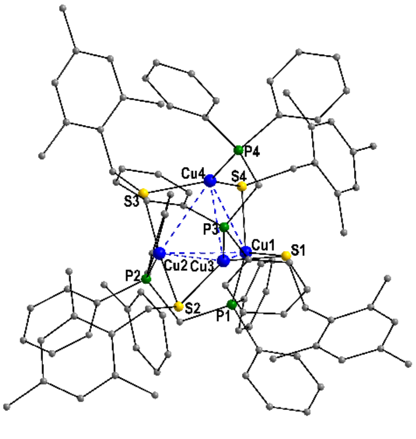

5.22 [Cu_2(Strimethyl-benzyl)$_2$(dppb)$_2$]·(C_6H_{14}) (**21**·(C_6H_{14}))

Compound	**21**·(C_6H_{14})
Empirical formula	$C_{82}H_{96}Cu_2P_4S_2$
Formula mass	1396.66
Temperature/K	150
Crystal system	triclinic
Space group	$P\overline{1}$
a/Å	9.8045(3)
b/Å	13.7698(4)
c/Å	14.2855(4)
α/°	108.955(2)
β/°	95.622(2)
γ/°	98.072(2)
Volume/Å^3	1784.62(9)
Z	1
ρ_{calc}/g·cm^{-3}	1.300
μ/mm^{-1}	4.338
F(000)	738.0
Crystal size/mm^3	0.25 × 0.22 × 0.21
Radiation	GaK_α (λ = 1.34143)
2Θ range for data collection/°	5.76 to 125.002
Index ranges	$-12 \le h \le 12$, $-6 \le k \le 17$, $-18 \le l \le 17$
Reflections collected	21822
Independent reflections	8460 (R_{int} = 0.0275, R_{sigma} = 0.0247)
Indep. refl. with ($I \ge 2\sigma(I)$)	7387
Data/restraints/parameters	8460/0/409
Goodness-of-fit on F^2	1.058
Final R indexes ($I \ge 2\sigma(I)$)	R_1 = 0.0526, wR_2 = 0.1437
Final R indexes [all data]	R_1 = 0.0606, wR_2 = 0.1521
Largest diff. peak/hole/e Å^{-3}	1.22/-0.94

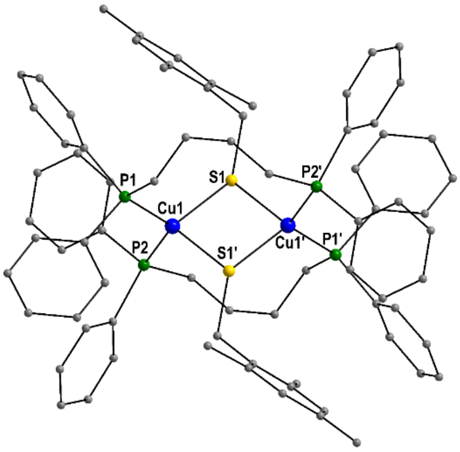

5.23 $[Cu_{12}S_6(dppox)_4]\cdot(C_7H_8)\cdot2(C_7H_{16})$ ($22\cdot(C_7H_8)\cdot2(C_7H_{16})$)

Compound	**22**$\cdot(C_7H_8)\cdot2(C_7H_{16})$
Empirical formula	$C_{149}H_{152}Cu_{12}P_8S_6$
Formula mass	3145.30
Temperature/K	180
Crystal system	monoclinic
Space group	$P2_1/n$
a/Å	16.5497(3)
b/Å	22.5492(6)
c/Å	18.3000(6)
α/°	90
β/°	91.791(2)
γ/°	90
V/Å^3	6825.9(3)
Z	2
ρ_{calc}/g·cm^{-3}	1.530
μ/mm^{-1}	11.267
F(000)	3220.0
Crystal size/mm^3	0.18 × 0.04 × 0.03
Radiation	GaK_α (λ = 1.34143)
2Θ range for data collection/°	5.412 to 125.18
Index ranges	$-21 \le h \le 20$, $-24 \le k \le 29$, $-24 \le l \le 18$
Reflections collected	70528
Independent reflections	16445 (R_{int} = 0.0461, R_{sigma} = 0.0401)
Indep. refl. with ($I \ge 2\sigma(I)$)	12308
Data/restraints/parameters	16445/8/747
Goodness-of-fit on F^2	1.017
Final R indexes ($I \ge 2\sigma(I)$)	R_1 = 0.0551, wR_2 = 0.1342
Final R indexes (all data)	R_1 = 0.0807, wR_2 = 0.1486
Largest diff. peak/hole/e Å^{-3}	1.15/-0.85

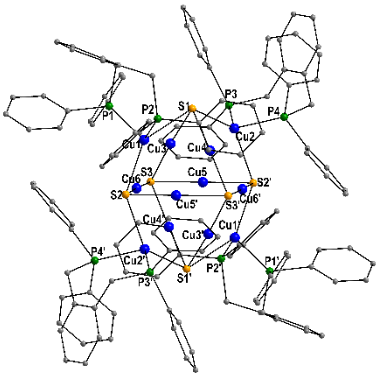

5.2 $(HDMF)_2[Cu_6(SPh)_5(dppe)_3]_2(Mo_8O_{26})\cdot 2DMF\cdot (Et_2O)$

($\mathbf{23}\cdot 2DMF\cdot (Et_2O)$)

Compound	**23**·2DMF·(Et_2O)
Empirical formula	$C_{232}H_{234}Cu_{12}Mo_8N_4O_{31}P_{12}S_{10}$
Formula mass	5796.46
Temperature/K	180.0
Crystal system	triclinic
Space group	$P\bar{1}$
a/Å	20.6639(16)
b/Å	21.2087(8)
c/Å	32.4361(13)
α/°	87.516(3)
β/°	88.732(5)
γ/°	72.913(5)
V/Å^3	13574.4(13)
Z	2
ρ_{calc}/g·cm^{-3}	1.418
μ/mm^{-1}	1.478
F(000)	5852.0
Crystal size/mm^3	0.16 × 0.14 × 0.12
Radiation	MoK_α (λ = 0.71073)
2Θ range for data collection/°	2.772 to 56
Index ranges	$-27 \leq h \leq 26$, $-28 \leq k \leq 26$, $-42 \leq l \leq 39$
Reflections collected	152127
Independent reflections	63960 (R_{int} = 0.0351, R_{sigma} = 0.0556)
Data/restraints/parameters	63960/8/2724
Goodness-of-fit on F^2	1.050
Final R indexes ($I \geq 2\sigma(I)$)	R_1 = 0.0745, wR_2 = 0.2291
Final R indexes (all data)	R_1 = 0.1144, wR_2 = 0.2496
Largest diff. peak/hole/e Å^{-3}	2.03/-1.66

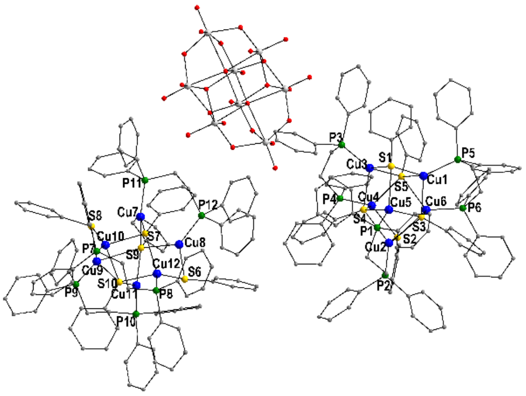

5.25 $[(Cu_5(SPh)_5(dppe)_2)_2(dppe)]\cdot 2DMF$ (24·2DMF)

Compound	**24**·2DMF
Empirical formula	$C_{196}H_{184}Cu_{10}N_2O_2P_{10}S_{10}$
Formula mass	3865.14
Temperature/K	180
Crystal system	monoclinic
Space group	$P2_1/n$
a/Å	25.0557(10)
b/Å	15.3922(4)
c/Å	25.6079(10)
α/°	90
β/°	110.006(3)
γ/°	90
V/Å^3	9280.1(6)
Z	2
ρ_{calc}/g·cm^{-3}	1.383
μ/mm^{-1}	7.540
F(000)	3980.0
Crystal size/mm^3	0.15 × 0.14 × 0.13
Radiation	GaK_α (λ = 1.34143)
2Θ range for data collection/°	5.93 to 90
Index ranges	$-24 \leq h \leq 26, -13 \leq k \leq 16, -26 \leq l \leq 26$
Reflections collected	50989
Independent reflections	11340 (R_{int} = 0.0987, R_{sigma} = 0.0727)
Indep. refl. with ($I \geq 2\sigma(I)$)	6778
Data/restraints/parameters	11340/6/748
Goodness-of-fit on F^2	1.541
Final R indexes ($I \geq 2\sigma(I)$)	R_1 = 0.1336, wR_2 = 0.3773
Final R indexes (all data)	R_1 = 0.1861, wR_2 = 0.4025
Largest diff. peak/hole/e Å^{-3}	2.71/-1.33

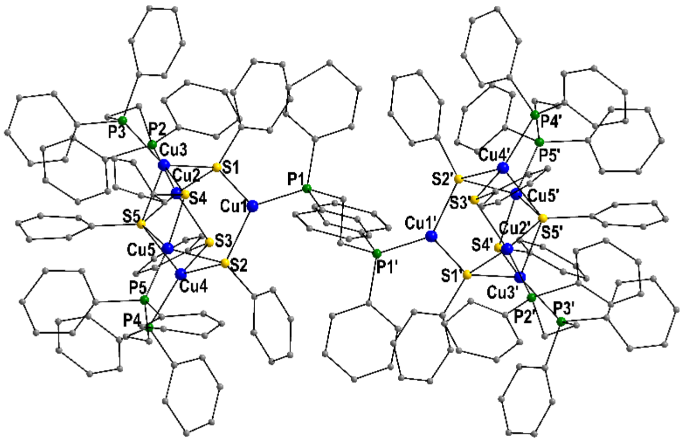

5.26 $[Cu_6(SPh)_4(dppm)_4](Mo_6O_{19})\cdot 2DMF$ (25·2DMF)

Compound	**25**·2DMF
Empirical formula	$C_{130}H_{122}Cu_6Mo_6N_2O_{21}P_8S_4$
Formula mass	3381.17
Temperature/K	150
Crystal system	triclinic
Space group	$P\overline{1}$
a/Å	15.114(2)
b/Å	17.388(3)
c/Å	29.050(11)
α/°	89.17(2)
β/°	76.76(2)
γ/°	66.642(10)
V/Å^3	6798(3)
Z	2
ρ_{calc}/g·cm^{-3}	1.652
μ/mm^{-1}	1.671
F(000)	3388.0
Crystal size/mm^3	0.14 × 0.12 × 0.02
Radiation	MoK_α (λ = 0.71073)
2Θ range for data collection/°	2.83 to 65.106
Index ranges	$-22 \le h \le 22$, $-26 \le k \le 23$, $-41 \le l \le 43$
Reflections collected	105099
Independent reflections	44902 (R_{int} = 0.0635, R_{sigma} = 0.1403)
Data/restraints/parameters	44902/0/1601
Goodness-of-fit on F^2	0.975
Final R indexes ($I \ge 2\sigma(I)$)	R_1 = 0.0776, wR_2 = 0.2001
Final R indexes (all data)	R_1 = 0.1732, wR_2 = 0.2446
Largest diff. peak/hole/e Å^{-3}	5.59/-3.72

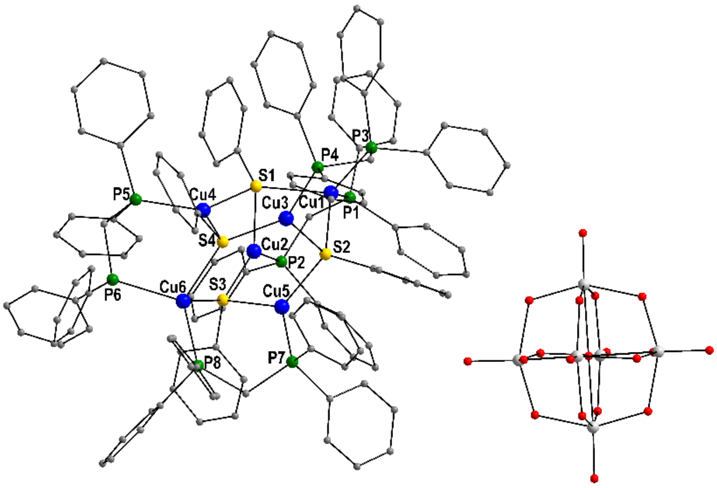

5.27 $[Cu_4(SPh)_4(PPh_3)_4]\cdot 2(C_7H_8)$ $(26\cdot 2(C_7H_8))$

Compound	**26**·$2(C_7H_8)$
Empirical formula	$C_{110}H_{96}Cu_4P_4S_4$
Formula mass	1924.14
Temperature/K	180
Crystal system	triclinic
Space group	$P\bar{1}$
a/Å	12.5525(4)
b/Å	13.0929(5)
c/Å	14.7533(5)
α/°	75.466(3)
β/°	84.629(3)
γ/°	84.691(3)
V/Å^3	2330.78(14)
Z	1
ρ_{calc}/g·cm^{-3}	1.371
μ/mm^{-1}	6.073
F(000)	996.0
Crystal size/mm^3	0.22 × 0.2 × 0.18
Radiation	GaK_α (λ = 1.34143)
2*Θ* range for data collection/°	5.398 to 124.998
Index ranges	$-15 \le h \le 16$, $-17 \le k \le 17$, $-8 \le l \le 19$
Reflections collected	29711
Independent reflections	11037 (R_{int} = 0.0279, R_{sigma} = 0.0314)
Indep. refl. with ($I \ge 2\sigma(I)$)	9003
Data/restraints/parameters	11037/0/551
Goodness-of-fit on F^2	1.050
Final *R* indexes ($I \ge 2\sigma(I)$)	R_1 = 0.0333, wR_2 = 0.0802
Final *R* indexes (all data)	R_1 = 0.0506, wR_2 = 0.0888
Largest diff. peak/hole / e Å^{-3}	0.35/-0.49

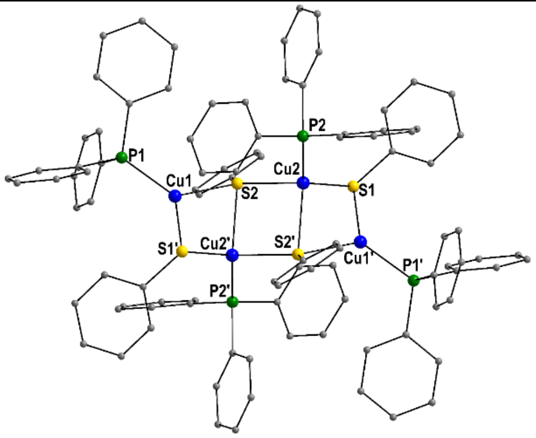

5.28 $[Cu_3S_3(SCp)(MoO)(PPh_3)_2]_2\cdot 2DMF$ (27·2DMF)

Compound	**27**·2DMF
Empirical formula	$C_{88}H_{92}Cu_6Mo_2N_2O_4P_4S_8$
Formula mass	2195.11
Temperature/K	180
Crystal system	monoclinic
Space group	$P2_1/n$
a/Å	13.6584(3)
b/Å	20.2089(3)
c/Å	17.0352(3)
α/°	90
β/°	108.0800(10)
γ/°	90
V/Å^3	4469.91(14)
Z	2
ρ_{calc}/g·cm^{-3}	1.631
μ/mm^{-1}	10.877
F(000)	2224.0
Crystal size/mm^3	0.16 × 0.14 × 0.12
Radiation	GaK_α (λ = 1.34143)
2Θ range for data collection/°	6.084 to 115
Index ranges	$-6 \le h \le 17$, $-25 \le k \le 25$, $-21 \le l \le 20$
Reflections collected	49218
Independent reflections	9294 (R_{int} = 0.0418, R_{sigma} = 0.0253)
Data/restraints/parameters	9294/0/676
Goodness-of-fit on F^2	1.029
Final R indexes ($I \ge 2\sigma(I)$)	R_1 = 0.0446, wR_2 = 0.1162
Final R indexes (all data)	R_1 = 0.0524, wR_2 = 0.1241
Largest diff. peak/hole/e Å^{-3}	0.92/-0.84

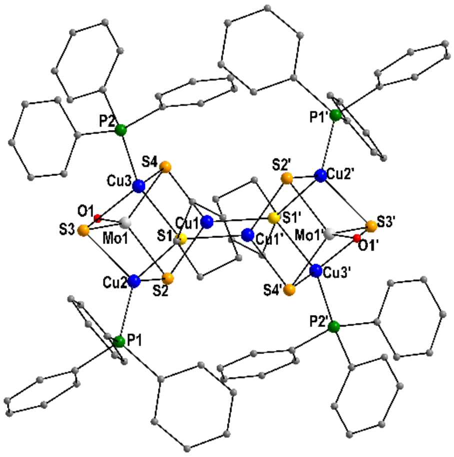

5.29 [$Cu_{16}Se_8(dppp)_6$] (28)

Compound	**28**·2THF·(Et_2O)	**28**·THF·(Et_2O)
Empirical formula	$C_{174}H_{182}Cu_{16}O_3P_{12}Se_8$	$C_{170}H_{174}Cu_{16}O_2P_{12}Se_8$
Formula mass	4341.15	4269.04
Temperature/K	150	150
Crystal system	monoclinic	triclinic
Space group	$P2_1/n$	$P\bar{1}$
a/Å	24.5871(9)	17.9679(5)
b/Å	31.7387(10)	18.1929(6)
c/Å	26.1161(11)	27.6592(7)
α/°	90	80.295(2)
β/°	102.441(3)	85.371(2)
γ/°	90	86.092(2)
V/Å^3	19901.5(13)	8869.3(4)
Z	4	2
ρ_{calc}/g·cm^{-3}	1.449	1.599
μ/mm^{-1}	11.004	12.336
F(000)	8664.0	4252.0
Crystal size/mm^3	0.16 × 0.12 × 0.03	0.18 × 0.06 × 0.05
Radiation	GaK_α (λ = 1.34143)	GaK_α (λ = 1.34143)
2Θ range for data collection/°	4.588 to 125.098	4.3 to 119.998
Index ranges	$-32 \le h \le 28$, $-17 \le k \le 41$, $-32 \le l \le 34$	$-23 \le h \le 23$, $-23 \le k \le 10$, $-35 \le l \le 32$
Reflections collected	118208	94640
Independent reflections	46675 (R_{int} = 0.0466, R_{sigma} = 0.0489)	38893 (R_{int} = 0.0340, R_{sigma} = 0.0334)
Reflections collected		30474
Data/restraints/parameters	46675/0/1870	38893/0/1893
Goodness-of-fit on F^2	1.050	1.037
Final R indexes ($I \ge 2\sigma(I)$)	R_1 = 0.0575, wR_2 = 0.1469	R_1 = 0.0468, wR_2 = 0.1198
Final R indexes (all data)	R_1 = 0.0798, wR_2 = 0.1616	R_1 = 0.0644, wR_2 = 0.1301
Largest diff. peak/hole/e Å^{-3}	0.90/-0.74	1.08/-0.48

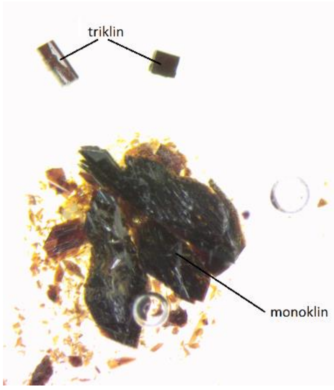

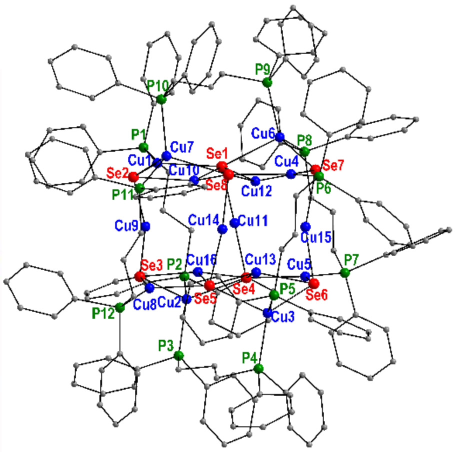

5.30 $[Cu_{12}Se_4(SCp)_4(dppfc)_4]\cdot(C_7H_8)$ ($\mathbf{29}\cdot(C_7H_8)$)

Compound	**29**·(C_7H_8)
Empirical formula	$C_{163}H_{156}Cu_{12}Fe_4P_8S_4Se_4$
Formula mass	3792.59
Temperature/K	150
Crystal system	monoclinic
Space group	*C*2/*c*
a/Å	33.9501(5)
b/Å	34.2686(7)
c/Å	36.5113(5)
α/°	90
β/°	93.6130(10)
γ/°	90
V/Å^3	42393.6(12)
Z	8
ρ_{calc}/g·cm^{-3}	1.188
μ/mm^{-1}	9.124
F(000)	15248.0
Crystal size/mm^3	0.14 × 0.13 × 0.12
Radiation	GaK_α (λ = 1.34143)
2*Θ* range for data collection/°	4.486 to 100.014
Index ranges	$-38 \le h \le 38$, $-38 \le k \le 39$, $-41 \le l \le 23$
Reflections collected	129259
Independent reflections	32851 (R_{int} = 0.0497, R_{sigma} = 0.0557)
Data/restraints/parameters	32851/0/1722
Goodness-of-fit on F^2	1.078
Final *R* indexes ($I \ge 2\sigma(I)$)	R_1 = 0.0516, wR_2 = 0.1295
Final *R* indexes (all data)	R_1 = 0.0882, wR_2 = 0.1433
Largest diff. peak/hole/e Å^{-3}	0.38/-0.29

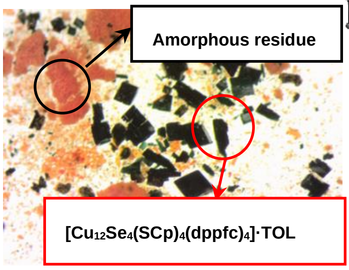

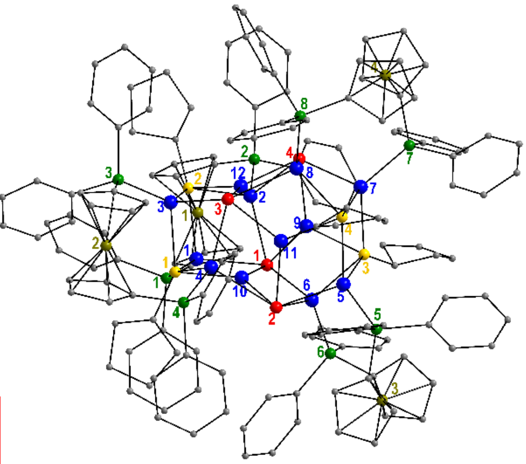

5.31 $[Cu_{14}Se_6(SAd)_2(dppm)_6]\cdot 6(C_7H_8)$ ($\mathbf{30}\cdot 6(C_7H_8)$)

Compound	**30**·6(C_7H_8)
Empirical formula	$C_{212}H_{210}Cu_{14}P_{12}S_2Se_6$
Formula mass	4556.87
Temperature/K	150
Crystal system	trigonal
Space group	$R\bar{3}c$
a/Å	27.1645(7)
b/Å	27.1645(7)
c/Å	44.6660(10)
α/°	90
β/°	90
γ/°	120
V/Å^3	28543.7(16)
Z	6
ρ_{calc}/g·cm^{-3}	1.591
μ/mm^{-1}	10.196
F(000)	13824.0
Crystal size/mm^3	0.16 × 0.15 × 0.14
Radiation	GaK_α (λ = 1.34143)
2Θ range for data collection/°	4.746 to 124.904
Index ranges	$-34 \le h \le 29$, $-25 \le k \le 34$, $-57 \le l \le 42$
Reflections collected	22908
Independent reflections	7505 (R_{int} = 0.0410, R_{sigma} = 0.0332)
Data/restraints/parameters	7505/0/371
Goodness-of-fit on F^2	1.019
Final R indexes ($I \ge 2\sigma(I)$)	R_1 = 0.0844, wR_2 = 0.2254
Final R indexes (all data)	R_1 = 0.1113, wR_2 = 0.2516
Largest diff. peak/hole/e Å^{-3}	4.72/-0.86

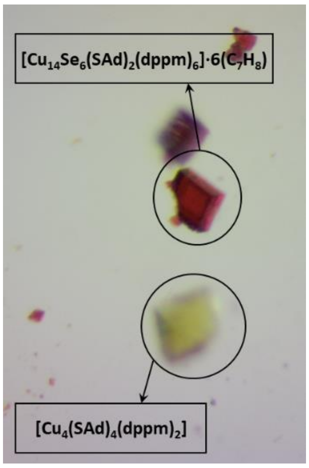

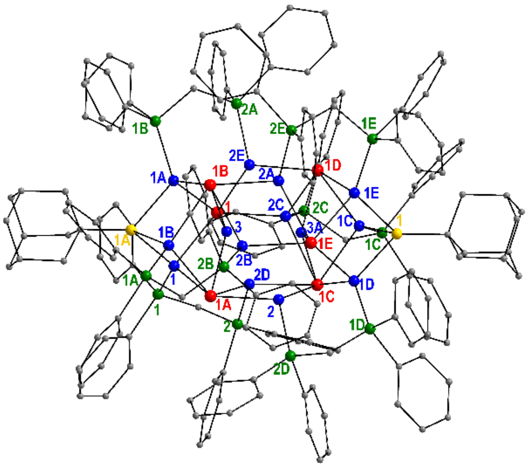

5.32 $[Cu_4(SAd)_4(dppm)_2]$ (31)

Compound	**31**
Empirical formula	$C_{90}H_{104}Cu_4P_4S_4$
Formula mass	1692.01
Temperature/K	150.0
Crystal system	monoclinic
Space group	$P2_1/n$
a/Å	13.1200(13)
b/Å	21.7181(16)
c/Å	13.9762(14)
α/°	90
β/°	97.899(8)
γ/°	90
V/Å^3	3944.6(6)
Z	2
ρ_{calc}/g·cm^{-3}	1.425
μ/mm^{-1}	7.118
F(000)	1768.0
Crystal size/mm^3	0.16 × 0.14 × 0.12
Radiation	GaK_α (λ = 1.34143)
2Θ range for data collection/°	6.588 to 123.99
Index ranges	$-15 \le h \le 17$, $-28 \le k \le 12$, $-18 \le l \le 16$
Reflections collected	23231
Independent reflections	9190(R_{int} = 0.0201, R_{sigma} = 0.0234)
Data/restraints/parameters	9190/0/460
Goodness-of-fit on F^2	1.036
Final R indexes ($I \ge 2\sigma(I)$)	R_1 = 0.0332, wR_2 = 0.0784
Final R indexes (all data)	R_1 = 0.0427, wR_2 = 0.0818
Largest diff. peak/hole/e Å^{-3}	0.35/-0.33

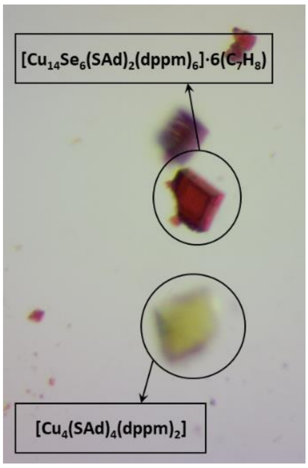

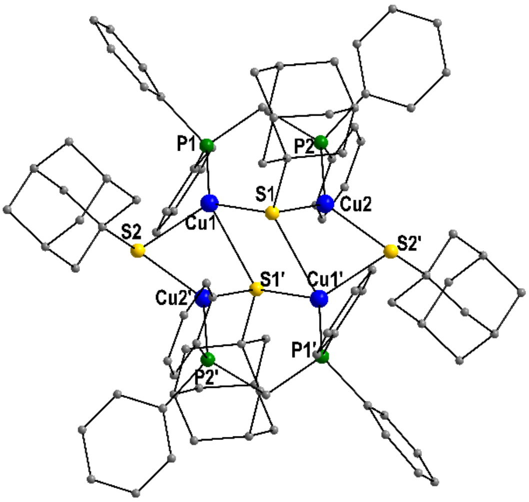

5.33 $[Cu_{92}S_{44}(SAd)_4(dppp)_{12}]$ (32)

Compound	**32**
Empirical formula	$C_{364}H_{372}Cu_{92}P_{24}S_{48}$
Formula mass	12874.43
Temperature/K	150
Crystal system	monoclinic
Space group	$P2_1/c$
a/Å	26.0399(7)
b/Å	37.0750(7)
c/Å	27.6809(8)
α/°	90
β/°	105.457(2)
γ/°	90
V/Å^3	25757.4(12)
Z	2
ρ_{calc}/g·cm^{-3}	1.660
μ/mm^{-1}	21.857
F(000)	12704.0
Crystal size/mm^3	0.12 × 0.1 × 0.08
Radiation	GaK_α (λ = 1.34143)
2Θ range for data collection/°	4.156 to 80
Index ranges	$-24 \le h \le 23$, $-23 \le k \le 35$, $-24 \le l \le 26$
Reflections collected	74966
Independent reflections	23209 (R_{int} = 0.1472, R_{sigma} = 0.1430)
Data/restraints/parameters	23209/2/1407
Goodness-of-fit on F^2	1.232
Final R indexes ($I \ge 2\sigma(I)$)	R_1 = 0.1190, wR_2 = 0.2905
Final R indexes (all data)	R_1 = 0.1824, wR_2 = 0.3278
Largest diff. peak/hole / e Å^{-3}	2.81/-1.66

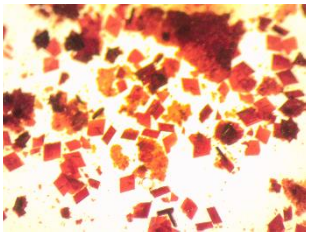

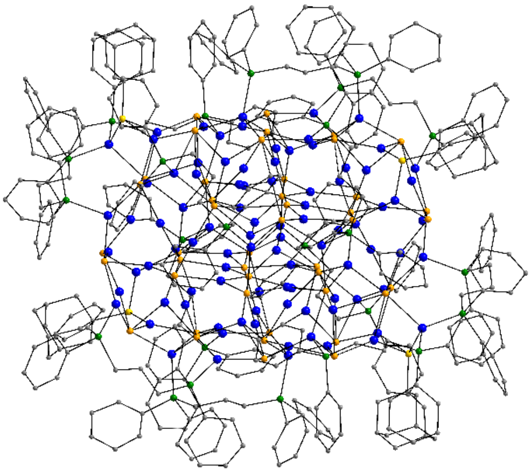

5.34 [$Cu_{90}S_{44}(SCp)_4(dppp)_{10}(dpppS)_2$] (33)

Compound	**33**
Empirical formula	$C_{344}H_{348}Cu_{90}P_{24}S_{50}$
Formula mass	12547.08
Temperature/K	150.0
Crystal system	monoclinic
Space group	*C*2/*c*
a/Å	40.5026(18)
b/Å	23.7202(8)
c/Å	50.296(3)
α/°	90
β/°	94.407(4)
γ/°	90
V/Å^3	48178(4)
Z	4
ρ_{calc}/g·cm^{-3}	1.730
μ/mm^{-1}	22.948
F(000)	24728.0
Crystal size/mm^3	0.14 × 0.12 × 0.02
Radiation	GaK_α (λ = 1.34143)
2Θ range for data collection/°	6.568 to 79.996
Index ranges	$-38 \le h \le 31$, $-22 \le k \le 9$, $-46 \le l \le 48$
Reflections collected	58850
Independent reflections	22046 (R_{int} = 0.0530, R_{sigma} = 0.0699)
Data/restraints/parameters	22046/6/1351
Goodness-of-fit on F^2	1.111
Final *R* indexes ($I \ge 2\sigma(I)$)	R_1 = 0.1190, wR_2 = 0.3301
Final *R* indexes (all data)	R_1 = 0.1546, wR_2 = 0.3450
Largest diff. peak/hole / e Å^{-3}	0.99/-0.82

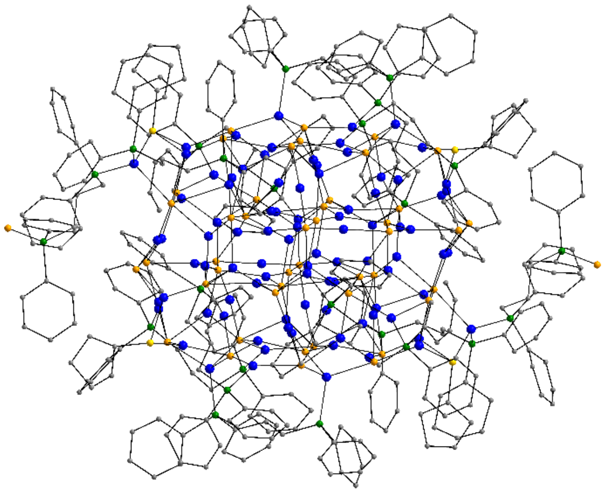

5.35 $[Cu_{40}Se_{15}(SCp)_{10}(dppp)_6]$ (34)

Compound	**34**
Empirical formula	$C_{212}H_{246}Cu_{40}P_{12}S_{10}Se_{15}$
Formula mass	7212.31
Temperature/K	150
Crystal system	monoclinic
Space group	$P2_1/n$
a/Å	19.8923(7)
b/Å	38.5781(12)
c/Å	35.6842(13)
α/°	90
β/°	92.360(3)
γ/°	90
V/Å^3	27361.1(16)
Z	4
ρ_{calc}/g·cm^{-3}	1.751
μ/mm^{-1}	19.077
F(000)	14112.0
Crystal size/mm^3	0.08 × 0.05 × 0.04
Radiation	GaK_α (λ = 1.34143)
2Θ range for data collection/°	4.352 to 95.062
Index ranges	$-12 \leq h \leq 21$, $-42 \leq k \leq 38$, $-39 \leq l \leq 39$
Reflections collected	106061
Independent reflections	37054 (R_{int} = 0.0948, R_{sigma} = 0.1521)
Data/restraints/parameters	37054/17/2386
Goodness-of-fit on F^2	0.951
Final R indexes ($I \geq 2\sigma(I)$)	R_1 = 0.0767, wR_2 = 0.1865
Final R indexes (all data)	R_1 = 0.1692, wR_2 = 0.2267
Largest diff. peak/hole / e Å^{-3}	1.14/-1.55

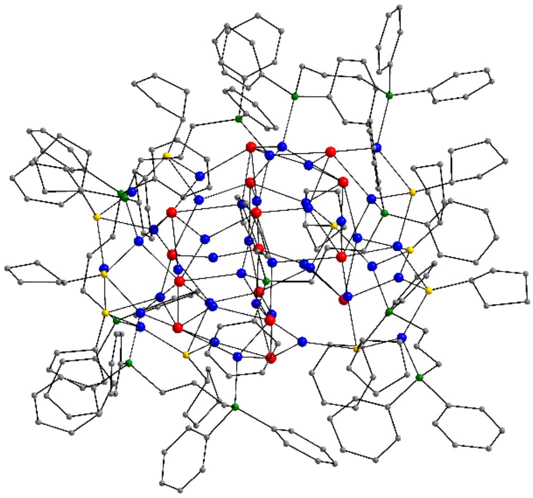

5.36 [$Cu_{61}Se_{31}(dppp)_{10}$] (35)

Compound	**35**
Empirical formula	$C_{270}H_{260}Cu_{61}P_{20}Se_{31}$
Formula mass	10447.86
Temperature/K	150.0
Crystal system	triclinic
Space group	$P\bar{1}$
a/Å	23.0061(6)
b/Å	24.6430(7)
c/Å	35.0155(10)
α/°	93.660(2)
β/°	90.474(2)
γ/°	115.341(2)
V/Å^3	17890.9(9)
Z	2
ρ_{calc}/g·cm^{-3}	1.939
μ/mm^{-1}	22.375
F(000)	10006.0
Crystal size/mm^3	0.14 × 0.03 × 0.02
Radiation	GaK_α (λ = 1.34143)
2Θ range for data collection/°	4.404 to 95
Index ranges	$-15 \le h \le 25$, $-27 \le k \le 25$, $-38 \le l \le 38$
Reflections collected	118678
Independent reflections	47666 (R_{int} = 0.0842, R_{sigma} = 0.1030)
Data/restraints/parameters	47666/78/3308
Goodness-of-fit on F^2	1.030
Final R indexes ($I \ge 2\sigma(I)$)	R_1 = 0.0945, wR_2 = 0.2400
Final R indexes (all data)	R_1 = 0.1484, wR_2 = 0.2736
Largest diff. peak/hole/e Å^{-3}	2.69/-1.70

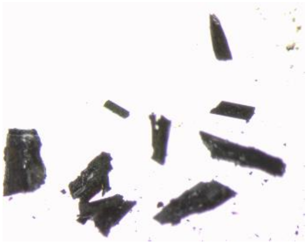

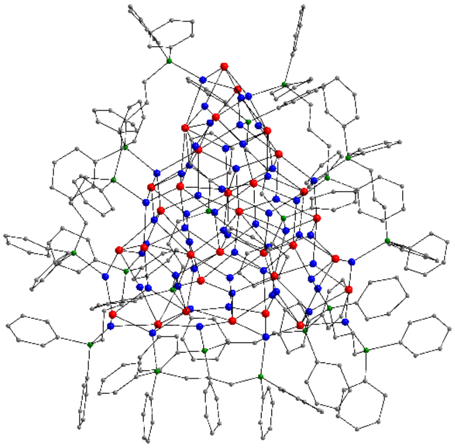

5.37 $[Cu_{61}Se_{26}(SCy)_9(PPh_3)_{14}]$ (36)

Compound	**36**
Empirical formula	$C_{306}H_{309}Cu_{61}P_{14}S_9Se_{26}$
Formula mass	10637.53
Temperature/K	150
Crystal system	monoclinic
Space group	$P2_1/c$
a/Å	25.2148(4)
b/Å	33.9030(5)
c/Å	50.0869(9)
α/°	90
β/°	92.6360(10)
γ/°	90
V/Å^3	42771.8(12)
Z	4
ρ_{calc}/g·cm^{-3}	1.652
μ/mm^{-1}	18.520
F(000)	20608.0
Crystal size/mm^3	0.12 × 0.02 × 0.01
Radiation	GaK_α (λ = 1.34143)
2Θ range for data collection/°	4.536 to 89.7
Index ranges	$-26 \leq h \leq 26$, $-35 \leq k \leq 13$, $-52 \leq l \leq 52$
Reflections collected	144318
Independent reflections	49695 (R_{int} = 0.1111, R_{sigma} = 0.1225)
Data/restraints/parameters	49695/90/3745
Goodness-of-fit on F^2	0.987
Final R indexes ($I \geq 2\sigma(I)$)	R_1 = 0.0850, wR_2 = 0.2088
Final R indexes (all data)	R_1 = 0.1403, wR_2 = 0.2411
Largest diff. peak/hole/e Å^{-3}	1.75/-1.86

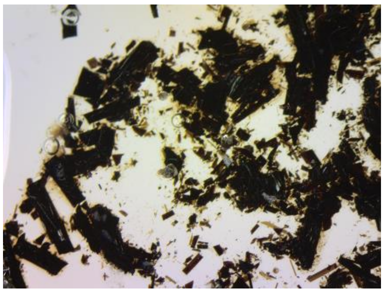

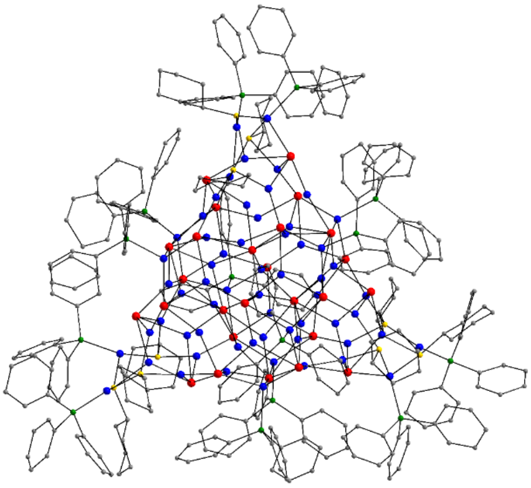

5.38 [$Cu_{51}Se_{26}(PPh_3)_{16}$] (37)

Compound	**37**
Empirical formula	$C_{288}H_{240}Cu_{51}P_{16}Se_{26}$
Formula mass	9489.81
Temperature/K	180
Crystal system	triclinic
Space group	$P\bar{1}$
a/Å	20.7053(5)
b/Å	22.4934(5)
c/Å	42.4419(8)
α/°	101.385(2)
β/°	93.023(2)
γ/°	115.160(2)
V/Å^3	17329.9(7)
Z	2
ρ_{calc}/g·cm^{-3}	1.819
μ/mm^{-1}	19.331
F(000)	9142.0
Crystal size/mm^3	0.12 × 0.11 × 0.1
Radiation	GaK_α (λ = 1.34143)
2Θ range for data collection/°	4.244 to 120.188
Index ranges	$-26 \leq h \leq 21$, $-15 \leq k \leq 29$, $-54 \leq l \leq 54$
Reflections collected	184124
Independent reflections	76196 (R_{int} = 0.0525, R_{sigma} = 0.0570)
Data/restraints/parameters	76196/12/3430
Goodness-of-fit on F^2	1.051
Final R indexes ($I \geq 2\sigma(I)$)	R_1 = 0.0864, wR_2 = 0.2316
Final R indexes (all data)	R_1 = 0.1271, wR_2 = 0.2668
Largest diff. peak/hole/e Å^{-3}	7.73/-3.46

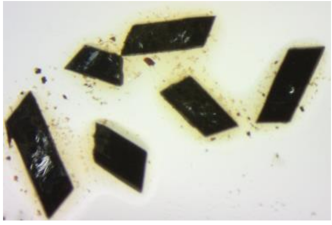

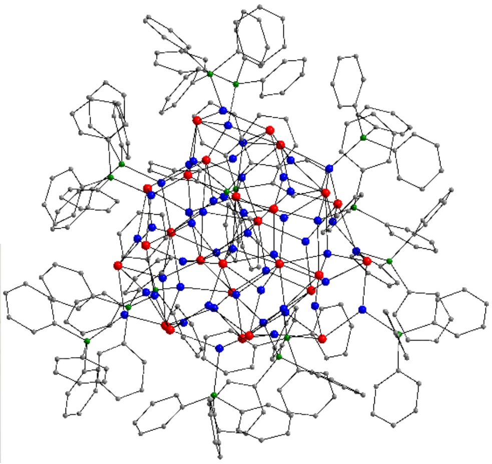

5.39 $[Cu_{73}Se_{37}(PPh_3)_{19}]\cdot(C_7H_{16})$ (**38**$\cdot(C_7H_{16})$)

Compound	**38**$\cdot(C_7H_{16})$
Empirical formula	$C_{349}H_{301}Cu_{73}P_{19}Se_{37}$
Formula mass	12643.25
Temperature/K	150
Crystal system	triclinic
Space group	$P\overline{1}$
a/Å	21.0781(7)
b/Å	28.6239(10)
c/Å	37.2347(19)
α/°	87.020(3)
β/°	85.993(3)
γ/°	69.926(3)
V/Å^3	21039.4(15)
Z	2
ρ_{calc}/g·cm^{-3}	1.996
μ/mm^{-1}	22.650
F(000)	12110.0
Crystal size/mm^3	0.12 × 0.1 × 0.02
Radiation	GaK_α (λ = 1.34143)
2Θ range for data collection/°	5.718 to 100.106
Index ranges	$-20 \le h \le 24$, $-17 \le k \le 32$, $-41 \le l \le 42$
Reflections collected	161747
Independent reflections	63699 (R_{int} = 0.0950, R_{sigma} = 0.1582)
Data/restraints/parameters	63699/12/3596
Goodness-of-fit on F^2	0.987
Final R indexes ($I \ge 2\sigma(I)$)	R_1 = 0.0844, wR_2 = 0.1921
Final R indexes (all data)	R_1 = 0.1873, wR_2 = 0.2392
Largest diff. peak/hole/e Å^{-3}	1.68/-1.66

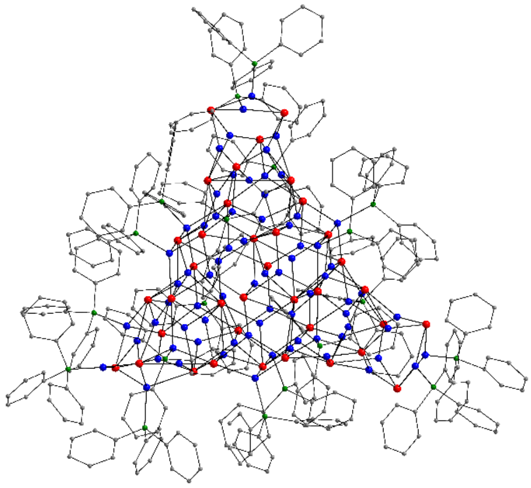

5.40 [$Cu_{94}Se_{43}(SCy)_9(PPh_3)_{18}$] (39)

Compound	**39**
Empirical formula	$C_{378}H_{369}Cu_{94}P_{18}S_9Se_{43}$
Formula mass	15125.75
Temperature/K	130
Crystal system	monoclinic
Space group	*P*2/*c*
a/Å	48.0606(11)
b/Å	28.2637(9)
c/Å	41.8364(11)
α/°	90
β/°	114.339(2)
γ/°	90
V/Å^3	51778(3)
Z	4
ρ_{calc}/g·cm^{-3}	1.940
μ/mm^{-1}	23.507
F(000)	28956.0
Crystal size/mm^3	0.2 × 0.14 × 0.07
Radiation	GaK_α (λ = 1.34143)
2Θ range for data collection/°	4.114 to 90
Index ranges	$-50 \le h \le 42$, $-28 \le k \le 29$, $-44 \le l \le 43$
Reflections collected	118524
Independent reflections	60421 (R_{int} = 0.0803, R_{sigma} = 0.1348)
Data/restraints/parameters	60421/423/2353
Goodness-of-fit on F^2	1.020
Final *R* indexes ($I \ge 2\sigma(I)$)	R_1 = 0.0922, wR_2 = 0.2362
Final *R* indexes (all data)	R_1 = 0.1590, wR_2 = 0.2600
Largest diff. peak/hole/e Å^{-3}	7.94/-2.52

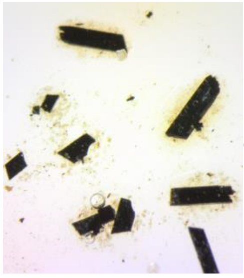

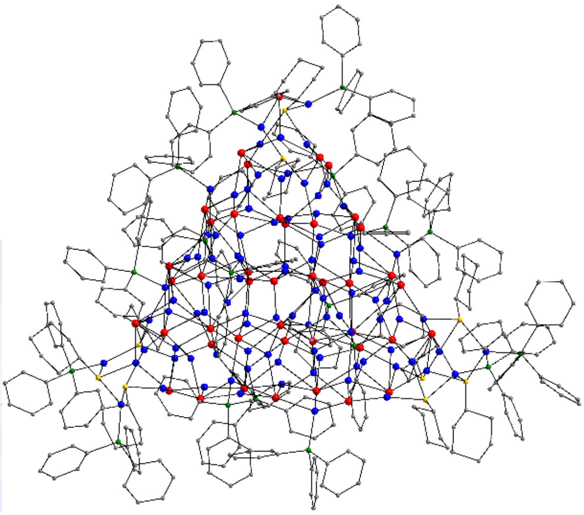

5.41 [$Ag_{15}S(SCy)_{12}(dppb)_3$]($BPh_4$) (40)

Compound	**40**
Empirical formula	$C_{180}H_{236}Ag_{15}BP_6S_{13}$
Formula mass	4631.13
Temperature/K	150
Crystal system	orthorhombic
Space group	$C222_1$
a/Å	21.9757(5)
b/Å	53.2574(12)
c/Å	17.5275(4)
α/°	90
β/°	90
γ/°	90
V/Å^3	20513.6(8)
Z	4
ρ_{calc}/g·cm^{-3}	1.500
μ/mm^{-1}	8.814
F(000)	9296.0
Crystal size/mm^3	0.12 × 0.1 × 0.08
Radiation	GaK_α (λ = 1.34143)
2Θ range for data collection/°	5.568 to 118.454
Index ranges	$-28 \leq h \leq 21$, $-68 \leq k \leq 53$, $-22 \leq l \leq 20$
Reflections collected	99555
Independent reflections	21905 (R_{int} = 0.0462, R_{sigma} = 0.0354)
Data/restraints/parameters	21905/341/715
Goodness-of-fit on F^2	1.022
Final R indexes ($I \geq 2\sigma(I)$)	R_1 = 0.0678, wR_2 = 0.1969
Final R indexes (all data)	R_1 = 0.0969, wR_2 = 0.2139
Largest diff. peak/hole/e Å^{-3}	1.01/-0.76
Flack parameter	0.132(19)

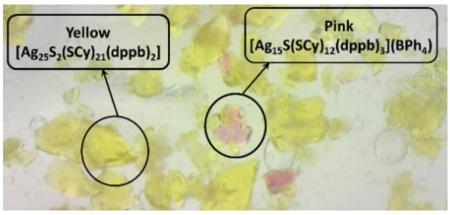

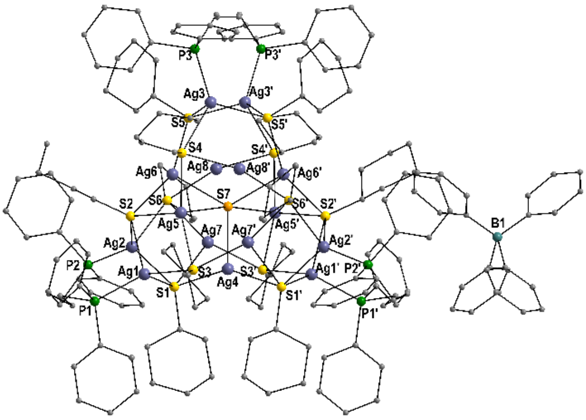

5.42 [$Ag_{25}S_2(SCy)_{21}(dppb)_2$] (41)

Compound	**41**
Empirical formula	$C_{182}H_{287}Ag_{25}P_4S_{23}$
Formula mass	6033.11
Temperature/K	180
Crystal system	monoclinic
Space group	*C*2/*c*
a/Å	65.6987(9)
b/Å	19.9436(4)
c/Å	36.0126(4)
α/°	90
β/°	96.5000(10)
γ/°	90
V/Å^3	46882.9(13)
Z	8
ρ_{calc}/g·cm^{-3}	1.709
μ/mm^{-1}	12.553
F(000)	23856.0
Crystal size/mm^3	0.2 × 0.17 × 0.15
Radiation	GaK_α (λ = 1.34143)
2Θ range for data collection/°	4.63 to 125
Index ranges	$-86 \leq h \leq 53$, $-26 \leq k \leq 25$, $-41 \leq l \leq 47$
Reflections collected	234449
Independent reflections	53921 (R_{int} = 0.1141, R_{sigma} = 0.0809)
Data/restraints/parameters	53921/2373/2071
Goodness-of-fit on F^2	0.929
Final *R* indexes ($I \geq 2\sigma(I)$)	R_1 = 0.0807, wR_2 = 0.2269
Final *R* indexes (all data)	R_1 = 0.1378, wR_2 = 0.2472
Largest diff. peak/hole/e Å^{-3}	3.24/-1.14

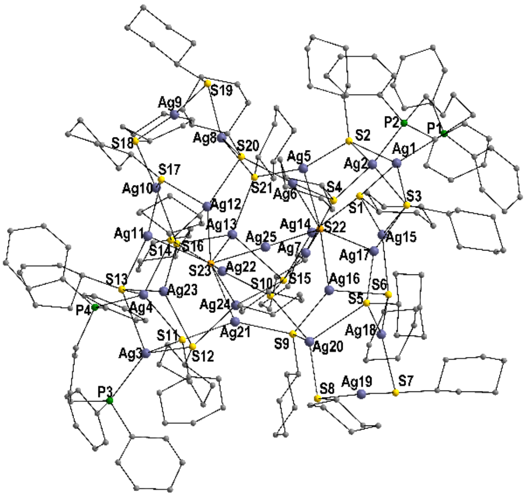

5.43 $[Ag_{15}Se(SCy)_{12}(dppb)_3](BPh_4)$ (42)

Compound	**42**
Empirical formula	$C_{180}H_{236}Ag_{15}BP_6S_{12}Se$
Formula mass	4678.03
Temperature/K	150.0
Crystal system	orthorhombic
Space group	$C222_1$
a/Å	21.9116(4)
b/Å	53.2425(9)
c/Å	17.5824(4)
α/°	90
β/°	90
γ/°	90
V/Å^3	20512.1(7)
Z	4
ρ_{calc}/g·cm^{-3}	1.515
μ/mm^{-1}	8.887
F(000)	9368.0
Crystal size/mm^3	0.15 × 0.14 × 0.13
Radiation	GaK_α (λ = 1.34143)
2Θ range for data collection/°	3.794 to 124.994
Index ranges	$-28 \leq h \leq 14$, $-67 \leq k \leq 70$, $-22 \leq l \leq 23$
Reflections collected	105830
Independent reflections	24656 (R_{int} = 0.0392, R_{sigma} = 0.0249)
Data/restraints/parameters	24656/226/863
Goodness-of-fit on F^2	1.082
Final R indexes ($I \geq 2\sigma(I)$)	R_1 = 0.0685, wR_2 = 0.1964
Final R indexes (all data)	R_1 = 0.0773, wR_2 = 0.2047
Largest diff. peak/hole/e Å^{-3}	1.53/-1.01
Flack parameter	0.099(16)

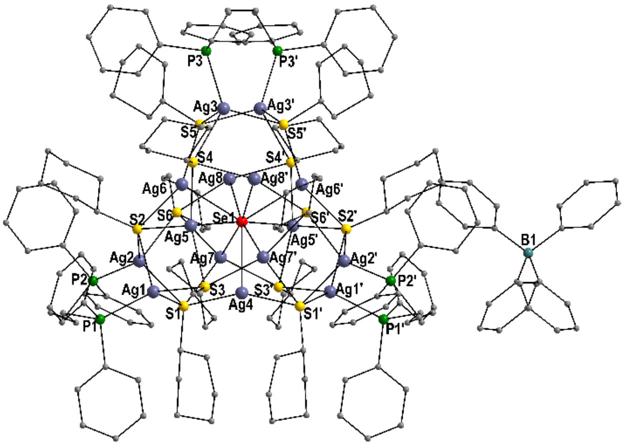

5.44 $[Ag_{27}Se_2(SCy)_{20}(dppb)_4](BPh_4)_3$ (43)

Compound	**43**
Empirical formula	$C_{304}H_{392}Ag_{27}B_3P_8S_{20}Se_2$
Formula mass	8037.95
Temperature/K	130
Crystal system	triclinic
Space group	$P\overline{1}$
a/Å	24.3666(4)
b/Å	24.5682(3)
c/Å	29.9613(5)
α/°	98.1930(10)
β/°	99.7310(10)
γ/°	104.0400(10)
V/Å^3	16831.1(5)
Z	2
ρ_{calc}/g·cm^{-3}	1.586
μ/mm^{-1}	9.615
F(000)	8016.0
Crystal size/mm^3	0.1 × 0.07 × 0.04
Radiation	GaK_α (λ = 1.34143)
2Θ range for data collection/°	3.79 to 125.19
Index ranges	$-32 \le h \le 29$, $-32 \le k \le 31$, $-39 \le l \le 34$
Reflections collected	195743
Independent reflections	77960 (R_{int} = 0.0621, R_{sigma} = 0.0769)
Data/restraints/parameters	77960/113/3085
Goodness-of-fit on F^2	0.964
Final R indexes ($I \ge 2\sigma(I)$)	R_1 = 0.0719, wR_2 = 0.1960
Final R indexes (all data)	R_1 = 0.1051, wR_2 = 0.2104
Largest diff. peak/hole/e Å^{-3}	4.03/-2.71

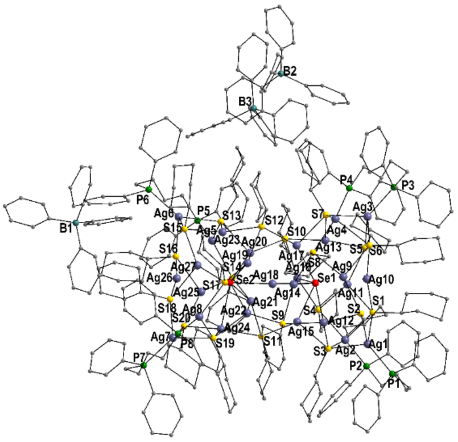

5.45 $[Ag_{86}S_{19}(SCy)_{48}]\cdot 2(C_7H_8)$ (**44**$\cdot 2(C_7H_8)$)

Compound	**44**	**44**$\cdot 2(C_7H_8)$
Empirical formula	$C_{288}H_{528}Ag_{86}S_{67}$	$C_{302}H_{544}Ag_{86}S_{67}$
Formula mass	15415.91	15600.18
Temperature/K	150.0	150.0
Crystal system	triclinic	triclinic
Space group	$P\overline{1}$	$P\overline{1}$
a/Å	24.0961(9)	24.1691(5)
b/Å	25.1345(11)	24.0782(5)
c/Å	41.2695(16)	24.2804(6)
α/°	74.679(3)	91.090(2)
β/°	75.427(3)	116.435(2)
γ/°	63.104(3)	118.953(2)
V/Å^3	21243.7(16)	10563.5(5)
Z	2	1
ρ_{calc}/g·cm^{-3}	2.410	2.452
μ/mm^{-1}	22.944	23.081
F(000)	14740.0	7470.0
Crystal size/mm^3	0.08 × 0.07 × 0.06	0.12 × 0.1 × 0.08
Radiation	GaK_α (λ = 1.34143)	GaK_α (λ = 1.34143)
2Θ range for data collection/°	3.91 to 104.998	3.824 to 115
Index ranges	$-28 \le h \le 28$, $-13 \le k \le 29$, $-48 \le l \le 48$	$-13 \le h \le 30$, $-30 \le k \le 29$, $-30 \le l \le 26$
Reflections collected	221645	126953
Independent reflections	71409 (R_{int} = 0.1020, R_{sigma} = 0.1398)	42947 (R_{int} = 0.0703, R_{sigma} = 0.0891)
Data/restraints/parameters	71409/492/2527	42947/484/1289
Goodness-of-fit on F^2	0.803	0.972
Final R indexes ($I \ge 2\sigma(I)$)	R_1 = 0.0643, wR_2 = 0.1509	R_1 = 0.0901, wR_2 = 0.2573
Final R indexes (all data)	R_1 = 0.1342, wR_2 = 0.1653	R_1 = 0.1561, wR_2 = 0.2879
Largest diff. peak/hole/e Å^{-3}	3.11/-2.27	4.56/-2.90

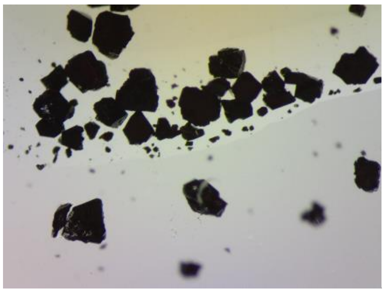

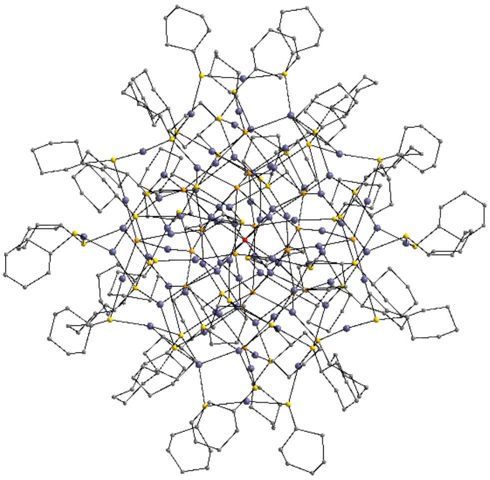

5.46 $[Ag_6(SCy)_4(dppm)_4](NO_3)_2 \cdot 5THF$ (45·5THF)

Compound	**45**·5THF
Empirical formula	$C_{144}H_{172}Ag_6N_2O_{11}P_8S_4$
Formula mass	3130.05
Temperature/K	180
Crystal system	monoclinic
Space group	$P2_1/c$
a/Å	24.5045(6)
b/Å	17.6923(3)
c/Å	32.8770(8)
α/°	90
β/°	98.410(2)
γ/°	90
V/Å^3	14100.3(5)
Z	4
ρ_{calc}/g·cm^{-3}	1.474
μ/mm^{-1}	5.607
F(000)	6416.0
Crystal size/mm^3	0.14 × 0.04 × 0.03
Radiation	GaK_α (λ = 1.34143)
2Θ range for data collection/°	4.946 to 125.278
Index ranges	$-32 \leq h \leq 25$, $-23 \leq k \leq 14$, $-43 \leq l \leq 34$
Reflections collected	87296
Independent reflections	32958 (R_{int} = 0.0294, R_{sigma} = 0.0368)
Data/restraints/parameters	32958/17/1468
Goodness-of-fit on F^2	0.970
Final R indexes ($I \geq 2\sigma(I)$)	R_1 = 0.0410, wR_2 = 0.1102
Final R indexes (all data)	R_1 = 0.0589, wR_2 = 0.1166
Largest diff. peak/hole/e Å^{-3}	1.04/-0.69

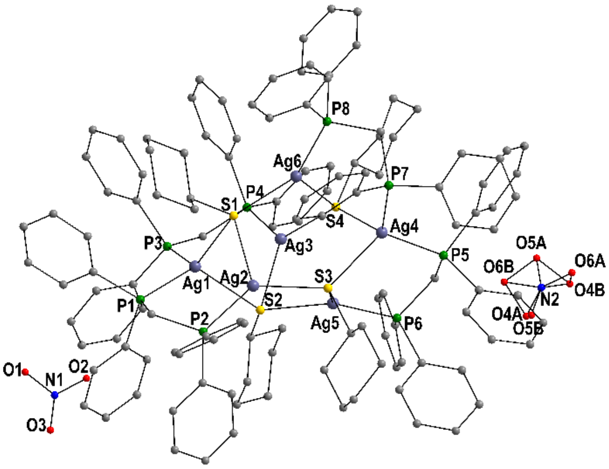

5.47 $[Ag_{25}Se_6S_2(SCy)_8(dppm)_6]$ (46)

Compound	**46**
Empirical formula	$C_{198}H_{220}Ag_{25}P_{12}S_{10}Se_6$
Formula mass	6462.48
Temperature/K	180
Crystal system	triclinic
Space group	$P\overline{1}$
a/Å	20.5415(4)
b/Å	21.7107(4)
c/Å	31.1981(6)
α/°	103.735(2)
β/°	92.362(2)
γ/°	105.351(2)
V/Å^3	12952.7(5)
Z	2
ρ_{calc}/g·cm^{-3}	1.657
μ/mm^{-1}	11.710
F(000)	6254.0
Crystal size/mm^3	0.14 × 0.03 × 0.02
Radiation	GaK_α (λ = 1.34143)
2Θ range for data collection/°	3.8 to 115.072
Index ranges	$-25 \le h \le 25$, $-27 \le k \le 27$, $-26 \le l \le 39$
Reflections collected	145622
Independent reflections	52120 (R_{int} = 0.0640, R_{sigma} = 0.0716)
Data/restraints/parameters	52120/77/984
Goodness-of-fit on F^2	0.928
Final R indexes ($I \ge 2\sigma(I)$)	R_1 = 0.0765, wR_2 = 0.2202
Final R indexes (all data)	R_1 = 0.1332, wR_2 = 0.2465
Largest diff. peak/hole/e Å^{-3}	2.38/-1.45

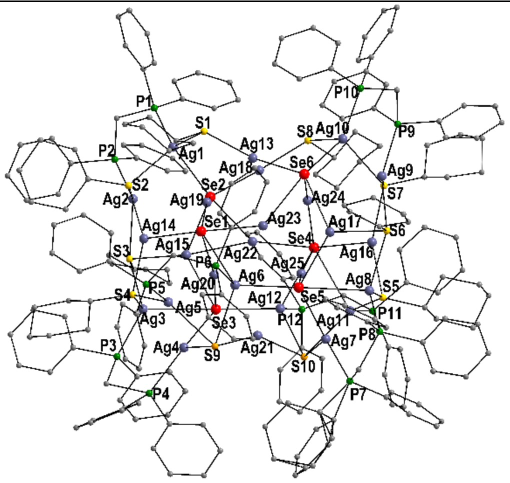

5.48 [$Ag_{12}Se_6(dppfc)_4$]·20THF (47·20THF)

Compound	**47**·20THF
Empirical formula	$C_{216}H_{272}Ag_{12}Fe_4O_{20}P_8Se_6$
Formula mass	5427.68
Temperature/K	150
Crystal system	tetragonal
Space group	$I4_1/a$
a/Å	34.8977(4)
b/Å	34.8977(4)
c/Å	17.7367(3)
α/°	90
β/°	90
γ/°	90
V/Å^3	21600.6(6)
Z	4
ρ_{calc}/g·cm^{-3}	1.669
μ/mm^{-1}	8.580
F(000)	10880.0
Crystal size/mm^3	0.14 × 0.12 × 0.11
Radiation	GaK_α (λ = 1.34143)
2Θ range for data collection/°	4.862 to 124.988
Index ranges	$-46 \leq h \leq 38$, $-31 \leq k \leq 46$, $-23 \leq l \leq 23$
Reflections collected	110847
Independent reflections	13036 (R_{int} = 0.0263, R_{sigma} = 0.0132)
Data/restraints/parameters	13036/2/475
Goodness-of-fit on F^2	1.039
Final R indexes ($I \geq 2\sigma(I)$)	R_1 = 0.0393, wR_2 = 0.1132
Final R indexes (all data)	R_1 = 0.0429, wR_2 = 0.1155
Largest diff. peak/hole/e Å^{-3}	1.51/-0.82

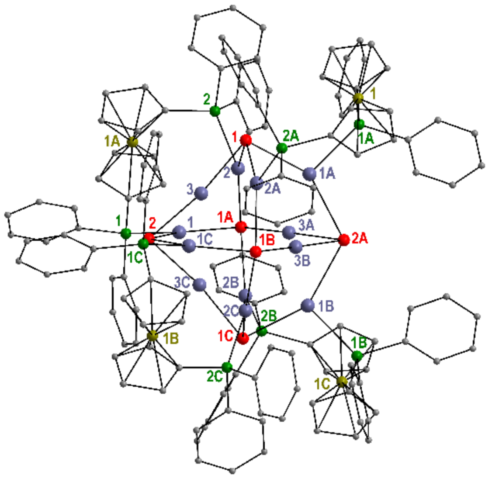

5.49 $[Ag_{97}S_{32}(SAd)_{33}(dppb)_3]$ (48)

Compound	**48**
Empirical formula	$C_{414}H_{579}Ag_{97}P_6S_{65}$
Formula mass	18288.85
Temperature/K	150.0
Crystal system	triclinic
Space group	$P\bar{1}$
a/Å	28.5603(7)
b/Å	29.4575(7)
c/Å	39.3667(12)
α/°	89.285(2)
β/°	80.944(2)
γ/°	83.674(2)
V/Å^3	32507.4(15)
Z	2
ρ_{calc}/g·cm^{-3}	1.868
μ/mm^{-1}	16.828
F(000)	17504.0
Crystal size/mm^3	0.14 × 0.12 × 0.03
Radiation	GaK_α (λ = 1.34143)
2Θ range for data collection/°	37.738 to 105.108
Index ranges	$-33 \leq h \leq 31$, $-33 \leq k \leq 34$, $-36 \leq l \leq 46$
Reflections collected	194021
Independent reflections	100195 (R_{int} = 0.0812, R_{sigma} = 0.1602)
Data/restraints/parameters	100195/76/3023
Goodness-of-fit on F^2	0.896
Final R indexes ($I \geq 2\sigma(I)$)	R_1 = 0.0893, wR_2 = 0.2268
Final R indexes (all data)	R_1 = 0.1592, wR_2 = 0.2586
Largest diff. peak/hole/e Å^{-3}	3.86/-3.73

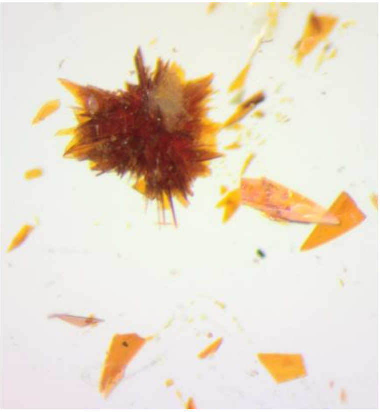

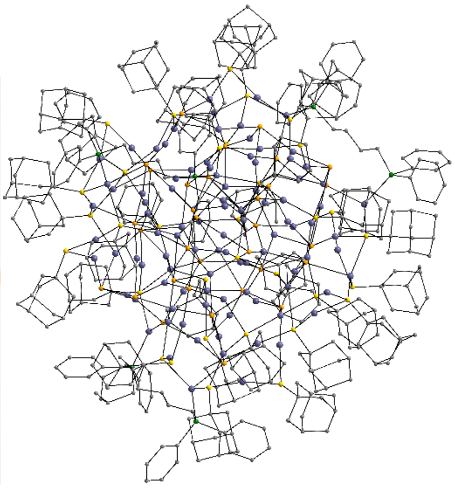

5.50 $[Ag_{42}Se_{13}(SAd)_{14}(dppm)_6](BPh_4)_2\cdot14THF$ (49·14THF)

Compound	**49**·14THF
Empirical formula	$C_{394}H_{494}Ag_{42}B_2O_{14}P_{12}S_{14}Se_{13}$
Formula mass	11852.98
Temperature/K	150.0
Crystal system	monoclinic
Space group	$P2_1/n$
a/Å	24.7503(4)
b/Å	31.2168(4)
c/Å	29.1781(6)
α/°	90
β/°	105.488(2)
γ/°	90
V/Å^3	21725.1(7)
Z	2
ρ_{calc}/g·cm^{-3}	1.812
μ/mm^{-1}	11.672
F(000)	11600.0
Crystal size/mm^3	0.12 × 0.1 × 0.08
Radiation	GaK_α (λ = 1.34143)
2Θ range for data collection/°	3.628 to 125.262
Index ranges	$-32 \leq h \leq 30$, $-37 \leq k \leq 41$, $-38 \leq l \leq 26$
Reflections collected	135350
Independent reflections	50449 (R_{int} = 0.0443, R_{sigma} = 0.0335)
Data/restraints/parameters	50449/1/2037
Goodness-of-fit on F^2	1.046
Final R indexes ($I \geq 2\sigma(I)$)	R_1 = 0.0448, wR_2 = 0.1193
Final R indexes (all data)	R_1 = 0.0516, wR_2 = 0.1224
Largest diff. peak/hole/e Å^{-3}	1.63/-2.37

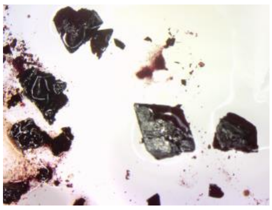

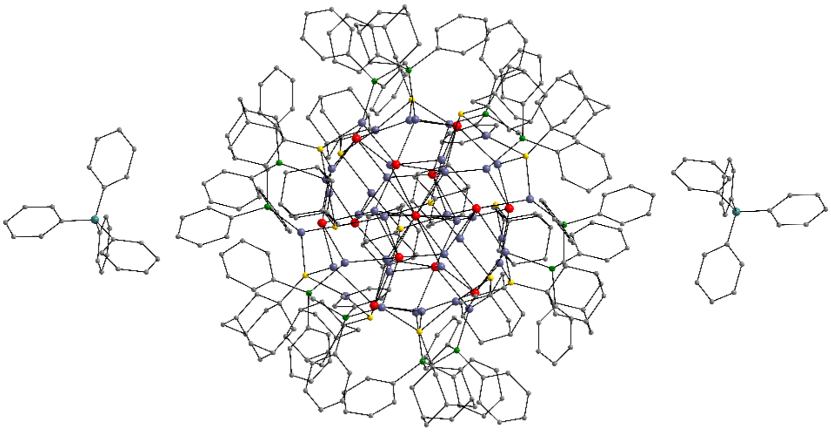

5.51 $[Ag_4(SAd)_4(dppe)]_n\cdot 2THF$ (50·2THF)

Compound	**50**·2THF
Empirical formula	$C_{74}H_{100}Ag_4O_2P_2S_4$
Formula mass	1643.19
Temperature/K	180.0
Crystal system	triclinic
Space group	$P\overline{1}$
a/Å	11.6074(7)
b/Å	14.8336(9)
c/Å	22.5202(17)
α/°	97.515(5)
β/°	104.202(5)
γ/°	103.756(5)
V/Å^3	3576.8(4)
Z	2
ρ_{calc}/g·cm^{-3}	1.526
μ/mm^{-1}	7.013
F(000)	1684.0
Crystal size/mm^3	0.16 × 0.03 × 0.02
Radiation	GaK_α (λ = 1.34143)
2Θ range for data collection/°	6.996 to 114.996
Index ranges	$-5 \le h \le 14$, $-18 \le k \le 18$, $-28 \le l \le 28$
Reflections collected	34808
Independent reflections	14397 (R_{int} = 0.0258, R_{sigma} = 0.0260)
Data/restraints/parameters	14397/2/725
Goodness-of-fit on F^2	1.038
Final R indexes ($I \ge 2\sigma(I)$)	R_1 = 0.0533, wR_2 = 0.1541
Final R indexes (all data)	R_1 = 0.0621, wR_2 = 0.1577
Largest diff. peak/hole/e Å^{-3}	1.33/-0.68

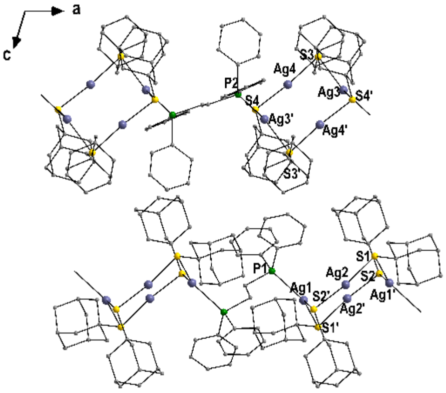

6 Miscellaneous structures

In this part 32 crystalline compounds are summarized that did not appear in the section of ‘results and discussion’. Some of them could not be reproduced others are mononuclear complexes. Herein, further characterizations such as IR and EA of these compounds have not been carried out. In this part synthesis, structures and crystallography data of these compounds are shown in the following table.

Table 6-1 *Basic information of miscellaneous structure*

Nr.	Reaction	Product	Comment
M1	0.5 mmol AgSCy + 0.5 mmol PPh_3 + 0.5 mmol $NaBF_4$ + 10 mL toluene + 20 mL *n*-hexane	$[Ag(PPh_3)_2][BF_4]$	
M2	0.6 mmol CuSPh + 0.3 mmol PPh_3 + 10 mL toluene + 15 mL *n*-heptane	$[Cu_4(SPh)_4(PPh_3)_4]\cdot 2(C_7H_8)$	Published *Inorg. Chem.* 1985, 24, 2547-2550
M3	0.6 mmol CuSCp + 1.2 mmol dppbz + 12 mL toluene + 20 mL *n*-heptane	$[Cu_2(SCp)_2(dppbz)_2]\cdot(C_7H_8)$	
M4	0.075 g Cu(SBz) + 0.035 g dppm + 50 *µ*L $S(SiMe_3)_2$ + 20 mL toluene	$((CH_3)_3SiSO_4)[Cu(dppmS)_2]\cdot(C_7H_8)$	
M5	0.3 g CuSCp + 0.15 g dppm + 150 *µ*L $S(SiMe_3)_2$ + 20 mL toluene	$((CH_3)_3SiSO_4)[Cu(dppmS)_2]\cdot 2(C_7H_8)$	
M6	0.3 mmol CuSBz + 0.15 mmol dppb + 5 mL toluene + 10 mL *n*-heptane	$[Cu_2(SBz)_2(dppb)_2]$	
M7	0.3 mmol CuSCp + 0.3 mmol PPh_3 + 5 mL toluene + 10 mL *n*-heptane	$[Cu_{14}S(SCp)_{12}(PPh_3)_4]$	Structurally the same with compound **12**
M8	0.3 mmol CuSAd + 0.6 mmol dppb + 5 mL toluene + 10 mL *n*-heptane	Molecule A $[Cu_4(SAd)_4(dppb)]_n\cdot(C_7H_8)$ Molecule B $[Cu_3(SAd)_3(dppb)](dppb)[Cu_3(SAd)_3(dppb)]\cdot(C_7H_8)$	

Miscellaneous structures

M9	0.3 mmol CuSAd + 0.3 mmol dppox + 5 mL toluene + 10 mL *n*-heptane	$[Cu_{12}S_6(dppox)_4]\cdot 3(C_7H_8)$	Structurally the same as compound **22** but one more solvent molecule in the lattice.
M10	0.3 mmol CuSAd + 0.6 mmol dppe + 5 mL toluene + 10 mL *n*-heptane	$[Cu_4(SAd)_4(dppe)]_n\cdot 2(C_7H_8)$	
M11	0.3 mmol CuSBz + 0.15 mmol dppb + 5 mL toluene + 10 mL *n*-heptane	$[Cu_2(SBz)_2(dppb)_2]$	
M12	0.3 mmol CuSBz + 0.6 mmol dppb + 5 mL toluene + 10 mL *n*-heptane	$[Cu_2(SBz)_2(dppb)_2]$	
M13	0.3 mmol CuSPh + 0.3 mmol PPh_3 + 5 mL toluene + 10 mL *n*-heptane	$[(PPh_3)_2Cu](SO_4)[(PPh_3)_2Cu]\cdot(C_7H_8)$	
M14	0.3 mmol CuSPh + 0.6 mmol PPh_3 + 5 mL toluene + 10 mL *n*-heptane	$[(PPh_3)_2Cu](SO_4)[(PPh_3)_2Cu]$	
M15	0.45 mmol CuSPh + 0.3 mmol PPh_3 + 0.15 mmol $K_6[P_2W_{18}O_{62}]\cdot 14H_2O$ + 2 mL DMF + 5 mL Et_2O + 2 mL ethanol	$[Cu_8(SPh)_8(PPh_3)_4]$	
M16	0.3 mmol CuSAd + 0.3 mmol dppp + 50 μL $S(SiMe_3)_2$ + 7.5 mL toluene	$[Cu_{24}S_8(SAd)_8(dppp)_4]$	
M17	0.3 mmol CuSCy + 0.9 mmol dppp + 36 μL $Se(SiMe_3)_2$ + 4 mL THF + 8 mL Et_2O	$[(dppp)_2CuSeSi(CH_3)_3]\cdot ½(C_6H_{12})$	
M18	0.3 mmol CuSCy + 0.05 mmol dppp + 36 μL $Se(SiMe_3)_2$ + 4 mL THF + 8 mL Et_2O	$[Cu_{42}Se_{17}(SCy)_8(dppp)_6]\cdot 2THF$	

Miscellaneous structures

M19	0.3 mmol CuSCp + 0.9 mmol dppe + 36 μL $Se(SiMe_3)_2$ + 4 mL toluene + 8 mL Et_2O	$[Cu_2(SCp)_2(dppe)_3]$	
M20	0.3 mmol CuSCp + 0.9 mmol dppfc + 36 μL $Se(SiMe_3)_2$ + 4 mL THF + 8 mL Et_2O	$[Cu_8Se_6(dppfc)_4(THF)_2]$	
M21	0.5 mmol CuSBz + 0.5 mmol dppb + 72 μL $Se(SiMe_3)_2$ + 4 mL THF + 8 mL Et_2O	$[Cu_2(SeBz)_2(dppb)_2]$	
M22	0.5 mmol AgSCy + 0.25 mmol dpph + 40 μL $S(SiMe_3)_2$ + 10 mL toluene + 20 mL *n*-pentane	$[Ag_{10}(SCy)_{10}(dpph)_2]\cdot 2(C_5H_{12})$	
M23	0.5 mmol AgSCy + 0.5 mmol dppb + 20 μL $S(SiMe_3)_2$ + 20 mL toluene	$[Ag_2(SCy)_2(dppb)_2]$	
M24	0.5 mmol AgSCy + 0.25 mmol dpph + 20 μL $S(SiMe_3)_2$ + 20 mL toluene	$[Ag_3(SCy)_2(dpph)_2](NO_3)$	
M25	0.5 mmol AgSCy + 0.25 mmol dppb + 16 μL $Se(SiMe_3)_2$ + 4 mL THF	$[Ag_{15}Se(SCy)_{12}(dppb)_3]$	Unknown anion
M26	1 mmol AgSAd + 0.5 mmol dppm + 32 μL $Se(SiMe_3)_2$ + 5 mL THF	$[Ag_{42}Se_{13}(SAd)_{14}(dppm)_6]\cdot 4THF$	Unknown anion
M27	0.5 mmol AgSCy + 0.25 mmol dppb+ 16 μL $Se(SiMe_3)_2$ + 4 mL THF + 1 mL ethanol + 8 mL Et_2O	$[Ag_2Se(SCy)(dppb)_2]\cdot(C_2H_5OH)$	Unknown cation
M28	0.5 mmol AgSCy + 0.25 mmol dppfc + 32 μL $Se(SiMe_3)_2$ + 4 mL THF	$[Ag_2(SH)_2(dppfc)_2]\cdot 3THF$	

M29	0.5 mmol AgSAd + 0.25 mmol dppfc + 16 μL $Se(SiMe_3)_2$ + 4 mL THF	$[Ag_2(SeH)_2(dppfc)_2]\cdot 2THF$	
M30	0.6 mmol CuSCp + 0.6 mmol dppox + 10 mL toluene + 20 mL *n*-heptane	$[Cu(SCp)(dppox)]\cdot(C_7H_8)$	
M31	0.5 mmol AgSCy + 0.5 mmol dppb + 10 μL $S(SiMe_3)_2$ + 20 mL toluene	$[Ag_2(SCy)_2(dppb)_2]$	
M32	0.3 mmol CuSCy + 0.05 mmol dppp + 72 μL $Se(SiMe_3)_2$ + 4 mL THF + 8 mL Et_2O	$[Cu_2(SeH)_2(dppp)_2]$	

6.1 $[Ag(PPh_3)_2](BF_4)$ (M1)

Compound	**M1**
Empirical formula	$C_{36}H_{30}AgBF_4P_2$
Formula mass	719.22
Temperature/K	150.15
Crystal system	monoclinic
Space group	*C*2/*c*
a/Å	24.7174(8)
b/Å	9.4527(2)
c/Å	14.8896(5)
α/°	90
β/°	115.877(2)
γ/°	90
V/Å^3	3130.08(17)
Z	4
ρ_{calc}/g·cm^{-3}	1.526
μ/mm^{-1}	4.413
F(000)	1456.0
Crystal size/mm^3	0.28 × 0.27 × 0.26
Radiation	GaK_α (λ = 1.34143)
2Θ range for data collection/°	6.916 to 117.978
Index ranges	$-31 \leq h \leq 23$, $-10 \leq k \leq 12$, $-19 \leq l \leq 16$
Reflections collected	8301
Independent reflections	3228 (R_{int} = 0.0117, R_{sigma} = 0.0089)
Indep. refl. with ($I \geq 2\sigma(I)$)	3154
Data/restraints/parameters	3228/0/260
Goodness-of-fit on F^2	1.058
Final R indexes ($I \geq 2\sigma(I)$)	R_1 = 0.0189, wR_2 = 0.0506
Final R indexes (all data)	R_1 = 0.0194, wR_2 = 0.0508
Largest diff. peak/hole/e Å^{-3}	0.26/-0.49

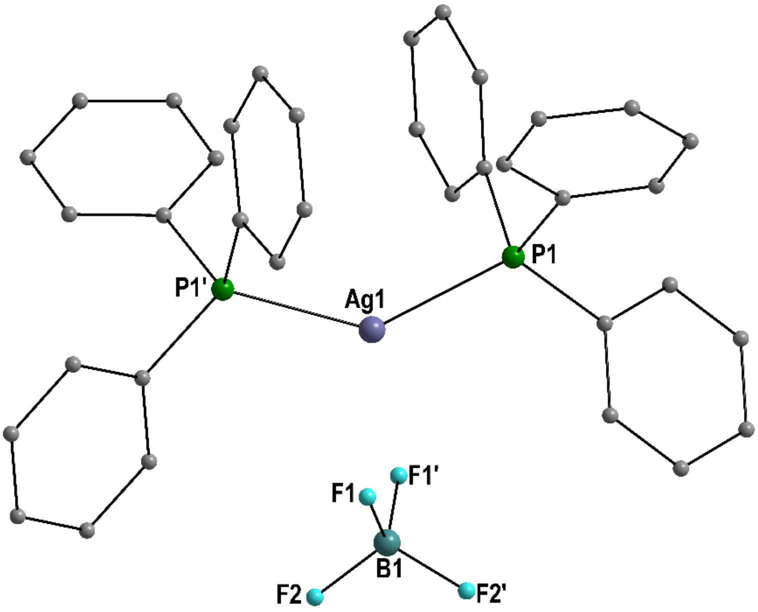

***Figure 6-1** Molecular structure of compound **M1** in the solid state (H atoms omitted).*

Compound **M1** is an ionic species with an $[Ag(PPh_3)_2]^+$ cation and a BF_4^- anion. For the cation, the silver ion coordinates with two phosphine ligands.

6.2 $[Cu_4(SPh)_4(PPh_3)_4]\cdot 2(C_7H_8)$ (M2·$2(C_7H_8)$)

Compound	**M2**·$2(C_7H_8)$
Empirical formula	$C_{55}H_{48}Cu_2P_2S_2$
Formula mass	962.07
Temperature/K	180
Crystal system	triclinic
Space group	$P\overline{1}$
a/Å	12.5532(5)
b/Å	13.1046(6)
c/Å	14.7483(6)
α/°	75.577(3)
β/°	84.690(3)
γ/°	84.766(4)
V/Å^3	2333.76(17)
Z	2
ρ_{calc}/g·cm^{-3}	1.369
μ/mm^{-1}	1.106
F(000)	996.0
Radiation	MoK_α (λ = 0.71073)
2Θ range for data collection/°	3.75 to 60
Index ranges	$-15 \leq h \leq 17$, $-18 \leq k \leq 18$, $-18 \leq l \leq 20$
Reflections collected	28286
Independent reflections	13312 (R_{int} = 0.0300, R_{sigma} = 0.0591)
Data/restraints/parameters	13312/0/551
Goodness-of-fit on F^2	0.972
Final R indexes ($I \geq 2\sigma(I)$)	R_1 = 0.0366, wR_2 = 0.0819
Final R indexes (all data)	R_1 = 0.0722, wR_2 = 0.0939
Largest diff. peak/hole/e Å^{-3}	0.56/-0.48

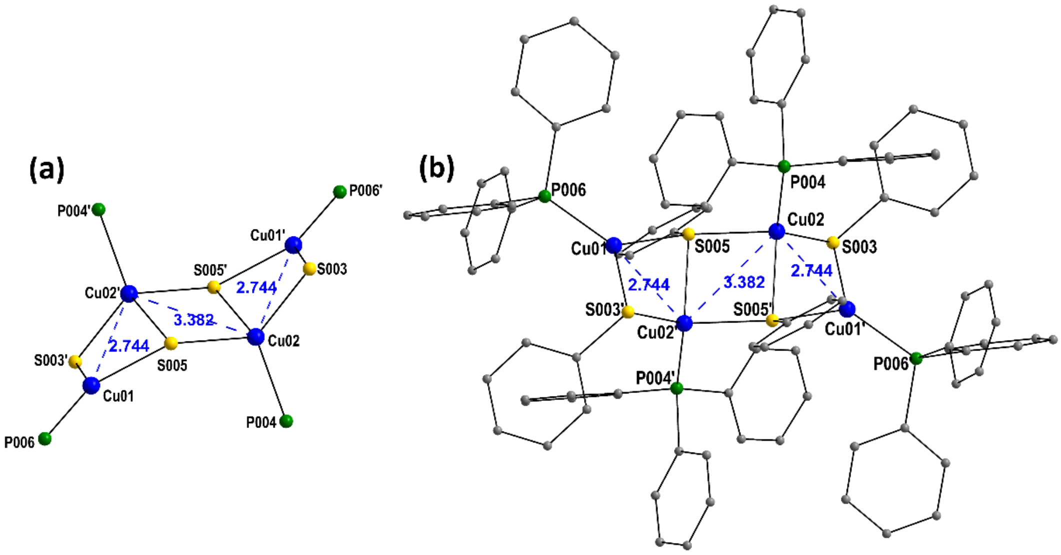

Figure 6-2 (a) *Structure of heavy atoms core of compound* ***M2*** *in the solid state;* ***(b)*** *molecular structure of compound* ***M2*** *in the solid state (H atoms omitted).*

Compound **M2** crystallizes in the triclinic space group $P\overline{1}$ with two molecules per unit cell. There is an inversion center locating on the middle point of Cu02…Cu02'. Core of this tetranuclear complex is a ladder-like Cu_4S_4 eight-membered ring. Copper atoms are triangularly or tetrahedrally coordinate with sulphur atoms and phosphine ligands.

6.3 [$Cu_2(SCp)_2(dppbz)_2$]·(C_7H_8) (M3·(C_7H_8))

Compound	**M3**·(C_7H_8)
Empirical formula	$C_{77}H_{74}Cu_2P_4S_2$
Formula mass	1314.44
Temperature/K	150.15
Crystal system	triclinic
Space group	$P\overline{1}$
a/Å	13.8326(4)
b/Å	13.8966(4)
c/Å	19.3678(5)
α/°	92.451(2)
β/°	108.739(2)
γ/°	90.579(2)
V/Å^3	3521.30(17)
Z	2
ρ_{calc}/g·cm^{-3}	1.240
μ/mm^{-1}	4.379
F(000)	1372.0
Crystal size/mm^3	0.26 × 0.05 × 0.04
Radiation	GaK_α (λ = 1.34143)
2Θ range for data collection/°	5.54 to 125
Index ranges	$-18 \le h \le 18$, $-18 \le k \le 7$, $-24 \le l \le 25$
Reflections collected	41900
Independent reflections	16350 (R_{int} = 0.0414, R_{sigma} = 0.0367)
Indep. refl. with ($I \ge 2\sigma(I)$)	13213
Data/restraints/parameters	16350/1/737
Goodness-of-fit on F^2	1.048
Final R indexes ($I \ge 2\sigma(I)$)	R_1 = 0.0990, wR_2 = 0.3100
Final R indexes (all data)	R_1 = 0.1137, wR_2 = 0.3198
Largest diff. peak/hole/e Å^{-3}	2.15/-0.97

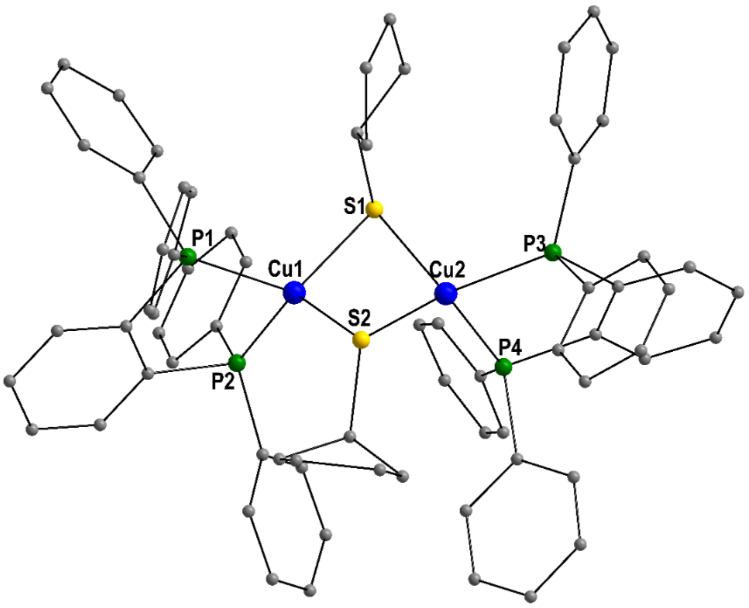

Figure 6-3 *Molecular structure of compound* ***M3*** *in the solid state (H atoms omitted).*

Compound **M3** crystallizes in the triclinic space group $P\overline{1}$ with two molecules per unit cell. **M3** consists of a butterfly-like Cu_2S_2 four-membered ring. The two thiolates present *trans*-orientation. The copper atoms are tetrahedrally coordinated by two sulphur atoms and two phosphorus ligands.

6.4 $((CH_3)_3SiSO_4)[Cu(dppmS)_2]\cdot(C_7H_8)$ (M4·(C_7H_8))

Compound	**M4**·(C_7H_8)
Empirical formula	$C_{60}H_{61}CuO_4P_4S_3Si$
Formula mass	1157.77
Temperature/K	180
Crystal system	triclinic
Space group	$P\overline{1}$
a/Å	11.4833(7)
b/Å	14.2884(10)
c/Å	19.2919(9)
α/°	82.516(5)
β/°	76.334(5)
γ/°	68.308(5)
V/Å^3	2854.7(3)
Z	2
ρ_{calc}/g·cm^{-3}	1.347
μ/mm^{-1}	3.788
F(000)	1208.0
Crystal size/mm^3	0.2 × 0.18 × 0.15
Radiation	GaK_α (λ = 1.34143)
2Θ range for data collection/°	4.106 to 125.31
Index ranges	$-15 \leq h \leq 14$, $-18 \leq k \leq 10$, $-24 \leq l \leq 25$
Reflections collected	33852
Independent reflections	13523 (R_{int} = 0.0220, R_{sigma} = 0.0226)
Indep. refl. with ($I \geq 2\sigma(I)$)	11341
Data/restraints/parameters	13523/0/662
Goodness-of-fit on F^2	1.044
Final R indexes ($I \geq 2\sigma(I)$)	R_1 = 0.0485, wR_2 = 0.1263
Final R indexes (all data)	R_1 = 0.0586, wR_2 = 0.1328
Largest diff. peak/hole/e Å^{-3}	0.51/-0.75

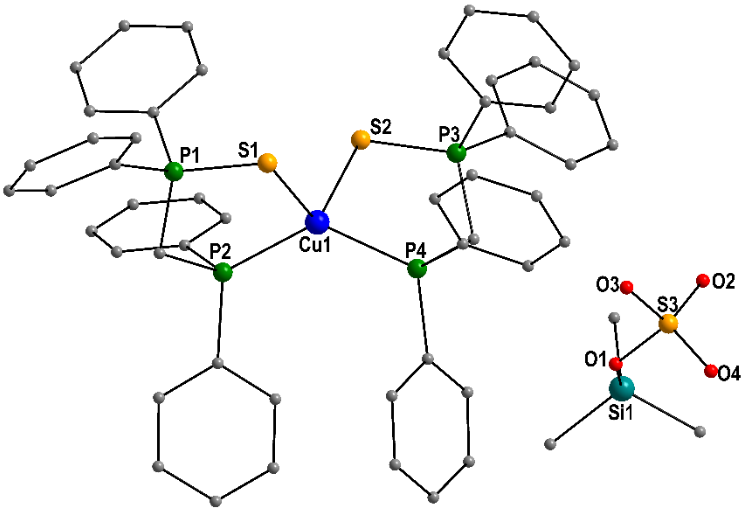

***Figure 6-4** Molecular structure of compound **M4** in the solid state (H atoms omitted).*

Compound **M4** is a mononuclear complex where Cu1 coordinate with two dppmS ligands *via* sulphur and phosphorus.

6.5 $((CH_3)_3SiSO_4)[Cu(dppmS)_2]\cdot 2(C_7H_8)$ (M5·$2(C_7H_8)$)

Compound	**M5**·$2(C_7H_8)$
Empirical formula	$C_{67}H_{69}CuO_4P_4S_3Si$
Formula mass	1249.91
Temperature/K	150
Crystal system	monoclinic
Space group	*Cc*
a/Å	23.3438(11)
b/Å	13.5431(6)
c/Å	19.9200(8)
α/°	90
β/°	92.308(4)
γ/°	90
V/Å^3	6292.5(5)
Z	4
ρ_{calc}/g·cm^{-3}	1.319
μ/mm^{-1}	3.462
F(000)	2616.0
Crystal size/mm^3	0.23 × 0.04 × 0.03
Radiation	GaK_α (λ = 1.34143)
2Θ range for data collection/°	6.566 to 125.038
Index ranges	$-30 \leq h \leq 30$, $-17 \leq k \leq 17$, $-25 \leq l \leq 9$
Reflections collected	38180
Independent reflections	9330 (R_{int} = 0.0561, R_{sigma} = 0.0546)
Indep. refl. with ($I \geq 2\sigma(I)$)	6635
Data/restraints/parameters	9330/3/707
Goodness-of-fit on F^2	0.965
Final R indexes ($I \geq 2\sigma(I)$)	R_1 = 0.0544, wR_2 = 0.1320
Final R indexes (all data)	R_1 = 0.0814, wR_2 = 0.1456
Largest diff. peak/hole/e Å^{-3}	0.46/-0.65
Flack parameter	-0.013(5)

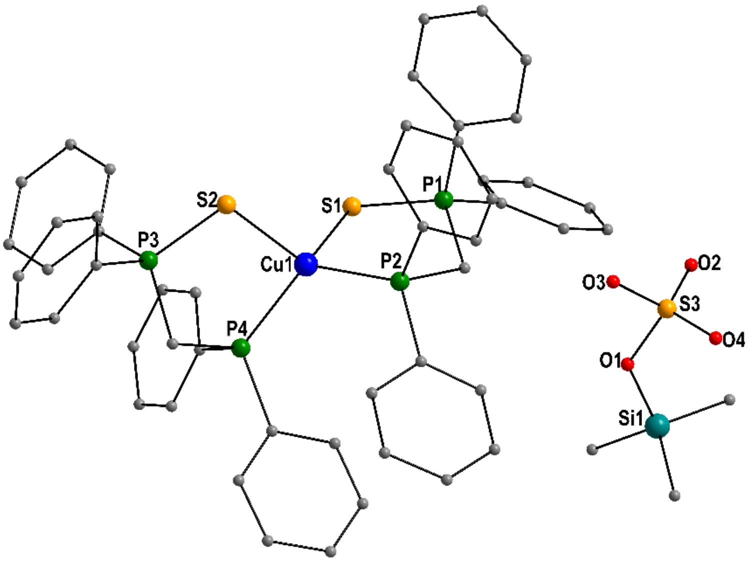

Figure 6-5 *Molecular structure of compound **M5** in the solid state (H atoms omitted).*

Compound **M5** is analogous with **M4**.

6.6 $[Cu_2(SBz)_2(dppb)_2]$ (M6, M11 and M12)

Compound	**M6**	**M11**	**M12**
Empirical formula	$C_{70}H_{70}Cu_2P_4S_2$	$C_{70}H_{70}Cu_2P_4S_2$	$C_{70}H_{70}Cu_2P_4S_2$
Formula mass	1226.34	1226.34	1226.34
Temperature/K	150	150	180
Crystal system	triclinic	triclinic	monoclinic
Space group	$P\overline{1}$	$P\overline{1}$	$P2_1/c$
a/Å	9.7010(8)	9.7125(5)	9.8826(3)
b/Å	11.4163(10)	11.4313(9)	22.1769(4)
c/Å	15.0297(10)	15.0425(8)	13.7393(3)
α/°	109.169(6)	109.298(5)	90
β/°	99.810(6)	99.779(4)	90.322(2)
γ/°	104.403(7)	104.372(5)	90
V/Å^3	1463.9(2)	1467.86(17)	3011.13(13)
Z	1	1	2
ρ_{calc}/g·cm^{-3}	1.391	1.387	1.353
μ/mm^{-1}	5.239	5.225	5.094
F(000)	640.0	640.0	1280.0
Crystal size/mm^3	0.2 × 0.19 × 0.18	0.23 × 0.21 × 0.16	0.21 × 0.17 × 0.16
Radiation	GaK_α (λ = 1.34143)	GaK_α (λ = 1.34143)	GaK_α (λ = 1.34143)
2Θ range for data collection/°	5.634 to 125.204	5.634 to 120.088	6.584 to 125
Index ranges	$-5 \leq h \leq 12$ $-15 \leq k \leq 15$ $-19 \leq l \leq 19$	$-5 \leq h \leq 12$ $-14 \leq k \leq 14$ $-19 \leq l \leq 19$	$-13 \leq h \leq 8$ $-29 \leq k \leq 29$ $-18 \leq l \leq 16$
Reflections collected	18816	17169	35037
Independent reflections	6956 (R_{int} = 0.0335, R_{sigma} = 0.0449)	6526 (R_{int} = 0.0434, R_{sigma} = 0.0510)	7249 (R_{int} = 0.0519, R_{sigma} = 0.0367)
Indep. refl. with ($I \geq 2\sigma(I)$)	4939	4840	5200
Data/restraints/parameters	6956/0/352	6526/0/352	7249/0/352
Goodness-of-fit on F^2	1.050	1.061	1.154
Final R indexes ($I \geq 2\sigma(I)$)	R_1 = 0.0519 wR_2 = 0.1429	R_1 = 0.0647 wR_2 = 0.1666	R_1 = 0.0813 wR_2 = 0.1702
Final R indexes (all data)	R_1 = 0.0779 wR_2 = 0.1551	R_1 = 0.0912 wR_2 = 0.1793	R_1 = 0.1073 wR_2 = 0.1786
Largest diff. peak/hole/e Å^{-3}	0.75/-0.46	0.80/-0.42	0.35/-0.48

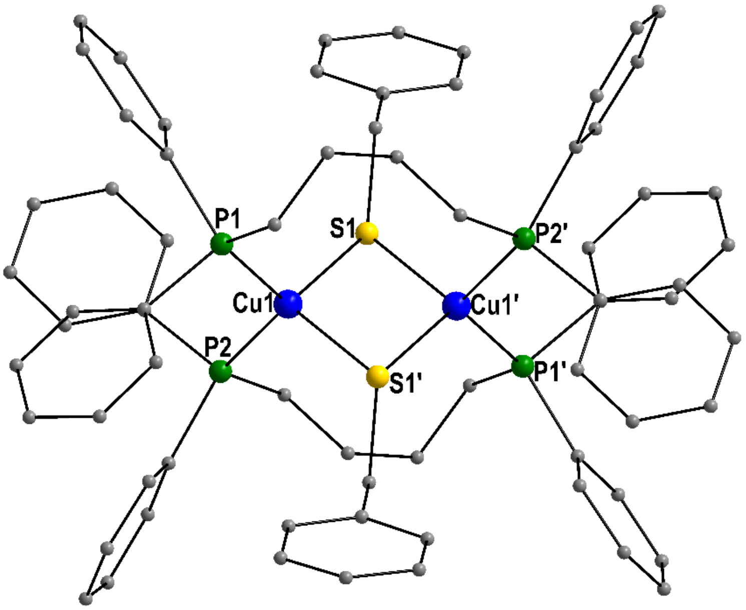

***Figure 6-6** Molecular structure of compound **M6, M11** and **M12** in the solid state (H atoms omitted).*

Compound **M6**, **M11** and **M12** share the same structure. There is an inversion center located on the central Cu_2S_2 plane. Copper atoms coordinate with two phosphorus atoms and two sulphur atoms.

6.7 $[Cu_{14}S(SCp)_{12}(PPh_3)_4]$ (M7)

Compound	**M7**
Empirical formula	$C_{132}H_{168}Cu_{14}P_4S_{13}$
Formula mass	3184.87
Temperature/K	180
Crystal system	trigonal
Space group	$R\overline{3}$
a/Å	17.8484(11)
b/Å	17.8484(11)
c/Å	88.324(6)
α/°	90
β/°	90
γ/°	120
V/Å^3	24367(3)
Z	6
ρ_{calc}/g·cm^{-3}	1.302
μ/mm^{-1}	11.134
F(000)	9804.0
Crystal size/mm^3	0.18 × 0.16 × 0.04
Radiation	GaK_α (λ = 1.34143)
2Θ range for data collection/°	5.05 to 127.346
Index ranges	$-23 \leq h \leq 14$, $-11 \leq k \leq 23$, $-114 \leq l \leq 114$
Reflections collected	54405
Independent reflections	13020 (R_{int} = 0.1854, R_{sigma} = 0.1054)
Indep. refl. with ($I \geq 2\sigma(I)$)	8568
Data/restraints/parameters	13020/13/486
Goodness-of-fit on F^2	1.349
Final R indexes ($I \geq 2\sigma(I)$)	R_1 = 0.1180, wR_2 = 0.2980
Final R indexes (all data)	R_1 = 0.1479, wR_2 = 0.3212
Largest diff. peak/hole/e Å^{-3}	1.60/-1.25

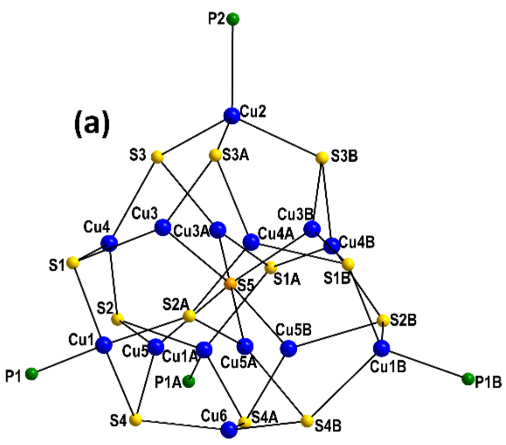

Figure 6-7 (a) *Structure of the heavy atoms core of compound* ***M7*** *in the solid state;* ***(b)*** *the central* Cu_6 *octahedron in* ***M7*** *highlighted in blue in the solid state.*

Compound **M7** is analogous to compound **12**.

6.8 $[Cu_4(SAd)_4(dppb)]_n·(C_7H_8)$ (**M8A**$·(C_7H_8)$) and $[Cu_3(SAd)_3(dppb)](dppb)[Cu_3(SAd)_3(dppb)]·(C_7H_8)$ (**M8B**$·C_7H_8$)

Compound	**M8A**$·(C_7H_8)$	**M8B**$·(C_7H_8)$
Empirical formula	$C_{41}H_{52}Cu_2PS_2$	$C_{151}H_{182}Cu_6P_6S_6$
Formula mass	2766.99	2756.38
Temperature/K	150	150
Crystal system	triclinic	triclinic
Space group	$P\overline{1}$	$P\overline{1}$
a/Å	10.1373(7)	14.8968(4)
b/Å	13.1428(12)	15.5210(3)
c/Å	16.1237(14)	15.7471(3)
α/°	70.649(6)	88.904(2)
β/°	74.157(6)	69.911(2)
γ/°	67.254(6)	81.606(2)
V/Å^3	1843.1(3)	3380.91(14)
Z	2	1
ρ_{calc}/g·cm^{-3}	1.382	1.354
μ/mm^{-1}	7.318	6.257
F(000)	806.0	1448.0
Crystal size/mm^3	0.28 × 0.04 × 0.03	0.24 × 0.05 × 0.04
Radiation	GaK_α (λ = 1.34143)	GaK_α (λ = 1.34143)
2Θ range for data collection/°	5.126 to 119.984	5.558 to 125.13
Index ranges	$-13 \leq h \leq 13$ $-16 \leq k \leq 10$ $-20 \leq l \leq 20$	$-19 \leq h \leq 9$ $-20 \leq k \leq 20$ $-20 \leq l \leq 18$
Reflections collected	17821	45093
Independent reflections	7817 (R_{int} = 0.0488, R_{sigma} = 0.0424)	16113 (R_{int} = 0.0252, R_{sigma} = 0.0286)
Indep. refl. with ($I \geq 2\sigma(I)$)	6347	12769
Data/restraints/parameters	7817/0/410	16113/0/747
Goodness-of-fit on F^2	1.270	1.041
Final R indexes ($I \geq 2\sigma(I)$)	R_1 = 0.1051, wR_2 = 0.2600	R_1 = 0.0431, wR_2 = 0.1079
Final R indexes (all data)	R_1 = 0.1194, wR_2 = 0.2752	R_1 = 0.0601, wR_2 = 0.1155
Largest diff. peak/hole/e Å^{-3}	3.76/-0.95	0.80/-0.56

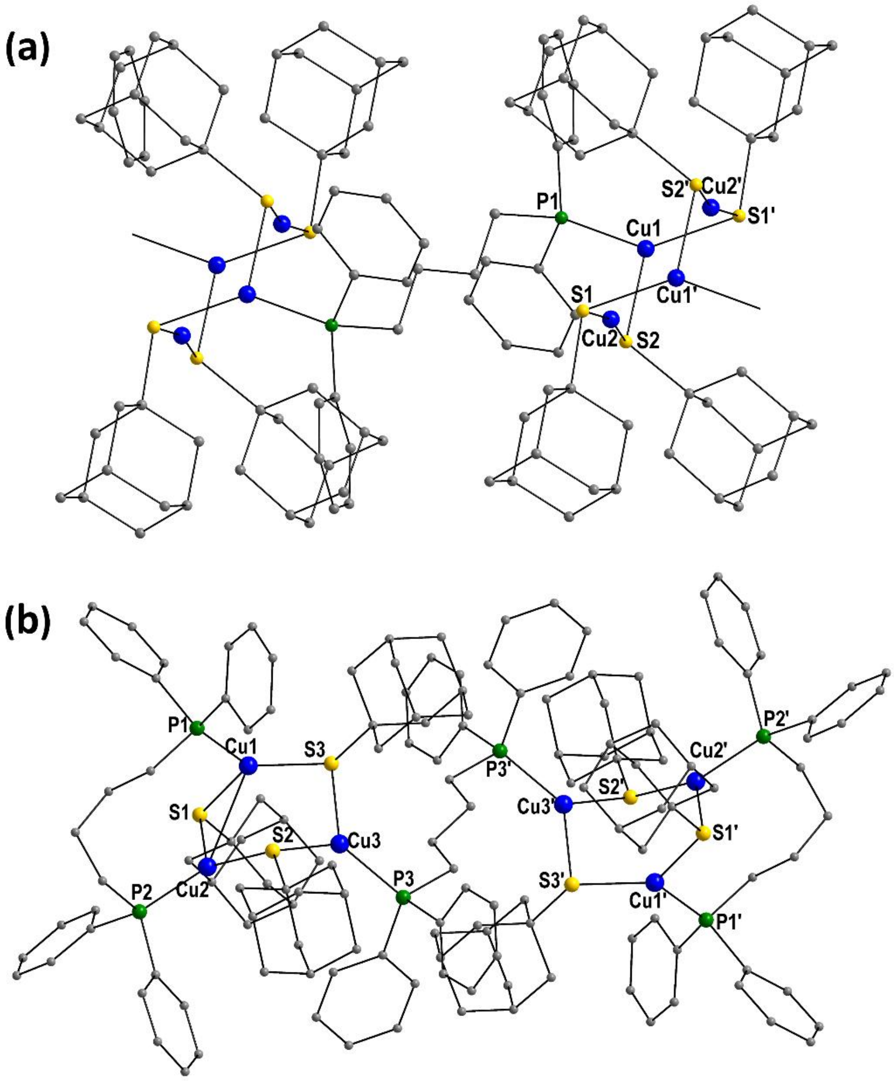

Figure 6-8 *Top: Molecular structure of the chain-like polymeric compound* ***M8A*** *in the solid state (H atoms omitted); bottom: Molecular structure of dimeric compound* ***M8B*** *in the solid state (H atoms omitted).*

There are two kinds of compounds in reaction **M8**, that is [Cu$_4$(SAd)$_4$(dppb)]$_n$ (**M8A**) and [Cu$_3$(SAd)$_3$(dppb)](dppb)[Cu$_3$(SAd)$_3$(dppb)] (**M8B**). Molecule **A** is a polymeric 1D chain. The core of these nodes is a Cu$_4$S$_4$ eight-membered ring, linked by dppb ligands; molecule **B** is a dimer. Each monomer consists of three copper atoms, three SAd$^-$ groups and one dppb ligand. The two units are connected by one dppb ligand.

6.9 $[Cu_{12}S_6(dppox)_4]\cdot 3(C_7H_8)$ (M9·$3(C_7H_8)$)

Compound	**M9**·$3(C_7H_8)$
Empirical formula	$C_{149}H_{136}P_8S_6Cu_{12}$
Formula mass	3129.17
Temperature/K	150.0
Crystal system	triclinic
Space group	$P\overline{1}$
a/Å	14.8217(5)
b/Å	15.6174(8)
c/Å	16.9613(11)
α/°	117.311(3)
β/°	104.554(5)
γ/°	92.082(4)
V/Å^3	3323.7(3)
Z	1
ρ_{calc}/g·cm^{-3}	1.563
μ/mm^{-1}	11.569
F(000)	1594.0
Crystal size/mm^3	0.22 × 0.2 × 0.18
Radiation	GaK_α (λ = 1.34143)
2Θ range for data collection/°	5.444 to 125.176
Index ranges	$-19 \le h \le 18$, $-20 \le k \le 18$, $-22 \le l \le 21$
Reflections collected	44592
Independent reflections	15822 (R_{int} = 0.0288, R_{sigma} = 0.0305)
Indep. refl. with ($I \ge 2\sigma(I)$)	11985
Data/restraints/parameters	15822/0/740
Goodness-of-fit on F^2	1.018
Final R indexes ($I \ge 2\sigma(I)$)	R_1 = 0.0434, wR_2 = 0.1032
Final R indexes (all data)	R_1 = 0.0640, wR_2 = 0.1139
Largest diff. peak/hole/e Å^{-3}	0.78/-0.44

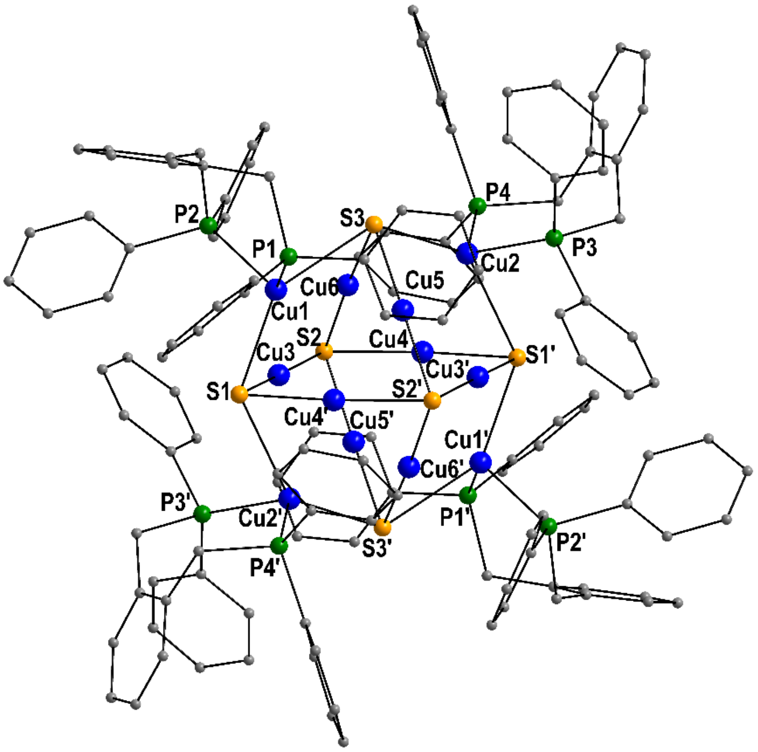

Figure 6-9 *Molecular structure of compound* ***M9*** *in the solid state (H atoms omitted).*

Compound **M9** is analogous with compound **22**.

6.10 $[Cu_4(SAd)_4(dppe)]_n\cdot 2(C_7H_8)$ (M10·2(C_7H_8))

Compound	**M10**·2(C_7H_8)
Empirical formula	$C_{80}H_{98}Cu_4P_2S_4$
Formula mass	1503.92
Temperature/K	150
Crystal system	monoclinic
Space group	*C*2/*c*
a/Å	25.6368(10)
b/Å	11.4547(2)
c/Å	26.3435(8)
α/°	90
β/°	111.292(3)
γ/°	90
V/Å^3	7208.0(4)
Z	4
ρ_{calc}/g·cm^{-3}	1.386
μ/mm^{-1}	7.478
F(000)	3152.0
Crystal size/mm^3	0.1 × 0.07 × 0.04
Radiation	GaK_α (λ = 1.34143)
2Θ range for data collection/°	6.438 to 125.124
Index ranges	$-30 \le h \le 33$, $-8 \le k \le 15$, $-34 \le l \le 33$
Reflections collected	37625
Independent reflections	8692 (R_{int} = 0.0281, R_{sigma} = 0.0214)
Data/restraints/parameters	8692/0/407
Goodness-of-fit on F^2	1.036
Final *R* indexes ($I \ge 2\sigma(I)$)	R_1 = 0.0515, wR_2 = 0.1344
Final *R* indexes (all data)	R_1 = 0.0630, wR_2 = 0.1441
Largest diff. peak/hole/e Å^{-3}	1.72/-0.67

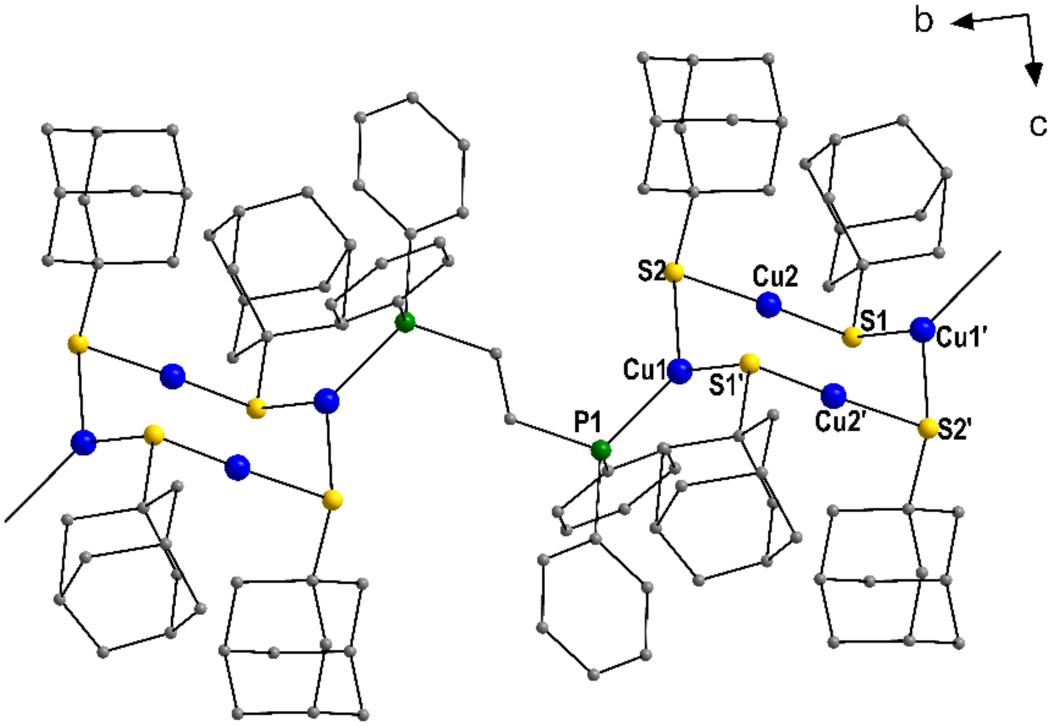

Figure 6-10 *Molecular structure of compound* ***M12*** *in the solid state (H atoms omitted).*

Compound **M12** is a polymeric 1D chain growing alongside *b* axis. The node is a chair-like Cu_4S_4 eight-membered ring. In this ring there is an inversion center locating on the middle point of the connection of Cu1···Cu1'. The $Cu_4(SAd)_4$ units are bridged by dppe ligands.

6.11 $[(PPh_3)_2Cu](SO_4)[Cu(PPh_3)_2]\cdot(C_7H_8)$ (**M13**$\cdot$(C_7H_8)) and $[(PPh_3)_2Cu](SO_4)[Cu(PPh_3)_2]$ (M14)

Compound	**M13**·(C_7H_8)	**M14**
Empirical formula	$C_{79}H_{68}Cu_2O_4P_4S$	$C_{72}H_{60}Cu_2O_4P_4S$
Formula mass	1364.35	1272.22
Temperature/K	150	150
Crystal system	triclinic	triclinic
Space group	$P\overline{1}$	$P\overline{1}$
a/Å	16.6900(5)	21.8188(9)
b/Å	18.4338(5)	22.1128(7)
c/Å	24.1681(9)	25.5140(10)
α/°	94.341(3)	94.151(3)
β/°	107.619(3)	90.824(3)
γ/°	109.039(2)	103.558(3)
V/Å^3	6572.3(4)	11929.2(8)
Z	4	8
ρ_{calc}/g·cm^{-3}	1.379	1.417
μ/mm^{-1}	4.549	4.985
F(000)	2832.0	5264.0
Crystal size/mm^3	0.23 × 0.22 × 0.2	0.18 × 0.16 × 0.03
Radiation	GaK_α (λ = 1.34143)	GaK_α (λ = 1.34143)
2Θ range for data collection/°	4.496 to 120.092	3.626 to 117.998
Index ranges	$-21 \le h \le 15$ $-23 \le k \le 23$ $-30 \le l \le 31$	$-27 \le h \le 9$ $-26 \le k \le 28$ $-32 \le l \le 32$
Reflections collected	76615	139742
Independent reflections	29048 (R_{int} = 0.0548, R_{sigma} =	51049 (R_{int} = 0.0528, R_{sigma} =
Data/restraints/parameters	29048/3/1552	51049/0/2989
Goodness-of-fit on F^2	1.021	1.040
Final R indexes ($I \ge 2\sigma(I)$)	R_1 = 0.0585, wR_2 = 0.1415	R_1 = 0.0590, wR_2 = 0.1536
Final R indexes (all data)	R_1 = 0.1050, wR_2 = 0.1629	R_1 = 0.1291, wR_2 = 0.1690
Largest diff. peak/hole/e Å^{-3}	1.62/-0.60	0.91/-0.40

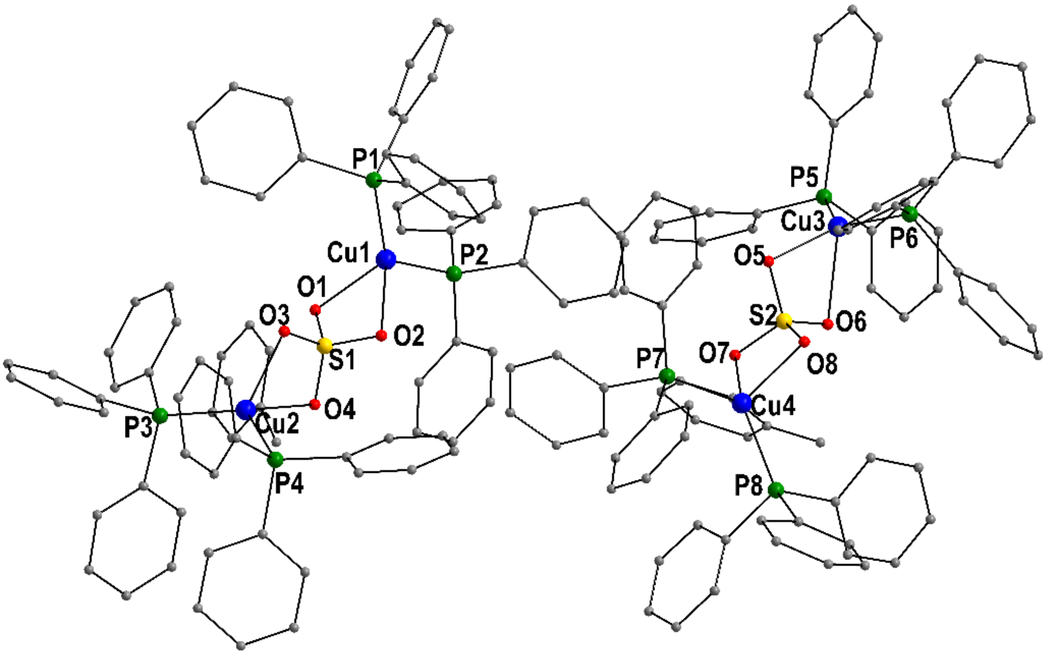

Figure 6-11 *Molecular structure of the two crystallographically independent molecules in compound* ***M13*** *in the solid state (H atoms omitted).*

Molecules in compound **M13** can be viewed as two mononuclear $[Cu(PPh_3)_2]^+$ cations bridged by the SO_4^{2-} anion.

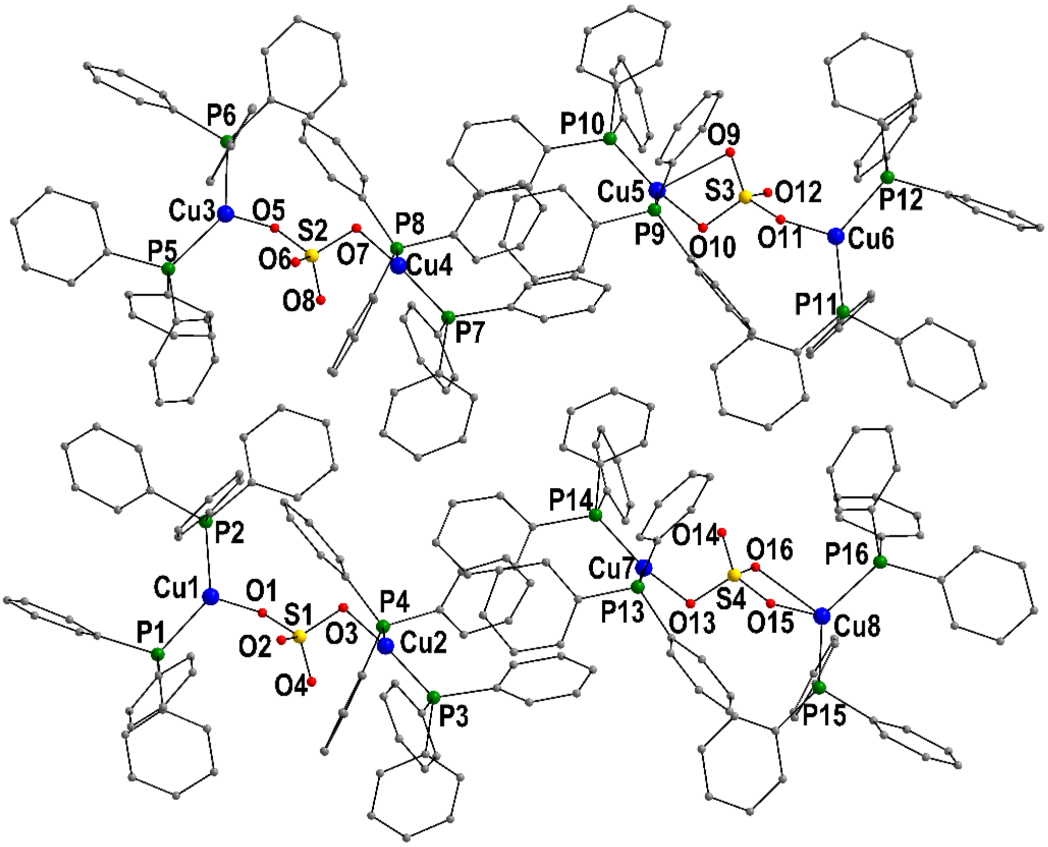

Figure 6-12 *Molecular structures of the four crystallographically independent molecules in the asymmetric unit of compound* ***M14*** *in the solid state (H atoms omitted).*

Compound **M14** structurally related to compound **M13**. The four molecules are distinguished by the different coordination modes of the bridging SO$_4^{2-}$ anions.

6.12 [$Cu_8(SPh)_8(PPh_3)_4$] (M15)

Compound	**M15**
Empirical formula	$C_{120}H_{100}Cu_8P_4S_8$
Formula mass	2430.67
Temperature/K	150
Crystal system	triclinic
Space group	$P\overline{1}$
a/Å	12.0545(6)
b/Å	14.5005(6)
c/Å	16.9006(7)
α/°	73.733(3)
β/°	70.955(4)
γ/°	78.315(4)
V/Å^3	2660.5(2)
Z	1
ρ_{calc}/g·cm^{-3}	1.517
μ/mm^{-1}	10.057
F(000)	1240.0
Crystal size/mm^3	0.18 × 0.16 × 0.14
Radiation	GaK_α (λ = 1.34143)
2Θ range for data collection/°	4.946 to 125.284
Index ranges	$-15 \leq h \leq 12$, $-16 \leq k \leq 19$, $-22 \leq l \leq 22$
Reflections collected	33266
Independent reflections	12558 (R_{int} = 0.0164, R_{sigma} = 0.0173)
Indep. refl. with ($I \geq 2\sigma(I)$)	11136
Data/restraints/parameters	12558/0/831
Goodness-of-fit on F^2	1.027
Final R indexes ($I \geq 2\sigma(I)$)	R_1 = 0.0281, wR_2 = 0.0693
Final R indexes (all data)	R_1 = 0.0342, wR_2 = 0.0721
Largest diff. peak/hole/e Å^{-3}	0.74/-0.43

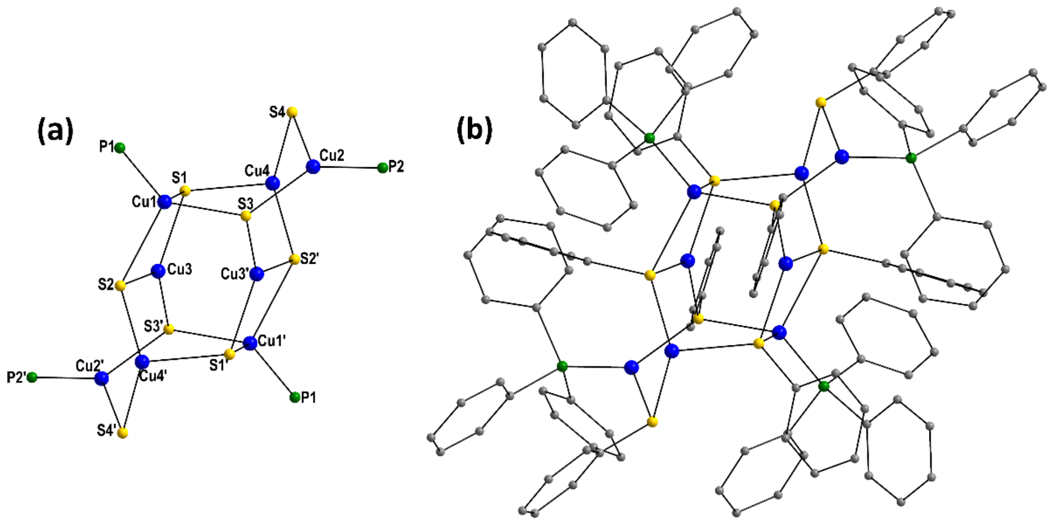

Figure 6-13 (a) *Structure of the heavy atoms core of compound* ***M15****;* ***(b)*** *Molecular structure of compound* ***M15*** *in the solid state in the same orientation as in* ***(a)*** *(H atoms omitted).*

Compound **M15** consist of a hexagonal prism build of six copper and six sulphur atoms capped by two CuSPh groups and phosphine ligands.

6.13 [$Cu_{24}S_8(SAd)_8(dppp)_4$] (M16)

Compound	**M16**
Empirical formula	$C_{188}H_{224}Cu_{24}P_8S_{16}$
Formula mass	4769.34
Temperature/K	150
Crystal system	orthorhombic
Space group	*Fddd*
a/Å	37.3336(4)
b/Å	40.9050(7)
c/Å	50.2158(6)
α/°	90
β/°	90
γ/°	90
V/Å^3	76686.1(18)
Z	16
ρ_{calc}/g·cm^{-3}	1.652
μ/mm^{-1}	15.762
F(000)	38784.0
Crystal size/mm^3	0.14 × 0.04 × 0.03
Radiation	GaK_α (λ = 1.34143)
2Θ range for data collection/°	11.582 to 89.998
Index ranges	$-39 \le h \le 20$, $-43 \le k \le 43$, $-52 \le l \le 52$
Reflections collected	111210
Independent reflections	11738 (R_{int} = 0.0458, R_{sigma} = 0.0281)
Data/restraints/parameters	11738/57/970
Goodness-of-fit on F^2	1.762
Final *R* indexes ($I \ge 2\sigma(I)$)	R_1 = 0.1289, wR_2 = 0.3732
Final *R* indexes (all data)	R_1 = 0.1644, wR_2 = 0.4025
Largest diff. peak/hole/e Å^{-3}	3.60/-1.87

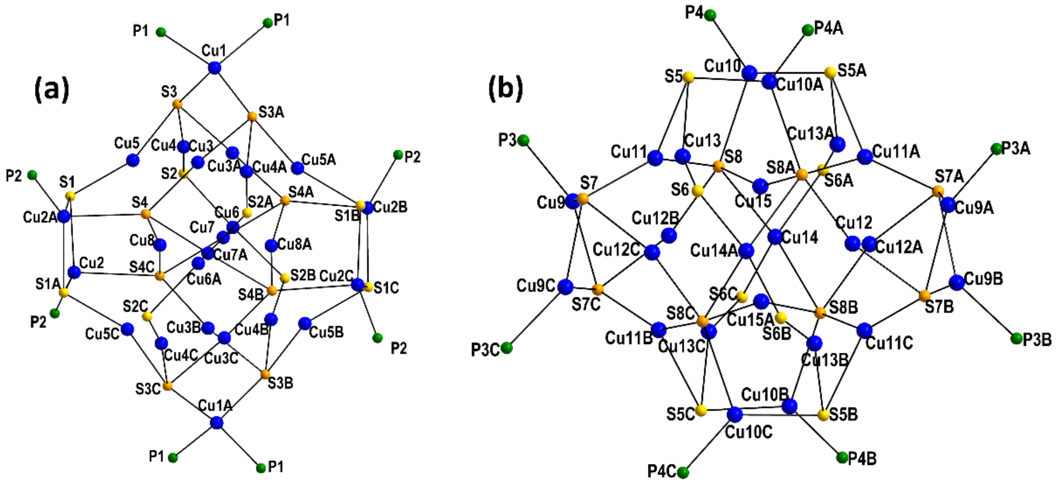

__Figure 6-14__ Structure of the heavy atoms core of the crystallographically independent molecules __A (a)__ and __B (b)__ in compound __M16__ in the solid state.

There are two isomers **A** and **B** present in the unit cell of **M16**. The main difference between these isomers is the coordination behavior of the copper atoms on the cluster surface. In molecule **A** there are two kind of copper atoms coordinating to phosphorus atoms:

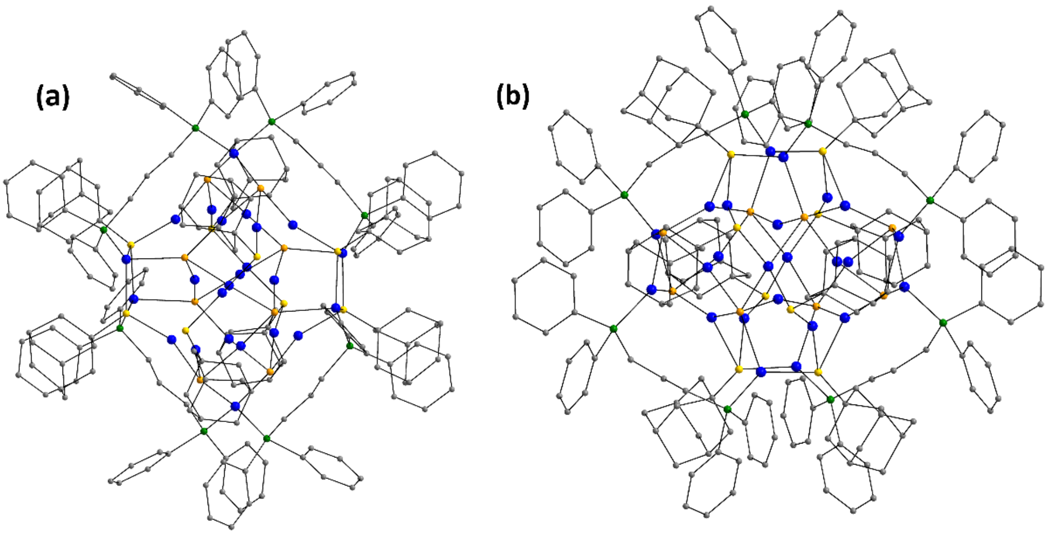

__Figure 6-15__ Molecular structure of molecule A __(a)__ and molecule B __(b)__ in compound __M16__ in the same orientation as in __Figure 6-14__ in the solid state (H atoms omitted).

6.14 $[(dppp)_2CuSeSi(CH_3)_3]\cdot½(C_6H_{12})$ (M17·½(C_6H_{12}))

Compound	**M17**·½(C_6H_{12})
Empirical formula	$C_{60}H_{63}CuP_4SeSi$
Formula mass	1078.57
Temperature/K	150
Crystal system	monoclinic
Space group	$P2_1/c$
a/Å	22.3778(15)
b/Å	10.3208(4)
c/Å	23.3586(15)
α/°	90
β/°	92.990(5)
γ/°	90
V/Å^3	5387.5(5)
Z	4
ρ_{calc}/g·cm^{-3}	1.330
μ/mm^{-1}	3.773
F(000)	2240.0
Crystal size/mm^3	0.14 × 0.04 × 0.03
Radiation	GaK_α (λ = 1.34143)
2Θ range for data collection/°	6.882 to 125.326
Index ranges	$-29 \leq h \leq 27$, $-13 \leq k \leq 4$, $-26 \leq l \leq 30$
Reflections collected	29625
Independent reflections	12580 (R_{int} = 0.0430, R_{sigma} = 0.0434)
Data/restraints/parameters	12580/20/548
Goodness-of-fit on F^2	1.532
Final R indexes ($I \geq 2\sigma(I)$)	R_1 = 0.1077, wR_2 = 0.3336
Final R indexes (all data)	R_1 = 0.1273, wR_2 = 0.3492
Largest diff. peak/hole/e Å^{-3}	1.72/-2.40

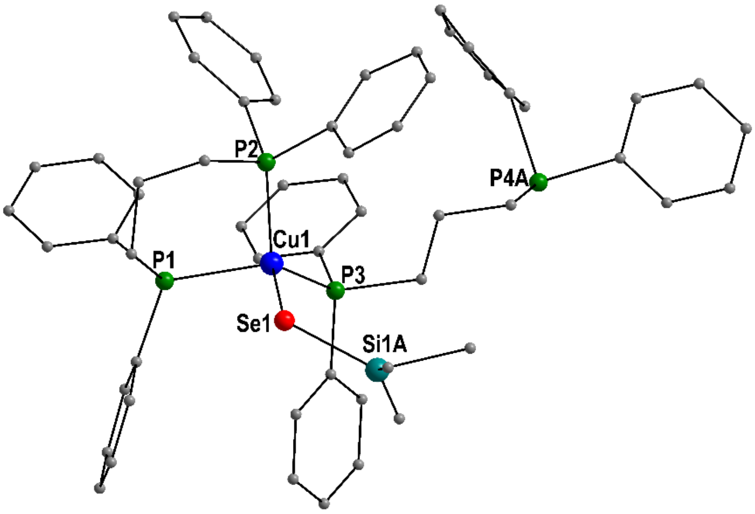

Figure 6-16 *Molecular structure of compound **M17** in the solid state (H atoms omitted).*

Compound **M17** is a mononuclear complex. Copper atoms tetrahedrally coordinate with three phosphorus atoms and one selenium atom.

6.15 $[Cu_{42}Se_{17}(SCy)_8(dppp)_6]\cdot 2THF$ (M18·2THF)

Compound	**M18**·2THF
Empirical formula	$C_{218}H_{260}Cu_{42}O_2P_{12}S_8Se_{17}$
Formula mass	7551.36
Temperature/K	180
Crystal system	monoclinic
Space group	*C*2/*c*
a/Å	38.6501(6)
b/Å	20.0112(4)
c/Å	36.8821(5)
α/°	90
β/°	109.1720(10)
γ/°	90
V/Å^3	26943.8(8)
Z	4
ρ_{calc}/g·cm^{-3}	1.862
μ/mm^{-1}	5.706
F(000)	14752.0
Crystal size/mm^3	0.16 × 0.14 × 0.12
Radiation	MoK_α (λ = 0.71073)
2Θ range for data collection/°	3.724 to 60.05
Index ranges	$-54 \le h \le 45$, $-27 \le k \le 27$, $-44 \le l \le 51$
Reflections collected	168701
Independent reflections	38902 (R_{int} = 0.0353, R_{sigma} = 0.0329)
Data/restraints/parameters	38902/18/1360
Goodness-of-fit on F^2	1.034
Final *R* indexes ($I \ge 2\sigma(I)$)	R_1 = 0.0645, wR_2 = 0.2047
Final *R* indexes (all data)	R_1 = 0.1027, wR_2 = 0.2418
Largest diff. peak/hole/e Å^{-3}	1.60/-1.01

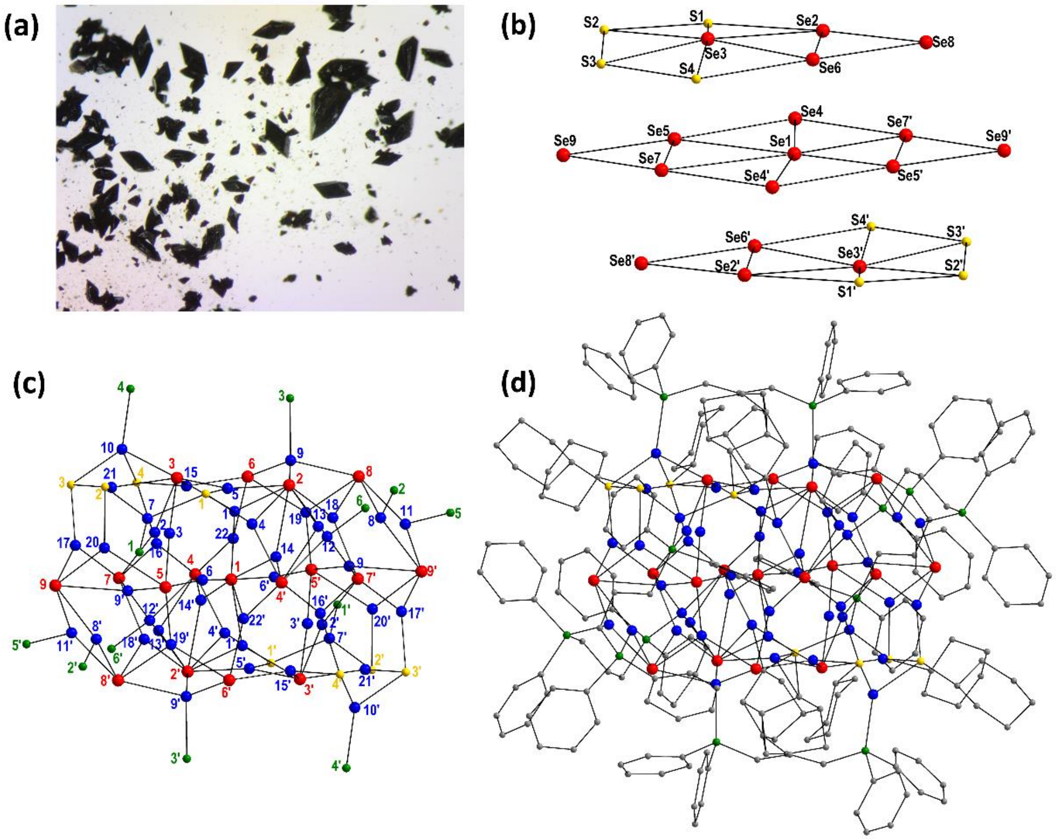

Figure 6-17* (a)** *Crystal image;* **(b)** *layer-type arrangement of chalcogen atoms;* **(c)** *structure of the heavy atoms core and* **(d)** *molecular structure of compound* ***M18 *in the solid state in the same orientation as in* **(c)** *(H atoms omitted).*

Compound **M18** consist of 42 Cu^+, 17 Se^{2-}, eight SCy^- groups and six dppp ligands. The 17 selenium atoms and eight sulphur atoms are arranged in three layers. The layers consist of 8, 9 and 8 atoms, respectively.

6.16 $[Cu_2(SCp)_2(dppe)_3]$ (M19)

Compound	**M19**
Empirical formula	$C_{88}H_{90}Cu_2P_6S_2$
Formula mass	1524.61
Temperature/K	150
Crystal system	monoclinic
Space group	$P2_1/c$
a/Å	12.6660(3)
b/Å	16.2369(3)
c/Å	18.3526(4)
α/°	90
β/°	97.630(2)
γ/°	90
V/Å^3	3740.92(14)
Z	2
ρ_{calc}/g·cm^{-3}	1.354
μ/mm^{-1}	4.432
F(000)	1596.0
Crystal size/mm^3	0.14 × 0.12 × 0.04
Radiation	GaK_α (λ = 1.34143)
2Θ range for data collection/°	6.126 to 125.062
Index ranges	$-16 \le h \le 16$, $-21 \le k \le 11$, $-20 \le l \le 24$
Reflections collected	23806
Independent reflections	8805 (R_{int} = 0.0158, R_{sigma} = 0.0192)
Data/restraints/parameters	8805/0/442
Goodness-of-fit on F^2	1.042
Final R indexes ($I \ge 2\sigma(I)$)	R_1 = 0.0379, wR_2 = 0.0971
Final R indexes (all data)	R_1 = 0.0451, wR_2 = 0.1013
Largest diff. peak/hole/e Å^{-3}	0.91/-0.42

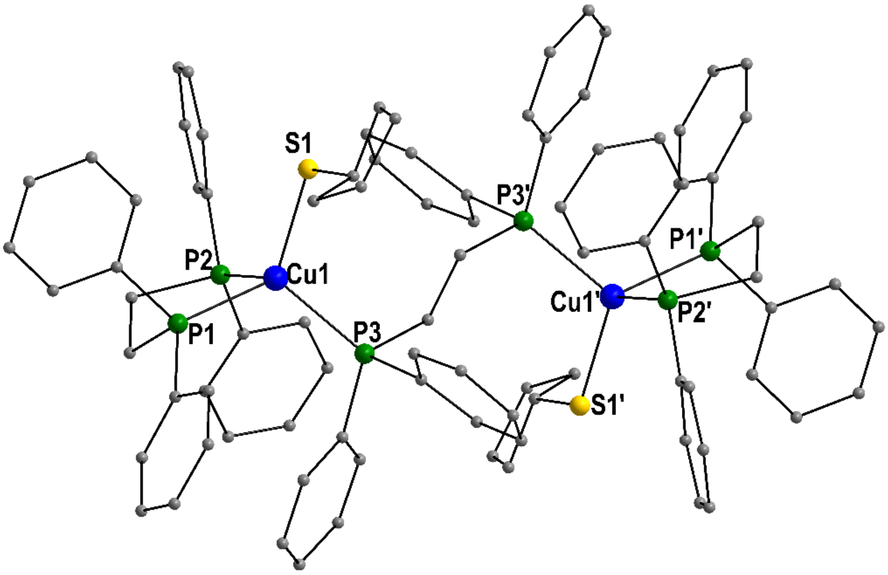

Figure 6-18 *Molecular structure of compound* ***M19*** *in the solid state (H atoms omitted).*

Compound **M19** is a dimer. In this compound, two [Cu(SCp)(dppe)] units are connected by a bridging dppe ligand.

6.17 [Cu_8Se_6(dppfc)$_4$(THF)$_2$] (M20)

Compound	**M20**
Empirical formula	$C_{110}H_{100}Cu_8Fe_3O_2P_6Se_6$
Formula mass	2789.34
Temperature/K	180
Crystal system	monoclinic
Space group	$C2/c$
a/Å	21.4015(5)
b/Å	18.0385(3)
c/Å	29.8705(8)
α/°	90
β/°	102.972(2)
γ/°	90
V/Å^3	11237.2(4)
Z	4
ρ_{calc}/g·cm^{-3}	1.649
μ/mm^{-1}	12.330
F(000)	5520.0
Crystal size/mm^3	0.17 × 0.16 × 0.15
Radiation	GaK_α (λ = 1.34143)
2Θ range for data collection/°	5.282 to 125.01
Index ranges	$-28 \leq h \leq 26$, $-23 \leq k \leq 10$, $-36 \leq l \leq 39$
Reflections collected	63472
Independent reflections	13547 (R_{int} = 0.0483, R_{sigma} = 0.0389)
Indep. refl. with ($I \geq 2\sigma(I)$)	8828
Data/restraints/parameters	13547/12/598
Goodness-of-fit on F^2	1.073
Final R indexes ($I \geq 2\sigma(I)$)	R_1 = 0.0790, wR_2 = 0.2409
Final R indexes (all data)	R_1 = 0.1113, wR_2 = 0.2717
Largest diff. peak/hole/e Å^{-3}	1.32/-1.25

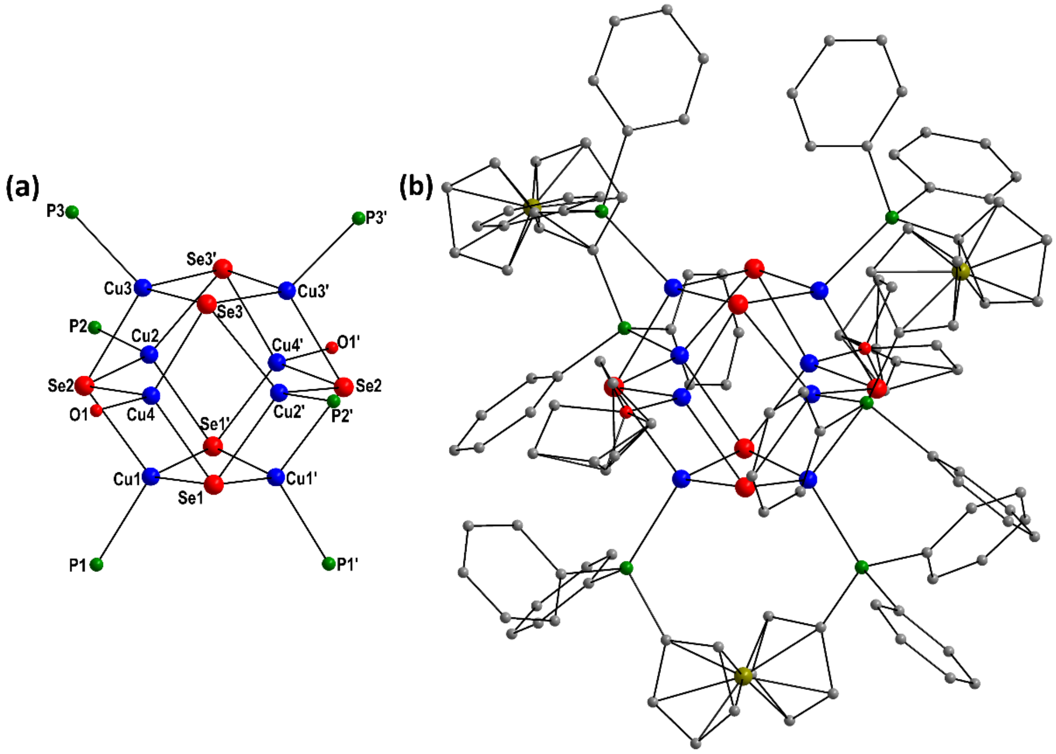

Figure 6-19* *(a) *Structure of the heavy atoms core of compound* ***M20 i****n the solid state;* ***(b)*** *Molecular structure of compound* ***M20*** *in the solid statein the same orientation as in* ***(a)*** *(H atoms omitted).*

In compound **M20,** two asymmetric units are combined in one molecule *via* a 2-fold axis. The core of this structure is a rhombic dodecahedron in which copper and selenium atoms occupy the corners of the polyhedron.

6.18 [$Cu_2(SeBz)_2(dppb)_2$] (M21)

Compound	**M21**
Empirical formula	$C_{70}H_{70}Cu_2P_4Se_2$
Formula mass	1320.14
Temperature/K	150.0
Crystal system	triclinic
Space group	$P\bar{1}$
a/Å	9.5770(7)
b/Å	11.6858(8)
c/Å	15.0279(12)
α/°	103.992(6)
β/°	107.236(6)
γ/°	104.366(6)
V/Å^3	1462.9(2)
Z	1
ρ_{calc}/g·cm^{-3}	1.498
μ/mm^{-1}	5.795
F(000)	676.0
Crystal size/mm^3	0.16 × 0.14 × 0.12
Radiation	GaK_α (λ = 1.34143)
2Θ range for data collection/°	5.698 to 125.208
Index ranges	$-12 \leq h \leq 11$, $-15 \leq k \leq 11$, $-17 \leq l \leq 19$
Reflections collected	17764
Independent reflections	6927 (R_{int} = 0.0231, R_{sigma} = 0.0252)
Data/restraints/parameters	6927/42/340
Goodness-of-fit on F^2	1.053
Final R indexes ($I \geq 2\sigma(I)$)	R_1 = 0.0813, wR_2 = 0.2471
Final R indexes (all data)	R_1 = 0.0904, wR_2 = 0.2585
Largest diff. peak/hole/e Å^{-3}	2.83/-2.31

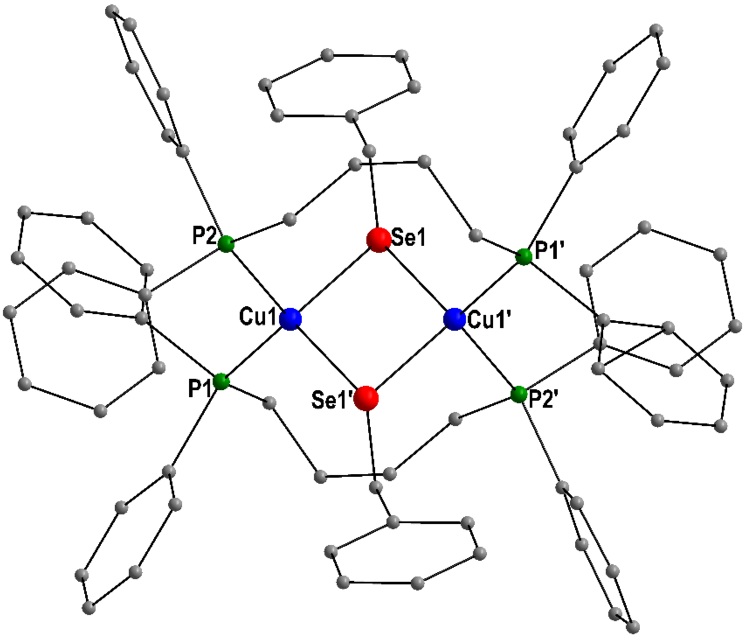

Figure 6-20 *Molecular structure of compound* ***M20*** *in the solid state (H atoms omitted).*

Compound **M21** is a binuclear complex with a planar Cu_2Se_2 core. Two copper atoms are bridged by two dppb ligands and two $SeBz^-$ ligands in *trans*-orientation.

6.19 $[Ag_{10}(SCy)_{10}(dpph)_2]\cdot 2(C_5H_{12})$ (M22·$2(C_5H_{12})$)

Compound	**M22**·$2(C_5H_{12})$
Empirical formula	$C_{130}H_{198}Ag_{10}P_4S_{10}$
Formula mass	3284.05
Temperature/K	150
Crystal system	monoclinic
Space group	$P2_1/n$
a/Å	15.3244(9)
b/Å	16.9718(8)
c/Å	26.5227(17)
α/°	90
β/°	90.193(5)
γ/°	90
V/Å^3	6898.1(7)
Z	2
ρ_{calc}/g·cm^{-3}	1.581
μ/mm^{-1}	8.882
F(000)	3336.0
Crystal size/mm^3	0.14 × 0.12 × 0.1
Radiation	GaK_α (λ = 1.34143)
2Θ range for data collection/°	5.378 to 114.98
Index ranges	$-19 \leq h \leq 11$, $-21 \leq k \leq 19$, $-33 \leq l \leq 33$
Reflections collected	65150
Independent reflections	14298 (R_{int} = 0.1590, R_{sigma} = 0.1057)
Data/restraints/parameters	14298/0/671
Goodness-of-fit on F^2	0.950
Final R indexes ($I \geq 2\sigma(I)$)	R_1 = 0.0840, wR_2 = 0.2081
Final R indexes (all data)	R_1 = 0.1219, wR_2 = 0.2291
Largest diff. peak/hole / e Å^{-3}	3.50/-2.14

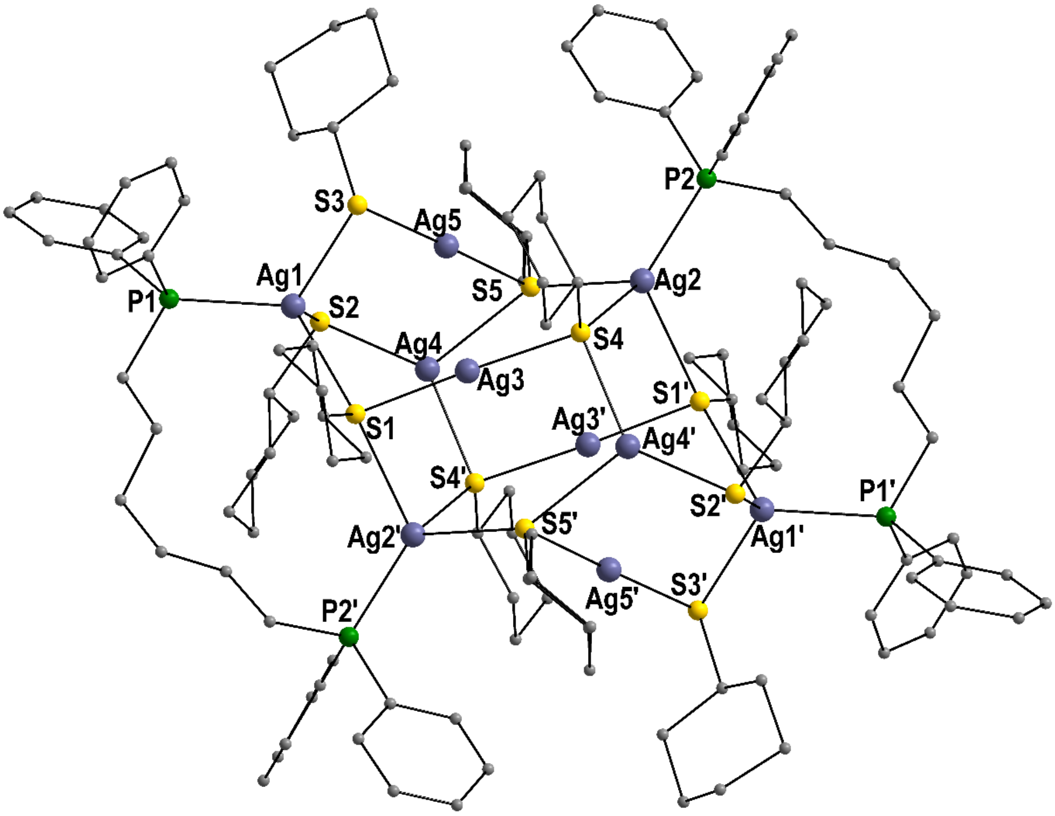

***Figure 6-21** Molecular structure of compound **M22** in the solid state (H atoms omitted).*

Compound **M22** is an irregular centrosymmetric structure combined by multiple rings.

6.20 [$Ag_2(SCy)_2(dppb)_2$] (M23)

Compound	**M23**
Empirical formula	$C_{68}H_{78}Ag_2P_4S_2$
Formula mass	1299.04
Temperature/K	180
Crystal system	monoclinic
Space group	$P2_1/c$
a/Å	14.3100(12)
b/Å	21.5470(14)
c/Å	10.1270(7)
α/°	90
β/°	100.340(6)
γ/°	90
V/Å^3	3071.8(4)
Z	2
ρ_{calc}/g·cm^{-3}	1.404
μ/mm^{-1}	0.850
F(000)	1344.0
Crystal size/mm^3	0.1 × 0.03 × 0.02
Radiation	MoK_α (λ = 0.71073)
2Θ range for data collection/°	4.504 to 60.008
Index ranges	$-20 \leq h \leq 19$, $-30 \leq k \leq 30$, $-11 \leq l \leq 14$
Reflections collected	44277
Independent reflections	8948 (R_{int} = 0.0481, R_{sigma} = 0.0436)
Data/restraints/parameters	8948/0/343
Goodness-of-fit on F^2	1.015
Final R indexes ($I \geq 2\sigma(I)$)	R_1 = 0.0388, wR_2 = 0.0894
Final R indexes (all data)	R_1 = 0.0643, wR_2 = 0.0969
Largest diff. peak/hole/e Å^{-3}	0.90/-0.78

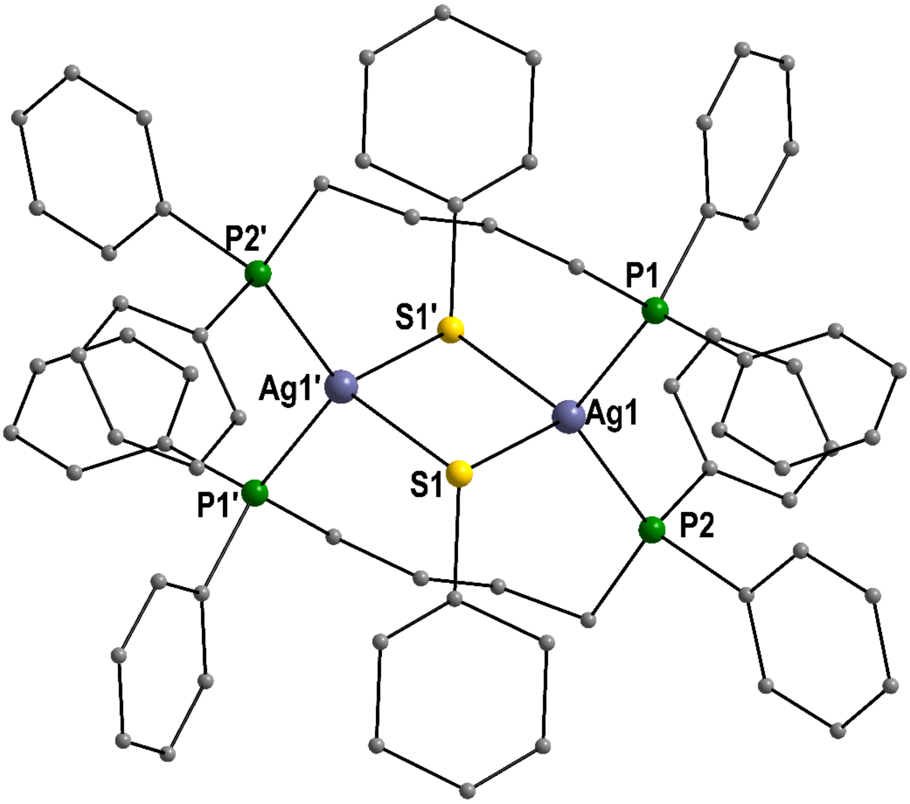

Figure 6-22 *Molecular structure of compound* ***M23*** *in the solid state (H atoms omitted).*

Compound **M23** is a binuclear complex. Its core is a planar Ag_2S_2 ring. Two silver atoms are bridged by two dppb ligands and two SCy^- ligands in *trans*-orientation.

6.21 $[Ag_3(SCy)_2(dpph)_2](NO_3)$ (M24)

Compound	**M24**
Empirical formula	$C_{72}H_{86}Ag_3NO_3P_4S_2$
Formula mass	1525.02
Temperature/K	130.0
Crystal system	triclinic
Space group	$P\overline{1}$
a/Å	9.8242(3)
b/Å	12.7167(4)
c/Å	16.1753(7)
α/°	103.451(3)
β/°	99.743(3)
γ/°	103.136(3)
V/Å^3	1860.58(12)
Z	1
ρ_{calc}/g·cm^{-3}	1.361
μ/mm^{-1}	5.285
F(000)	782.0
Crystal size/mm^3	0.14 × 0.13 × 0.12
Radiation	GaK_α (λ = 1.34143)
2Θ range for data collection/°	6.474 to 125.136
Index ranges	$-12 \leq h \leq 10$, $-16 \leq k \leq 16$, $-15 \leq l \leq 21$
Reflections collected	21180
Independent reflections	8613 (R_{int} = 0.0192, R_{sigma} = 0.0187)
Data/restraints/parameters	8613/3/383
Goodness-of-fit on F^2	1.117
Final R indexes ($I \geq 2\sigma(I)$)	R_1 = 0.0396, wR_2 = 0.1159
Final R indexes (all data)	R_1 = 0.0425, wR_2 = 0.1180
Largest diff. peak/hole/e Å^{-3}	0.87/-1.43

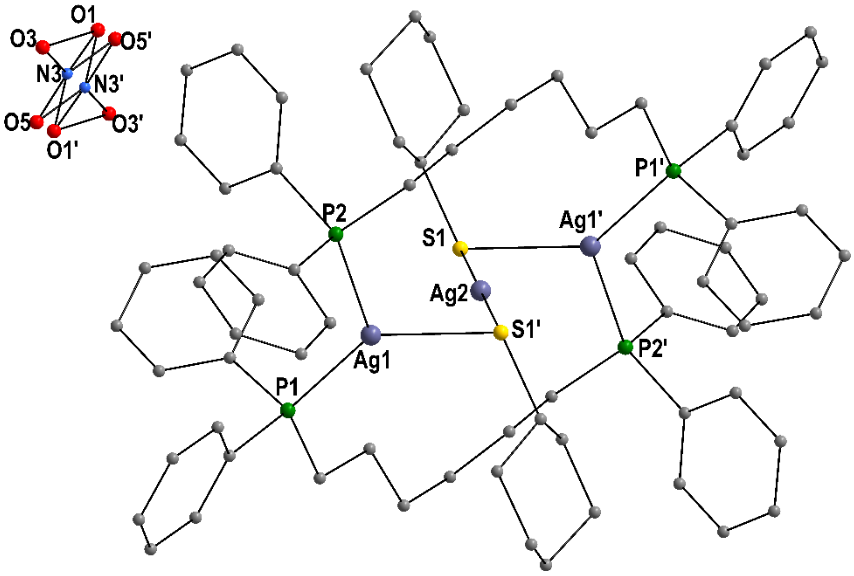

Figure 6-23 *Molecular structure of compound* ***M24*** *in the solid state (H atoms omitted).*

The $[Ag_3(SCy)_2(dpph)_2]^+$ cation in **M24** can be seen as two mononuclear substructures [Ag(SCy)(dpph)] connected by Ag2. Ag1 and Ag1’ are additionally bridged by dpph ligands. The nitrate counterion is disordered.

6.22 $[Ag_{15}Se(SCy)_{12}(dppb)_3]$ (M25)

Compound	**M25**
Empirical formula	$C_{156}H_{216}Ag_{15}P_6S_{12}Se$
Formula mass	4358.83
Temperature/K	170
Crystal system	trigonal
Space group	$P3_1c$
a/Å	19.0604(2)
b/Å	19.0604(2)
c/Å	28.2084(2)
α/°	90
β/°	90
γ/°	120
V/Å^3	8875.1(2)
Z	2
ρ_{calc}/g·cm^{-3}	1.631
μ/mm^{-1}	10.248
F(000)	4346.0
Crystal size/mm^3	0.16 × 0.14 × 0.12
Radiation	GaK_α (λ = 1.34143)
2Θ range for data collection/°	5.396 to 124.984
Index ranges	$-25 \leq h \leq 24$, $-25 \leq k \leq 24$, $-16 \leq l \leq 37$
Reflections collected	79346
Independent reflections	10264 (R_{int} = 0.0269, R_{sigma} = 0.0133)
Data/restraints/parameters	10264/6/572
Goodness-of-fit on F^2	1.040
Final R indexes ($I \geq 2\sigma(I)$)	R_1 = 0.0637, wR_2 = 0.1692
Final R indexes (all data)	R_1 = 0.0644, wR_2 = 0.1703
Largest diff. peak/hole/e Å^{-3}	3.34/-0.88
Flack parameter	0.011(8)

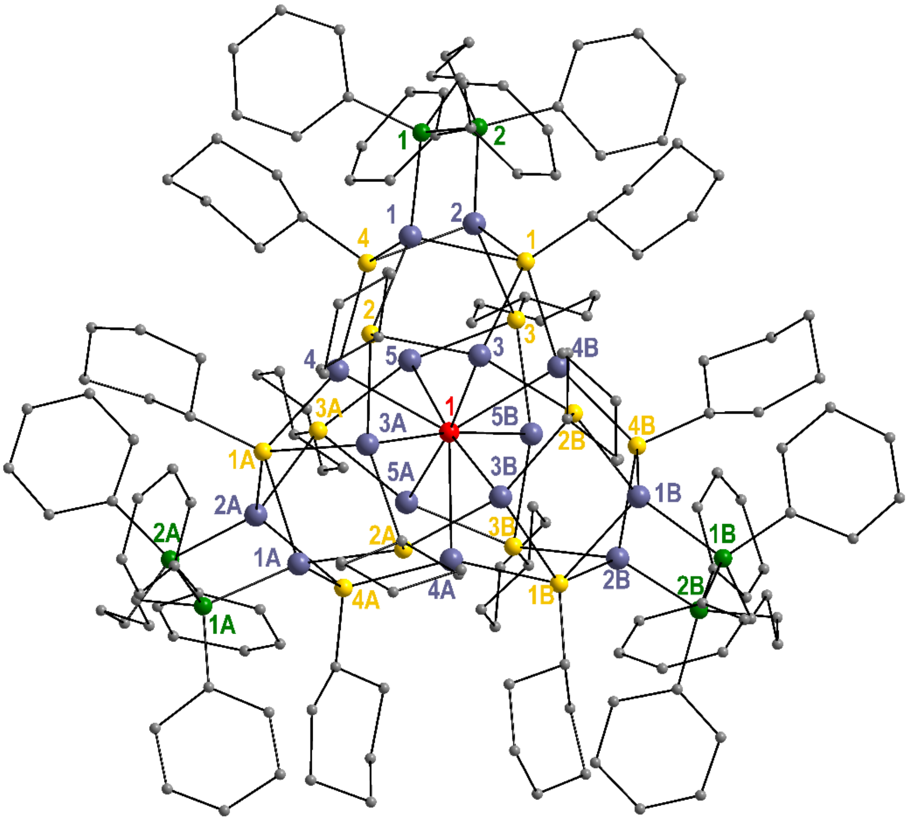

***Fig 6-24** Molecular structure of the cation in compound **M25** in the solid state (H atoms omitted).*

Compound **M25** shares the same cation with compound **42**. The anion – probably a nitrate – could not be found.

6.23 [$Ag_{42}Se_{13}(SAd)_{14}(dppm)_6$]·4THF (M26·4THF)

Compound	**M26**·4THF
Empirical formula	$C_{306}H_{374}Ag_{42}O_4P_{12}S_{14}Se_{13}$
Formula mass	10493.53
Temperature/K	150.0
Crystal system	triclinic
Space group	$P\overline{1}$
a/Å	22.5404(4)
b/Å	22.9462(3)
c/Å	23.8332(3)
α/°	107.9840(10)
β/°	106.7250(10)
γ/°	111.7660(10)
V/Å^3	9694.1(3)
Z	1
ρ_{calc}/g·cm^{-3}	1.797
μ/mm^{-1}	13.049
F(000)	5062.0
Crystal size/mm^3	0.14 × 0.12 × 0.06
Radiation	GaK_α (λ = 1.34143)
2Θ range for data collection/°	4.078 to 125.112
Index ranges	$-29 \leq h \leq 14$, $-29 \leq k \leq 30$, $-31 \leq l \leq 31$
Reflections collected	108745
Independent reflections	45110 (R_{int} = 0.0240, R_{sigma} = 0.0227)
Ind. refl. with ($I \geq 2\sigma(I)$)	38017
Data/restraints/parameters	45110/0/1762
Goodness-of-fit on F^2	1.071
Final R indexes ($I \geq 2\sigma(I)$)	R_1 = 0.0407, wR_2 = 0.1147
Final R indexes (all data)	R_1 = 0.0471, wR_2 = 0.1180
Largest diff. peak/hole/e Å^{-3}	3.73/-2.59

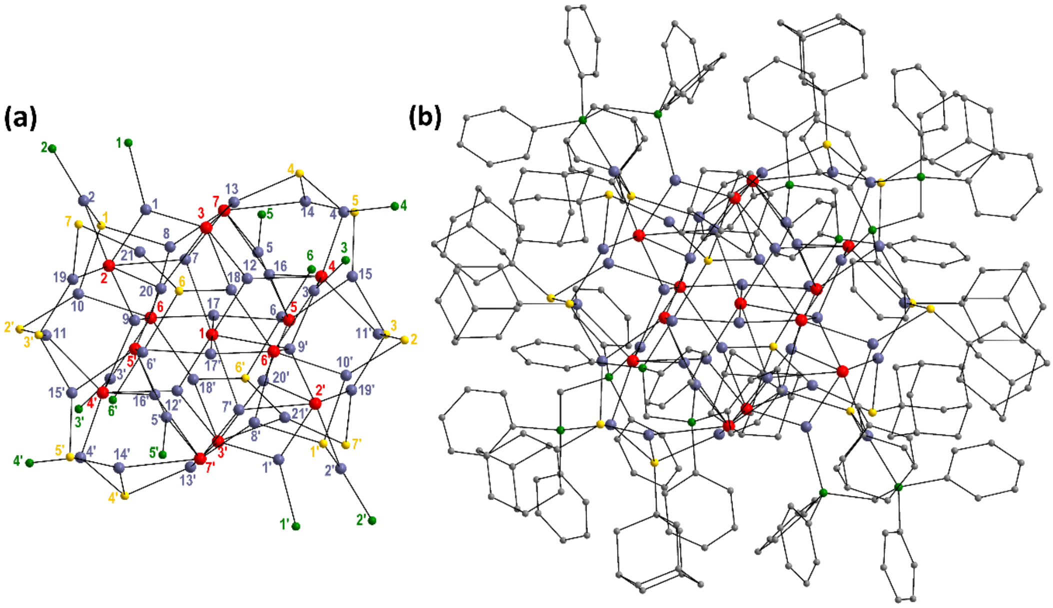

***Fig 6-25 (a)** Structure of heavy atoms core of compound **M26** in the solid state; **(b)** Molecular structure of compound **M26** in the solid state in the same orientation as in **(a)** (H atoms omitted).*

Compound **M26** shares the same cation with compound **49**. There is an inversion center locating on the Se1 atom. However, the anion – probably nitrate – of compound **M26** could not be localized.

6.24 $[Ag_2Se(SCy)(dppb)_2]\cdot(C_2H_5OH)$ (M27·(C_2H_5OH))

Compound	**M27**·(C_2H_5OH)
Empirical formula	$C_{64}H_{73}Ag_2OP_4SSe$
Formula mass	1308.86
Temperature/K	150.0
Crystal system	monoclinic
Space group	$P2_1/n$
a/Å	10.4572(4)
b/Å	42.349(2)
c/Å	13.6375(5)
α/°	90
β/°	98.607(3)
γ/°	90
V/Å^3	5971.4(5)
Z	4
ρ_{calc}/g·cm^{-3}	1.456
μ/mm^{-1}	5.077
F(000)	2676.0
Crystal size/mm^3	0.16 × 0.14 × 0.02
Radiation	GaK_α (λ = 1.34143)
2Θ range for data collection/°	5.984 to 114.996
Index ranges	$-12 \le h \le 13$, $-48 \le k \le 53$, $-9 \le l \le 17$
Reflections collected	31976
Independent reflections	11896 (R_{int} = 0.0366, R_{sigma} = 0.0565)
Data/restraints/parameters	11896/1/645
Goodness-of-fit on F^2	0.955
Final R indexes ($I \ge 2\sigma(I)$)	R_1 = 0.0448, wR_2 = 0.1103
Final R indexes (all data)	R_1 = 0.0711, wR_2 = 0.1172
Largest diff. peak/hole/e Å^{-3}	1.77/-0.76

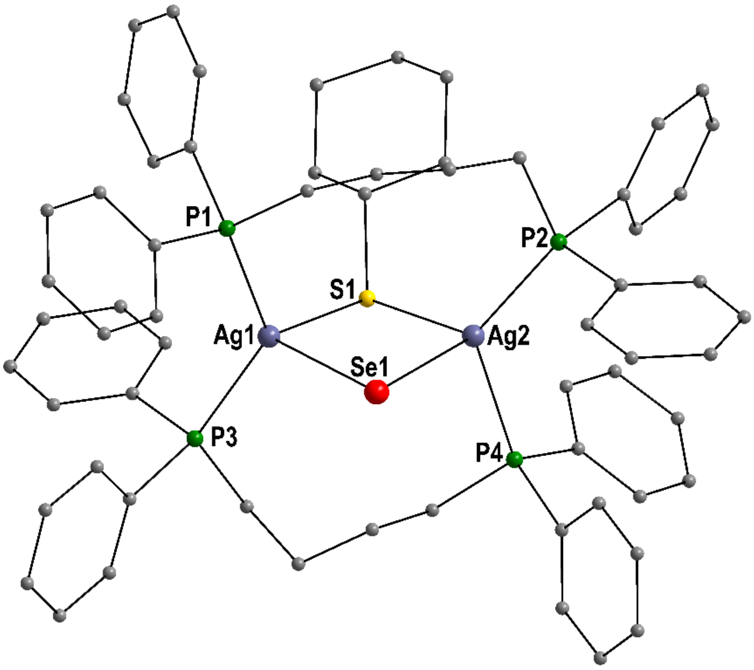

***Figure 6-26** Molecular structure of compound **M27** in the solid state (H atoms omitted).*

Compound **M27** is a binuclear complex consisting of a planar Ag_2SSe four-membered ring, probably the selenium atom carries one hydrogen atom, which could not be found in the Fourier analysis. The two silver atoms are additionally bridged by two dppb ligands.

6.25 [$Ag_2(SH)_2(dppfc)_2$]·3THF (M28·3THF)

Compound	**M28**·3THF
Empirical formula	$C_{80}H_{82}Ag_2Fe_2O_3P_4S_2$
Formula mass	1606.89
Temperature/K	180
Crystal system	triclinic
Space group	$P\overline{1}$
a/Å	10.9201(6)
b/Å	12.3244(6)
c/Å	13.8990(7)
α/°	71.247(4)
β/°	88.448(4)
γ/°	82.663(4)
V/Å^3	1756.58(16)
Z	1
ρ_{calc}/g·cm^{-3}	1.519
μ/mm^{-1}	6.310
F(000)	824.0
Crystal size/mm^3	0.14 × 0.13 × 0.12
Radiation	GaK_α (λ = 1.34143)
2Θ range for data collection/°	5.842 to 125.114
Index ranges	$-14 \le h \le 14$, $-15 \le k \le 16$, $-18 \le l \le 11$
Reflections collected	23767
Independent reflections	8378 (R_{int} = 0.0479, R_{sigma} = 0.0465)
Data/restraints/parameters	8378/10/393
Goodness-of-fit on F^2	1.066
Final R indexes ($I \ge 2\sigma(I)$)	R_1 = 0.0741, wR_2 = 0.2105
Final R indexes (all data)	R_1 = 0.0917, wR_2 = 0.2312
Largest diff. peak/hole/e Å^{-3}	1.38/-1.62

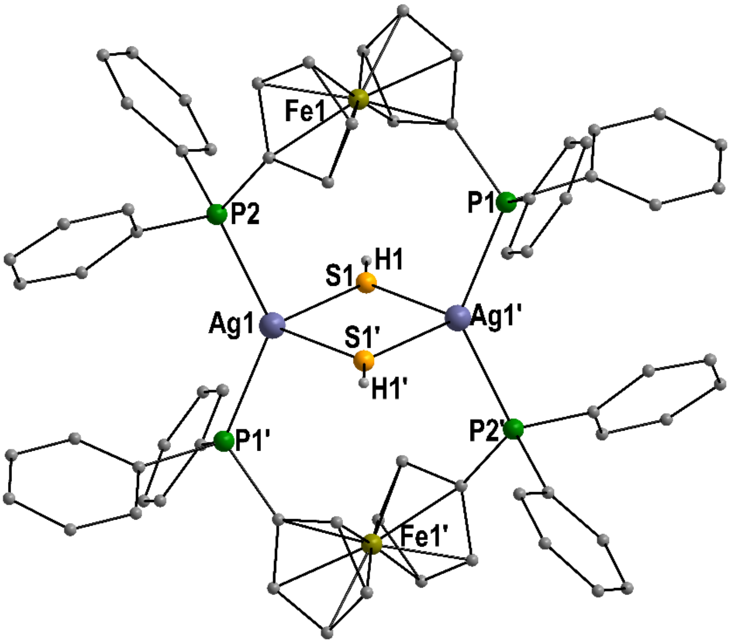

Figure 6-27 *Molecular structure of compound* ***M28*** *in the solid state (H atoms except for H1 omitted).*

Compound **M28** is a binuclear complex. Core of this compound is a planar Ag_2S_2 four-membered ring. There is an inversion center locating on the middle point of the Ag_2S_2 plane.

6.26 [Ag$_2$(SeH)$_2$(dppfc)$_2$]·2THF (M29·2THF)

Compound	**29**·2THF
Empirical formula	$C_{76}H_{74}Ag_2Fe_2O_2P_4Se_2$
Formula mass	1628.59
Temperature/K	180.0
Crystal system	triclinic
Space group	$P\bar{1}$
a/Å	10.9852(4)
b/Å	12.3224(4)
c/Å	13.8981(5)
α/°	71.130(3)
β/°	88.329(3)
γ/°	82.352(3)
V/Å^3	1764.16(11)
Z	1
ρ_{calc}/g·cm^{-3}	1.533
μ/mm^{-1}	6.716
F(000)	820.0
Crystal size/mm^3	0.14 × 0.1 × 0.02
Radiation	GaK_α (λ = 1.34143)
2Θ range for data collection/°	5.848 to 124.988
Index ranges	$-13 \le h \le 14$, $-15 \le k \le 16$, $-8 \le l \le 18$
Reflections collected	22774
Independent reflections	8384 (R_{int} = 0.0300, R_{sigma} = 0.0260)
Data/restraints/parameters	8384/3/372
Goodness-of-fit on F^2	1.081
Final R indexes ($I \ge 2\sigma(I)$)	R_1 = 0.0767, wR_2 = 0.2302
Final R indexes (all data)	R_1 = 0.0832, wR_2 = 0.2371
Largest diff. peak/hole/e Å^{-3}	1.79/-3.30

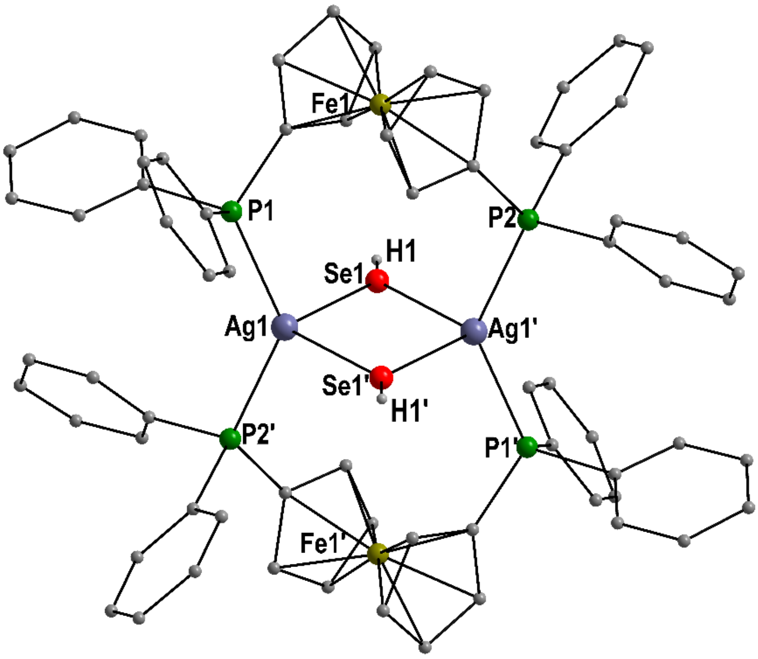

Figure 6-28 *Molecular structure of compound* ***M29*** *in the solid state (H atoms except for H1 omitted).*

Similar with compound **M28**, compound **M29** also has a planar four-membered Ag_2Se_2 ring. The two silver atoms are bridged by dppfc ligands.

6.27 [Cu(SCp)(dppox)]·(C_7H_8) (M30·(C_7H_8))

Compound	**M30**·(C_7H_8)
Empirical formula	$C_{44}H_{45}CuP_2S$
Formula mass	731.34
Temperature/K	150
Crystal system	monoclinic
Space group	$P2_1/c$
a/Å	13.596(4)
b/Å	11.5952(17)
c/Å	23.649(6)
α/°	90
β/°	94.58(2)
γ/°	90
V/Å^3	3716.3(15)
Z	4
ρ_{calc}/g·cm^{-3}	1.307
μ/mm^{-1}	4.184
F(000)	1536.0
Crystal size/mm^3	0.24 × 0.2 × 0.18
Radiation	GaK_α (λ = 1.34143)
2Θ range for data collection/°	6.524 to 125.322
Index ranges	$-17 \le h \le 17$, $-15 \le k \le 5$, $-31 \le l \le 30$
Reflections collected	41862
Independent reflections	8884 (R_{int} = 0.0258, R_{sigma} = 0.0235)
Data/restraints/parameters	8884/0/434
Goodness-of-fit on F^2	1.015
Final R indexes ($I \ge 2\sigma(I)$)	R_1 = 0.0321, wR_2 = 0.0728
Final R indexes (all data)	R_1 = 0.0432, wR_2 = 0.0775
Largest diff. peak/hole/e Å^{-3}	0.30/-0.32

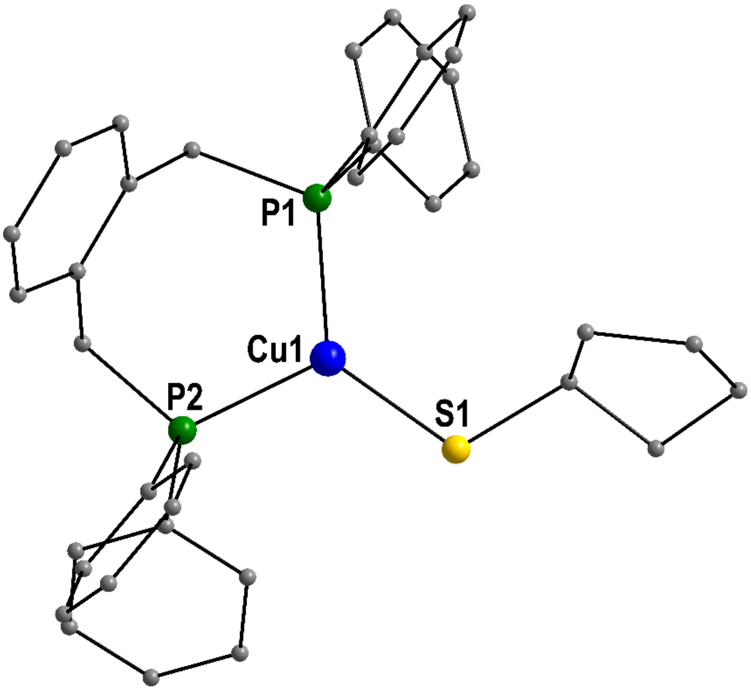

Figure 6-29 *Molecular structure of compound* ***M30*** *in the solid state (H atoms omitted).*

Compound **M30** co-crystallized with compound **11** and is a mononuclear complex consisting of one chelating dppox ligand and a terminal SCp⁻ group.

6.28 [$Ag_2(SCy)_2(dppb)_2$] (M31)

Compound	**M31**
Empirical formula	$C_{68}H_{78}Ag_2P_4S_2$
Formula mass	1299.04
Temperature/K	150.0
Crystal system	monoclinic
Space group	$P2_1/c$
a/Å	10.4689(2)
b/Å	20.7820(5)
c/Å	28.5292(7)
α/°	90
β/°	99.663(2)
γ/°	90
V/Å^3	6118.9(2)
Z	4
ρ_{calc}/g·cm^{-3}	1.410
μ/mm^{-1}	4.693
F(000)	2688.0
Crystal size/mm^3	0.18 × 0.03 × 0.02
Radiation	GaK_α (λ = 1.34143)
2Θ range for data collection/°	4.6 to 115.036
Index ranges	$-13 \leq h \leq 6$, $-26 \leq k \leq 25$, $-32 \leq l \leq 35$
Reflections collected	61736
Independent reflections	12625 (R_{int} = 0.0468, R_{sigma} = 0.0406)
Data/restraints/parameters	12625/0/685
Goodness-of-fit on F^2	1.169
Final R indexes ($I \geq 2\sigma(I)$)	R_1 = 0.1003, wR_2 = 0.2458
Final R indexes (all data)	R_1 = 0.1132, wR_2 = 0.2504
Largest diff. peak/hole/e Å^{-3}	3.33/-1.89

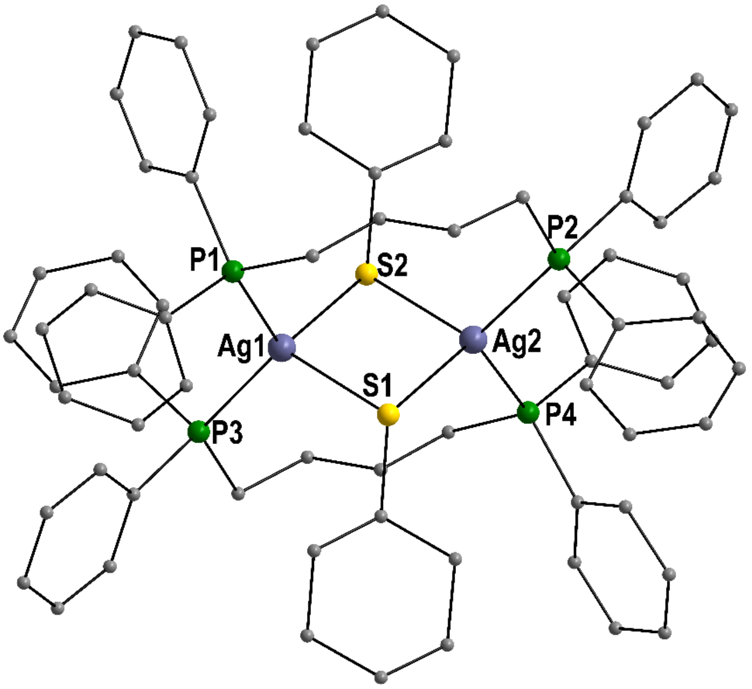

Figure 6-30 *Molecular structure of compound* ***M31*** *in the solid state (H atoms omitted).*

Compound **M31** consists of a planar Ag_2S_2 four-membered ring. The two silver atoms are additionally bridged by dppb ligands.

6.29 [$Cu_2(SeH)_2(dppp)_2$] (M32)

Compound	**M32**
Empirical formula	$C_{54}H_{54}Cu_2P_4Se_2$
Formula mass	1111.85
Temperature/K	150
Crystal system	monoclinic
Space group	$P2_1/n$
a/Å	10.3049(4)
b/Å	18.4742(6)
c/Å	13.1504(7)
α/°	90
β/°	104.698(4)
γ/°	90
V/Å^3	2421.58(18)
Z	2
ρ_{calc}/g·cm^{-3}	1.525
μ/mm^{-1}	6.874
F(000)	1128.0
Crystal size/mm^3	0.14 × 0.03 × 0.02
Radiation	GaK_α (λ = 1.34143)
2Θ range for data collection/°	8.77 to 125.152
Index ranges	$-7 \leq h \leq 13$, $-24 \leq k \leq 20$, $-17 \leq l \leq 17$
Reflections collected	16038
Independent reflections	5752 (R_{int} = 0.0150, R_{sigma} = 0.0121)
Data/restraints/parameters	5752/0/388
Goodness-of-fit on F^2	1.085
Final R indexes ($I \geq 2\sigma(I)$)	R_1 = 0.0255, wR_2 = 0.0631
Final R indexes (all data)	R_1 = 0.0268, wR_2 = 0.0639
Largest diff. peak/hole/e Å^{-3}	0.40/-0.77

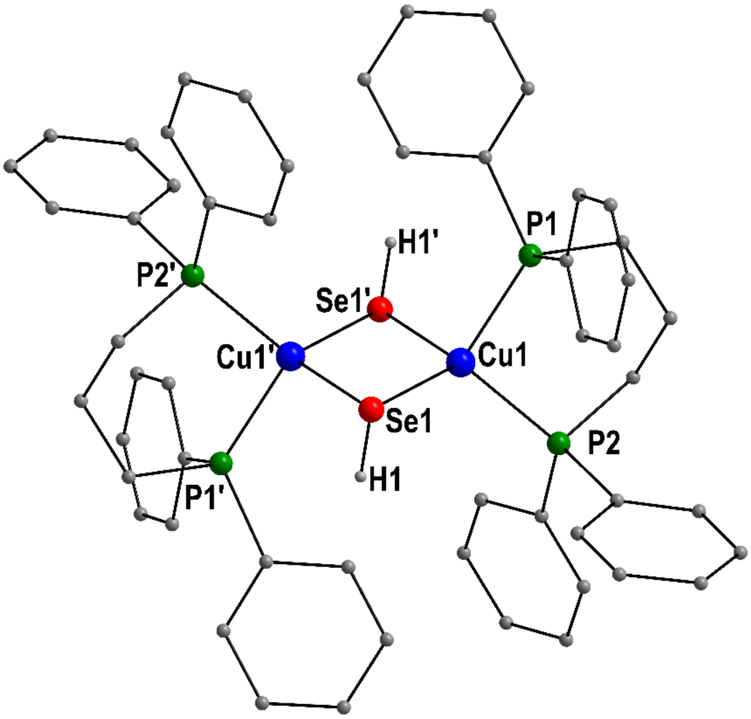

Figure 6-31 *Molecular structure of compound* ***M32*** *in the solid state (H atoms except for H1 omitted).*

Compound **M32** has the similar structure as compound **M29** but their metal atoms are different. Cu atoms are chelated by dppp ligands.

7 Summary

Inspired by the research work about coinage metal chalcogenide clusters, synthesis and structures of a series of silver or copper chalcogenide compounds have been reported in this thesis. In addition, photoluminescence properties of several compounds have been explored.

In the first part, the synthesis of smaller copper clusters obtained from copper thiolates and phosphine ligands is described. The solubility of copper thiolates in common solvents is low. But by the addition of phosphine ligands, copper thiolates phosphine oligomers can be dissolved. Then these species can be crystallized by layering with non-polar solvents. Actually, this kind of compounds can be understood as precursors of the following larger clusters. Nine compounds have been selected to carry out luminescence measurements. It is observed that their optical properties are influenced by the size of the clusters, shape of the core, nature of the ligands, etc. A possible reason for the light emission is a ligand to metal charge transfer (LMCT), which has been discussed in literature before.

In the second part the synthetic approach was widened from the isolation of binary to that of ternary compounds using an additional polyoxomolybdate source. Some new compounds are successfully obtained with copper cations and polyoxomolybdate anions but others are binary copper thiolate compounds.

In the third part $E(SiMe_3)_2$ (E = S, Se) has been added to the reactions. This $E(SiMe_3)_2$ acts as a chalcogenide source yielding metal-rich copper or silver chalcogenide clusters. Finally, these thermodynamically metastable clusters are protected by phosphine ligands or/and thiolates and isolated from solutions.

总结

随着 TEM, ESI, NMR 等表征方式的兴起，货币金属硫属簇的合成，表征和性能研究在过去几十年里得到了长足的发展。研究表明一方面由于其小的尺寸（≤10 nm），这些簇表现出很多纳米尺寸的材料所独有的性质，同时通过借助单晶测试等手段，我们可以精确确定这些簇的结构，进而研究结构与性能的关系；另一方面，从结构上来说，这些簇是链接小分子和体相材料的中间体，这对我们研究 M_2E（M = Ag, Cu; E = S, Se）的结构如何从小分子过渡到体相至关重要。

合成硫属簇的方式多种多样，我们课题组主要关注如何用膦配体保护 M_2E 核的方式。因此在本论文中，我们聚焦三个方面的工作。

（1） 将六种不同的硫醇铜与有机膦反应，得到 22 种结构简单，尺寸较小的 Cu-S 化合物。这些化合物通常有个多元环构成的 Cu-S 核，其外围被膦配体环绕。Cu 原子表现出线性、平面三角形和四面体三种配位模式。硫原子大多以 RS^-的形式存在，也有少量化合物种含有 S^{2-}的形式。此外，除了分立的小分子的结构，也有部分化合物是 1D 的聚合物。当然，我们也尝试将第二种金属 Mo 引入结构中，最终得到了 3 个 Cu – Mo - S 异金属化合物。此外，我们还对其中 9 个化合物进行了光学性能方面的初步研究。

（2） 将硫醇铜与有机磷进行反应，在这个过程中加入六甲基硅硫/硒烷 $E(SiMe_3)_2$，期望得到大的 Cu-E 簇。在这个过程中，我们成功获得了 8 个中大型的簇，这些簇中的 Cu 原子数从 34 增加到 94。这些簇的结构共同点是：所有的硫属原子呈层状排布，铜原子分布在这些层的间隙中或者是层的外围。有趣的是，仅通过不良溶剂的扩散，我们就可以获得不同尺寸和大小的三种化合物。

（3） 将硫醇银与有机磷进行反应，在这个过程中加入六甲基硅硫/硒烷 $E(SiMe_3)_2$，期望得到大的 Ag - E 簇。我们一共获得了 10 个 Ag - E 化合物，其中有三个大型簇。这些大型的结构特点是硫属原子成核-壳状分布，银原子排布在这些硫属原子壳的间隙或者外围。另外我们也获得了四种有关联的银簇。仅通过调整阴离子来源 $NaBPh_4$ 和 $E(SiMe_3)_2$ 比例我们即可获得不同的银簇。

8 References

[1] a) J. F. Corrigan, O. Fuhr, D. Fenske, *Adv. Mater.* **2009**, *21*, 1867-1871; b) M. D. Morse, *Chem. Rev.* **1986**, *86*, 1049-1109; c) J. Koutecky, P. Fantucci, *Chem. Rev.* **1986**, *86*, 539-587.

[2] X. Liu, D. Astruc, *Coord. Chem. Rev.* **2018**, *359*, 112-126.

[3] K. K.-W. Lo, V. W.-W. Yam, W. K.-M. Fung, C.-R. Wang, *Coord. Chem. Rev.* **1998**, *171*, 17-41.

[4] M. N. Pillay, W. E. van Zyl, C. W. Liu, *Nanoscale* **2020**, *12*, 24331-24348.

[5] O. Veselska, A. Demessence, *Coord. Chem. Rev.* **2018**, *355*, 240-270.

[6] a) S. Auer, D. Frenkel, *Nature* **2001**, *413*, 711-713; b) A. Henglein, *Chem. Rev.* **1989**, *89*, 1861-1873.

[7] R. R. Nasaruddin, T. Chen, N. Yan, J. Xie, *Coord. Chem. Rev.* **2018**, *368*, 60-79.

[8] a) V. W.-W. Yam, E. C.-C. Cheng, K.-K. Cheung, *Angew. Chem. Int. Ed.* **1999**, *38*, 197-199; b) Z. Luo, X. Yuan, Y. Yu, Q. Zhang, D. T. Leong, J. Y. Lee, J. Xie, *J. Am. Chem. Soc.* **2012**, *134*, 16662-16670; c) I. Dolamic, S. Knoppe, A. Dass, T. Bürgi, *Nat. Commun.* **2012**, *3*; 798; d) Z. Wu, R. Jin, *Nano Lett.* **2010**, *10*, 2568-2573; e) M. W. Heaven, A. Dass, P. S. White, K. M. Holt, R. W. Murray, *J. Am. Chem. Soc.* **2008**, *130*, 3754-3755.

[9] a) R.-W. Huang, J. Yin, C. Dong, P. Maity, M. N. Hedhili, S. Nematulloev, B. Alamer, A. Ghosh, O. F. Mohammed, O. M. Bakr, *ACS Mater.* **2021**, *3*, 90-99; b) R.-W. Huang, J. Yin, C. Dong, A. Ghosh, M. J. Alhilaly, X. Dong, M. N. Hedhili, E. Abou-Hamad, B. Alamer, S. Nematulloev, Y. Han, O. F. Mohammed, O. M. Bakr, *J. Am. Chem. Soc.* **2020**, *142*, 8696-8705; c) R. S. Dhayal, J.-H. Liao, S. Kahlal, X. Wang, Y.-C. Liu, M.-H. Chiang, W. E. van Zyl, J.-Y. Saillard, C. W. Liu, *Chem. Eur. J.* **2015**, *21*, 8369-8374.

[10] K. K. Chakrahari, R. P. B. Silalahi, J.-H. Liao, S. Kahlal, Y.-C. Liu, J.-F. Lee, M.-H. Chiang, J.-Y. Saillard, C. W. Liu, *Chem. Sci.* **2018**, *9*, 6785-6795.

[11] Z. Wang, Q.-P. Qu, H.-F. Su, P. Huang, R. K. Gupta, Q.-Y. Liu, C.-H. Tung, D. Sun, L.-S. Zheng, *Sci. China Chem.* **2019**, *63*, 16-20.

[12] F. Hu, J.-J. Li, Z.-J. Guan, S.-F. Yuan, Q.-M. Wang, *Angew. Chem. Int. Ed.* **2020**, *59*, 5312-5315.

[13] Y.-H. Feng, Z.-S. Lin, S.-Q. Liu, J.-F. Shi, K. Zhou, J.-Y. Ji, Y.-F. Bi, *New J. Chem.* **2020**, *44*, 663-667.

[14] S.-D. Bian, J.-H. Jia, Q.-M. Wang, *J. Am. Chem. Soc.* **2009**, *131*, 3422-3423.

[15] X.-Y. Li, Z. Wang, H.-F. Su, S. Feng, M. Kurmoo, C.-H. Tung, D. Sun, L.-S. Zheng, *Nanoscale* **2017**, *9*, 3601-3608.

[16] Y.-P. Xie, J.-L. Jin, X. Lu, T. C. W. Mak, *Angew. Chem. Int. Ed.* **2015**, *54*, 15176-15180.

[17] Z. Wang, H.-F. Su, X.-P. Wang, Q.-Q. Zhao, C.-H. Tung, D. Sun, L.-S. Zheng, *Chem. Eur. J.* **2018**, *24*, 1640-1650.

[18] L.-P. Cheng, Z. Wang, Q.-Y. Wu, H.-F. Su, T. Peng, G.-G. Luo, Y.-A. Li, D. Sun, L.-S. Zheng, *Chem. Commun.* **2018**, *54*, 2361-2364.

[19] J.-W. Liu, H.-F. Su, Z. Wang, Y.-A. Li, Q.-Q. Zhao, X.-P. Wang, C.-H. Tung, D. Sun, L.-S. Zheng, *Chem. Commun.* **2018**, *54*, 4461-4464.

[20] Q. Yao, T. Chen, X. Yuan, J. Xie, *Acc. Chem. Res.* **2018**, *51*, 1338-1348.

[21] S.-F. Yuan, Z.-J. Guan, W.-D. Liu, Q.-M. Wang, *Nat. Commun.* **2019**, *10*, 4032.

[22] X. Gao, S. He, C. Zhang, C. Du, X. Chen, W. Xing, S. Chen, A. Clayborne, W. Chen, *Adv. Sci.* **2016**, *3*, 1600126 (1-7).

[23] Z.-A. Nan, Y. Xiao, X.-Y. Liu, T. Wang, X.-L. Cheng, Y. Yang, Z. Lei, Q.-M. Wang, *Chem. Commun.* **2019**, *55*, 6771-6774.

[24] Y.-L. Li, J. Wang, P. Luo, X.-H. Ma, X.-Y. Dong, Z.-Y. Wang, C.-X. Du, S.-Q. Zang, T. C. W. Mak, *Adv. Sci.* **2019**, *6*, 1900833(1-6).

[25] O. Fuhr, S. Dehnen, D. Fenske, *Chem. Soc. Rev.* **2013**, *42*, 1871-1906.

[26] V. A. Fedorin, *Semicond.* **1993**, *27*, 196-198.

[27] B. A. Mansour, S. E. Demian, H. A. Zayed, *J. Mater. Sci.: Mater. Electron.* **1992**, *3*, 249-252.

[28] V. W.-W. Yam, K. K.-W. Lo, W. K.-M. Fung, C.-R. Wang, *Coord. Chem. Rev.* **1998**, *171*, 17-41.

[29] S. Dehnen, A. Schäfer, D. Fenske, R. Ahlrichs, *Angew. Chem. Int. Ed.* **1994**, *33*, 746-749.

[30] K. Tang, T. Xia, X. Jin, Y. Tang, *Polyhedron* **1993**, *12*, 2895-2898.

[31] O. Fuhr, L. Fernandez-Recio, D. Fenske, *Eur. J. Inorg. Chem.* **2005**, *2005*, 2306-2314.

[32] M. Semmelmann, D. Fenske, J. F. Corrigan, *J. Chem. Soc*., *Dalton Trans*., **1998**, 2541-2545.

[33] M.-L. Fu, I. Issac, D. Fenske, O. Fuhr, *Angew. Chem. Int. Ed.* **2010**, *49*, 6899-6903.

[34] S. Dehnen, D. Fenske, *Chem. Eur. J.* **1996**, *2*, 1407-1416.

[35] M. Bettenhausen, A. Eichhöfer, D. Fenske, M. Semmelmann, *Z. Anorg. Allg. Chem.* **1999**, *625*, 593-601.

[36] S. Dehnen, D. Fenske, A. C. Deveson *J. Cluster Sci.* **1996**, *7*, 351-368.

[37] A. Deveson, S. Dehnen. D. Fenske, *J. Chem. Soc., Dalton Trans.,* **1997**, 4491-4497.

[38] R. Langer, W. Yu, L. Wünsche, G. Buth, O. Fuhr, D. Fenske, *Z. Anorg. Allg. Chem.* **2011**, *637*, 1834-1840.

[39] X.-X. Yang, I. Issac, S. Lebedkin, M. Kuhn, F. Weigend, D. Fenske, O. Fuhr, A. Eichhöfer, *Chem. Commun.* **2014**, *50*, 11043-11045.

[40] H. Krautscheid, D. Fenske, *Angew. Chem. Int. Ed.* **1990**, *29*, 1452-1454.

[41] M.-L. Fu, D. Fenske, B. Weinert, O. Fuhr, *Eur. J. Inorg. Chem.* **2010**, *2010*, 1098-1102.

[42] C. Nitschke, D. Fenske, J. F. Corrigan, *Inorg. Chem.* **2006**, *45*, 9394-9401.

[43] O. Fuhr, A. Meredith, D. Fenske, *Dalton Trans.* **2002**, 4091-4094.

[44] A. Eichhöfer, G. Buth, S. Lebedkin, M. Kuhn, F. Weigend, *Inorg. Chem.* **2015**, *54*, 9413-9422.

[45] L. Fernandez-Recio, D. Fenske, O. Fuhr, *Z. Anorg. Allg. Chem.* **2008**, *634*, 2853-2857.

[46] D. Fenske, H. Krautscheid, S. Balter, *Angew. Chem. Int. Ed.* **1990**, *29*, 796-799.

[47] O. Fuhr, L. Fernandez-Recio, A. Castineiras, D. Fenske, *Z. Anorg. Allg. Chem.* **2007**, *633*, 700-704.

[48] A. Eichhöfer, D. Fenske, *J. Chem. Soc., Dalton Trans.* **1998**, 2969-2962.

[49] N. Zhu, D. Fenske, *J. Chem. Soc., Dalton Trans.* **1999**, 1067-1075.

[50] S. Dehnen, D. Fenske, *Angew. Chem. Int. Ed.* **1994**, *33*, 2287-2289.

[51] C. Nitschke, D. Fenske, J. F. Corrigan, *Inorg. Chem.* **2006**, *45*, 9394-9401.

[52] A. Eichhöfer, E. Beckmann, D. Fenske, D. Herein, H. Krautscheid, R. Schlögl, *Isr. J. Chem.* **2001**, *41*, 31-37.

[53] H. Krautscheid, D. Fenske, G. Baum, M. Semmelmann, *Angew. Chem. Int. Ed.* **1993**, *32*, 1303-1305.

[54] V. Stylidou, K. Kavaratzi, I. Papazoglou, A. G. Hatzidimitriou, A. G. Papadopoulos, P. Angaridis, P. Aslanidis, *Eur. J. Inorg. Chem.* **2018**, *2018*, 2915-2926.

[55] A. Koutsari, F. Karasmani, E. Kapetanaki, D. I. Zainuddin, A. G. Hatzidimitriou, P. Angaridis, P. Aslanidis, *Inorg. Chim. Acta* **2017**, *458*, 138-145.

[56] K. Shimada, A. Kobayashi, Y. Ono, H. Ohara, T. Hasegawa, T. Taketsugu, E. Sakuda, S. Akagi, N. Kitamura, M. Kato, *J. Phys. Chem. C* **2016**, *120*, 16002-16011.

[57] R. Langer, M. Yadav, B. Weinert, D. Fenske, O. Fuhr, *Eur. J. Inorg. Chem.* **2013**, *2013*, 3623-3631.

[58] B. K. Maiti, K. Pal, S. Sarkar, *Eur. J. Inorg. Chem.* **2007**, *2007*, 5548-5555.

[59] H. Xie, I. Kinoshita, T. Karasawa, K. Kimura, T. Nishioka, I. Akai, K. Kanemoto, *J. Phys. Chem. B* **2005**, *109*, 9339-9345.

[60] J.-F. Song, S.-Z. Li, R.-S. Zhou, J. Shao, X.-M. Qiu, Y.-Y. Jia, J. Wang, X. Zhang, *Dalton Trans.* **2016**, *45*, 11883-11891.

[61] A. Oppermann, R. Dick, C. Wehrhahn, U. Flörke, S. Herres-Pawlis, G. Henkel, *Eur. J. Inorg. Chem.* **2016**, *2016*, 3744-3755.

[62] A. M. Polgar, A. Zhang, F. Mack, F. Weigend, S. Lebedkin, M. J. Stillman, J. F. Corrigan, *Inorg. Chem.* **2019**, *58*, 3338-3348.

[63] C. B. Khadka, B. K. Najafabadi, M. Hesari, M. S. Workentin, J. F. Corrigan, *Inorg. Chem.* **2013**, *52*, 6798-6805.

[64] R. Langer, D. Fenske, O. Fuhr, *Z. Naturforsch. B* **2013**, *68*, 575-580.

[65] S. Bestgen, O. Fuhr, P. W. Roesky, D. Fenske, *Dalton Trans.* **2016**, *45*, 14907-14910.

[66] A. Eichhöfer, D. Fenske, *unpublished results*.

[67] X. Yang, I. Isaac, C. Persau, R. Ahlrichs, O. Fuhr, D. Fenske, *Inorg. Chim. Acta* **2014**, *421*, 233-245.

[68] B. K. Najafabadi, J. F. Corrigan, *Dalton Trans.* **2014**, *43*, 2104-2111.

[69] V. W.-W. Yam, E. C.-C. Cheng, N. Zhu, *New J. Chem.* **2002**, *26*, 279-284.

[70] K. Nomiya, H. Yokoyama, R. Noguchi, K. Machida, *Chem. Lett.* **2002**, *9*, 922-923.

[71] D. Habibia, E. Gheami, R. V. Parishb, R. G. Pritchardb, *Polyhedron* **1999**, *18*, 2977-2979.

[72] *Non-Tetrahedrally Bonded Elements and Binary Compounds I*, ed. O. Madelung, U. Rössler, M. Schulz, Springer-Verlag Berlin Heidelberg, **1998**, *41C*, PP 1-4.

[73] X.-J. Wang, T. Langetepe, C. Persau, B.-S. Kang, G. M. Sheldrick, D. Fenske, *Angew. Chem. Int. Ed.* **2002**, *41*, 3818-3822.

[74] D. Fenske, C. Persau, S. Dehnen, C. E. Anson, *Angew. Chem. Int. Ed.* **2004**, *43*, 305-309.

[75] D. Fenske, C. E. Anson, A. Eichhöfer, O. Fuhr, A. Ingendoh, C. Persau, C. Richert, *Angew. Chem. Int. Ed.* **2005**, *44*, 5242-5246.

[76] C. E. Anson, A. Eichhöfer, I. Issac, D. Fenske, O. Fuhr, P. Sevillano, C. Persau, D. Stalke, J. Zhang, *Angew. Chem. Int. Ed.* **2008**, *47*, 1326-1331.

[77] S. Bestgen, X. Yang, I. Issac, O. Fuhr, P. W. Roesky, D. Fenske, *Chem. Eur. J.* **2016**, *22*, 9933-9937.

[78] S. Bestgen, O. Fuhr, B. Breitung, V. S. K. Chakravadhanula, G. Guthausen, F. Hennrich, W. Yu, M. M. Kappes, P. W. Roesky, D. Fenske, *Chem. Sci.* **2017**, *8*, 2235-2240.

[79] J.-W. Liu, L. Feng, H.-F. Su, Z. Wang, Q.-Q. Zhao, X.-P. Wang, C.-H. Tung, D. Sun, L.-S. Zheng, *J. Am. Chem. Soc.* **2018**, *140*, 1600-1603.

[80] R. Langer, B. Breitung, L. Wünsche, D. Fenske, O. Fuhr, *Z. Anorg. Allg. Chem.* **2011**, *637*, 995-1006.

[81] H. P. Nayek, W. Massa, S. Dehnen, *Inorg. Chem.* **2010**, *49*, 144-149.

[82] D. Fenske, T. Langetepe, *Angew. Chem. Int. Ed.* **2002**, *41*, 300-304.

[83] S. Chitsaz, D. Fenske, O. Fuhr, *Angew. Chem. Int. Ed.* **2006**, *45*, 8055-8059.

[84] X.-J. Wang, T. Langetepe, D. Fenske, *Z. Anorg. Allg. Chem.* **2002**, *628*, 1158-1167.

[85] D. Fenske, N. Zhu, T. Langetepe, *Angew. Chem. Int. Ed.* **1998**, *37*, 2639-2644.

[86] K. Tang, X. Xie, L. Zhao, Y. Zhang, X. Jin, *Eur. J. Inorg. Chem.* **2004**, *2004*, 78-85.

[87] X. Jin, K. Tang, W. Liu, H. Zeng, H. Zhao, Y. Ouyang, Y. Tang, *Polyhedron* **1996**, *15*, 1207-1211.

[88] F. Kirchhoff, J. M. Holender, M. J. Gillan, *Phys. Rev. B* **1996**, *54*, 190 - 202.

[89] Y. Jin, S. Li, Z. Han, B.-J. Yan, H.-Y. Li, X.-Y. Dong, S.-Q. Zang, *Angew. Chem. Int. Ed.* **2019**, *58*, 12143-12148.

[90] Y.-H. Chen, T. T.Y. Lin, H.-Y. Chen, C.-L. Kao, H.-Y. Chen, S. C.N. Hsu, J. R. Carey, M. Y. Chiang, *J. Inorg. Biochem.* **2013**, *120*, 24-31.

[91] O. Fuhr, L. Fernandez-Recio, D. Fenske, *Eur. J. Inorg. Chem.* **2005**, *2005*, 2306-2314.

[92] a) J.-P. Lang, X.-Q. Xin, *Acta Chimica Sinica* **1996**, *54*, 461-467; b) H. Kawaguchi, K. Yamada, J.-P. Lang, K. Tatsumi, *J. Am. Chem. Soc.* **1997**, *119*, 10346-10358; c)

J.-P. Lang, S.-J. Ji, Q.-F. Xu, Q. Shen, K. Tatsumi, *Coord. Chem. Rev.* **2003**, *241*, 47-60; d) J. -P. Lang, Q.-F. Xu, W.-H. Zhang, H.-X. Li, Z.-G. Ren, J.-X. Chen, Y. Zhang, *Inorg. Chem.* **2006**, *45*, 10487-10496; e) W.-H. Zhang, Z.-G. Ren, J.-P. Lang, *Chem. Soc. Rev.* **2016**, *45*, 4995-5019; f) Q. Liu, W.-H. Zhang, J.-P. Lang, *Coord. Chem. Rev.* **2017**, *350*, 248-274.

[93] S. F. Gheller, T. W. Hambley, J. R. Rodgers, R. T. C. Brownlee, M. J. O'Connor, M. R. Snow, A. G. Wedd, *Inorg. Chem.* **1984**, *23*, 2519-2528

[94] C.-P. Cui, S.-M. Hu, J.-J. Zhang, W.-X. Du, X.-T. Wu, *Inorg. Chem. Commun.* **2005**, *8*, 704-707.

[95] J. Zhang, C. Wang, Y. Wang, W. Chen, M. P. Cifuentes, M. G. Humphrey, C. Zhang, *J. Solid State Chem.* **2015**, *231*, 230-238.

[96] J. Zhang, D. Jia, M. G. Humphrey, S. Meng, M. J. Zaworotko, M. P. Cifuentes, C. Zhang, *Chem. Commun.* **2016**, *52*, 3797-3800.

[97] a) V. Shivaiah, S. K. Das, *Inorg. Chem.* **2005**, *44*, 7313-7315; b) D. Hagrman, P. Hagrman, J. Zubieta, *Inorg. Chim. Acta* **2000**, *300*, 212-224.

[98] a) H. Abbas, A. L. Pickering, D.-L. Long, P. Kogerler, L. Cronin, *Chem. Eur. J.* **2005**, *11*, 1071-1078; b) Y.-Q. Lan, S.-L. Li, X.-L. Wang, K.-Z. Shao, D.-Y. Du, H.-Y. Zang, Z.-M. Su, *Inorg. Chem.* **2008**, *47*, 8179-8187; c) H.-Y. Zang, Y.-Q. Lan, G.-S. Yang, X.-L. Wang, K.-Z. Shao, G.-J. Xu, Z.-M. Su, *CrystEngComm* **2010**, *12*, 434-445; d) J. Du, J. Yu, J. Tang, J. Wang, W. Zhang, W. R. Thiel, M. Jia, *Eur. J. Inorg. Chem.* **2011**, *2011*, 2361-2365; e) Y. Gong, Y.-X. Yang, M.-M. Zhang, X.-L. Gao, J.-L. Yin, J.-H. Lin, *Dalton Trans.* **2014**, *43*, 16928-16936.

[99] Z.-K. Qu, K. Yu, Z.-F. Zhao, Z.-H. Su, J.-Q. Sha, C.-M. Wang, B.-B. Zhou, *Dalton Trans.* **2014**, *43*, 6744-6751.

[100] V. W.-W. Yam, K. K.-W. Lo, *Chem. Soc. Rev.* **1999**, *28*, 323-334.

[101] L.-X. Hu, F. Wang, Y. Kang, J. Zhang, *Cryst. Growth Des.* **2016**, *16*, 7139-7144.

[102] Y.-M. Su, W. Liu, Z. Wang, S.-A. Wang, Y.-A. Li, F. Yu, Q.-Q. Zhao, X.-P. Wang, C.-H. Tung, D. Sun, *Chem. Eur. J.* **2018**, *24*, 4967-4972.

[103] M. Osawa, *Chem. Commun.* **2014**, *50*, 1801-1803.

[104] B. K. Teo, Y.-H. Xu, B.-Y. Zhong, Y.-K. He, H.-Y. Chen, W. Qian, Y.-J. Deng, Y.-H. Zou, *Inorg. Chem.* **2001**, *40*, 6794-6801.

[105] L. M. Nguyen, M. E. Dellinger, J. T. Lee, R. A. Quinlan, A. L. Rheingold, R. D. Pike, *Inorg. Chim. Acta* **2005**, *358*, 1331-1336.

[106] J.-H. So, P. Boudjouk, *Synthesis-Stuttgart* **1989**, 306-307.

[107] a) G. M. Sheldrick, *Acta Cryst. A* **2008**, *64*, 112-122; b) G. M. Sheldrick, *Acta Cryst. C* **2015**, *71*, 3-8.

[108] O. V. Dolomanov, L. J. Bourhis, R. J. Gildea, J. A. K. Howard, H. Puschmann, *J. Appl. Crystallogr.* **2009**, *42*, 339-341.

[109] K. Brandenburg, *DIAMOND3.2i, Visual Crystal Structure Information System, Crystal Impact GbR, Bonn,* **2012**.

[110] a) B. K. Maiti, K. Pal, S. Sarkar, *Eur. J. Inorg. Chem.* **2007**, *2007*, 5548-5555; b) M.-J. Zhang, H.-X. Li, H.-Y. Li, J.-P. Lang, *Dalton Trans.* **2016**, *45*, 17759-17769.

9 Abbreviations

dppm	bis(diphenylphosphino)methan
dppe	1,2-bis(diphenylphosphino)ethane
dppp	1,3-bis(diphenylphosphino)propane
dppb	1,4-bis(diphenylphosphino)butane
dpppt	1,5-bis(diphenylphosphino)pentane
dpph	1,6-bis(diphenylphosphino)hexane
dppox	1,2-bis(diphenylphosphinomethyl)benzene
dppbz	1,2-bis(diphenylphosphino)benzene
dppfc	1,1'-bis(diphenylphosphino)ferrocene
PPh_3	triphenylphosphine
HSCy	cyclohexanethiol
HSCp	cyclopentanethiol
HSAd	1-adamanetanethiol
HSPh	phenylthiol
HSBz	benzylthiol
Strimethyl-benzyl	(2,4,6-trimethyl)benzylthiol
DMF	dimethylformamide
Diethyl ether	Et_2O
THF	tetrahydrofuran
Å	Ångstrom (10^{-10} m)
°C	Celsius degree
μL	microliter
mL	milliliter
mmol	millimole
IR	Infrared Spectrum
ATR	Attenuated Total Reflection
EA	Elemental Analysis
UV-vis	Ultraviolet Visible

Abbreviations

LUMO	Lowest Unoccupied Molecular Orbital
HOMO	Highest Occupied Molecular Orbital
DFT	Density Functional Theory
TEM	Transmission Electron Microscope
NMR	Nuclear Magnetic Resonance.
ESI-MS	Electrospray Ionization Mass Spectrometry
MLCT	Metal Core to Ligands Transfer
LMCT	Ligands to Metal Core Transfer
OLED	Organic Light Emitting Diode
POM	Polyoxometalates
fcc	Face Centred Cubic
hcp	Hexagonal Close Packing
symm. equiv.	Symmetric Equivalence

In the presentation of the molecular structures, the following colour code has been used.

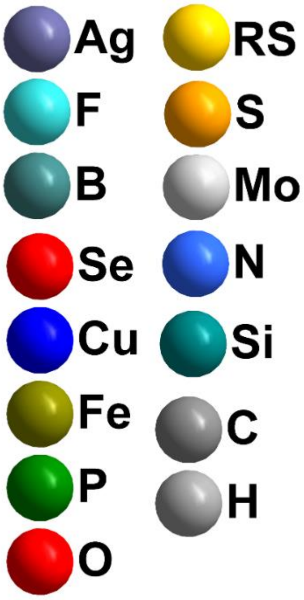

10 Acknowledgements

First of all, I would like to express my sincerest gratitude to my supervisor Prof. Dr. Dieter Fenske. During the past three years, Prof. Dr. Dieter Fenske helped me to test every compound’s crystallography data and provided me with great suggestion and encouragement throughout my PhD study. I have learned a lot from him, not only from his profound knowledge, but also from his enthusiasm for academics, his decades of persistence in the field of chemistry and how to treat every detail at daily work. All of this help means immeasurably to this thesis and me.

I would like to thank Dr. Olaf Fuhr. He taught me the rules in laboratory, the synthetic approaches of many compounds and the usage of IR, UV-vis and fluorescence. Besides. Dr. Olaf Fuhr also helped me to solve the crystal structure and gave me a lot of suggestions during my writing.

I would like to thank Prof. Dr. Peter W. Roesky and every member in Prof. Dr. Peter W. Roesky’s group. They helped me a lot about how to start research in KIT, especially when I freshly arrived here.

I would like to thank Dr. Sergei Lebedkin for revising the fluorescent section of my thesis.

I would like to thank Nikolai Bartnick for the elemental analysis measurement.

I would like to thank my friend Tingting Ruan and Xiaofei Sun. They helped me analyze some complicated experimental phenomena and inspired me to synthesis new compounds.

I would like to thank my parents and the other family members for their support and encouragement for my study and live in Karlsruhe.

I would like to thank all the other colleagues for their help and suggestion during my work.

Finally, I would like to thank of the China Scholarship Council (201808350100) for providing the financial support for my PhD study.